

Mountain pine beetle dispersal: morphology, genetics, and range expansion

by

Victor Aaron Shegelski

A thesis submitted in partial fulfillment of the requirements for the degree of

Doctor of Philosophy

in

Systematics and Evolution

Department of Biological Sciences

University of Alberta

Abstract

Dispersal by flight is a complex life history phase in many insects that is essential to gene flow and range expansion. Many elements contribute to realized dispersal, including biotic and abiotic environmental conditions, as well as intrinsic factors such as morphology, physiology and behavior. Dispersal is often associated with economic consequences in pest species, and understanding its correlates can inform control efforts. In this thesis I investigate dispersal from a micro to macro scale using the mountain pine beetle (*Dendroctonus ponderosae*) as a study system. I begin by testing relationships between empirically observable flight morphology and dispersal capacity, as measured using computer-linked flight mills. I also relate dispersal capacity to genetic variation using RNA-seq and a targeted association study to identify genes and genetic markers associated with a dispersal phenotype. I then shift focus to identify large scale patterns of dispersal across the landscape, using genomic single nucleotide polymorphisms (SNPs).

In this research I found several flight-related traits and genes. Morphologically, variation in dispersal capacity is related to wing size and body weight. These traits, however, only explained approximately 20% of the variation, indicating that other factors, such as genetic variation, also contribute to a “dispersal phenotype”. Analysis of gene expression by comparing beetles with strong and weak dispersal capacity revealed over 2,700 differentially expressed genes and 4 genetic markers associated with flight performance. Many of these genes related to physiology, hormonal control, behavior, and detoxification, which may have implications for landscape-scale dispersal success. By investigating dispersal dynamics of mountain pine beetle across central Alberta, I identified the sources of current outbreaks at leading-edge populations and found evidence for long-range dispersal and high rates of gene flow between populations.

This work represents a synthesis of different approaches to dispersal-related research in which I investigated morphological, physiological and behavioral traits, as well as landscape-scale patterns of dispersal, using empirical measurements, genetics, and flight mill-measured dispersal capacity. I present a methodological approach to studying dispersal on several scales and contribute to our understanding of the many factors associated with insect dispersal by flight.

Preface

A version of Chapter 2 has been published as Shegelski VA, Evenden ML, Sperling FAH (2019) “Morphological variation associated with dispersal capacity in a tree-killing bark beetle *Dendroctonus ponderosae* Hopkins”, Agriculture and Forest Entomology volume 21, pages 79-97. VAS performed the analysis and drafted the manuscript. Flight mills in the lab of MLE were used to acquire flight data. All authors contributed to the study design and manuscript revisions.

A version of Chapter 4 has been submitted for publication, authored by Shegelski VA, Campbell EO, Thompson KM, Whitehouse CM, and Sperling FAH. Structure analysis was performed by EOC, and all other aspects of the analysis, as well as drafting of the manuscript, were performed by VAS. Many samples were supplied by CMW or KMT. All authors contributed to study design and manuscript revisions.

Acknowledgements

To get to this point, I have been supported by a veritable army, but I would like to start by thanking my supervisor, who took a chance on an ex-military wildcard. Thank you, Felix. You have been the ideal supervisor. You provided a perfect blend of direction and creative freedom. I can understand that a student like me could not always have been easy; we have butted heads on several occasions, but, like a true “Bayesian” intellectual, you were flexible in your thinking, and you certainly taught me to do the same.

Thank you, Maya and Dezene, for being on my committee and supporting me through these trials. Maya, you gave me the chance to be a part of your field research (chainsaw and shotgun training was a blast... no pun intended), and you had some serious patience in helping me get my first paper published. Dezene, you have provided some great theoretical insight, and your encouragement has been invaluable.

I would also like to thank the “army” that helped with this research through sample collection, advice and great discussion: Stephane Bordeleau, Jackson Lai, Dylan Sjolie, Caroline Whitehouse, Bryan Brunet, Phil Batista, Sebastian Lackey, Corey Davis, Devin Letourneau, Melodie Kunegel-Lion, Stephen Trevoy, Nils Koch, Nathan Marculis, John Haley, Tiago Simões, Oksana Vernygora, Andrew Sperling, William Sperling, Janet Sperling, Neil Thompson, Jennifer McCormack, Fraser McKee, Asha Wijerathna, and the crew down at the MBSU (Troy and Sophie). Also, Julian Dupuis, Ronald Batallas, members of the Sperling Lab, and, of course, the wonderful “Core Four”, Tyler, Brittany, and Erin. We had some doggone good times.

Thank you, Mom, Dad, Adam, Mandy, Trevor and Lianne, for your support, and for forging who I am today. Thank you, Kyla, my wife, for your unwavering support through the last

few years. It has been an adventure having children as we simultaneously faced the constant challenge of clawing out our respective professional niches. Regardless, with your support I have overcome insurmountable difficulties. I love you, and I am capable of anything when I have you by my side. Isaac, you have been amazingly patient with ‘Dah-dee’ and have made life infinitely richer. And Hazel, welcome to the world! Thank you for being patient enough to wait until after I wrote this thesis.

Thank you to all my in-laws. Many cringe at the thought of having one set of in-laws, but I have two, and I love you all. In this, I know I have won the lottery. Shannon, Thank you for your weekly help with caring for Isaac. I would not have been able to complete my work in time if not for you.

I also thank my late wife, Michelle Shegelski (née Ernst) for setting me on this path. Without your guidance, I never would have discovered my love of teaching and the academic world.

This research was supported by: (1) a grant to Dr. Maya Evenden and Dr. Felix Sperling from the Natural Science and Engineering Research Council of Canada to the TRIA Network, with contributions from Alberta Agriculture and Forestry, fRI Research, Manitoba Conservation and Water Stewardship, Natural Resources Canada - Canadian Forest Service, Northwest Territories Environment and Natural Resources, Ontario Ministry of Natural Resources and Forestry, Saskatchewan Ministry of Environment, West Fraser and Weyerhaeuser; (2) an NSERC Discovery Grant to F. Sperling; and (3) the Government of Alberta.

Table of Contents

Abstract	ii
Preface	iv
Acknowledgements	v
List of Figures	x
List of Tables	xi
List of Abbreviations	xii
List of Appendices	xiii
Introduction	1
1.1 Insect dispersal	1
1.2 Investigating the correlates of dispersal	2
1.3 Systematics, life history and impact of the mountain pine beetle	4
1.4 Morphological and genetic correlates of flight in mountain pine beetle.....	8
1.5 Population dynamics of mountain pine beetle	10
1.6 Thesis Objectives	11
Morphological variation associated with dispersal capacity in a tree-killing bark beetle <i>Dendroctonus ponderosae</i> Hopkins	13
2.1 Summary	13
2.2 Introduction	14
2.3 Methods.....	17
2.3.1 Beetle data collection.....	17
2.3.2 Statistical analysis.....	20
2.4 Results	22
2.4.1 Morphology associations.....	22
2.4.2 Regression models	23
2.4.3 Heteroscedasticity and quantile regression.....	23
2.5 Discussion	24
2.5.1 Morphology associations with dispersal capacity	24
2.5.2 Heteroscedasticity in flight distance and future directions.....	27
2.6 Conclusions	29
2.7 Literature cited	35

Identification of genes and gene expression associated with dispersal capacity in the mountain pine beetle, *Dendroctonus ponderosae* Hopkins (Coleoptera: Curculionidae).45

3.1 Summary45

3.2 Introduction45

 3.3.1 Sample collection and preparation47

 3.3.2 Flight mill bioassay and sample selection48

 3.3.3 RNA extractions, RNA-Seq library preparation & sequencing49

 3.3.4 Sequence data mapping & differential expression analysis55

 3.3.5 Enrichment analysis & KEGG pathway analysis49

 3.3.6 DNA extractions, sequencing & mapping for association study50

 3.3.7 Targeted association study.....51

3.4 Results51

 3.4.1 Flight mill bioassay51

 3.4.2 Differential expression analysis.....52

 3.4.3 GO enrichment analysis.....54

 3.4.4 KEGG pathways55

 3.4.5 Targeted association study.....56

3.5 Discussion57

 3.5.1 Metabolism57

 3.5.2 Muscle form & function58

 3.5.3 Oxidative stress & detoxification58

 3.5.4 Endocrine system.....59

 3.5.5 Behavior.....60

 3.5.6 Association study.....61

3.6 Conclusions61

Source and spread dynamics of mountain pine beetle (*Dendroctonus ponderosae*) in central Alberta, Canada75

4.1 Summary75

4.2 Introduction76

4.3 Methods77

 4.3.1 Beetle sampling, DNA extraction, and sequencing77

 4.3.2 Data filtering and SNP calling.....78

 4.3.3 Population structure analysis79

4.4 Results	81
4.5 Discussion	82
4.6 Conclusions	84
General Conclusions	91
5.1 Thesis Overview.....	91
5.2 Future directions.....	94
5.2.1 Future work on flight-related morphology (Chapter 2).....	94
5.2.2 Future work on flight-related genetics (Chapter 3)	95
5.2.3 Future work on landscape-scale dispersal (Chapter 4).....	96
Biography.....	98
Works Cited.....	100
Appendices	137

List of Figures

Figure 2.1 The dispersal kernel of mountain pine beetle.....	31
Figure 2.2 Morphological differences between weak and strong flight	32
Figure 2.3 Quantile regression of individual morphological traits associated with flight.....	33
Figure 2.4 Comparison of trends in dispersal and morphology, and comparison to quantile regression of wing loading.....	34
Figure 3.1 Chapter 3 methods flowchart.....	63
Figure 3.2 Measured flight patterns of mountain pine beetle in relation to lighting conditions and actual sunset/sunrise.....	64
Figure 3.3 Principal component analysis and MA plots of differential expression analysis comparing strong, weak and non-fliers.....	65
Figure 3.4 GO annotations associated with mountain pine beetle dispersal capacity	66
Figure 3.5 KEGG pathways associated with dispersal capacity.....	67
Figure 3.6 Results of a targeted association study comparing variant sites to flight propensity and total distance flown	68
Figure 4.1 Principal component analyses of Alberta mountain pine beetle populations.....	86
Figure 4.2 Structure analysis of Alberta mountain pine beetle populations	87
Figure 4.3 Population expansion dynamics of mountain pine beetle in Alberta	88

List of Tables

Table 3.1 Sequence data for RNA-Seq experiment	69
Table 3.2 Differentially expressed candidate genes related to flight performance.....	70
Table 4.1 Population differentiation statistics of mountain pine beetle in Alberta	90

List of Abbreviations

20E – 20-hydroxyecdysone

BP – Breusch-Pagan

DAPC – discriminant analysis of principal components

FDR – false discovery rate

GLM - generalized linear model

GO – gene ontology

GST – glutathione-s-transferase

IBIS - Institut de Biologie Intégrative et des Systèmes

IGF - Insulin-like growth factor

JH – juvenile hormone

JHEH – juvenile hormone epoxide hydrolase

KEGG – Kyoto Encyclopedia of Genes and Genomes

LD – linkage disequilibrium

MBSU – Molecular Biology Service Unit

MPB – mountain pine beetle

PCA – principal component analysis

perm p – permuted p-value

SNP – single nucleotide polymorphism

VIF – variance inflation factor

List of Appendices

Appendix 2.1.....	137
Appendix 2.2.....	143
Appendix 3.1.....	144
Appendix 3.2.....	225
Appendix 4.1.....	231
Appendix 4.2.....	233

Chapter 1

Introduction

1.1 Insect dispersal

Dispersal in insects involves movement across a landscape that potentially results in gene flow and range expansion (Saastamoinen et al. 2018). Dispersal range and complexity are increased by the ability to fly, and this can make prediction difficult (Stinner et al. 1983; Bowler and Benton 2005; Ward et al. 2020). Several insect species are economically disruptive (Machado et al. 2020; Huang et al. 2020; Fetting et al. 2020) and invasive spread of insects is enhanced by climate change and increasing globalization (Hulme 2017). Thus, the need to predict dispersal for control measures and damage mitigation has become increasingly urgent.

Predicting insect dispersal is difficult, in part due to complex interactions that make up the dispersal phenotype (Jones et al. 2019). Dispersal within a population can be described using a probability density function called a dispersal kernel, which represents the distribution of dispersal distances within a population and is used to characterize dispersal patterns (Nathan et al. 2012). Dispersal distances are highly variable (Eviden et al. 2014), as they involve morphological, physiological, and behavioral trait interactions (Roff and Fairbairn 2007; Saastamoinen et al. 2018; Jones et al. 2019), and can be affected by factors such as temperature (Atkins 1959; Aukema et al. 2008), wind (Safranyik et al. 1989; Ainslie and Jackson 2011), humidity (Safranyik and Carroll 2006), chemical cues (Atkins 1966; Robertson et al. 2007), and parasitic infection (Eveleigh et al. 2007). However, intrinsic factors such as wing and body morphology (Hassall 2015; Dominguez and Abdala 2019), joint resilin (Haas et al. 2000; Bäumler and Büsse 2019), and genetics (Jones et al. 2015; Zhou et al. 2020) can also be influential. In this thesis I hope to improve the body of

knowledge surrounding insect dispersal flights by focusing on morphology and genetics, as well as landscape-scale patterns, associated with dispersal by the destructive forest pest, mountain pine beetle (*Dendroctonus ponderosae* Hopkins).

1.2 Investigating the correlates of dispersal

Some species have obvious traits that differentiate dispersal phenotypes (Zhang et al. 2019). In other species these phenotypes are not easily discerned (Shegelski et al. 2019). In such situations individual flight capacity can be measured using computer-linked flight mills (Jones et al. 2019; Naranjo 2019) which are capable of recording data on distance, velocity, and propensity. However, drawing a clear relationship between natural dispersal and flight measured on mills can be difficult. There is debate that flight mill data may be underestimated (Taylor et al. 2010) or overestimated (Robertson and Roitberg 1998), as insects on flight mills are suspended and do not have to carry their own weight but must overcome the inertia of the mill arm (Minter et al. 2018). It is also possible that attempts by the insect to fly in a straight line may increase energetic costs associated with the circular flight path of the mill (Ribak et al. 2017). Flight mills also do not allow measurement of orientation that can be an important factor in dispersing insects (Reynolds et al. 2016; Ribak et al. 2017). Ultimately, because of the contrast from a natural setting, flight mill data is most useful in testing relative differences and identifying flight phenotypes based on comparative performance (Minter et al. 2018; Naranjo 2019).

Once individuals have been characterized, dispersal data should be compared to other variables in order to identify relationships (Minter et al. 2018). Morphological data can be acquired through precise measurements taken by hand with calipers, ocular units on a microscope, or through software programs such as ImageJ (Schneider et al. 2012) or Image J2 (Rueden et al.

2017). Once these data are collected, relationships can be identified using regression-based analyses in programs such as R (R Core Team 2018).

Flight mill data can also be compared to genetic information (Minter et al. 2018). Many analyses focus on pre-identification of candidate loci for testing relationships, but RNA-seq can be used to compare the instantaneous gene expression profiles of samples to find differentially expressed genes associated with particular conditions (Stark et al. 2019). RNA-seq technologies have been developing rapidly; short-read technologies still remain dominant in the field, but recent advances in long-read sequencing have reduced read ambiguity and allow complete identification of longer transcripts that are otherwise difficult to capture (Oikonomopoulos et al. 2016). Regardless, short-read RNA-seq remains a powerful and popular tool in identifying candidate genes (Stark et al. 2019).

One drawback of RNA-seq is that sample acquisition and preparation is highly sensitive and may be difficult to achieve in the field. Alternatively, DNA is comparatively easy to work with. Association studies are one way to use DNA to test a large number of loci for variants related to a particular trait (Visscher et al. 2017). This kind of association study can be done using programs like TASSEL (Bradbury et al. 2007), and can account for continuous, non-normally distributed data through permutation testing (Che et al. 2014). Statistical power for such analyses is low due to necessary p-value corrections, but this can be countered by increasing sample sizes (estimated at hundreds to thousands of individuals; Visscher et al. 2017), or minimizing the area of focus in the genome, reducing the number of tested loci.

1.3 Systematics, life history and impact of the mountain pine beetle

The term bark beetle generally refers to the subfamily Scolytinae within the family Curculionidae. Scolytine beetles have a shortened snout and several “stumpy” features that are adapted to tunneling within plant tissues (Hulcr et al. 2015). Within Scolytinae, the bark beetles *sensu stricto* include those that feed and breed within the inner bark of a host tree (Raffa et al. 2015), such as *D. ponderosae*.

The genus *Dendroctonus* Erichson is the sister genus to *Hylurgus* (Jordal and Cognato 2012; Pistone et al. 2018) and is currently within the tribe Hylurgini, although this tribe is currently paraphyletic and will be undergoing major revisions (Pistone et al. 2018). Within the genus *Dendroctonus*, *D. ponderosae* and *D. jeffreyi* Hopkins are sister species based on COI sequence data (Victor and Zúñiga 2016), genomic SNP data (Godefroid et al. 2019), as well as morphological features, such as similarities in elytral declivity, tubercles on the head and base of the mandibles, and mycangia (Victor and Zúñiga 2016), which are sac-like structure on the mouthparts used to carry symbiotic fungi. Aside from morphology, these two species have similar life histories involving facultative predation on host trees, are sympatric, and have similar gallery structures (Wood 1982). Differences occur in the primary female pheromone constituents (Paine et al. 1999) and the host trees they occupy; *D. jeffreyi* is only found in *Pinus jeffreyi* Balf., and *D. ponderosae* is found in every pine species within its range except *P. jeffreyi* (Fettig 2016).

The general life cycle of bark beetles involves (i) colonization of a host tree and reproduction, (ii) overwintering and development under the bark of the tree, and (iii) emergence and dispersal to find new host (Raffa et al. 2015). Although there are many variations on this life cycle within the bark beetles, the general pattern remains the same. There are two main attack

strategies used by *Dendroctonus* bark beetles during colonization: some are true parasites that will attack alone or in pairs around the base of the tree, and the larvae develop within the living tree; others use pheromones to coordinate mass attacks to kill the host tree (Reeve et al. 2012; Godefroid et al. 2019). This latter strategy is used by *D. ponderosae* and has the potential to develop epidemic population outbreaks (Burke and Carroll 2017).

In order to begin colonization, the pioneering beetle must select a host tree. Three hypotheses have been used to explain host choice and colonization behavior in mountain pine beetle (Latty and Reid 2010; Chubaty et al. 2014; Jones et al. 2020): (a) the “safe site” hypothesis postulates that beetles will select trees with low defenses in order to maximize the probability of success, (b) the “desperation” hypothesis predicts that beetles with lower energy reserves will attempt to colonize a tree regardless of its condition, and (c) the “condition matching” hypothesis proposes that the condition of the tree and beetle are both important in such a way that fit beetles may colonize a healthy tree. In *D. ponderosae*, females are the pioneering sex (Blomquist et al. 2010). They will perform the initial attack on a host tree and coordinate aggregation using the pheromone *trans*-verbenol (Chiu et al. 2019). The strength of this pheromone signal increases with dispersal distance, likely enhancing the ability to aggregate at distant attack sites (Jones et al. 2020). Males that join in the attack will produce *exo*-brevicomin and frontalin, both of which also initially act as aggregation pheromones (Aw et al. 2010; Keeling et al. 2013a). Once host defenses have been overcome, and to avoid overcrowding in the host, both sexes use antiaggregation pheromones to signal the end of the attack; females produce verbenone (Taft et al. 2015), and a build up of male-produced frontalin also has an anti-aggregation effect when in high concentrations (Blomquist et al. 2010).

After the attack, female *D. ponderosae* will excavate a nuptial chamber, mate with a male under the bark of the host tree, then bore a J-shaped vertical gallery and lay eggs, alternating along the sides (Esch et al. 2016). In order to maximize reproductive capacity, many bark beetles, including mountain pine beetle, degrade their flight muscles (McCambridge and Mata 1969; Sahota 1975) to reallocate resources for reproduction (Atkins and Farris 1962; Bhakthan et al. 1970; Robertson 1998).

Development takes place under the bark of the host tree (Wertman et al.2018) and is largely dependent on symbiotic blue stain fungi species such as *Grosmannia clavigera* (Rob.-Jeffer. & R.W. Davidson) Zipfel, Z.W. de Beer & M.J. Wingf., *Leptographium longiclavatum* S.W. Lee, J.J. Kim & C. Breuil, and *Ophiostoma montium* (Rumbold) Arx (Lee et al. 2007). Associated fungi species vary based on geographic location (Rice et al. 2008) and may change over time (Six and Bentz 2007). These fungi, carried in the mycangia of the beetle, inoculate the tree during colonization and the excavation of natal galleries (Bleiker et al. 2009; Six 2020). The mutualist fungi effectively stop the flow of phloem (Hubbard et al.2013), which ultimately kills the host tree. These fungi also transfer nitrogen into the phloem where it can be ingested by developing larvae (Bleiker and Six 2007; Six 2020).

Mountain pine beetles typically overwinter as larvae (Cooke 2009), as they have reduced cold tolerance as eggs (Bleiker et al. 2017) and pupae (Bleiker and Smith 2019). Winter survival can be difficult in the northern range of mountain pine beetle, as low temperatures can cause mass mortality (Safranyik 1998; Bleiker and Smith 2019). To survive winter, beetles build up cryoprotectants such as glycerol (Fraser et al.2017) and potentially other proline-related compounds (Thompson et al. 2020).

Beetles that survive winter and predation while under the bark typically emerge mid-summer to perform a dispersal flight (Wertman and Bleiker 2019). Dispersal distances can be highly variable and may be performed above or below the forest canopy (Jackson et al. 2008; Evenden et al. 2014). Above-canopy dispersal, also known as long range dispersal, is mostly mediated by wind (Jackson et al. 2008) and may be influenced by strong updrafts caused by terrain features (de la Giroday et al. 2011). It is estimated that only 2.4% of beetles disperse this way (Jackson et al. 2008), but this type of dispersal during the current outbreak led to the establishment of populations in Alberta (Jackson et al. 2008; Janes et al. 2014).

The majority of mountain pine beetle dispersal is below the forest canopy and is more dependent on individual flight capabilities (Steyn et al. 2016). In laboratories, beetle flight, as measured on flight mills, is highly variable, ranging from no flight to over 30 km (Evenden et al. 2014). While these distances do not necessarily directly translate to dispersal flights in nature, they indicate substantial variation in dispersal capacity (Jones et al. 2019), which provides short and long-term advantages to a population. Short-distance dispersers have greater survival rates, with more energetic resources available to colonize and reproduce, while those that fly long distances take more risks and use more energy but may colonize new resource rich regions (Roff and Fairbairn 2007; Latty and Reid 2010).

Bark beetles play an important ecological role in maintaining forest health (Axelson et al. 2009). Under endemic conditions, *D. ponderosae* generally only attack older, unhealthy trees (Safranyik and Carroll 2006; Axelson et al. 2009); however, during epidemic conditions, mass attacks can kill entire pine stands, which can have tremendous social and economic impact (Kurz et al. 2008; Corbett et al. 2015). To reach epidemic population sizes there must be an abundance

of weak host trees (Safranyik and Carroll 2006), which can result from drought, fire suppression, or range expansion into novel habitat due to climate change (Taylor and Carroll 2004; Safranyik and Carroll 2006). Epidemic beetles are able to attack and overcome the defenses of healthy trees (Lindgren and Raffa 2013), which perpetuates the outbreak as this epidemic behavior is passed down from parent to offspring (Burke and Carroll 2017).

The current outbreak is the largest in recent history and has damaged more than 71,000 km² of pine forest since the mid 1990's (Hart et al. 2015). During this outbreak, MPB has spread across the Rocky Mountains and become established in Alberta (Jackson et al. 2008; Janes et al. 2014), colonizing a novel host species, jack pine. The leading edge of mountain pine beetle infestation is now near Lac La Biche, Alberta (Mac Cormick 2020), and its spread threatens to continue eastward into the pine forests of eastern Canada and the USA. Understanding factors that contribute to this spread is crucial to mitigating damage through control efforts (Safranyik and Carroll 2006; Jackson et al. 2008).

1.4 Morphological and genetic correlates of flight in mountain pine beetle

Variation in flight-related morphology and genetics may have significant impacts on dispersal and range expansion (Hill et al. 1999a; Jones et al. 2015). Morphology may include wing size and shape, flight muscle, and fitness (Azevedo et al. 1998; Hassall 2015). Fitness is often measured as body size and weight, as larger, heavier bodies are generally indicative of greater energy stores (lipids) in mountain pine beetle (Evenden et al. 2014; Wijerathna and Evenden 2019). Lipid content influences flight and dispersal of bark beetles in three main ways: heavier beetles are more inclined to initiate flight (Atkins 1966; Jactel 1993; Evenden et al. 2014), they have more energy stores to sustain flight (Thompson and Bennett 1971; Williams and Robertson

2008), and they have shown reduced response to olfactory cues (Bennett and Borden 1971; Jones 2019), which could prolong flight in the presence of susceptible hosts. Wing morphology has also been linked to flight by influencing wing-beat frequency, which may impact flight capabilities (Atkins 1960). Wing morphology in other insects is often correlated with flight ability; variation in aspect ratio (ratio of wing length to chord) and wing size have been linked to improved flight capabilities under different environmental conditions (Azvedo et al. 1998; Frazier et al. 2008; Hassall 2015), and wing size has a positive correlation with flight muscle, as well as flight frequency, speed, and duration (Palmer and Dingle 1989; Dudley 1990; Fairbairn and Roff 1990). Differences in flight muscle have also been associated with flight capacity (Marden 2000) and may influence flight capability in mountain pine beetle.

Flight has also been linked to genes under selection identified in population genetics studies of mountain pine beetle (Janes et al. 2014; Batista et al. 2016), but these were never specifically tested for relationships with flight. Other life phases of mountain beetle have been studied more rigorously; genes have been identified that relate to detoxification of host defenses (Keeling et al. 2013b), pheromone biosynthesis (Huber and Robert 2016), and overwintering (Robert et al. 2016; Fraser et al. 2017), but research on the genes influencing dispersal flight is lacking. Flight-related genes have been identified in several other insects. These genes relate to metabolism (Niitepold et al. 2009, Zhou et al. 2020), muscle function (Marden et al. 2012), wing morphology (Rogulja et al. 2008), and generally improved flight capacity (Wheat et al. 2010; Jones et al. 2015). Identification of such genes in mountain pine beetle would provide understanding of the behavioral, physiological and morphological adaptations that contribute to its success, but also provide insight into bark beetle and insect dispersal in general.

1.5 Population dynamics of mountain pine beetle

The range of mountain pine beetle extends from near the border of Yukon and B.C., Canada, in the north, to as far south as Mexico (Six and Bracewell 2015). Throughout this range there are genetic patterns of isolation by distance with the exception of areas in which barriers to dispersal occur (Mock et al. 2007). There are also indications of recent range expansion, such as low genetic diversity, in the northern USA populations that extend into Canada (Mock et al. 2007; Janes et al. 2018).

Historically, mountain pine beetle was native to southwestern Alberta and BC. These populations are generally endemic and contribute to forest health (Axelson et al. 2009), but with periodic outbreaks that do immense damage to pine stands, and, consequently, a long history of control efforts, largely within the pine forests of BC (Alfaro et al. 2010). Such reports of beetle outbreaks in BC occur as early as the 1900s, and subsequent outbreaks have occurred in the 1930s, 1940s, 1970s, and 1980s. The current outbreak began in the 1990s and led to the establishment of mountain pine beetle in Alberta in the early 2000s (Alfaro et al. 2010).

The newest leading-edge populations in Alberta are found in Hinton and Lac La Biche (Town of Hinton [accessed 2020]; Mac Cormick 2020) and both are of particular concern. Part of the economy in Hinton relies on local forestry, and the presence of mountain pine beetle in Lac La Biche demonstrates population establishment in the novel host species, jack pine (*Pinus banksiana*).

Several studies have focused on population structure and gene flow in mountain pine beetle (Cullingham et al. 2019), and evidence has revealed genetically distinct populations in

Alberta: a northern invasive population, a southern resident population (Samarasekera et al. 2012; Janes et al. 2014; Batista et al. 2016), and a population that is a genetic intermediate that is likely a product of admixture between the northern and southern populations (Trevoy et al. 2018b). Identification of the north and intermediate populations also indicates that, during the recent outbreak, mountain pine beetle entered Alberta on two fronts; one arrived near Grande Prairie in the early 2000s, and the intermediate population entered through Jasper National Park more recently. Speculation on the nature of the genetically intermediate population has indicated some potentially important concerns relating to management, particularly if this admixture has produced novel adaptive genetic elements (Trevoy et al. 2018b).

1.6 Thesis Objectives

In this thesis I investigate dispersal of mountain pine beetle on 3 scales: (i) I compare empirically observable morphology to flight performance; (ii) I explore genetic and transcriptomic elements related to flight and dispersal; and (iii) I look at overall population dynamics resulting from dispersal across the landscape in Alberta.

There are many potential factors affecting dispersal (Hill et al. 1999), and identifying morphology associated with flight of mountain pine beetle can help us understand variation in dispersal. In **Chapter 2** I compare body, wing and flight muscle morphology to identify features related to dispersal capacity, as measured by a computer-linked flight mill bioassay.

Some variation in dispersal capacity is related to genetic factors (Minter et al. 2018), which can involve large suites of genes (Jones et al. 2015). In **Chapter 3** I survey the transcriptome for genetic systems and candidate flight genes, and I use this data to inform a targeted association

study to identify genetic markers associated with differential flight performance in mountain pine beetle.

Mountain pine beetles are expanding their range across Alberta and have recently established in Hinton and Lac La Biche (Town of Hinton [accessed 2020], Mac Cormick 2020). Genetic information can provide substantial insight into this movement across the landscape (Janes et al. 2018; Cullingham et al. 2019). In **Chapter 4** I use genetic variation among and between sample sites to identify population structure of mountain pine beetle populations across central Alberta.

Through this research, I hope to not only identify factors related to flight and dispersal in insects, but also to draw connections between these three scales by identifying genes and morphology linked to dispersal-related behaviors that may, in turn, affect landscape-scale dispersal success.

Chapter 2

Morphological variation associated with dispersal capacity in a tree-killing bark beetle *Dendroctonus ponderosae* Hopkins

A version of Chapter 2 has been published as Shegelski VA, Evenden ML, Sperling FAH (2019) "Morphological variation associated with dispersal capacity in a tree-killing bark beetle Dendroctonus ponderosae Hopkins", Agriculture and Forest Entomology volume 21, pages 79-97.

2.1 Summary

Intrinsic factors influencing the dispersal of insect pests during outbreaks are poorly understood, yet these factors need to be quantified to parameterize dispersal in models that predict population spread. The present study related wing and body morphology of female mountain pine beetles (*Dendroctonus ponderosae*) to flight distance, as measured by flight mill bioassays. Beetles that flew long distances (> 11 km) had a greater body weight and larger wings than beetles that flew short distances (< 1 km). These heavier female beetles should also be more capable pioneers because other studies have shown that body weight is positively correlated with lipid content.

Wing and body morphology of females are significant predictors of flight distance; heavy beetles with large wings generally flew further than smaller beetles, although this relationship is heteroscedastic. Dispersion of flight distance values increases with wing loading (weight/wing

area) as a result of a cohort of ‘lazy’ individuals that fly short distances (< 1 km) regardless of flight phenotype. The observed morphology explained less than 20% of the variation in flight capacity, indicating a substantial contribution from other intrinsic factors that remain to be investigated. The present study may have implications for dispersal modelling, providing estimates of flight capacity using morphological measurements.

2.2 Introduction

Dispersal leading to range expansion can exert selective pressures on the physical traits associated with dispersal phenotypes (Olivieri and Gouyon 1997; Hassall 2015). In many insects, traits like wing morphology, flight muscle and body condition can influence flight capacity and dispersal potential (Azevedo et al. 1998; Hassall 2015). Measurements of such flight-related traits can be used to infer an individual’s ability to disperse and may also be correlated with successful establishment after dispersal (Manning and Reid 2013; Evenden et al. 2014). Models that predict dispersal capacity by pest species have become important tools for environmental conservation and resource management through the refinement of damage prevention, especially in cases of range expansion and invasion of novel habitats (Safranyik and Carroll 2006).

The mountain pine beetle (MPB) *Dendroctonus ponderosae* Hopkins (Coleoptera: Curculionidae) is a tree-killing bark beetle that attacks and kills pine trees across western North America. MPB has recently expanded its range eastward (Safranyik et al. 2010). This spread is threatening to continue; historically, MPB distribution has been limited by climate rather than host availability (Safranyik 1978), but climate change has made previously unsuitable regions available to this species (Carroll et al. 2004). Milder climate and protection of large overmature trees from natural fires have created conditions in which the beetles can thrive and reproduce to reach

epidemic population levels (Taylor and Carroll 2004; Safranyik and Carroll 2006). This has led to the destruction of over 723 million m³ of merchantable pine in British Columbia and Alberta during the last outbreak (NRCan 2017), with subsequent ecological and economic impacts (Kurz et al. 2008; Corbett et al. 2015). These losses can be reduced through effective allocation of management resources based on early risk detection (Safranyik and Carroll 2006). Resource allocation is increasingly important in epidemic scenarios in which total control of MPB is not realistic. In such scenarios, equipment and manpower must be allocated in accessible areas that will maximize the impact on MPB spread while minimizing cost. Predictive modelling of MPB spread is one means of risk detection, and such models need to be parameterized with variables such as regional climate and dispersal capacity (Atkins 1961; Robertson et al. 2007; Aukema et al. 2008; Goodsman et al. 2016). Climatic data are often available, but the ability to identify MPB dispersal phenotypes is lacking.

The variable dispersal behaviour of MPB poses a challenge for predicting its range expansion. Beetles can utilize updrafts to disperse above the forest canopy (Jackson et al. 2008; de la Giroday et al. 2012), but research has shown that a majority of dispersal can take place below the canopy (Safranyik et al. 1992). In below-canopy dispersal, many beetles ignore susceptible host trees immediately upon emergence in order to colonize new locations (Safranyik et al. 1989; Robertson et al. 2007). Below-canopy dispersal is self-propelled and can be parameterized in vitro with computer-linked flight mill bioassays. Many models predict MPB dispersal at both landscape and stand levels based on spatio-temporal patterns (Robertson et al. 2007; Aukema et al. 2008; Chen and Walton 2011), climate (Aukema et al. 2008), host vigor (Lewis et al. 2009) and other environmental conditions (Safranyik et al. 1989; Robertson et al. 2007; Ainslie and Jackson 2011). Inclusion of flight mill data can improve model accuracy by providing detailed data on flight

behavior and patterns such as stopping frequency and length of uninterrupted flight times (Goodsman et al. 2016). Finding the relationships of MPB wing and body morphology to measured flight capacity should improve our ability to predict bark beetle dispersal in nature.

In insects, wing morphology (*e.g.*, shape and size) and flight muscle mass are often correlated with dispersal capability. Factors such as variance in aspect ratio (ratio of wing length to width) have been linked to greater dispersal in populations at higher latitudes (Azevedo et al. 1998; Hassall 2015). For example, small wing aspect ratio and large relative wing size can increase the flight capacity of *Drosophila* in cool climates (Azevedo et al. 1998; Frazier et al. 2008). In several insect species, such as milkweed bugs, neotropical butterflies and sand crickets, there are positive relationships between wingspan and flight frequency, duration and speed (Palmer and Dingle 1989; Dudley 1990; Fairbairn and Roff 1990). Along with wing size, thoracic muscle mass can influence flight capability in butterflies (Dempster et al. 1976; Chai and Srygley 1990). In bark beetles, body mass correlates with flight distance and duration (Williams and Robertson 2008; Evenden et al. 2014). In general, body mass has been a primary factor in body condition quantification (Elkin and Reid 2004; Elkin and Reid 2005). Body condition is considered to represent the intrinsic resources available for growth, survival and reproduction, and is consequently important for successful colonization (Boggs 1992).

Dispersal is necessary in MPB as adults must find a new host tree in order to reproduce (Safranyik and Carroll 2006), and females are pioneers in host colonization. Females initiate the attack once they arrive on a host and release aggregation pheromones to attract conspecifics (Blomquist et al. 2010), and bark beetle body condition determines the quality and quantity of their offspring (Kautz et al. 2016). Correlations among lipid content, attack success and reproduction

in bark beetles have been well documented (Elkin and Reid 2005; Reid and Purcell 2011; Manning and Reid 2013; Kautz et al. 2016); larger, heavier beetles have greater lipid content (Evenden et al. 2014), resulting in increased fecundity (Elkin and Reid 2005), and greater ability to resist host defences (Reid and Purcell 2011). Larger females therefore are potentially better pioneers through their capacity to facilitate range expansion.

As the condition of females is influential in colonizing novel regions, this study aims to identify and quantify the morphological factors associated with female MPB dispersal capacity. These morphological features of females could provide a way to characterize the flight potential of individuals and dispersal capacity of populations (Hill et al. 1999b; Hassall et al. 2009). Given that flight performance is often associated with phenotypic traits such as wing size and body condition, larger individuals with larger wings should have greater dispersal capacity.

2.3 Methods

2.3.1 Beetle data collection

All MPB used for this study were collected near Grande Prairie, Alberta, Canada (55.17 N, 118.80 W). The sample group was reared from bolts collected in October 2015. Four lodgepole pine trees infested by MPB were selected (3 from site 1 at 54.57 N, 119.42 W; and 1 from site 2 at 54.19 N, 118.68 W), and two 50-cm bolts were cut from each tree at 1m above ground level. All bolts were sealed with paraffin wax on the cut ends upon felling. These bolts, containing larval MPB, were stored at 4°C until use.

Bolts were removed from 4°C and placed in separate 136 L opaque plastic emergence chambers at 24±1°C in April 2016. Emerged beetles were collected daily. A total of 173 females were collected and flown; however, 49 beetles that flew less than 10 m, 44 of which did not fly at

all, were removed from this study in order to exclude individuals that had irregular flight behaviours that were unlikely to be related to observed morphological features. Overall, the experimental group consisted of 124 female beetles, including 53 collected from site 1 bolts and 71 from site 2 bolts. Individual beetles were separated by sex based on the incidence of beetle stridulation, which is considered to be ~98% accurate for identifying males (Rosenberger et al. 2016). This was performed at $24\pm 1^{\circ}\text{C}$. The beetles were then placed in 2 mL centrifuge tubes with a small piece of paper and stored at 4°C to reduce use of metabolic resources until the flight assay (Evenden et al. 2014), which was performed 3 to 5 days post emergence.

Flight distance, duration and frequency data was collected for female beetles using the methods for computer-linked flight mill bioassays of Evenden et al. (2014). Flight distance was calculated as the total distance flown over a flight period, flight duration was calculated as total time spent in-flight, and flight frequency was calculated as the number of times flight was initiated after a minimum 5 second period of non-flight. Females were weighed prior to flight (Mettler Toledo, XS105 accurate to 0.01mg), and body dimensions (total length and pronotum width) were measured using digital calipers (Pro.Point 1-150mm, accurate to 0.01mm; remeasuring of 10 randomly selected specimens verified 99.01% precision). Beetles were then attached to a 2 cm long tether of 0.32 mm-diameter aluminum wire using LePage® Heavy Duty Contact Cement. Tethers were carefully attached to the pronotum to ensure no interference of elytra and wing movement. Length of the flight bioassay was 22 hours. This duration was chosen to allow for processing of samples and switch over of specimens between flight cohorts. During the flight assay the flight mill chamber had a photoperiod of 16:8 (L:D) h and a temperature of 22.5°C . Flight assays began 2 hours after initiation of the light phase of the photoperiod, which allowed

time to process the previous flight group, and to prepare the next group of beetles for the 22-hour flight assay. Female beetles were flown in groups ranging from 8 to 20.

After flights were complete, beetles were weighed again and stored in 85% ethanol at -20°C. For morphological data collection, wings were removed and suspended in a 50% ethanol solution. Wings were unfolded using paintbrushes and positioned, then removed from the solution by sliding a small strip of card stock below the wing and gently lifting it, maintaining the unfolded wing shape. The wings were fixed to the card stock strip by applying a thin layer of diluted glue with a fine paintbrush. Dried wings were scanned and measured using ImageJ version 1.51j8 (Schneider et al. 2012).

Sixty-two MPB individuals were available for muscle dissection. The metathoracis medianus, lateralis posterior and lateralis medius flight muscles were identified for dissection based on Reid (1958) and Chapman (1998). After removal of the wings and elytra, the metathorax was opened by removing the dorsal tergites. Once the flight muscles were exposed, fibre length and lateral width of the metathoracis medianus were measured using an ocular micrometer in a dissection microscope under 50x magnification. The anterior edge of a medial segment of the metathoracis medianis was then detached from the metathoracic prephragma and its transverse thickness was measured. Subsequently, the transverse thickness and lateral width of the lateralis medius and the lateralis posterior were measured. The lateralis medius was then carefully separated from the metacoxa, extracted from the metathorax, placed flat and its length measured. Measurements of the volume of individual muscles were then summed into 2 groups: dorsal longitudinal flight muscle volume, which included the metathoracis medianus muscle group, and dorsal ventral flight muscle volume, which included measurements of the lateralis medius and the

lateralis posterior. Individual muscle measurements were each included in preliminary models but were not found to provide additional explanatory power individually. To simplify variables and interactions in the presented models, these measurements were consolidated by calculating the volume of an elliptical cylinder, representing the flight muscle volume, and this value was used for further analyses.

2.3.2 Statistical analysis

All statistical analyses were conducted in R version 3.3.2 (R Core Team 2017). Model R^2 values were obtained using the R package piecewiseSEM (Lefcheck 2015) which finds R^2 values for non-fixed effect linear models, based on Nakagawa and Schielzeth (2013) and Johnson (2014). Flight models were created and analysed using R packages nlme (Pinheiro et al. 2017) and lme4 (Bates et al. 2015).

ANOVA hypothesis testing was used to determine whether differences exist between the strongest and weakest fliers observed in this study. Samples were separated by quartiles based on flight distance in order to apply the ANOVA tests. The upper quartile beetles, with flight distances > 11.13 km (n=31), represented strong fliers. They were compared to the lower quartile beetles that represented weak fliers, with flight distances < 1.05 km, (n=31; this number excludes any beetles that flew less than 10 m). Muscle volume was also compared using ANOVA hypothesis tests on the top and bottom quartiles, but with smaller sample sizes since fewer beetles with dissected flight muscle were available. The top quartile group contained 16 beetles, with flight distances > 8.0 km, and the bottom quartile group contained 16 beetles, with flight distances < 3.5 km. Morphological features tested included body weight, body size (calculated as ellipsoid volume [$\frac{4}{3} * \pi * \text{body length} * \text{pronotum width}^2$]), preflight weight, postflight weight, density

$\left(\frac{\text{preflight weight}}{\text{body size}}\right)$, absolute weight lost, proportional weight lost, wing size (measured as two-dimensional surface area), and wing shape (calculated as aspect ratio: $\frac{\text{wing length}}{\text{wing width}}$).

A linear mixed effects model was produced using distance flown as the dependent variable. Each included emergence bolt and flight mill as random variables. Each full model included the independent variables: pre-flight weight, body size, wing size, age (days since emergence) and wing shape, as well as all two-way interactions. Stepwise model simplification was achieved by removal of the least significant variables (highest p-values) until only significant ($p < 0.05$) variables remained, and reduced models were compared to previous models and the full model using AIC and ANOVA hypothesis testing until the most parsimonious model was found. Following model refinement methods by Crawley (2013), interactions between variables were preferred for removal over basic variables in instances where both variables and interactions had a p-value greater than 0.05. All models were tested for significance using F-tests, and the included independent variables were tested with ANOVA. The residuals of each regression model were observed for random dispersal, and a variance inflation factor test was performed on each model before and after refinement using the R package *fmsb* (Nakazawa 2017)

We tested the significant regression variables of distance flown for heteroscedasticity using Breusch-Pagan tests. When heteroscedasticity was present, quantile regressions were used to regress the data at separate quantiles of the independent variable, using the R package *quantreg* (Koenker 2017). Because variables can only be tested independently in quantile regression, a third variable, wing loading ($\frac{\text{preflight weight}}{\text{wing area}}$), was introduced to combine the significant independent variables into a single term. Tests were conducted at the quantiles of 0.12 to 0.96 in increments of 0.12 in order to maximize resolution while retaining an adequate number of samples per

quantile. When heteroscedasticity was observed, ANOVA hypothesis testing was used to compare slopes to an average quantile slope.

2.4 Results

2.4.1 Morphology associations

Variability in the following data is reported as standard error. Female MPB flew an average distance of 7.4 ± 0.58 km over the 22-hour flight period, with a maximum flight distance of 28.81 km. On average, beetles flew for 3.70 ± 0.29 hours and initiated flight 176 ± 27.52 times; 81.8% of the total flight distance occurred during the light stage of the photoperiod. Strong fliers flew longer, and more frequently, than weak fliers ($F_{(1,60)}=402.230$, $P<0.0001$; and $F_{(1,60)}=7.433$, $P=0.0084$, respectively). Strong fliers flew an average of 7.60 ± 0.36 hours with an average frequency of 144.8 ± 29.65 flights, while weak fliers flew an average of 0.170 ± 0.03 hours with 55.5 ± 12.67 flights. Forty-four beetles did not fly at all, while 5 flew less than 10 m. Dispersal distance data was not normally distributed (Figure 2.1). A complete table to flight and morphology data can be seen in Appendix 2.1.

Long distance and short distance fliers were morphologically different (Figure 2.2). Beetles that flew longer distances had greater body weight, both preflight ($F_{(1,60)}=9.021$, $P=0.0039$) and postflight ($F_{(1,60)}=6.637$, $P=0.0125$), as well as greater body density ($F_{(1,60)}=15.741$, $P=0.0002$). Long distance fliers also lost more absolute weight ($F_{(1,60)}=10.990$, $P=0.0016$) and proportional weight ($F_{(1,60)}=5.467$, $P=0.0227$) during the flight bioassay. Long distance fliers tended to have larger wings, but this only bordered significance ($F_{(1,60)}=3.740$, $P=0.0578$; Figure 2.2). There was no significant difference between long and short distance fliers in wing shape ($F_{(1,60)}=1.453$, $P=0.2328$), body size ($F_{(1,60)}=1.332$, $P=0.2530$), or flight muscle volume ($F_{(1,30)}=0.1008$,

P=0.7530). Plots containing all 124 samples showing the relationship between total distance flown and preflight weight, postflight weight, wing area, body density, proportional weight lost, and absolute weight lost can be seen in Appendix 2.2. The age of beetles in this study (3-5 days) had no relationship with flight distance ($F_{(1,60)}=0.440$, $P=0.5095$).

2.4.2 Regression models

After model refinement, flight distance of MPB was significantly related to both wing size ($F_{(1,121)}=8.512$, $P=0.0042$) and preflight weight ($F_{(1,121)}=12.466$, $P=0.0006$). Heavier beetles with larger wings flew farther than lighter beetles with smaller wings. Wing data was essential in predicting flight performance; exclusion of wing size data resulted in a significant loss of explanatory power in the flight distance model ($F_{(121,122)}=8.512$, $P=0.0042$), as well as an increase in AIC (AIC 2516.0 to 2522.4). Ultimately, these linear mixed effects models explained only a limited amount of the flight performance in female MPB. The models predicted 19% of variation in flight distance ($R^2=0.1910$).

A variance inflation factor (VIF) of 10 or more indicates multicollinearity; VIF tests showed that there was no multicollinearity before or after model refinement (VIF=1.32 and VIF=1.17, respectively).

2.4.3 Heteroscedasticity and quantile regression

Breusch-Pagan tests showed potential heteroscedasticity in the relationship of distance flown to preflight weight ($BP_{(1)}=10.447$, $P=0.0012$) and wing area ($BP_{(1)}=4.028$, $P=0.0447$), which were more prevalent when both variables were tested simultaneously as wing loading ($BP_{(1)}=16.811$, $P<0.0001$).

Preflight weight and wing area were first tested with quantile regression separately (Figure 2.3). Distance flown had a significantly different response to preflight weight at the 96% quantile ($F_{(1,247)}=5.399$, $P=0.0210$), but showed no significant difference at the 12% quantile ($F_{(1,247)}=3.369$, $P=0.0676$). Preflight weight had a significantly stronger effect on flight distance when it was greater, with an increase of 1.63 km in flight distance per 1 mg increase in beetle weight, while it otherwise had an average increase of 0.67 km per 1 mg increase in preflight weight.

When both variables were combined into wing loading, the tests for heteroscedasticity revealed a general trend in which the dispersion of distance flown values increased with wing loading. Distance flown had a significantly different response from the average at both the 12% quantile ($F_{(1,247)}=12.132$, $P=0.0006$; Figure 2.4 and the 96% quantile ($F_{(1,247)}=4.495$, $P=0.0350$; Figure 2.4). At the 96% quantile, the predicted distance flown increases by 38.5 km per 1 mg/mm^2 increase wing loading, while at the 12% quantile this relationship was reduced to an increase of 1.6 km per 1 mg/mm^2 . Otherwise, the average increase was 19.3 km per 1 mg/mm^2 wing loading.

2.5 Discussion

2.5.1 Morphology associations with dispersal capacity

We found that heavier beetles with larger wings flew farther than lighter beetles with smaller wings. After simplification, linear mixed effects models showed that the primary variables explaining distance flown were wing size and preflight body weight. Increased dispersal capacity by heavier individuals has also been found in other studies (Hill et al. 1999a; Williams and Robertson 2008; Evenden et al. 2014). Although body weight was a significant predictor of dispersal in this study, body size was not related to flight distance. Reid and Purcell (2011) found no relationship between body size and fat content but demonstrated that relative body weight is

correlated with fat content. Other research has also shown the relationship between weight and lipid content (Williams and Robertson 2008; Evenden et al. 2014), implying that denser beetles have a greater store of flight fuel per unit of body size that allows them to fly further. This is also supported by our findings of increased density in long distance fliers.

An increase in stored lipids can also influence dispersal behaviour in bark beetles through behavioural responses to olfactory stimuli. Some newly emerged beetles will ignore both visual and chemical cues from susceptible hosts (Shepherd 1966; Safranyik et al. 1989; Eidson et al. 2017). In the Douglas-fir beetle, *Dendroctonus pseudotsugae*, beetles with higher fat content are less responsive to aggregation pheromones and spend more time selecting a host to colonize (Atkins 1966; Bennett and Borden 1971), thereby increasing dispersal; depletion of fat reserves through flight initiates a behavioural response in which the beetles are more responsive to olfactory cues. Fat content likely has a similar effect on dispersal in MPB, as well as impacting colonization success (Seybold et al. 2006; Reid and Purcell 2011) and reproduction (Manning and Reid 2013) after dispersal.

We have shown that long range dispersing beetles not only have higher preflight weight, but postflight weight as well, which can influence the success of pioneers. Successful colonization requires large amounts of stored fat to detoxify monoterpenes produced by the host tree (Reid and Purcell 2011), and to produce offspring (Elkin and Reid 2005; Manning and Reid 2013). Greater postflight weight provides a substantial advantage to MPB, since the heaviest individuals are most likely to disperse long distances and also have the greatest chance of succeeding in host colonization.

While weight is important in dispersal capacity of MPB (Evenden et al. 2014), the inclusion of wing morphology significantly increased the predictive power of the regression models tested in this study. Wing size is often important for flight performance in insects (Betts and Wootton 1988; Taylor and Merriam 1995; Hill 1999a), and larger wings increase lift and carrying capacity (Wootton 1992), allowing longer distance travel with a greater load of resources for dispersal and colonization, such as lipids. Large wings are also important for flight capacity in cold climates; cold temperatures can reduce flight muscle function and wing beat frequency, but larger wings allow for increased lift generation with lower input power (Azevedo et al. 1998; Frazier et al. 2008). Individuals with such an advantage could have contributed to the recent range expansion of MPB north into the Northwest Territories (NRCan 2017), and eastward across the Rocky Mountains, although this hypothesis remains to be tested.

The ability to predict range expansion can be challenged by difficulties in acquiring data for predicting dispersal phenotype; however, morphological data related to dispersal capacity can be obtained from specimens that are already available from population monitoring. Currently, 4-inch diameter disks are collected from infested trees in many mass attack regions, and larvae are observed under the bark to determine the reproductive success of a population (Alberta Agriculture and Forestry 2016). Quantification of the relationship between larval instars and adult size is needed, but, with some modification of sampling procedure, collected data, such as larval weight, could be incorporated into this data collection and subsequently used in dispersal models that distinguish between regional populations.

Although not investigated in this study, wing size may also affect above-canopy passive dispersal. Range expansion in MPB can also occur through long distance dispersal events in which

beetles are caught in updrafts and carried up to 300 km (Cerezke 1989; Jackson et al. 2008). Certain behaviours exhibited by MPB hint at adaptations to passive dispersal: 44 of the beetles that were tethered to flight mills did not actually fly, but many of these displayed a “drifting” behaviour in which they would open the elytra and spread their wings fully, without flapping. Similar behaviors have been documented by Atkins (1959) when testing flight preparation and response in the Douglas-fir beetle, *D. pseudotsugae*. They found that some beetles fully extended their wings, but did not vibrate them, when tossed in the air. We suggest that such behaviour, when caught in an updraft, could maximize the exposed wing area while minimizing energy consumption. Associations between stationary wing size and passive dispersal distance occur in winged seeds of plants, (Augspurger 1986) and this relationship could be similar in insects dispersed by the wind.

2.5.2 Heteroscedasticity in flight distance and future directions

Many factors can affect flight performance, and although the morphological variation observed in our study follows a normal distribution, the distribution of flight capacities follow a well-known non-normal pattern of dispersal, the dispersal kernel (Figure 2.1; Bateman 1950; Chapman et al. 2006). We found that many individuals fly only short distances on the flight mill while very few fly long distances. There are population-wide advantages to this distribution of dispersal behaviours, as it gives the greatest survivorship in the largest portion of the population while still allowing some risk for colonization. Beetles that fly short distances use less lipid (Williams and Robertson 2008; Evenden et al. 2014) and tend to be more successful in colonizing host trees than similarly sized beetles that burn more of their lipid reserves to disperse (Reid and Purcell 2011; Manning and Reid 2013; Kautz et al. 2016). In our study, we found that body weight and wing size were associated with flight distance and, consequently, a population of larger

individuals with larger wings is likely to have a greater proportion of long distance dispersers; however, the strong positive skew in the dispersal kernel of MPB causes inconsistencies with predictions based on linear relationships with morphology.

Even with both wing and body morphology included, the power of these models to predict flight distance remains relatively low. Part of the weakness in the relationship of morphology with flight distance is due to heteroscedasticity in the coefficients of the variables. Quantile regression shows that preflight weight and wing area, when considered separately, do not show a clear relationship with flight distance (Figure 2.3); however, when combined as wing loading, the heteroscedastic nature of the relationship becomes evident (Figure 2.4). When wing loading is low, morphology has little power to predict dispersal, but the relationship at high wing loading values has a significantly higher slope, indicating that small increases can have a significant positive impact on dispersal capacity (Figure 2.4). This inconsistent relationship is caused by an increase in the dispersion of flight distance at different quantiles of wing loading and is likely due to the large cohort of ‘lazy’ individuals that fly only short distances regardless of high wing loading (Figure 2.4). These ‘lazy’ beetles increase the disparity between individuals with low and high wing loading within each quantile, which subsequently increases the quantile slope coefficient. This creates difficulties in predicting the relationship between morphology and flight capacity and indicates that there is more than morphology associated with dispersal capacity. The natural tendency to disperse is an important contributor to flight distance in other insects (Steyn et al. 2016), and further research should focus on identifying factors that contribute to variation in dispersal behaviour, such as the ‘lazy’ dispersal phenotype seen in our study.

Other factors involved in dispersal capacity in the natural environment that could not be tested in this lab study include abiotic conditions such as temperature (Atkins 1959; Aukema et al. 2008), wind (Safranyik et al. 1989; Ainslie and Jackson 2011), and humidity (Safranyik and Carroll 2006). Biotic factors that can influence dispersal include host presence, density and distance from the beetle (Atkins 1966; Robertson et al. 2007), wing flexibility (Mountcastle and Combes 2013), joint resilin content (Haas et al. 2000), as well as parasitic infections (Everleigh et al. 2007). Some of the variation in the relationship between beetle morphology and flight performance may be mediated by behaviour. Atkins (1966) has shown that different female dispersal behavioural types exist within Douglas-fir beetle populations, but the behaviours exhibited by these types did not appear to have a strong correlation with body weight. Our results similarly reveal that some ‘lazy’ individuals do not fly to their capacity as indicated by wing size and body weight. Although morphological characteristics demonstrably have an impact on flight capacity in MPB, other factors that govern dispersal-related behaviour, such as gene expression, should also be investigated.

2.6 Conclusions

Body weight and wing size contribute to dispersal capacity in mountain pine beetle, and such data can potentially be useful in improving dispersal model quality (Goodsman et al. 2016). Although many other factors must also be considered in the parameterization of dispersal models, we have shown that large female beetles with large wings generally have increased dispersal capacity, flying farther than smaller beetles with smaller wings; autonomous populations in dispersal models can be assigned flight capacities based on morphology observed *in situ* through use of samples already being collected for monitoring purposes.

As large females are better colonizers (Seybold et al. 2006; Reid and Purcell 2011; Manning and Reid 2013), our study expands understanding of the mechanisms by which MPB establish new populations and increase their range; however, due to the heteroscedasticity of the data, morphological variation alone provides limited power to predict flight capacity; many individuals fly short distances despite having the morphology of long distance dispersers. This suggests that, even in a controlled laboratory setting, other intrinsic factors also influence flight and dispersal behaviour. Further research should target these intrinsic influences so that we can better understand the elements governing dispersal-related behaviours of MPB and other economically significant insect species.

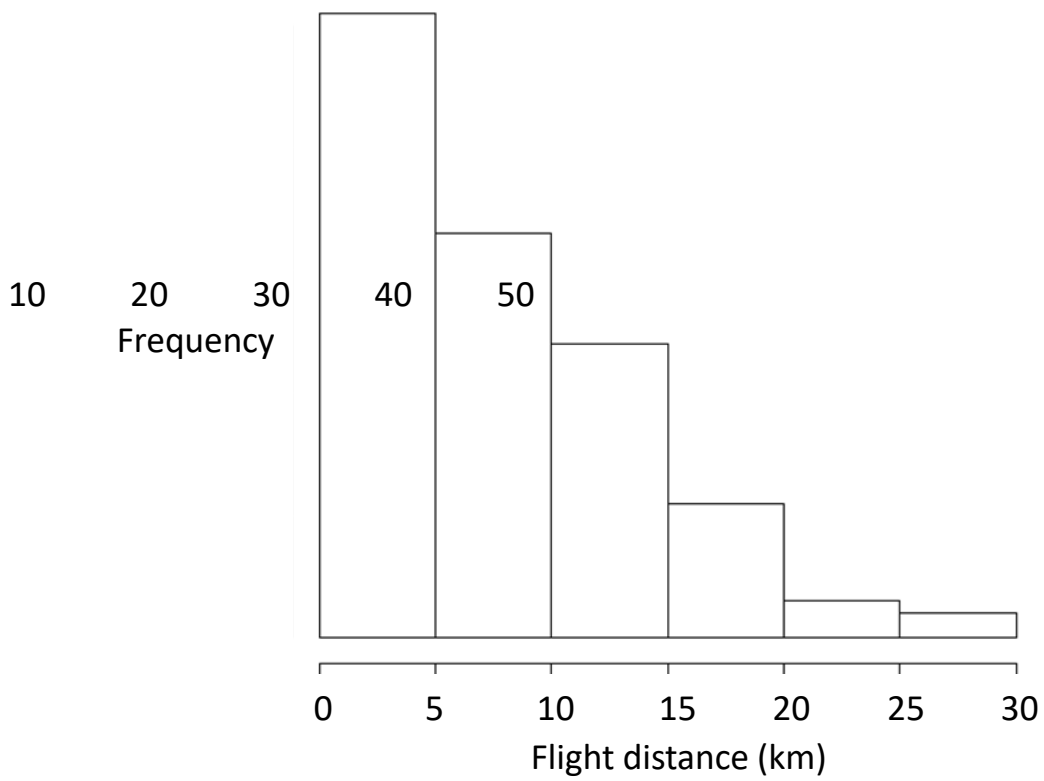


Figure 2.1. The positive skew in the distribution of flight distances for 124 female mountain pine beetles. Beetles that flew less than 10 m were excluded from this study; the minimum flight distance is 0.01 km.

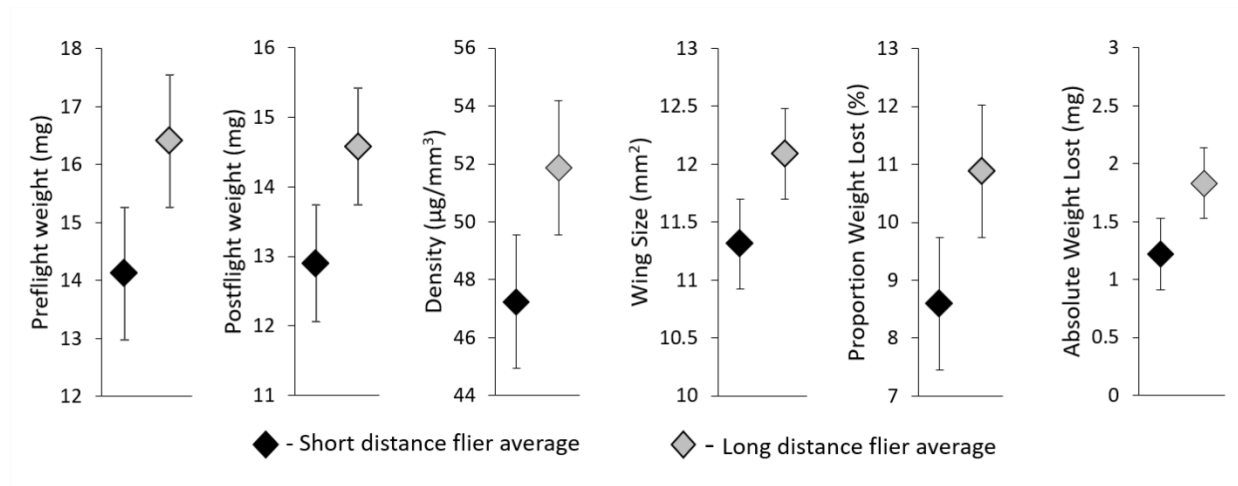


Figure 2.2. Morphological differences between 31 longest distance (> 11.13 km) and 31 shortest distance (< 1.05 km) dispersing female mountain pine beetles. Long distance dispersers have greater preflight and post flight weight, wing size, proportional and absolute weight loss. Points represent group averages and bars show standard error. Comparisons were done using ANOVA. All graphs depict significant results.

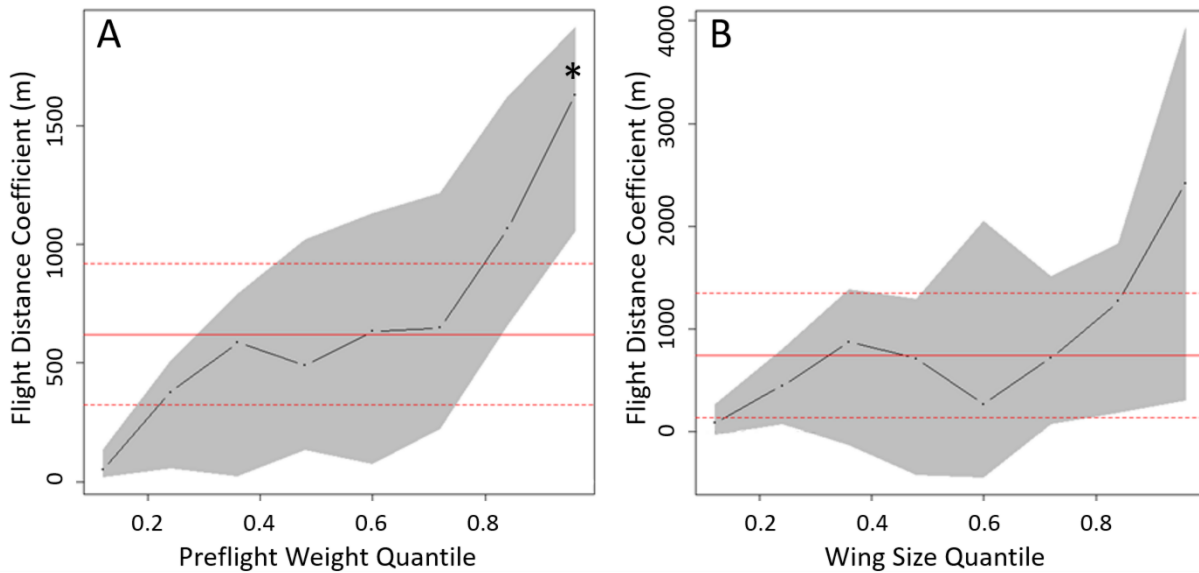


Figure 2.3. Quantile regressions showing the relationships of (A) preflight weight and (B) wing size with flight distance at 12% quantiles of 124 female mountain pine beetles. The solid horizontal line is the average relationship between flight distance and wing loading (dashed line is standard error). Grey shaded area represents the 90 percent confidence band for the quantile estimates. Preflight weight shows a significant deviation from the average relationship at the 96% quantile, showing that higher preflight weight has an increasing effect on flight distance. Although other potential sources of heteroscedasticity may exist, no other significant differences in slope coefficients were found. The asterisk in (A) indicates a significantly different quantile from the average.

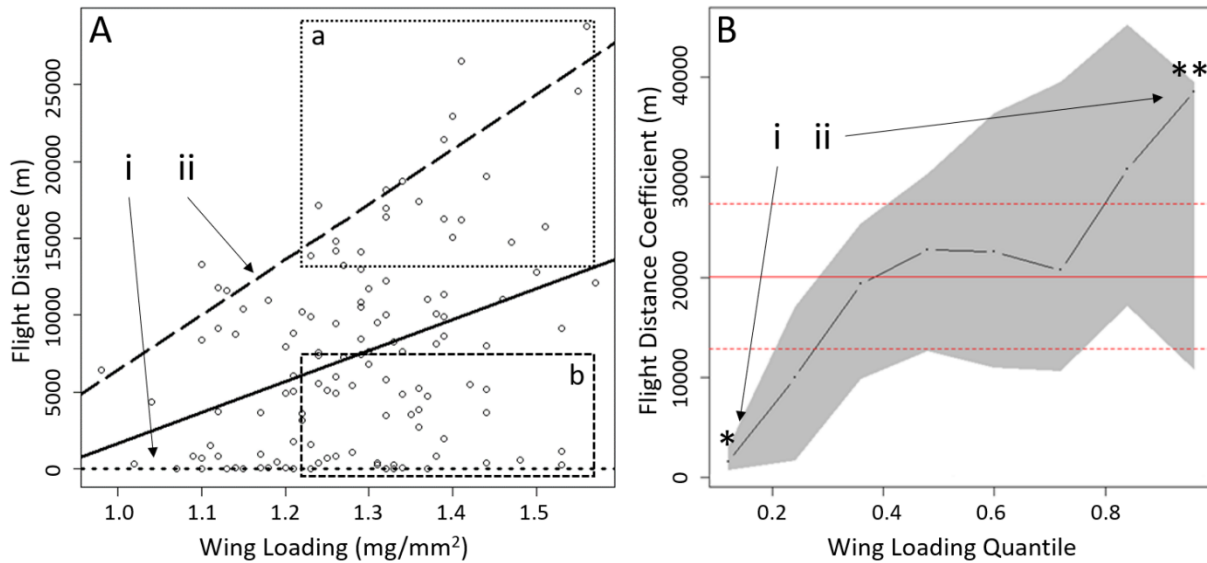


Figure 2.4. (A) Wing loading vs flight distance of 124 mountain pine beetles, with regression lines of the lowest 12% of dispersers (i) shown as a dotted trendline, and the highest 12% of dispersers (ii) shown as a dashed trendline. (B) Regression at each 12% quantile shows a significant change in the relationship, resulting in heteroscedasticity. The solid horizontal line is the average relationship between flight distance and wing loading (dashed line is standard error). Grey shaded area represents the 90 percent confidence band for the quantile estimates. At lower quantiles of wing loading (i) the relationship approaches 0; at higher quantiles (ii) the relationship becomes more pronounced. All strong fliers show high wing loading ((A), box 'a'), but many "lazy" individuals have high wing loading and do not fly long distances ((A), box 'b'), causing heteroscedasticity in the relationship. Asterisks in (B) indicate quantiles with significantly different coefficients from the average.

2.7 Literature cited

- Ainslie B, Jackson PL. 2011. Investigation into mountain pine beetles above canopy dispersion using weather radar and an atmospheric dispersion model. *Aerobiologia*, **27**: 51-65.
- Alberta Agriculture and Forestry. 2016. Mountain pine beetle detection and management in Alberta (Blue Book). Government of Alberta. Available at:
<[https://www1.agric.gov.ab.ca/\\$department/deptdocs.nsf/all/formain15619/\\$FILE/MPB%20Blue%20Book%20-%20Complete%20Guide%202016.pdf](https://www1.agric.gov.ab.ca/$department/deptdocs.nsf/all/formain15619/$FILE/MPB%20Blue%20Book%20-%20Complete%20Guide%202016.pdf)> [Accessed 17 April 2018]
- Atkins MD. 1959. A study of the flight of the Douglas-fir beetle, *Dendroctonus pseudotsugae* Hopk. (Coleoptera: Scolytidae). I. Flight preparation and response. *The Canadian Entomologist* **91**: 283-291.
- Atkins MD. 1961. A study of the flight of the Douglas-fir beetle *Dendroctonus pseudotsugae* Hopk. (Coleoptera: Scolytidae). III. Flight Capacity. *The Canadian Entomologist*, **93**: 467-474.
- Atkins MD. 1966. Laboratory Studies on the Behaviour of the Douglas-fir Beetle, *Dendroctonus pseudotsugae* Hopkins. *Canadian Entomologist*, **98**: 953-991.
- Augspurger, CK. 1986. Morphology and Dispersal Potential of Wind-Dispersed Diaspores of Neotropical Trees. *American Journal of Botany*, **73**: 353-363.

- Aukema BH, Carroll AL, Zheng Y, Zhu J, Raffa KF, Moore RD, Stahl K, Taylor SW. 2008. Movement of outbreak populations of mountain pine beetle: influences of spatiotemporal patterns of climate. *Ecography*, **31**: 348-358.
- Azevedo RBR, James AC, McCabe J, Partridge L. 1998. Latitudinal variation of wing: thorax size ratio and wing-aspect ratio in *Drosophila melanogaster*. *Evolution*, **52**: 1353-1362.
- Bateman AJ. 1950. Is gene dispersion normal? *Heredity*, **4**: 353–363.
- Bates D, Maechler M, Bolker B, Walker S. 2015. Fitting Linear Mixed Effects Models Using lme4. *Journal of Statistical Software*, **67**: 1-48.
- Bennett RB, Borden JH. 1971. Flight Arrestment of Tethered *Dendroctonus pseudotsugae* and *Trypodendron lineatum* (Coleoptera: Scolytidae) in Response to Olfactory Stimuli. *Annals of the Entomological Society of America*, **64**: 1273-1286.
- Betts CR, Wootton RJ. 1988. Wing shape and flight behaviour in butterflies (Lepidoptera: Papilionoidea and Hesperioidea): A preliminary analysis. *Journal of Experimental Biology*, **138**: 271-288.
- Blomquist GJ, Figueroa-Teran R, Aw M, Song M, Gorzalski A, Abbott NL, Chang E, Tittiger C. 2010. Pheromone production in bark beetles. *Insect Biochemistry and Molecular Biology*, **40**: 699-712.
- Boggs CL. 1992. Resource Allocation: exploring connections between foraging and life history. *Functional Ecology*, **6**: 508-518.

- Carroll AL, Taylor SW, Régnière J, Safranyik L. 2004. Effects of climate and climate change on the mountain pine beetle (pp 221-230) in Shore TL, Brooks JE, Stone JE (eds) *Challenges and Solutions: Proceedings of the Mountain Pine Beetle Symposium*. Kelowna, British Columbia, Canada October 30 - 31, 2003. Canadian Forest Services.
- Cerezke HF. 1989. Mountain pine beetle aggregation semiochemical use in Alberta and Saskatchewan, 1983-1987. In Amman GD. (Compiler). *Proceedings-Symposium on the management of lodgepole pine to minimize losses to the mountain pine beetle, July 12-14, 1988, Kalispell, Montana* (pp 108-113). Ogden, Utah: USDA Forest Service, Intermountain Research Station.
- Chai P, Srygley RB. 1990. Predation and the flight, morphology, and temperature of neotropical rain-forest butterflies. *American Naturalist*. **135**: 748-765.
- Chapman DS, Dytham C, Oxford GS. 2006. Modelling population redistribution in a leaf beetle: an evaluation of alternative dispersal functions. *Journal of Animal Ecology*, **76**: 36-44.
- Chapman RF. 1998. *The Insects: Structure and function* (4th ed.). Cambridge: Cambridge University Press.
- Chen H, Walton A. 2011. Mountain pine beetle dispersal: spatiotemporal patterns and role in the spread and expansion of the present outbreak. *Ecosphere*, **2**: 1-17.
- Corbett LJ, Withey P, Lantz VA, Ochuodho TO. 2015. The economic impact of the mountain pine beetle infestation in British Columbia: provincial estimates from a CGE analysis. *Forestry*, **89**: 100-105.

Crawley MJ. 2013. Regression (Chapter 10). In *The R book* (2nd ed) (pp 449-497). West Sussex, United Kingdom: John Wiley & Sons, Ltd.

de la Giroday HC, Carroll AL, Aukema BH. 2012. Breach of the northern Rocky Mountain geoclimatic barrier: initiation of range expansion by the mountain pine beetle. *Biogeography*, **39**: 1112-1123.

Dempster JP, King ML, Lakhani KH. 1976. The status of the swallowtail butterfly in Britain. *Ecological Entomology*, **1**: 71-84.

Dudley R. 1990. Biomechanics of flight in neotropical butterflies: morphometrics and kinematics. *Journal of Experimental biology*, **150**: 37-53.

Eidson EL, Mock KE, Bentz BJ. 2017. Mountain pine beetle host selection behavior confirms high resistance in Great Basin bristlecone pine. *Forest Ecology and Management*, **402**: 12-20.

Elkin CM, Reid ML. 2004. Attack and reproductive success of mountain pine beetles (Coleoptera: Scolytidae) in fire-damaged lodgepole pines. *Environmental Entomology*, **33**: 1070-1080.

Elkin CM, Reid ML. 2005. Low energy reserves and energy allocation decisions affect reproduction by mountain pine beetles, *Dendroctonus ponderosae*. *Functional Ecology*, **19**: 102-109.

- Eveleigh ES, Lucarotti CJ, McCarthy PC, Morin B, Royama T, Thomas AW. 2007. Occurrence and effects of *Nosema fumiferanae* infections on adult spruce budworm caught above and within the forest canopy. *Agriculture and Forest Entomology*, **9**: 247-258.
- Evenden ML, Whitehouse CM, Sykes J. 2014. Factors influencing flight capacity of the mountain pine beetle (Coleoptera: Curculionidae: Scolytinae). *Environmental Entomology*, **43**: 187-196.
- Fairbairn DJ, Roff DA. 1990. Genetic correlations among traits determining migratory tendency in sand cricket *Gryllus firmus*. *Evolution*, **44**: 1787-1795.
- Frazier MR, Harrison JF, Kirkton SD, Roberts SP. 2008. Cold rearing improves cold-flight performance in *Drosophila* via changes in wing morphology. *The Journal of Experimental Biology*, **211**: 2116-2122.
- Goodsman DW, Koch D, Whitehouse C, Evenden ML, Cooke BJ, Lewis MA. 2016. Aggregation and a strong Allee effect in a cooperative outbreak insect. *Ecological Applications*, **26**: 2623-2636.
- Haas F, Gorb S, Blickhan R. 2000. The function of resilin in beetle wings. *Proceedings of the Royal Society of London B*, **267**: 1375-1381.
- Hassall C. 2015. Strong geographical variation in wing aspect ratio of a damselfly, *Calopteryx maculate* (Odonata: Zygoptera). *PeerJ*, **3**: e1219.

- Hassall C, Thompson DJ, Harvey IF. 2009. Variation in morphology between core and marginal populations of three British damselflies. *International Journal of Freshwater Entomology*, **31**: 187-197.
- Hill JK, Thomas CD, Blakeley DS. 1999a. Evolution of flight morphology in a butterfly that has recently expanded its geographic range. *Oecologia*, **121**: 165-170.
- Hill JK, Thomas CD, Lewis OT. 1999b. Flight morphology in fragmented populations of a rare British butterfly, *Hesperia comma*. *Biological Conservation*, **87**: 277-283.
- Jackson PL, Straussfogel D, Lindgren BS, Mitchell S, Murphy B. 2008. Radar observation and aerial capture of mountain pine beetle, *Dendroctonus ponderosae* Hopk. (Coleoptera: Scolytidae) above the forest canopy. *Canadian Journal of Forest Research*, **38**: 2313-2327.
- Johnson PCD. 2014. Extension of Nakagawa Schielzeth's R^2_{GLMM} to random slopes models. *Methods in Ecology and Evolution*, **5**: 944-946.
- Kautz M, Imron MA, Dworschak K, Schopf R. 2016. Dispersal variability and associated population-level consequences in tree-killing bark beetles. *Movement Ecology*, **4**: 9.
- Koenker R. 2017. Quantreg: Quantile Regression. R package version 5.29. URL <https://CRAN.R-project.org/package=quantreg>
- Kurz WA, Dymond CC, Stinson G, Rampley GJ, Neilson ET, Carroll AL, Ebata T, Safranyik L. 2008. Mountain pine beetle and forest carbon feedback to climate change. *Nature*, **452**: 987-990.

- Lefcheck JS. 2015 piecewiseSEM: Piecewise structural equation modeling in R for ecology, evolution, and systematics. *Methods in Ecology and Evolution*, **7**: 573-579.
- Lewis MA, Nelson W, Xu C. 2009. A structured threshold model for mountain pine beetle outbreak. *Bulletin of Mathematical Biology*, **72**: 565-589.
- Manning CG, Reid ML. 2013. Sub-lethal effects of monoterpenes on reproduction by mountain pine beetles. *Agriculture and Forest Entomology*, **15**: 262-271
- Mountcastle AM, Combes SA. 2013. Wing flexibility enhances load-lifting capacity in bumblebees. *Proceedings of the Royal Society B*, **280**: 23536604.
- Nakagawa S, Schielzeth H. 2013. A general and simple method for obtaining R^2 from generalized linear mixed-effects models. *Methods in Ecology and Evolution*, **4**: 133-142.
- Nakazawa M. 2017. fmsb: Functions for Medical Statistics Book with some Demographic Data. R package version 0.6.1. URL <https://cran.r-project.org/web/packages/fmsb/index.html>
- NRCan (Natural Resources Canada). 2017 [accessed February 21]. Mountain pine beetle (factsheet). Retrieved from <http://www.nrcan.gc.ca/forests/fire-insects-disturbances/top-insects/13397>
- Olivieri I, Gouyon P-H. 1997. Evolution of migration rate and other traits: the metapopulation effect (pp 293–323) In Hanski IA, Gilpin ME. (eds), *Metapopulation biology: ecology, genetics, and evolution*. San Diego, California: Academic Press.

- Palmer JO, Dingle H. 1989. Responses of selection on flight behaviour in a migratory population of milkweed bugs (*Oncopeltus fasciatus*). *Evolution*, **43**: 1805-1808.
- Pinheiro J, Bates D, DebRoy S, Sarkar D, R Core Team. 2017. nlme: Linear and Nonlinear Mixed Effects Models. R package version 3.1-131. URL: <https://CRAN.R-project.org/package=nlme>
- R Core Team. 2017. R: A language and environment for statistical computing. R Foundation for Statistical Computing, Vienna, Austria. URL <https://www.R-project.org/>.
- Reid ML, Purcell JRC. 2011. Condition-dependent tolerance of monoterpenes in an insect herbivore. *Arthropod-Plant Interactions*, **5**: 331-337.
- Reid RW. 1958. Internal changes in female mountain pine beetle *Dendroctonus monticolae* Hopk., Associated with Egg Laying and Flight. *The Canadian Entomologist*, **90**: 464-468.
- Robertson C, Nelson TA, Boots B. 2007. Mountain pine beetle dispersal: the spatial-temporal interaction of infestations. *Forest Science*, **53**: 395-405.
- Rosenberger DW, Venette RC, Aukema BH. 2016. Sexing live mountain pine beetles *Dendroctonus ponderosae*: refinement of a behavioral method for *Dendroctonus* spp.. *Entomologia Experimentalis et Applicata*, **160**: 195-199.
- Safranyik L, Carroll AL. 2006. The biology and epidemiology of the mountain pine beetle in lodgepole pine forests (Chapter 1). In Safranyik, L. Wilson, W.R. (Eds.), *The mountain pine beetle: a synthesis of biology, management, and impacts on lodgepole pine* (pp. 3-

- 66). Victoria, British Columbia: Natural Resources Canada, Canadian Forest Service, Pacific Forestry Centre.
- Safranyik L, Carroll AL, Régnière J, Langor DW, Riel WG, Shore TL, Peter B, Cooke BJ, Nealis VG, Taylor SW. 2010. Potential for range expansion of mountain pine beetle into the boreal forest of North America. *The Canadian Entomologist*, **142**: 415-442.
- Safranyik L, Silversides R, McMullen LH, Linton DA. 1989. An empirical approach to modeling the local dispersal of the mountain pine beetle (*Dendroctonus ponderosae* Hopk.) (Col., Scolytidae) in relation to sources of attraction, wind direction and speed. *Journal of Applied Entomology*, **108**: 498-511.
- Schneider CA, Rasband WS, Eliceiri KW. 2012. NIH Image to ImageJ: 25 years of image analysis. *Nature Methods*, **9**: 671-675.
- Seybold SJ, Huber DPW, Lee JC, Graves AD, Bohlmann J. 2006. Pine monoterpenes and pine bark beetles: a marriage of convenience for defense and chemical communication. *Phytochemistry Reviews*, **5**: 143-178.
- Shepherd RF. 1966. Factors influencing the orientation and rates of activity of *Dendroctonus ponderosae* Hopkins (Coleoptera: Scolytidae). *The Canadian Entomologist*, **98**: 507-518.
- Steyn VM, Mitchell KA, Terblanche JS. 2016. Dispersal propensity, but not flight performance, explains variation in dispersal ability. *Proceedings of the Royal Society B*, **283**: 20160905.

- Taylor S, Carroll AL. 2004. Disturbance, forest age, and mountain pine beetle outbreak dynamics in BC: A historical perspective (pp 41-51). In Shore, T.L., Brooks, J.E. Stone, J.E. (eds). *Mountain Pine Beetle Symposium: Challenges and Solutions*. Kelowna, British Columbia: Natural Resources Canada, Canadian Forest Service, Pacific Forestry Centre, Information Report BC-X-399, Victoria, BC. 298 p.
- Taylor PD, Merriam G. 1995. Wing morphology of a forest damselfly is related to landscape structure. *Oikos*, **73**: 43-48.
- Williams WI, Robertson IC. 2008. Using automated flight mills to manipulate fat reserves in Douglas-fir beetles (Coleoptera: Curculionidae). *Environmental Entomology*, **37**: 850-856.
- Wootton RJ. 1992. Functional morphology of insect wings. *Annual Review of Entomology*, **37**: 113-140.

Chapter 3

Identification of genes and gene expression associated with dispersal capacity in the mountain pine beetle, *Dendroctonus ponderosae* Hopkins (Coleoptera: Curculionidae)

3.1 Summary

Range expansion of the mountain pine beetle has caused significant damage in pine stands of Western Canada, but their dispersal flights are poorly understood. We examined the genetic basis of mountain pine beetle dispersal capacity, measured with flight mills, using RNA-seq and a targeted association study. There were no differentially expressed genes between non-fliers and weak flying beetles, but nearly 3000 differentially expressed genes between strong and weak fliers. These genes related to lipid metabolism, muscle maintenance, oxidative stress response, detoxification, hormones, and behavior, among others. We also found 4 genetic variant sites associated with flight capacity, although no specific link to flight is currently known for these genes. Our research shows that several systems are important for sustained flight, while others are downregulated to conserve energy before colonization. The candidate genes and SNPs identified here will inform further studies and contribute to our understanding of the mechanisms of insect dispersal flights.

3.2 Introduction

Insect dispersal flights are not well understood, largely because they are affected by many biotic and abiotic factors (Stinner et al. 1983; Bowler and Benton 2005; Jones et al. 2019). Intrinsicly, there are physiological, morphological, and behavioral adaptations that determine insect flight capabilities (Roff and Fairbairn 2007; Jones et al. 2019), and these can be influenced

by large suites of genes (Jones et al. 2015). Understanding the genetic mechanisms of flight can provide valuable insight into the dispersal and spread of economically important insect species (Kristensen et al. 2013).

Mountain pine beetles (*D. ponderosae*) contribute to the maintenance of healthy pine forests under endemic conditions (Safranyik and Carroll 2006), but periodic outbreaks can cause significant damage (Hart et al. 2015). The most recent outbreak in western Canada expanded the range of the mountain pine beetle to a novel host tree with a distribution that extends toward economically important forests in eastern Canada and USA.

Morphology plays a significant role in predicting flight capacity of *D. ponderosae* (Shegelski et al. 2019); however, many beetles with strong flight-related morphology fly very little, indicating a large amount of unexplained variation in flight performance. Genetic factors constitute a plausible component of this variation. Genes have been identified relating to several life phases of mountain pine beetle, including pheromone biosynthesis (Keeling et al. 2013a; Nadeau et al. 2017), detoxification of host defenses, reproduction (Robert et al. 2013; Huber and Robert 2016), and overwintering cold tolerance (Robert et al. 2016; Fraser et al. 2017). However, the dispersal phase remains relatively unexplored.

In this study we aim to identify the genetic correlates of dispersal capacity in *D. ponderosae*. Dispersal-related genes in other insects have been linked to regulation of metabolic rate (Wheat et al. 2010; Jones et al. 2015; Zhou et al. 2020), muscle tracheation (Marden et al. 2012), generally improved flight capability (Niitepold et al. 2009; Wheat et al. 2010), and increased dispersal behavior (Zhou et al. 2020). We expect to find suites of genes associated with several flight and dispersal-related functions such as metabolism, muscle form and function,

oxidative stress and detoxification, hormonal control, and behavior. To achieve this, we combine a computer-linked flight mill bioassay with differential gene expression analysis using RNA-Seq and a targeted association study. The identification of flight-related genes is intended to allow a better understanding of the mechanisms associated with flight and dispersal in insects.

3.3 Methods

A flowchart of the methods used for this study constitutes Figure 3.1.

3.3.1 Sample collection and preparation

Four lodgepole pine trees infested with mountain pine beetles were selected from sites near Grande Prairie, Alberta, Canada (3 from site 1 at 54.57 N, 119.42 W; and 1 from site 2 at 54.19 N, 118.68 W) in October 2015. Two 50-cm bolts were cut from each tree at 1m above ground level. The cut ends of the bolts were sealed with paraffin wax upon felling, and bolts were stored at 4°C for 6 months until use.

For beetle emergence, bolts were placed in separate 136 L opaque plastic emergence chambers at 24±1°C in April 2016, and emerged beetles were collected daily. Individual beetles were separated by sex based on the incidence of beetle stridulation, according to methods by Rosenberger et al. (2016), which was performed at 24±1°C. In order to reduce the use of metabolic resources before the flight assay, individual beetles were stored at 4°C in 2 mL centrifuge tubes with a small piece of paper until the flight bioassay (Evenden et al. 2014), which was performed 3 to 5 days post emergence.

3.3.2 Flight mill bioassay and sample selection

Prior to flight bioassay, female beetles were weighed and measured at $24 \pm 1^\circ\text{C}$ for separate morphological analysis (published under Shegelski et al. 2019). Beetles were then attached to individual 2-cm long aluminum wire tethers with a diameter of 0.32mm. LePage® Heavy Duty Contact Cement was used to adhere the tether to the pronotum of the specimen. Care was taken so tethering would not interfere with wing or elytra movement.

Data was recorded on flight distance, duration (time spent in flight), and propensity (the number of times flight was initiated after a minimum 5 second period of no flight), using methods for computer-linked flight mill bioassays described by Evenden et al. (2014). The flight bioassays were 22 hours long, which allowed a 2-hour period for specimen processing and turn-over. Conditions in the flight chamber involved a light:dark photoperiod of 16:8, and temperature was kept at 22.5°C . Flights began 2 hours after the initiation of the photoperiod's light phase, giving specimens a total of 14 hours of flight time in light, and 8 in dark.

Samples for RNA-seq were selected based on total distance flown during the 22 hr assay. All beetles that flew $<1\text{km}$ and $> 10 \text{ km}$ were flash frozen in liquid nitrogen and stored at -80°C . From these beetles, the 8 beetles with the highest and lowest total distances flown were used to represent the strongest and the weakest fliers, and four Beetles that did not fly, but demonstrated a full range of motion in the elytra and wings, were also selected to represent non-fliers. All other flown beetles were stored at -20°C in 85% EtOH until DNA extraction.

3.3.3 RNA extractions, RNA-Seq library preparation & sequencing

Total RNA extractions used direct-zol RNA MiniPrep kits, with a DNase I treatment and TRIzol as a medium for specimen homogenization. RNA was checked for quality using an Agilent 2100 Bioanalyzer system and quantified using Qubit. cDNA synthesis and RNA-seq library preparation used a TruSeq Stranded RNA LT Kit following recommended protocol, which included poly-A selection for mRNA purification. Prior to sequencing, quality and quantity of cDNA was checked again using an Agilent 2100 Bioanalyzer. Library sequencing was performed on an Illumina NextSeq 500 platform at the Molecular Biology Service Unit (MBSU) at the University of Alberta. Sample groups were evenly split between two NextSeq 500 runs for optimal number of reads.

3.3.5 Enrichment analysis & KEGG pathway analysis

In order to find trends in gene ontology (GO) annotations and Kyoto Encyclopedia of Genes and Genomes (KEGG; Kanehisa and Goto 2000) pathways for the differentially expressed gene transcripts we used Blast2GO version 5.2.5 (Götz et al. 2008). The nucleotide sequences of the transcripts were blasted against the NCBI nr database using blastx, scanned with interpro, and were then mapped and annotated with GO terms. Interpro and GO annotations were then merged to validate GO annotations, and an enrichment analysis using Fisher's exact test ($FDR < 0.05$) was used to test upregulated and downregulated genes separately for significant overrepresentation of GO terms between the strong and weak flight phenotypes. Also using Blast2GO, a KEGG pathway analysis was performed on all differentially expressed transcripts to identify flight-related pathways.

3.3.6 DNA extractions, sequencing & mapping for association study

DNA extractions used a Qiagen DNEasy Blood & Tissue kit, following standard protocol with an optional RNase A treatment. Library preparation involved the ddRAD protocol of Peterson et al. (2012). Single-end sequencing was performed at the University of Alberta MBSU using the Illumina NextSeq500 platform. Initial data processing and quality checking of the raw sequence data followed protocols by Campbell et al. (2017).

A common weakness of association studies is the large number of comparisons (Visscher et al. 2017); to increase statistical power, we reduced the number of tested loci by focusing on candidate regions identified through our RNA-seq experiment. Alignment for the association study used a subset of scaffolds from the mountain pine beetle genome (Keeling et al. 2013b) that contained 1 or more flight-related genes. This alignment used the BWT-SW algorithm in BWA version 0.7.17 (Li and Durbin 2009), and alignment quality was checked using SAMtools version 1.9 (Li et al. 2009).

Stacks 2.0 `ref_map.pl` (Rochette et al. 2019) was used to identify single nucleotide polymorphism (SNP) sites. We allowed a minor allele frequency of 1%, and loci were initially retained if present in at least 80% of the specimens (Paris et al. 2017). Further filtering used `vcftools` version 0.1.14 (Danecek et al. 2011), with reads with a genotype quality score below 30, and SNP sites with more than 2% missing data among individuals being excluded from the final data set.

3.3.7 Targeted association study

We used TASSEL version 5.2.54 (Bradbury et al. 2007) to perform an association study in which we tested SNP sites for associations with total flight distance and flight propensity. The study included 59 female beetles (31 strong and 28 weak fliers) that were randomly selected from the upper and lower quartiles based on total flight distance. We used a principal component analysis (PCA) to account for population structure and stratification, and a generalized linear model (GLM) with permutation test (1000 permutations) to account for non-normal distributions in the phenotypic data and FDR (Che et al. 2014). The permuted p-value (perm p) was used to determine significance at $\alpha=0.05$.

3.4 Results

3.4.1 Flight mill bioassay

Excluding non-fliers, beetles used for the differential expression analysis flew an average of 10.08 km, ranging 0.04-28.81 km, and initiated flight an average of 72.8 times, ranging 2-327. There was a significant difference in total flight distance between strong (n=7) and weak (n=7) flight phenotypes (t stat=8.2, df=6, $P<0.0001$), but there was no significant difference in flight propensity (t stat=-0.45, df=10, $p=0.333$). Beetles selected to represent the strong flight phenotype had an average flight distance of 19.9 km, ranging 9.9-22.8 km, and initiated flight an average of 83.9 times, ranging from 5-327 times. Average flight distance in the group representing the weak flight phenotype was 0.231 km, ranging 0.040-0.689 km, and initiated flight an average of 61.7 times, ranging 2-210 times. Although the majority (88.5%) of flight by beetles took place during the light period, beetles with a strong flight capacity flew significantly more in the dark than weak fliers (t stat=2.253, df=12, $p=0.0218$; Figure 3.2). On average, strong fliers flew 84.4% of their

total flight time in the light, and 15.6% in the dark. This compared to weak fliers that on average flew 95.6% of their total flight time in the light, and 4.4% in the dark.

The 59 beetles used for the association study flew an average of 6.4 km, ranging 0.01-24.6 km, and initiated flight an average of 229.8 times, ranging 4-2806. The strong fliers used for the association study flew significantly farther than the weak fliers (t stat=12.3, df =57, p <0.001). The 31 strong flight beetles in this data set flew an average of 11.4 km, ranging from 5.2-24.6 km, and the 28 weak fliers flew an average of 0.8 km, ranging from 10 m to 3.7 km.

There was no significant difference in flight propensity between the strong and weak fliers used for the association study (t stat = 1.1, df =57, p =0.297). The strong fliers initiated flight an average of 289.0 times, ranging from 23 to 2806, while the weak fliers initiated flight 164.4 times on average, ranging from 4 to 1968 instances.

3.4.2 Differential expression analysis

A total of 1.735 billion reads were sequenced via RNA-Seq, and 1.283 billion reads were > Q30. On average, there were 65.5 million reads per sample, and this ranged from 25.2 million to 108.8 million (Table 3.1). Principal component analysis of all 3 phenotypes (strong, weak & non fliers) showed a clear separation of strong fliers from weak and non-fliers. It also showed that non-fliers are nested within weak fliers, and that weak fliers have the highest variation in gene expression (Figure 3.3A). There were no significantly differentially expressed genes in the comparison between weak fliers and non-fliers (Figure 3.3B); therefore, further analyses focused on the differences between strong and weak fliers.

In comparisons of strong to weak fliers, differential expression analysis using DESeq2 revealed 2741 differentially expressed genes (Figure 3.3C). Of these, 1486 (54.2%) of the genes were upregulated and 1255 (45.8%) were downregulated. Of the differentially expressed genes, 387 were uncharacterized. In this study we focused on genes that could be broadly categorized as relating to metabolism, muscle form and function, oxidative stress and detoxification, endocrine system, and behavior (Table 3.2). A complete list of differentially expressed genes can be found in Appendix 3.1. 1,282,664,688

We identified 20 genes related to various stages of lipid metabolism, and all but 3 were upregulated (Table 3.2). The majority of these were lipases, although there were also reductases and dehydrogenases, among others.

We found 15 differentially expressed genes relating to muscle form and function (Table 3.2), including 4 collagen alpha chains (all upregulated), and 5 related to myosin (2 up and 3 downregulated), including paramyosin, which is structurally integral to indirect flight muscle (Liu et al. 2003). We also found 6 differentially expressed myotubularin transcripts (3 up and 3 downregulated), which relate to muscle maintenance (Laporte et al. 2001).

We also identified 10 differentially expressed genes involved in oxidative stress management (Table 3.2), including 5 glutathione-s-transferases (GST; 1 theta, 3 sigma, 1 ambiguous Delta/Epsilon), 1 microsomal GST, and 4 antioxidants (2 phospholipid hydroperoxide glutathione peroxidases, and 2 peroxiredoxins). We also found 23 differentially expressed cytochrome P450 genes, including 7 CYP4s, 9 CYP6s and 3 CYP9s, as well as 2 CYP307 genes, 1 CYP 302 and 1 CYP 28. Also related to stress response, we identified 7 heat shock protein transcripts that were differentially expressed.

There were 10 transcripts related to endocrine function, including 4 related to juvenile hormone (JH) and ecdysone, and 6 related to insulin and insulin-like growth factor (IGF; Table 3.2). All JH-related genes were upregulated; however, these were both for juvenile hormone epoxide hydrolase (JHEH), which deactivates JH. There was upregulation of ecdysone 20-monooxygenase, which catalyzes production of the hormone, 20-hydroxyecdysone (20E), but ecdysone-inducible protein E75, an orphan hormone receptor (Segraves and Hogness 1990), was downregulated. Insulin is involved in metabolism, growth, and development (Nässel et al. 2015), and of the 6 insulin family-related genes, there were 4 upregulated receptors (2 insulin receptors and 2 insulin-like growth factor receptors), 1 downregulated insulin-degrading enzyme, and 1 downregulated insulin-like growth factor-binding protein.

Some potential behavioral genes that were differentially expressed included 2 isoforms of nocturnin, which relates to light-mediated behavioral response, a circadian clock-controlled protein, and protein alan shepard, which is related to gravitaxis (Armstrong et al. 2006; Table 3.2).

There were 9 differentially expressed transcripts related to olfaction (Table 3.2). Of these, 2 chemosensory proteins, 3 odorant receptors, and 2 odorant binding proteins were downregulated, and 2 odorant binding proteins were upregulated.

3.4.3 GO enrichment analysis

Of the 2741 differentially expressed gene transcripts, 2,556 (93.3%) of the transcripts had InterPro hits, and 1,358 (49.5%) had one or more GO annotations. Enrichment analysis of upregulated GO terms was performed in the 2 categories, biological process and molecular function. The 100 significantly overrepresented GO terms (89 biological processes and 11 molecular functions; FDR=0.05), were reduced to 25 more specific GO terms. These included 8

molecular functions and 17 biological processes relating to oxidoreductase activity, coenzyme binding, oxidation-reduction processes, mitochondrial transport and organization, and coenzyme metabolic processes (Figure 3.4).

Enrichment analysis of the downregulated GO terms revealed 28 overrepresented terms (24 biological processes and 4 molecular functions; FDR=0.05), which were reduced to 4 more specific GO terms, including 2 molecular functions and 2 biological processes related to DNA transcription and signal transduction (Figure 3.4).

3.3.4 Sequence data mapping & differential expression analysis

Our experiment included 18 samples belonging to 3 flight phenotypes (7 strong fliers, 7 weak fliers and 4 non fliers). We began with 8 strong, 8 weak and 4 non fliers, but one strong flier sequenced poorly, and a weak flier was removed because it was in a bout of strong flight when it was collected, which was made apparent in downstream analysis of the beetle flight data.

Sequence data was aligned to the male mountain pine beetle draft genome (Keeling et al. 2013b) using Bowtie2 version 2.1.1.3 (Langmead and Salzberg 2012) and Tophat2 version 2.1.1 (Kim et al. 2013), with a maximum of 5 alignment sites, and otherwise default settings. This data was then sorted and indexed using SAMtools version 1.5 (Li et al. 2009).

Differential expression analysis was performed using the R package DESeq2 (Love et al. 2014), in R version 3.3.3 (R Core Team 2017). We chose to use DESeq2 for its stringency (Rajkumar et al. 2015), risking higher false negatives rather than false positives. BAM files were read using RSamtools (Morgan et al. 2017) and annotated read count tables were produced using the packages GenomicFeatures and GenomicAlignments (Lawrence et al. 2013). Differentially

expressed genes with a false discovery rate (FDR) < 0.01 were considered candidate genes related to flight. A principal component analysis (PCA) was performed on regularized-logarithm transformed gene expression data to visualize relationships between the specimens based on gene expression without bias towards highly expressed genes (Love et al. 2014).

3.4.4 KEGG pathways

KEGG pathway analysis of all differentially expressed genes revealed 52 pathways represented by at least 2 enzymes (Appendix 3.2), 42 of which were represented by at least 3 enzymes (Figure 3.5). Several metabolic pathways included: the metabolism of glycerolipids, purine, pyruvate, and sphingolipids, pantothenate and coenzyme A biosynthesis, glycolysis, and the citric acid cycle. Detoxification and stress response were also represented in the KEGG pathways, including detoxification, biosynthesis of antibiotics, drug metabolism, and metabolism of xenobiotics by P450s. We also found pathways associated with glutathione metabolism, which may relate to oxidative stress. The steroid hormone biosynthesis pathway, which may relate to hormone-mediated flight behaviors, was also represented, but only by 3 sequences that all coded for the same enzyme.

3.4.5 Targeted association study

We identified 714 scaffolds containing differentially expressed flight genes, and these contained 7781 SNP sites that passed filtering. Of these, 4 SNPs were significantly associated with flight performance: 1 SNP was found to be associated with flight distance (Figure 3.6A), and 3 were found to be associated with flight propensity (Figure 3.6B). The SNP associated with flight distance is located at position 3148638 on scaffold NW_017852012 (perm p=0.041). This is located in an exon (XM_019902532) of the gene LOC109536350 (Protein Brunelleschi). Of the

SNPs found to be associated with flight propensity, the first is located at position 642895 on scaffold NW_017852258 (perm $p=0.009$), which is an intron of the uncharacterized gene LOC109542038. The second SNP is located at position 193112 on scaffold NW_017852115 (perm $p=0.021$). This is located in an exon of the gene LOC109540157 (probable E3 ubiquitin-protein ligase HERC1). The third SNP is located at position 188406 on scaffold NW_017851689 (perm $p=0.046$), and this is located in an intron of the gene LOC109534071 (WD repeat-containing protein 55 homolog).

3.5 Discussion

Dispersal by flight is one of the most important phases in the life history of many insects (Roff and Fairbairn 2007). Our research shows that there are several genetic systems related to strong flight; gene expression profiles between flight-avid (strong fliers) and flight-averse (weak fliers and non-fliers) beetles are significantly different. However, no significant differences were found among the flight-averse weak and non-fliers (Figure 3.3), indicating that the physiological change between non-fliers and weak fliers is relatively minimal. Based on this, we focus on 2 main flight modes, a “dispersal” and “non-dispersal” mode, with clear differences in dispersal capacity and gene expression.

3.5.1 Metabolism

Upregulated metabolic activity is expected in response to insect flight, as it is one of the most physiologically demanding activities known (Wegener 1996). Several GO terms and KEGG pathways indicate the importance of metabolic processes, such as glycolysis, citric acid cycle, and serine metabolism. Serine, in particular, is associated with the metabolism of lipids (Gao et al. 2018), a known energy source in insects and the primary fuel source for sustained flight in *D.*

ponderosae (Evenden et al. 2014; Wijerathna and Evenden 2019). This is further supported by several upregulated lipid metabolism-related genes and pathways (Table 3.2; Figure 3.5).

3.5.2 Muscle form & function

Several differentially expressed genes indicate the importance of muscle function and maintenance in flight. We identified differentially expressed collagen genes, which are important for muscle development and function (Zhan et al. 2014) and have been linked to migratory behavior in insects (Zhan et al. 2014; Jones et al. 2015). Some myosins were also related to flight; in particular, paramyosin was upregulated in strong fliers, and is known to be structurally integral to thick filaments in indirect flight muscle (Liu et al. 2003). These genes may act in concert with differentially expressed myotubularin genes in order to maintain muscle structure and function during bouts of sustained flight (Laporte et al. 2001).

3.5.3 Oxidative stress & detoxification

Our data suggests several mechanisms are used by *D. ponderosae* to mitigate stress-induced damage during flight, including DNA repair pathways and GSTs. In strong fliers, DNA repair GO terms are upregulated and would mitigate genetic damage caused by oxidative stress (Figure 3.4). GSTs are also antioxidants (Pompella et al. 2003; Yamamoto et al. 2011; Yamamoto et al. 2016) and prevent build-up of potentially harmful lipid metabolism in flight muscle (Singh et al. 2001). Upregulated GSTs and glutathione-related pathways in strong female fliers may play other roles in successful dispersal and establishment, as females are the pioneering sex in mountain pine beetle (Blomquist et al. 2010). GSTs are involved in detoxification of host defenses during colonization (Robert et al. 2013; Keeling et al. 2013b); however, this process often involves

precursor steps that rely on reactions with other enzymes, such as cytochrome P450s (Sheehan et al. 2001).

Several P450s are differentially expressed during flight, and these are found mostly in 3 cytochrome P450 families that are believed to be adaptive in *D. ponderosae* (CYP4, CYP6, and CYP9 in the CYP4 clade; Keeling et al. 2013b). Many of these are likely involved in host defense detoxification (Sandstrom et al. 2006; Nadeau et al. 2017; Chiu et al. 2018). Others, in particular members of the CYP6 family, may be involved in pheromone biosynthesis (Chiu et al. 2019), which may relate to variation in pheromone production observed in different mountain pine beetle flight phenotypes (Jones et al. 2020). We also found 3 differentially expressed CYP9s; many CYP9 functions have not yet been characterized (Keeling et al. 2013b), and these may relate to dispersal. Other differentially expressed P450s in the CYP302 and CYP307 families may be related to the biosynthesis of hormones like 20E (Iga and Kataoka 2012), which may impact dispersal-related behaviors.

3.5.4 Endocrine system

Trends in gene expression indicate reduced levels of JH, and increases in 20E, insulin, and IGF; these are important hormones linked to dispersal and colonization in *D. ponderosae*. During flight, JH epoxide hydrolase (JHEH), an enzyme that deactivates JH, is upregulated, theoretically reducing overall JH levels. In other insects, decreases in JH have been linked to dispersal (Roff and Fairbairn 2007); however, increases in JH are linked to reproductive behavior (Gruntenko and Rauschenbach 2008), biosynthesis of sex and aggregation pheromones (Bridges 1982; Conn et al. 1984; Tillman et al. 2004), and degradation and reallocation of flight muscle resources (Borden and Slater 1969; Sahota 1975). Similar phenomena occur in *D. ponderosae* (McCambridge and

Mata 1969) and may also be mediated by JH; reduced levels of JH in strong fliers may act to maintain “dispersal mode” by preventing the onset of several colonization-associated behaviors.

Increased interactions of insulin and insulin-like growth factors (IGF) were differentially expressed and may be associated with metabolism and growth. In many bark beetles, including *D. ponderosae*, strong dispersers tend to be larger (Evenden et al. 2014; Shegelski et al. 2019). This may be influenced by increased IGF receptors (Nässel et al. 2015) and reduced IGF binding protein levels (Nazif and Partridge 2008). Insulin, which shares structural similarities with IGF, affects carbohydrate and lipid metabolism (Erion and Sehgal 2013) and is likely one of the metabolic hormones that increases metabolism in strong fliers.

We also identified upregulation of ecdysone 20-monooxygenase, which catalyzes the production of 20E (Nigg et al. 1976; Johnson and Rees 1977), and may affect flight behavior as it has links to lipid metabolism (Wang et al. 2010), reproduction (Gruntenko and Rauschenbach 2008; Sieber and Spradling 2015), and regulation of the circadian clock (Kumar et al. 2014).

3.5.5 Behavior

Several differentially expressed genes may mediate response to abiotic and biotic cues, affecting behavior. Strong fliers flew relatively more in the dark than weak fliers (Figure 3.2) which may be linked to differential expression of light-response and circadian clock genes (Table 3.2). Nocturnin, which is downregulated in strong fliers, may affect response to environmental light cues (Nagoshi et al. 2010). Flight patterns in strong fliers also appeared to be more aligned with actual day and night (Figure 3.2), which may be associated with differential response to a synchronized internal clock (Wertman and Bleiker 2019). Also, circadian clock-controlled protein has circadian-controlled expression (Lorenz and Rosbash 1989), and its upregulation in strong

fliers, coupled with differential temporal flight performance, indicates potential differences in circadian synchronization that may affect dispersal capacity.

Differentially expressed olfaction genes may also be important in determining dispersal behavior. In *Dendroctonus pseudotsugae*, larger, stronger dispersers will often ignore chemical cues (Bennet and Borden 1971), and this has similarly been observed in *D. ponderosae* (Jones 2019). Several differentially expressed chemosensory proteins, odorant receptors, and odorant-binding proteins, most of which are downregulated in strong fliers, are potentially related to altered response to host volatiles (Zhang et al. 2016), and these may be of interest in understanding the role chemical cues play in flight and dispersal behavior.

3.5.6 Association study

For the 4 SNPs that we found to be associated with dispersal capacity (Figure 3.6), one protein has no known function and may provide an interesting avenue of investigation, and 3 other genes involve cell functions that are not directly linked to flight, but are associated with flight propensity, which may be a better predictor of realized dispersal in the natural environment (Steyn et al. 2016). Regardless, sequence data associated with flight potentially provides a management tool. Current mountain pine beetle surveying methods involve collecting disks from the surface of infested trees to determine reproductive success of a population. These disks are often rife with specimens that could be sequenced to also provide dispersal potential data for that population based on prevalence of flight phenotypes.

3.6 Conclusions

We identified genetic distinctions between mountain pine beetles with strong and weak flight capacity but found no significant difference between weak and non-fliers in the flight-averse

grouping. The genetic systems associated with sustained flight appear to be involved in meeting the physiological demands of flight, while downregulated systems may represent mechanisms to conserve resources for post-flight host colonization. This demonstrates a level of genetic coordination between dispersal and colonization. Our research has also identified genes that may contribute to the “dispersal” phenotype behaviors, as well as genetic variants associated with flight performance that may be useful in predicting flight capacity through genetic testing. Our research sheds some light on the physiological nature of dispersal by flight and indicates several potential avenues for future research.

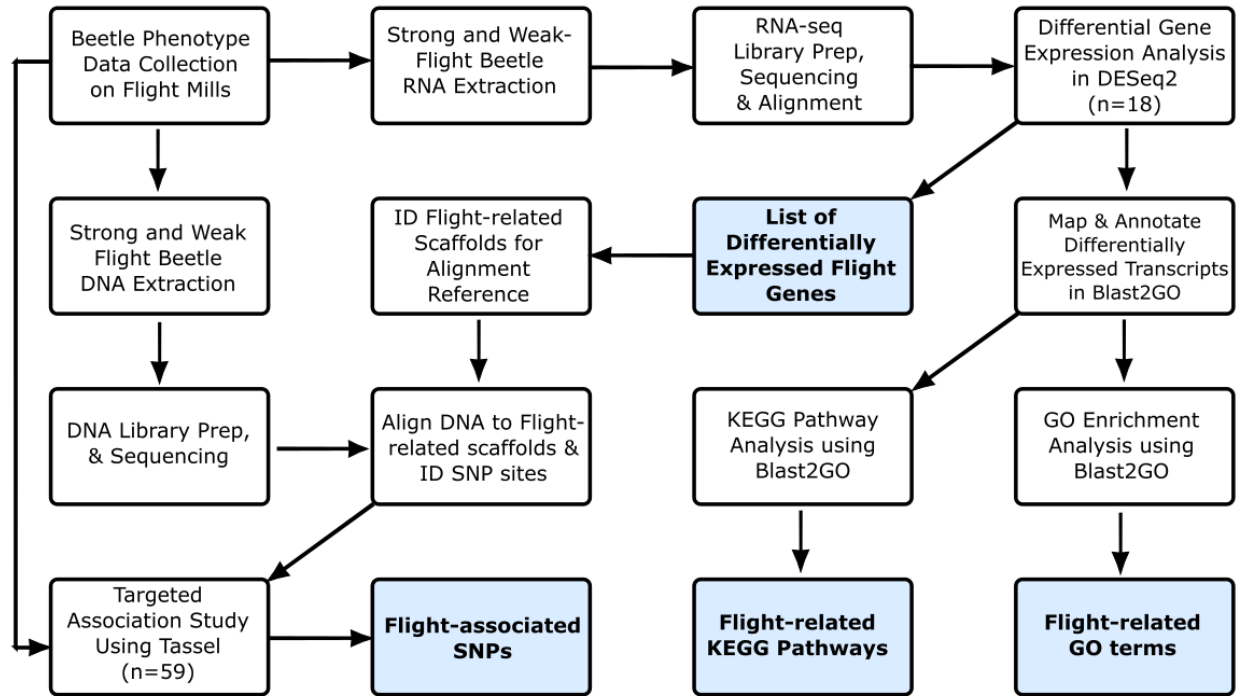


Figure 3.1: Flowchart of methods used for this study. Shaded boxes represent data endpoints that were used to determine differentially expressed genes and gene systems related to flight.

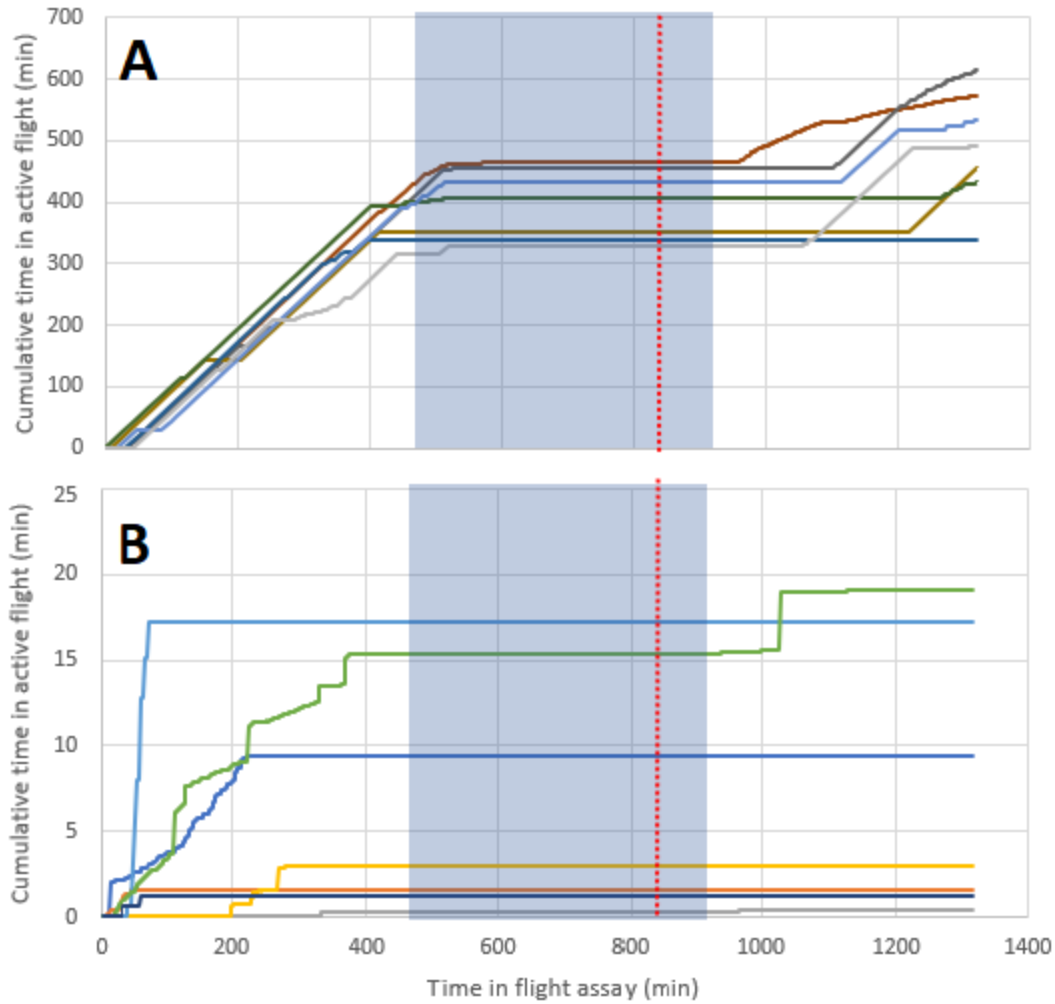


Figure 3.2: Flight patterns of strong fliers (A) and weak fliers (B). The dashed red line indicates the time at which the lights were switched off in the flight room to simulate night, and the shaded box indicates actual night based on June 20th (dusk at 22:00, dawn at 05:00).

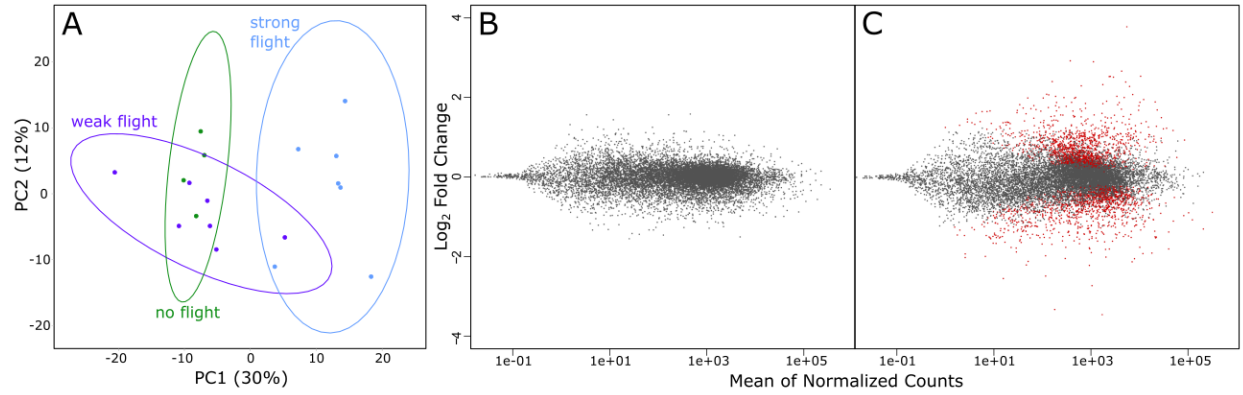


Figure 3.3: (A) rlog principal component analysis of the 3 flight groups based on variation in gene expression. (B) MA plot showing the results of a differential expression analysis between weak and non-fliers. There were no significantly differentially expressed genes at $\alpha=0.01$. (C) MA plot showing the results of a differential expression analysis between strong and weak fliers. Significantly differentially expressed genes ($\alpha=0.01$) are shown in red.

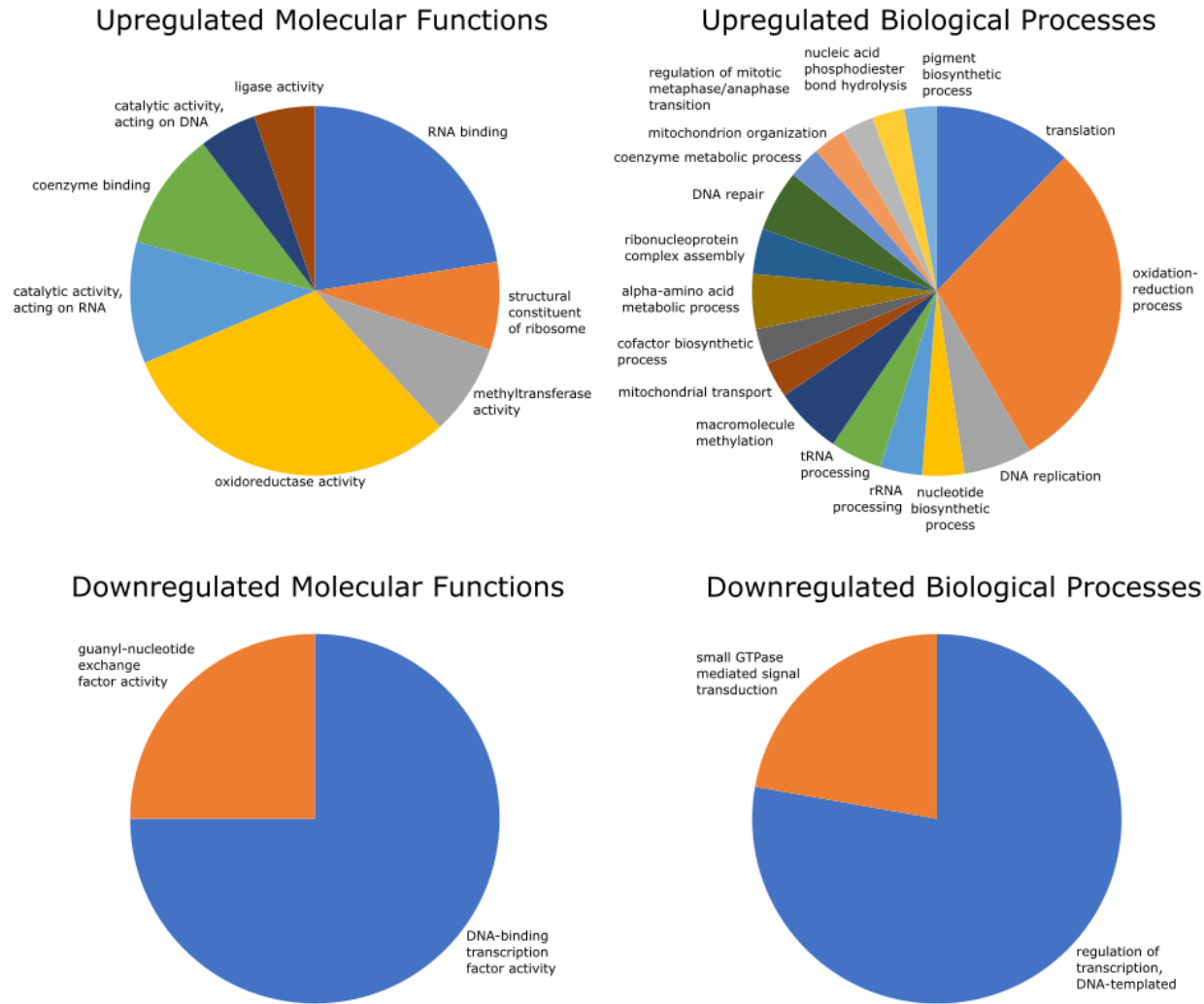


Figure 3.4: Results of GO enrichment analysis reduced to most specific terms where possible. All GO annotations shown were significantly different between strong and weak fliers (FDR=0.05). Pie charts are based on proportion of representation among the total number of sequences relating to differentially expressed GO terms.

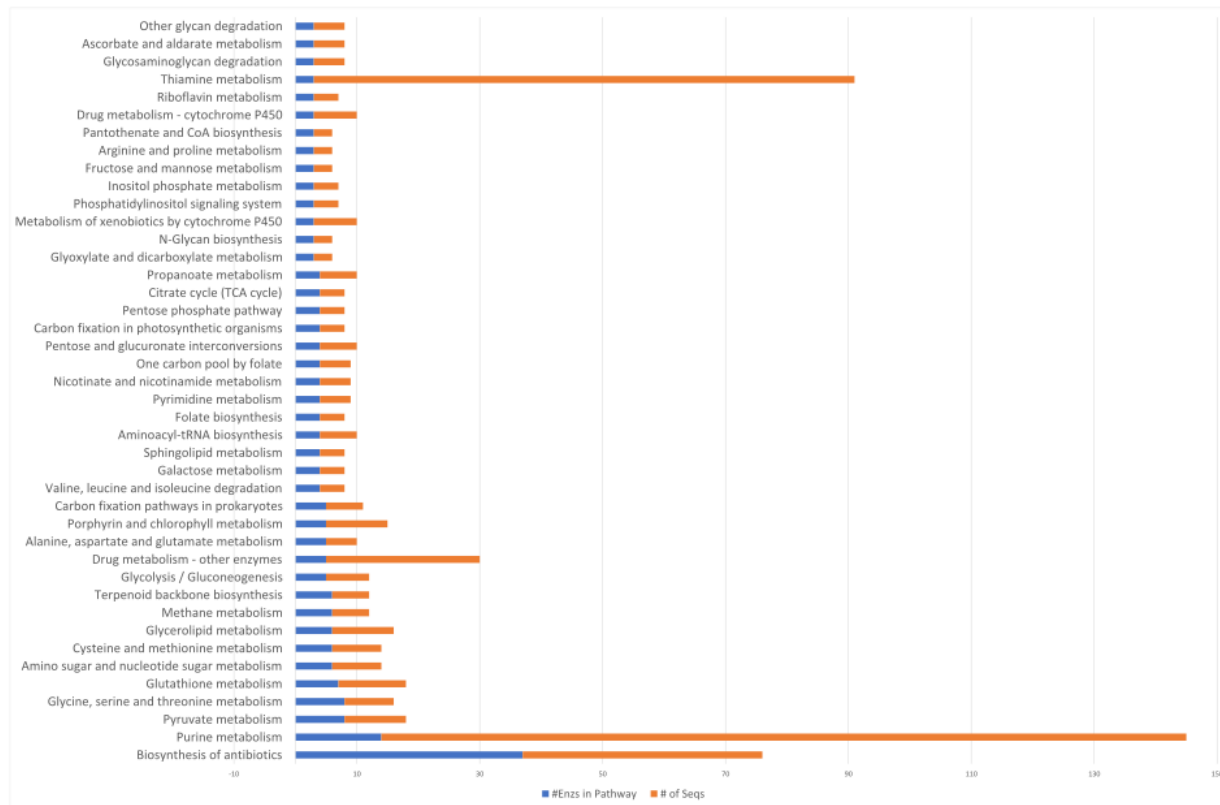


Figure 3.5: All KEGG pathways with more than 3 represented enzymes in the differentially expressed genes. Blue shows number of enzymes in the pathway represented in the data, and orange shows the total number of sequences related to enzymes in the pathway.

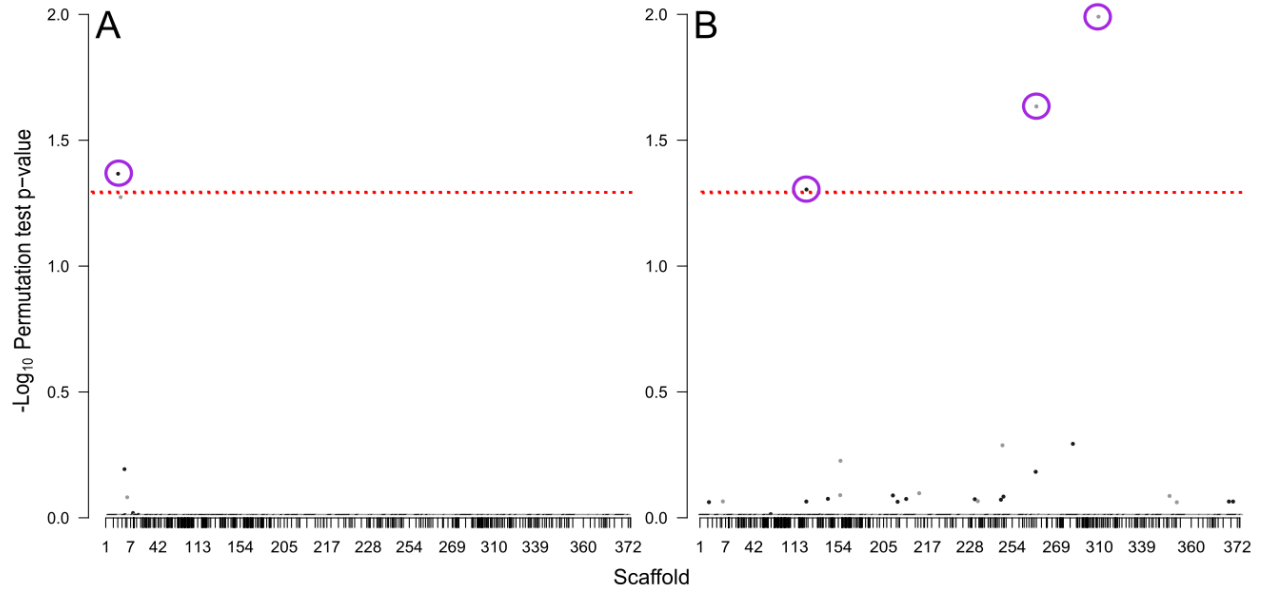


Figure 3.6: Manhattan plots showing $-\text{Log}_{10}$ permutation test p-values for each SNP based on testing for association with (A) total distance flown during the flight mill assay and (B) flight propensity. SNPs are shaded by scaffold, alternating between black and white, and a purple circle indicates the SNP is significantly associated with the tested trait.

Table 3.1: Sequence data for each specimen used for the differential expression analysis, including their flight phenotype. The number of reads shown have a quality score >Q30.

Sample ID	Flight phenotype	Millions of reads (>Q30)
289	Weak	44.322586
293	Weak	67.926129
387	Strong	45.72894
392	No Flight	108.826416
393	Strong	25.166942
404	Weak	64.687156
409	Strong	73.784869
410	No Flight	96.462167
418	Weak	91.495058
378	No Flight	49.056371
385	Strong	69.742723
306	Weak	62.060979
311	Strong	77.153324
320	Strong	73.660515
328	Weak	78.226999
332	Weak	78.979533
345	Strong	65.119831
358	Weak	46.989146
367	No Flight	25.603463

Table 3.2: Differentially expressed candidate genes. This table lists the Genbank accession number, annotation based on the mountain pine beetle draft genome (Keeling et al. 2013b), Log2 fold change (positive values are upregulated and negative values are downregulated in strong fliers), and the adjusted p-value based on a Benjamini-Hochberg correction for false discovery rate.

Accession	Annotation	log2 Fold Change	padj	Role
XM_019899335.1	nocturnin isoform X1	-1.43	8.8E-10	Behavior
XM_019907230.1	nocturnin isoform X2	-1.20	2.7E-06	Behavior
XM_019914674.1	protein alan shepard isoform X8	-0.72	6.5E-05	Behavior
XM_019911839.1	circadian clock-controlled protein-like	1.99	1.0E-05	Behavior
XM_019917055.1	probable cytochrome P450 9f2	-1.57	4.2E-04	Detoxification
XM_019909987.1	cytochrome P450 9e2-like	-1.55	3.1E-04	Detoxification
XM_019909983.1	cytochrome P450 9e2-like	-1.39	5.4E-04	Detoxification
XM_019906180.1	cytochrome P450 9e2-like	-1.26	2.1E-03	Detoxification
XM_019915611.1	probable cytochrome P450 28d1	-0.87	6.6E-03	Detoxification
XM_019904514.1	cytochrome P450 307a1-like	-0.84	7.6E-03	Detoxification
XM_019904602.1	cytochrome P450 307a1-like	-0.83	8.5E-03	Detoxification
XM_019916691.1	cytochrome P450 4d2-like isoform X1	-0.78	3.0E-03	Detoxification
XM_019916694.1	cytochrome P450 4d2-like	-0.78	5.0E-03	Detoxification
XM_019913251.1	cytochrome P450 6B1-like	0.37	5.5E-03	Detoxification
XM_019917741.1	cytochrome P450 302a1, mitochondrial-like	0.53	6.4E-05	Detoxification
XM_019917605.1	multidrug resistance-associated protein 4-like	0.73	1.3E-04	Detoxification
XM_019917607.1	multidrug resistance-associated protein 4-like	0.74	6.5E-03	Detoxification
XM_019898552.1	cytochrome P450 4g15-like	0.79	4.1E-03	Detoxification

XM_019917604.1	multidrug resistance-associated protein 4-like	0.85	8.6E-06	Detoxification
XM_019901159.1	probable cytochrome P450 4aa1	0.87	3.7E-05	Detoxification
XM_019898650.1	cytochrome P450 CYP6BW1	0.89	1.4E-03	Detoxification
XM_019913238.1	cytochrome P450 6B1-like	1.00	1.2E-03	Detoxification
XM_019918001.1	cytochrome P450 4C1-like	1.23	1.9E-03	Detoxification
XM_019915536.1	cytochrome P450 6k1-like	1.31	2.0E-03	Detoxification
XM_019901126.1	cytochrome P450 4g1-like	1.32	1.3E-04	Detoxification
XM_019908046.1	multidrug resistance-associated protein 4-like	1.32	2.1E-06	Detoxification
XM_019914207.1	probable cytochrome P450 6a13	1.36	1.4E-04	Detoxification
XR_002171627.1	cytochrome P450 6a2-like	1.46	6.8E-04	Detoxification
XM_019910044.1	cytochrome P450 6k1-like	1.53	2.1E-04	Detoxification
XM_019898560.1	cytochrome P450 6a2-like	1.71	3.6E-07	Detoxification
XM_019898558.1	cytochrome P450 6A1-like	1.89	4.1E-12	Detoxification
XM_019917057.1	cytochrome P450 4c3-like isoform X1	2.01	1.0E-06	Detoxification
XM_019902592.1	glutathione S-transferase theta-1-like isoform X1	-0.79	4.9E-06	Detoxification - antioxidant
XM_019915413.1	microsomal glutathione S-transferase 1-like	-0.52	1.2E-03	Detoxification - antioxidant
XM_019905169.1	glutathione S-transferase-like	-0.29	8.5E-03	Detoxification - antioxidant
XM_019899571.1	glutathione S-transferase 1-like	0.53	3.8E-04	Detoxification - antioxidant
XM_019916272.1	PREDICTED: peroxiredoxin-2-like	0.65	4.7E-05	Detoxification - antioxidant
XM_019905168.1	glutathione S-transferase-like	0.89	3.6E-05	Detoxification - antioxidant
XM_019909039.1	PREDICTED: peroxiredoxin-6	0.89	4.7E-07	Detoxification - antioxidant

XM_019915687.1	probable phospholipid hydroperoxide glutathione peroxidase%2C transcript variant X1	0.94	3.1E-04	Detoxification - antioxidant
XM_019906204.1	probable phospholipid hydroperoxide glutathione peroxidase%2C transcript variant X1	0.94	3.1E-04	Detoxification - antioxidant
XM_019899020.1	glutathione S-transferase-like	0.99	3.2E-03	Detoxification - antioxidant
XM_019907423.1	ecdysone-inducible protein E75 isoform X1	-0.80	2.7E-11	Endocrine
XM_019898632.1	ecdysone 20-monooxygenase isoform X1	0.57	6.5E-05	Endocrine
XM_019911438.1	juvenile hormone epoxide hydrolase 1-like	0.85	1.7E-03	Endocrine
XM_019906207.1	juvenile hormone epoxide hydrolase 1-like	0.99	5.8E-05	Endocrine
XM_019900280.1	putative molluscan insulin-related peptide(s) receptor	1.04	3.2E-06	Endocrine
XM_019900281.1	insulin receptor-like	1.02	4.3E-06	Endocrine
XM_019898016.1	insulin receptor-like	0.99	4.7E-05	Endocrine
XM_019913890.1	insulin-degrading enzyme	-0.33	1.3E-04	Endocrine
XM_019912320.1	insulin-like growth factor 1 receptor	0.96	1.4E-05	Endocrine
XM_019913102.1	insulin-like growth factor-binding protein complex acid labile subunit transcript variant X1	-1.11	1.1E-05	Endocrine
XM_019905105.1	heat shock protein 70 A1-like isoform X1	-1.39	3.2E-04	Heat Shock Proteins
XM_019905101.1	heat shock protein 68-like	-1.02	4.1E-03	Heat Shock Proteins
XM_019899536.1	heat shock 70 kDa protein II-like isoform X2	-0.68	2.1E-03	Heat Shock Proteins
XM_019904181.1	heat shock protein 83	-0.51	1.2E-03	Heat Shock Proteins
XM_019901242.1	heat shock 70 kDa protein 4 isoform X1	-0.49	1.3E-03	Heat Shock Proteins
XM_019905254.1	heat shock protein 75 kDa, mitochondrial	-0.45	5.5E-05	Heat Shock Proteins
XM_019899225.1	heat shock 70 kDa protein-like isoform X2	0.80	1.1E-04	Heat Shock Proteins
XM_019914951.1	pancreatic triacylglycerol lipase	-1.29	7.6E-03	Metabolism - Lipid
XM_019901458.1	putative fatty acyl-CoA reductase CG5065	-0.75	6.7E-03	Metabolism - Lipid

XM_019908951.1	abhydrolase domain-containing protein 2	-0.28	1.5E-03	Metabolism - Lipid
XM_019900381.1	acyl-CoA dehydrogenase family member 9, mitochondrial	0.47	1.9E-03	Metabolism - Lipid
XM_019915250.1	monoacylglycerol lipase ABHD12-like isoform X1	0.59	2.2E-04	Metabolism - Lipid
XM_019916253.1	pancreatic triacylglycerol lipase-like isoform X1	0.66	2.7E-03	Metabolism - Lipid
XM_019911517.1	lipase member H-A-like	0.67	2.8E-03	Metabolism - Lipid
XM_019903342.1	2-hydroxyacyl-CoA lyase 1	0.74	3.7E-03	Metabolism - Lipid
XM_019905050.1	very-long-chain 3-oxoacyl-CoA reductase	0.84	2.5E-03	Metabolism - Lipid
XM_019908494.1	short/branched chain specific acyl-CoA dehydrogenase, mitochondrial	0.87	5.1E-05	Metabolism - Lipid
XM_019908288.1	phospholipase B1, membrane-associated-like	0.96	5.0E-05	Metabolism - Lipid
XM_019899282.1	phospholipase DDHD2 isoform X1	1.03	2.4E-04	Metabolism - Lipid
XM_019906151.1	lipase 3-like	1.03	2.2E-04	Metabolism - Lipid
XM_019908331.1	fatty acyl-CoA reductase wat-like	1.08	1.4E-03	Metabolism - Lipid
XM_019899377.1	lipoprotein lipase-like	1.18	2.0E-03	Metabolism - Lipid
XM_019901196.1	lipase 3-like	1.37	3.6E-05	Metabolism - Lipid
XM_019917332.1	pancreatic lipase-related protein 3-like	1.49	1.1E-03	Metabolism - Lipid
XM_019899299.1	pancreatic triacylglycerol lipase-like	1.82	2.8E-05	Metabolism - Lipid
XM_019918004.1	putative fatty acyl-CoA reductase CG5065 isoform X1	1.99	1.8E-05	Metabolism - Lipid
XM_019915053.1	group XV phospholipase A2-like	2.28	3.9E-11	Metabolism - Lipid
XM_019906965.1	collagen alpha chain CG42342-like transcript variant X1	0.62	2.5E-04	Muscle form and function
XM_019912643.1	collagen alpha-1(XI) chain-like	0.71	1.4E-03	Muscle form and function
XM_019916633.1	collagen alpha-2(XI) chain-like	0.83	1.7E-03	Muscle form and function
XM_019905926.1	collagen alpha-5(IV) chain	0.80	1.3E-03	Muscle form and function

XM_019906403.1	myosin heavy chain non-muscle transcript variant X1	-0.49	2.1E-03	Muscle form and function
XM_019907520.1	paramyosin-like	0.83	4.9E-04	Muscle form and function
XM_019916148.1	myosin-10-like	1.00	5.8E-06	Muscle form and function
XM_019915840.1	myosin-IA transcript variant X1	-1.03	1.7E-05	Muscle form and function
XM_019899155.1	myosin-VIIa transcript variant X1	-0.47	7.3E-04	Muscle form and function
XM_019908500.1	myotubularin-related protein 10-A	0.40	9.3E-09	Muscle form and function
XM_019898786.1	myotubularin-related protein 13-like	-0.53	5.9E-05	Muscle form and function
XM_019898787.1	myotubularin-related protein 13-like	-0.49	7.5E-03	Muscle form and function
XM_019910219.1	myotubularin-related protein 13-like	-0.46	2.0E-03	Muscle form and function
XM_019903766.1	myotubularin-related protein 14%2C transcript variant X1	1.17	2.0E-07	Muscle form and function
XM_019908753.1	myotubularin-related protein 8	-0.40	6.9E-03	Muscle form and function
XM_019910296.1	odorant receptor 49b	-1.45	1.9E-03	Olfaction
XM_019902425.1	chemosensory protein 2	-1.17	2.7E-06	Olfaction
XM_019902670.1	chemosensory protein 4	-1.04	1.7E-03	Olfaction
XM_019902486.1	odorant-binding protein 4	-1.00	6.3E-03	Olfaction
XM_019915903.1	odorant receptor 63a-like isoform X1	-0.96	1.7E-03	Olfaction
XM_019902493.1	odorant-binding protein 28	-0.88	7.6E-03	Olfaction
XM_019901389.1	odorant receptor 67c-like isoform X2	-0.77	1.1E-04	Olfaction
XM_019913381.1	odorant-binding protein 26	0.80	5.0E-03	Olfaction
XM_019911214.1	odorant-binding protein 27	1.30	1.7E-03	Olfaction

Chapter 4

Source and spread dynamics of mountain pine beetle (*Dendroctonus ponderosae*) in central Alberta, Canada

A version of Chapter 4 has been submitted for publication, authored by Shegelski VA, Campbell EO, Thompson KM, Whitehouse CM, and Sperling FAH.

4.1 Summary

Mountain pine beetles (*Dendroctonus ponderosae* Hopkins; Coleoptera: Curculionidae) are a significant destructive force in the pine forests of western Canada and have the capacity to spread east into a novel host tree species. New populations have been documented in central Alberta, but the source populations for these outbreaks have yet to be identified. In this study we use genetic data to identify parent populations for recent outbreak sites near Slave Lake, Lac La Biche and Hinton. We found the northern population cluster that entered Alberta near Grande Prairie was the source of the most eastern established population near Lac La Biche, and the range expansion to this leading-edge population has been too rapid to establish evidence of population structure. However, some dispersal from a population in the Jasper and Hinton areas has been detected as far north and east as Slave Lake. We also identified two potential source populations for the current outbreak in Hinton; most beetles appear to be from Jasper National Park, but some also originated from the northern population cluster. These findings demonstrate the dynamic dispersal capabilities of mountain pine beetle across the Alberta landscape and the potential hazard of increased dispersal to newly established leading-edge populations.

4.2 Introduction

The mountain pine beetle, *Dendroctonus ponderosae* Hopkins (Coleoptera: Curculionidae), is a tree-killing bark beetle that is one of the most significant destructive forest pests in western North America (NRCan 2017). Historically, mountain pine beetle populations in Canada have largely been confined to British Columbia and southwestern Alberta within the range of their primary host, lodgepole pine (Safranyik et al. 2010). However, in the early 2000s populations expanded and established in northwestern Alberta (NRCan 2017), aided by wind updrafts (Jackson et al. 2008, Janes et al. 2014). Its eastward spread has continued, resulting in more than 500 million dollars being spent on mitigating damage in Alberta alone (Whittaker 2018). Northeastern Alberta is of particular concern as this is where lodgepole pine transitions to jack pine, a naive host species that provides a potential entry point into the boreal pine forests of eastern Canada and the northern United States (Cullingham et al. 2011; Bleiker et al. 2014).

Various genetic markers have been used to map mountain pine beetle population structure and range expansions in BC and Alberta (Langor and Spence 1991; Mock et al. 2007; Cullingham et al. 2012; Samarasekera et al. 2012; Janes et al. 2014; Batista et al. 2016; Janes et al. 2016; Janes et al. 2018). These studies have shown that MPB spread into Alberta was composed of two genetically distinct incursions (Samarasekera et al. 2012; Janes et al. 2014; Batista et al. 2016), and a third that is genetically intermediate (Trevoy et al. 2018b). The southern resident population has ranged as far north as Banff and Canmore (Hopping and Mathers 1945), and a more recently established northern population extends eastward past Grande Prairie (Janes et al. 2014). The intermediate population recently entered Alberta via Jasper National Park, and its genetic similarity to lab-produced hybrids between the northern and southern populations suggests that it resulted from admixture between them (Trevoy et al. 2018b).

Epidemic populations have been identified in Hinton, west-central Alberta, and Slave Lake, indicating continued northeastern range expansion in Alberta. Mountain pine beetle has now also been detected at very low densities on the eastern edge of Alberta toward the Saskatchewan border in novel jack pine habitat (Mac Cormick 2020). It is uncertain if beetles detected near Saskatchewan came from low-density, locally established populations from previous long-range dispersal events, or directly from larger outbreak populations to the west. These recently detected populations have not yet been included in demographic studies on mountain pine beetle spread. Determining their sources would allow optimisation of pheromone monitoring (Miller et al. 2005), guide forest management practices to limit localised population increases (Safranyik and Carroll 2006), and better inform assessments of outbreak risk (Bleiker 2019). In our study, we use genome-wide SNPs (single nucleotide polymorphisms) to characterize population structure and identify dispersal and spread of mountain pine beetle in northern Alberta, particularly in newly detected northeastern populations.

4.3 Methods

4.3.1 Beetle sampling, DNA extraction, and sequencing

A total of 306 specimens were collected at 44 different sites from 10 locations during 2014 to 2018, and specimens were assigned to populations based on proximity to other collection localities (Appendix 4.1). Beetles were preferentially taken from different trees or egg galleries to reduce the influence of genetic structuring due to the inclusion of siblings from single families. Once collected, beetles were preserved in 90-95% ethanol and placed in a freezer at -20°C until DNA extraction.

DNA extraction used the Qiagen DNEasy Blood & Tissue kit with an optional RNase A treatment. Library preparation for samples collected in 2014-2015 followed the two-enzyme GBS protocol of Poland et al. (2012) , and the ddRAD protocol of Peterson et al. (2012) for samples collected in 2016-2018, following the general procedure outlined in Campbell et al. (2017); single-end sequencing of 2014-2015 samples was performed on an Illumina HiSeq2000 at the Institut de biologie intégrative et des systèmes (IBIS) at Université Laval, and single-end sequencing of 2016-2018 samples was done on an Illumina NextSeq500 at the University of Alberta Molecular Biology Service Unit (MBSU).

4.3.2 Data filtering and SNP calling

Initial data demultiplexing was conducted in Stacks version 2.0b (Rochette et al. 2019) on the Graham cluster of Compute Canada. *PstI* restriction sites on the 5' end of each sequence read were trimmed using cutadapt version 1.9.1 (Martin 2011). Samples sequenced on a NextSeq 500 had a final read length of 67 base pairs after trimming. Following Campbell et al. (2017), longer reads produced on a HiSeq 2000 were additionally truncated on the 3' end to match the length of the NextSeq-generated data. The trimmed sequence reads were then aligned to the female mountain pine beetle draft genome (Keeling et al. 2013b) using BWA version 0.7.17 (Li and Durbin 2009) with the BWT-SW algorithm. Alignment quality was checked using SAMtools version 1.9 (Li et al. 2009).

SNPs were identified using the `ref_map.pl` script in Stacks (Catchen et al. 2011; Rochette et al. 2019). We specified a minimum minor allele frequency of 0.01 and adhered to the *r80* principle recommended by Paris et al. (2017), which requires a locus to be present in at least 80% of the individuals in a population in order to be retained in the final dataset. At each locus only a

single random SNP was retained. Further filtering of SNP data and samples was done using vcftools version 0.1.14 (Danecek et al. 2011). Reads were dropped if they had a genotype quality score below 30 or if a SNP locus had more than 5% missing data globally. Further filtering for linkage disequilibrium (LD) was conducted following Abdellaoui et al. (2013) and was calculated for all pairwise SNP combinations using the dartR package (Gruber and Georges 2019) in R (R Core Team 2018). For any groups of SNPs that were in LD ($R^2 > 0.5$), we retained only one random SNP from each to reduce the impact of LD on population clustering analyses.

Although we tried to reduce the incidence of sampling multiple specimens from a single family, preliminary data visualization using principal components analysis (PCA) indicated clustering patterns for 10 individuals that were consistent with family-level structure. To reduce the influence of such family structure in population-level analyses, all but one individual in each set of closely related specimens were removed from the dataset.

4.3.3 Population structure analysis

To explore and identify potential signs of population structure across northern Alberta, we used several approaches. A PCA was performed in adegenet (Jombart 2008; Jombart and Ahmed 2011) based on all samples that passed filtering. This was used to detect SNP covariance between specimens and identify population structure among the specimens without *a priori* population assignment. PCA plots were made using ggplot2 (Wickham 2016). We also used this set of samples to calculate observed heterozygosity, expected heterozygosity, and pairwise population F_{st} in dartR, and population differentiation based on genetic diversity using an exact G test of genic differentiation in the R package genepop (Raymond and Rousset 1995; Rousset 2008) with a Bonferroni correction based on the 36 pairwise tests.

To assess fine-scale population structure across the northernmost locations, we created a northern dataset by removing all southern and intermediate-cluster population samples, including any putative dispersers. We performed a PCA on this northern data set, then used discriminant analysis of principal components (DAPC, Jombart et al. 2010) in adegenet to detect potential weak signals of population structure using *a priori* population assignments. We then performed isolation by distance analysis using the R packages geosphere (Hijmans 2019) and sna (Butts 2016), and a Mantel test was calculated in adegenet.

The program Structure version 2.3.4 (Pritchard et al. 2000; Falush et al. 2003; Falush et al. 2007; Hubisz et al. 2009) was used to infer genetic population structure among all populations. We subsampled the full dataset to 125 individuals that were arbitrarily selected to represent potential sample site variation (10 to 16 individuals per location) in order to reduce bias due to differences in sampled population sizes (Appendix 4.1). In this data set, we attempted to include as many samples as possible per population while maintaining a roughly equal sample size among many sampling locations. We used the admixture model without specifying *a priori* population or location information, and tested values of K from 1 to 10 with 1 million MCMC generations and a burn-in period of 250,000. We replicated the analysis for each value of K a total of 10 times, and then used CLUMPAK (Kopelman et al. 2015) to average the ten independent replicates for each value of K . The optimal value of K was assessed using both the Evanno method, using the ΔK statistic (Evanno et al. 2005), and $\ln(\text{Pr}K)$ (Pritchard et al. 2000). We then ran a PCA using this subset of data to ensure our Structure results were comparable to the PCA of the full dataset described above.

4.4 Results

After filtering, 294 individuals and 2872 genomic SNPs were retained for data analysis. Pairwise F_{st} between populations ranged from ~ 0 to 0.13 (Table 4.1), with Canmore as the most distinct. Tests for differences in pairwise population genetic differentiation also identified Canmore as having significantly different allelic distributions from all other tested populations and found some significant differences between intermediate and northern locations (Table 4.1). Observed heterozygosity was similar among populations, ranging from 0.14 – 0.19, and differences between expected and observed heterozygosity were minimal (Table 4.1). Some of the most recently detected populations, such as Battle Lake and Lac La Biche, had higher heterozygosity than some older, established populations, such as Grande Prairie and Edson, but no clear trend was evident (Table 4.1).

In the PCA for the full dataset of 294 individuals (Figure 4.1A), the first principal component, which often relates to geographic population location (Abdellaoui et al. 2013), explained 3.6% of the variation in the SNP data and distinguished northern and southern populations, as well as a distinct intermediate group between the two; for this study we used $PC1 = -5.5$ and -0.06 to delimit the intermediate cluster. The second principal component explained 1.0% of the remaining variance, and related to variation within, rather than between, populations.

No population structure was detected in either PCA or DAPC analyses when we focused on a northern dataset that comprised a total of 201 specimens, after removing individuals from the intermediate and southern clusters (Figure 4.1B; Appendix 4.2). IBD analysis of the northern locations likewise did not indicate any patterns of population differentiation based on geographic distances (Mantel test: $p=0.75$).

ΔK and $\text{Ln}(\text{Pr}K)$ from the Structure results indicated an optimal K of 2 that distinguished northern and southern population clusters (Figure 4.2). No additional separation of populations was provided by $K = 3$ and subsequent K values, in contrast to the distinct grouping of the intermediate population cluster in the first PCA axis (Figure 4.1A). There was also no population structure among the northern locations. All Battle Lake specimens and most Hinton specimens had intermediate population assignments. Structure analysis also indicated individuals that did not cluster according to the locations in which they were collected; one individual collected near Edson and one from near Slave Lake grouped with the intermediate population. A PCA using this subset of 125 samples also produced similar divisions to the Structure analysis, and closely resembled patterns seen in Figure 4.1A, indicating that the results of the Structure analysis were comparable to the population structure identified using PCA of the full data set.

Based on the full data set PCA ($n=294$), we identified several additional individuals that were collected in the northern populations but grouped with the intermediate population cluster, bringing the totals to 3 beetles from Slave lake, 5 from Whitecourt, and 1 from Edson (Appendix 4.1). We also identified 11 specimens collected in Hinton and 1 from Jasper that grouped with the northern cluster. The presence of these geographically mismatched individuals is consistent with expectations for recent dispersal events (Figure 4.3). No putative dispersers from the intermediate population were found among the newly established Lac La Biche specimens.

4.5 Discussion

Our study used population structure to investigate the dispersal dynamics of mountain pine beetle in central Alberta, identifying primary source populations as well as fine-scale dispersal from other regions. We found the same distinct north-south genetic population structure previously

described in Alberta (Janes et al. 2014; Batista et al. 2016; Trevoy et al. 2018b; Figs. 1 and 2). When we focused on individuals from northern locations, however, we found no evidence of population structure (Figure 4.1B) or isolation by distance. This is consistent with a high rate of dispersal and gene flow between these regions. The long-range dispersal capability of mountain pine beetle (Jackson et al. 2008) likely promotes genetic admixture, particularly from west to east, and may have inhibited the further development of genetically distinct populations in this region.

The extensive dispersal of mountain pine beetle also applies to mixing of population clusters. While we saw no admixture involving the southern cluster, there was mingling among the north and intermediate populations. We identified several putative dispersers with affinities to Jasper and Hinton in sites across the northern locations, as far northeast as Slave Lake (Figure 4.3; Appendix 4.1). This illustrates the considerable dispersal capability of these populations, and their potential contribution to range expansion in the north. Hinton, and one specimen at Jasper, had the reverse pattern, with some beetles having affinities to the northern cluster, indicating that several individuals likely came from a northern source (Figure 4.3). This highlights the importance of considering multiple source populations when determining infestation origins in newly established regions.

High dispersal rates from the north and intermediate populations toward the northeast and admixture among populations may have important genetic ramifications. In particular, dispersal from the genetically intermediate Jasper and Hinton region is likely to increase genetic diversity in the currently expanding eastern range of mountain pine beetle, which would otherwise be solely composed of the genetically homogenous northern population. While this introduces the possibility of potential benefits from increased genetic diversity in the leading-edge populations,

high rates of dispersal and gene flow may also prevent local adaptation (Lenormand 2002). Regardless, genetic differences between regions allow us to monitor new populations and to identify the magnitude and composition of northeastward spread from different genetic sources.

Currently, the leading edge of the mountain pine beetle range is found in jack pine forests near Lac La Biche (Mac Cormick 2020), and this population is genetically indistinguishable from other northern populations as far west as Grande Prairie. This uniformity can be explained by high rates of dispersal and regular waves of reinforcing conspecifics from other populations. In another forest pest, the spruce budworm (*Choristoneura fumiferana* Clemens), reinforcing waves of dispersers from neighboring populations may allow endemic populations to become epidemic (Larroque et al. 2020). Although their life histories differ, mountain pine beetle and spruce budworm have similar overall dynamics with large increases in population size causing epidemic conditions (Royama 1984; Larroque et al. 2020). In jack pine forests, mountain pine beetle can face intense competition from heterospecifics, such as wood-boring beetles (Klutsch et al. 2016). This may serve to mediate local population growth, but populations near Slave Lake likely make contributions to the Lac La Biche infestation. Continued recruitment in this region risks establishing large, potentially epidemic populations in the eastern jack pine forests.

4.6 Conclusions

Mountain pine beetle dispersal has been difficult to predict, but our study has helped to identify large-scale dispersal patterns in central Alberta. We demonstrated that the current Hinton infestation was derived from two sources, these likely being Jasper and, to a lesser degree, Grande Prairie. Although there was no evidence of any dispersal from the southern population cluster, there was a general trend of population expansion from the Jasper region toward the northeast,

with occasional dispersal as far northeast as Slave Lake. To date, control efforts in Alberta have been largely successful at slowing its spread, but mountain pine beetle nonetheless remains capable of extensive and rapid range expansion. Long range dispersal may limit population structure within the northernmost regions, but it also may contribute to epidemic population development. Continued focus on reducing current outbreaking populations may be necessary to minimize long-range dispersal and reinforcement of populations at the leading-edge.

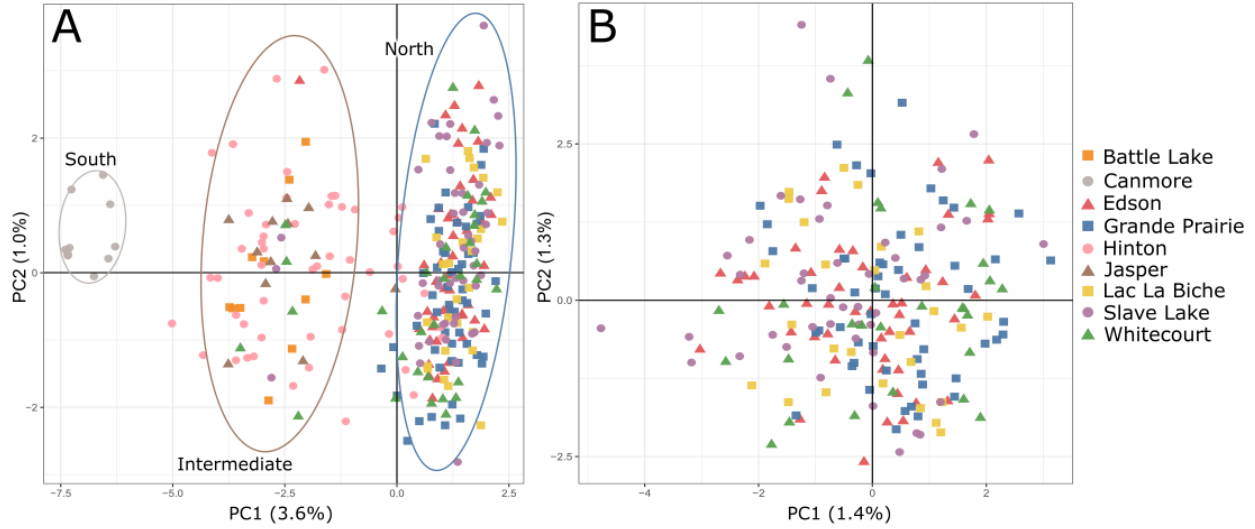


Figure 4.1: Principal component analyses (PCA) for (A) all sampling locations and individuals (n=294), and (B) northern locations (Edson, Grande Prairie, Lac La Biche, Slave Lake, and Whitecourt), with all intermediate-cluster individuals removed (n=201). In (A), ellipses were added to emphasize the south, intermediate and north clusters. These genetic population clusters were divided at $PC1 = -5.5$ and $PC1 = -0.06$ for assignment of individuals in Appendix 4.1.

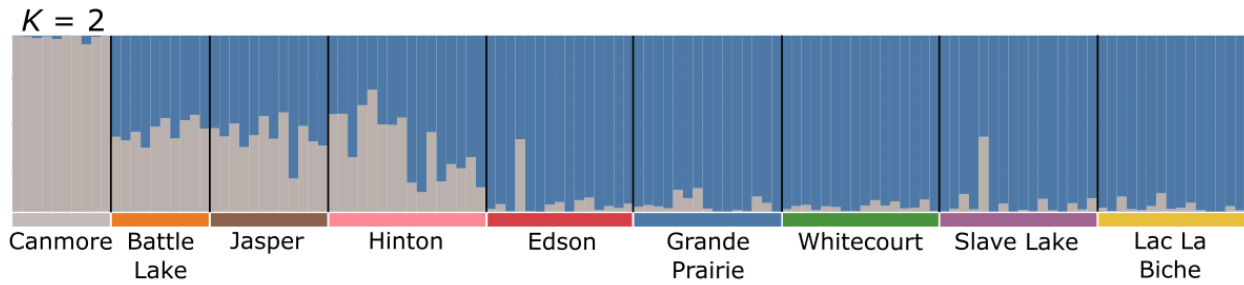


Figure 4.2: Structure analysis for equivalently sized population subsets, totaling 125 individuals. Structure assignments are shown individually. $K=2$ was the best supported number of populations. Based on individual assignments, Edson and Slave Lake populations each include a single admixed individual with a roughly equal assignment to both the northern and southern genetic clusters.

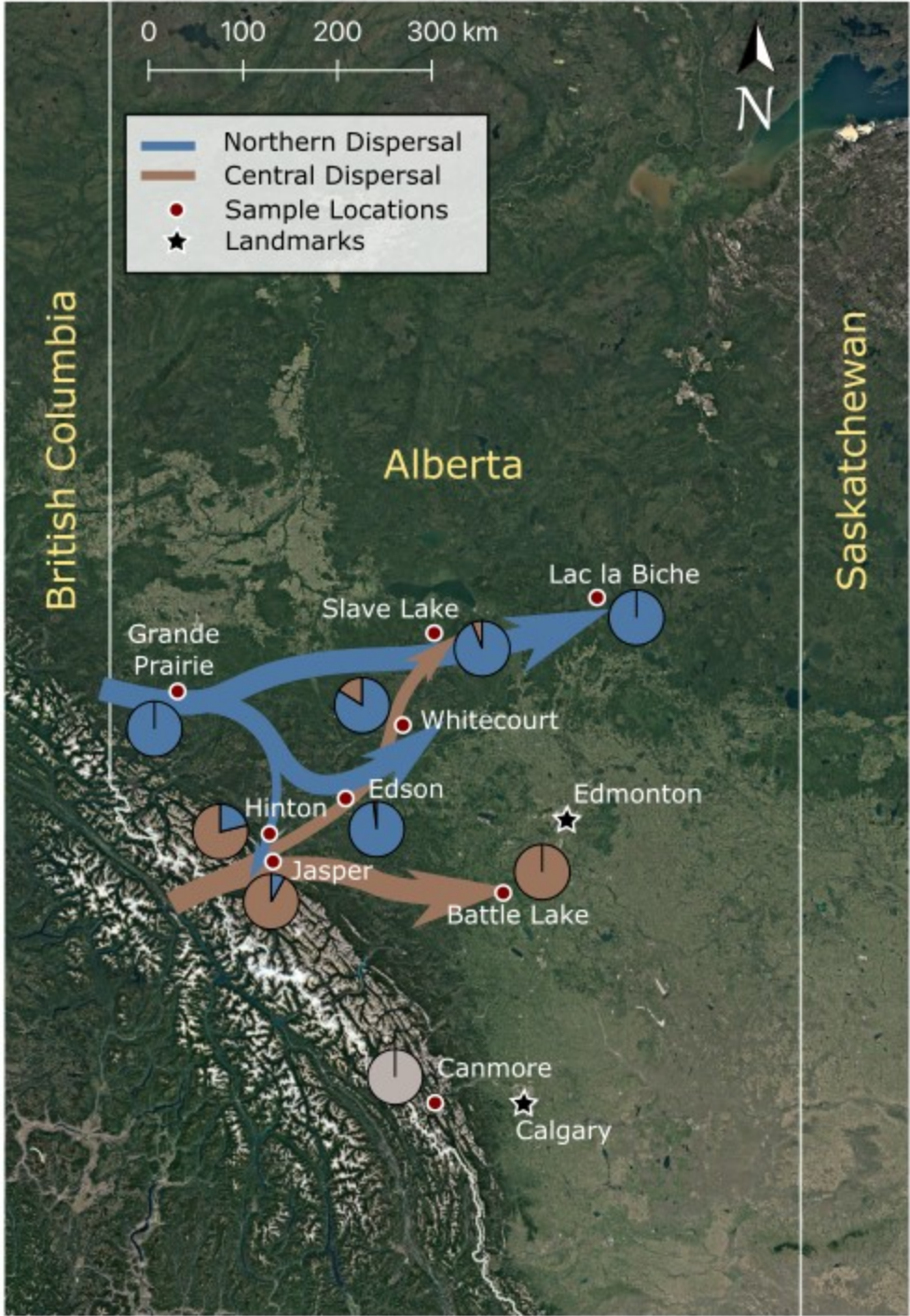


Figure 4.3: Population expansion dynamics inferred from genetic evidence based on 294 specimens collected from sites across Alberta. Pie charts for each sampling location are colored

by proportion of individuals assigned to the north (blue), intermediate (brown), and south (grey) population clusters, as determined using PCA (Figure 4.1A).

Table 4.1: Pairwise population differentiation p-values (above diagonal), Fst (below diagonal), and observed (Ho) and expected (He) population heterozygosity. Statistics were calculated using *n* individuals for each population group. Significantly differentiated population pairs (in bold) had genic differentiation values of $p < 0.001$ after Bonferroni correction.

Gen D Fst	Battle Lake	Canmore	Edson	Grande Prairie	Hinton	Jasper	Lac La Biche	Slave Lake	White-court	n	Ho	He
Battle Lake	--	0.018	0.000	0.000	1.000	1.000	0.000	0.000	0.187	52	0.19	0.19
Canmore	0.053	--	0.000	0.000	0.000	0.000	0.000	0.000	0.000	48	0.18	0.18
Edson	0.032	0.128	--	1.000	0.000	0.000	1.000	1.000	1.000	49	0.15	0.17
Grande Prairie	0.032	0.131	0.002	--	0.000	0.000	1.000	1.000	1.000	53	0.15	0.17
Hinton	0.002	0.065	0.019	0.018	--	1.000	0.000	0.000	0.000	32	0.14	0.19
Jasper	0.001	0.056	0.028	0.028	0.002	--	0.000	0.000	0.918	27	0.18	0.19
Lac La Biche	0.036	0.134	0.003	0.003	0.021	0.031	--	1.000	1.000	10	0.17	0.17
Slave Lake	0.030	0.126	0.001	0.001	0.017	0.024	0.003	--	1.000	12	0.14	0.18
White-court	0.021	0.113	0.001	0.001	0.012	0.018	0.003	0.001	--	11	0.16	0.18

Chapter 5

General Conclusions

5.1 Thesis Overview

The largest dispersals in insects involve flight that is inherently dangerous (Gatehouse 1997), energetically demanding (Wegener 1996; Wijerathna and Evenden 2019), and often involves trade-offs with capacity to colonize (Jones et al. 2020) and reproduce (Wijerathna et al. 2019). Variation in flight behavior can be an evolutionary stable strategy between different flight phenotypes (Kaitala et al. 1989; Jones et al. 2020); short-range dispersers ensure continuation of the local population, but long-range dispersers may colonize new regions, reducing intraspecific competition for resources in their source population and potentially founding new populations. This pattern of dispersal behavior can be seen in other insects (Kaitala et al. 1989), plants (Clark 1998) and fungi (Rieux et al. 2014). The research in this thesis has shown that the flight pattern of mountain pine beetle involves multiple dispersal phenotypes that are consistent with a stable dispersal strategy (Ohms et al. 2019), and there are genetic and morphological elements that influence this.

In **Chapter 2**, I characterized the general dispersal kernel (distribution of dispersal behaviors) of mountain pine beetle based on flight mill data. Although we do not capture the complete range of the dispersal kernel (Nathan et al. 2012), which would be attained by flying beetles to expiration, I showed that the majority of beetles conduct shorter distance flights, with a smaller proportion of the population flying longer distances. Several morphological factors are associated with long-range flight capacity, such as increased wing size and total weight (Shegelski et al. 2019). Many large beetles do not perform long flights, however, and this variation in flight

range could be considered an evolutionary stable strategy, as it reduces competition between flight phenotypes while providing population-wide benefits (Ohms et al. 2019; Jones et al. 2020). The lipids used to fuel flight are also important for successful host colonization (Reid and Purcell 2011; Jones et al. 2020) and reproduction (Manning and Reid 2013; Wijerathna et al. 2019); short-range dispersers, especially larger beetles with ample lipid stores, have more of such resources, as well as nearby conspecifics to assist in overcoming host defenses, ensuring a significant portion of the population succeeds in colonizing new hosts. Under most conditions, this is the most cost-effective behavior, but populations could become overcrowded, inbreeding could become detrimental, and local events (e.g.: forest fires, local host tree depletion) could cause extirpation. Beetles that succeed in long-range dispersal and colonization will experience less competition from non-dispersers, and are potentially able to outbreed due to a stronger pheromone signal (Jones et al. 2020). Maintenance of these dispersal types may be a product of different forms of selection; short range dispersers have fitness and reproductive advantages because less energy is used for dispersal, but they may have substantial competition for trees, or may face declining habitat quality, whereas long-range dispersers use more energy reserves for dispersal but may compete less for local resources upon arrival and may have better habitat quality than the site they left.

In **Chapter 3** I identified genes that may contribute to the dispersal strategy of mountain pine beetle. Many of these genes are related to increases in metabolism, but there were also several downregulated olfaction-related genes in strong fliers. In *Dendroctonus pseudotsugae* Hopkins and *D. ponderosae*, some large beetles that perform strong flights ignore important chemical cues (Bennet and Borden 1971, Jones 2019). Variable responses to olfactory cues may be a key difference in beetles that disperse long-distances, and this certainly warrants more in-depth

investigation. Further, we also identified several behavioral and endocrine system-related genes that likely also contribute to this variation in flight behavior.

Current epidemic conditions may cause a shift in the evolutionary stable dispersal strategy of mountain pine beetle. Aside from energetic costs, long distance dispersal brings the inherent risks in locating a host and conspecifics to assist in colonization. Mountain pine beetle, however, are ubiquitous across some regions, and, because of its current epidemic state, most pine trees are susceptible to mass attack. This increases the probability of finding conspecifics and a suitable host tree after a long-range dispersal flight. In **Chapter 4**, I identified several dispersers close to Slave Lake that originated from Alberta's genetically intermediate population, which could mean a dispersal distance of nearly 300 km. These dispersers likely succeeded because distant populations are already established in the Slave Lake area. Successful long-range dispersals increase genetic diversity through admixture but may also make the genetic basis of long-distance dispersal more prevalent within populations (Danchin et al. 2011), causing a shift in the equilibrium that promotes their dispersal strategy (Zhang et al. 2020). Expanded mountain pine beetle populations may signify a shift to include more long-distance dispersal phenotypes. These consequences, however, are largely dependent on a continuation of the current epidemic population state. Once populations shift back to an endemic state, population densities will reduce, and healthy trees will no longer be appropriate hosts (Burke and Carroll 2017), drastically reducing the number of susceptible hosts along with the probability of coordinating mass attacks with distant conspecifics. This would make conditions less favorable for long range dispersers.

In this thesis, I provide a methodological framework that characterizes dispersal on several scales, from geographic expansion to flight-related genetics, and this can be applied to other insect

systems. The identification of flight morphology and genetics highlights the importance of considering multiple systems and how they may interact to influence flight and potential dispersal across the landscape.

5.2 Future directions

5.2.1 Future work on flight-related morphology (Chapter 2)

We noted a “drifting behavior” in some of the beetles; such behaviors have also been noted in other *Dendroctonus* species (Atkins 1959) and may be related to long range dispersal events in which beetles can disperse hundreds of kilometers using updrafts of wind (Jackson et al. 2008). Beetles that perform “drifting behavior” during wind-mediated long-range dispersal events would conserve a significant amount of energy that would otherwise be used for active flight (Wijerathna and Evenden 2019). The duration of this “drifting behavior” may be observable in an updraft wind tunnel and quantified within a population. If a significant number of individuals show this behavior, it may have important ramifications as a long-range dispersal energy conservation strategy, and models used to predict passive seed dispersal may also be partially applicable to this form of spread. Future research on bark beetle flight morphology should thus include a broader variety of characters. There are several interesting candidates for future work, such as joint resilin (Bäumler and Büsse 2019) and wing flexibility (Mountcastle and Combes 2013), but there could be other less obvious factors involved. Perhaps the weight, angle or streamlining of the elytra are important in long flights, or the distribution of weight throughout the wing could affect wing pitch (Norberg 1972).

5.2.2 Future work on flight-related genetics (Chapter 3)

The discovery of a large set of differentially expressed flight genes is only the beginning of this research. While we identified nearly 3000 candidate flight genes, approximately 400 of these remain uncharacterized and would make interesting subjects for future studies. I am currently working with a group of researchers to produce a detailed mountain pine beetle genome, based on the Keeling et al. (2013b) draft genome, with near-chromosome-level location data. There is prominent linkage in the mountain pine beetle genome (Trevoy et al. 2018a), and, with this large group of candidate genes, we can now explore the potential relationships of dispersal capacity with genetic architecture and linkage.

There is also evidence that ketones may be involved in sustained flight in female *D. ponderosae*. Ketone bodies are found in flight muscle and fatty tissues in moths and locusts (Bailey et al. 1972; Candy et al. 1997), and we identified 3 upregulated ketone metabolism genes in females. In particular, the upregulated gene succinyl-CoA: 3-ketoacid coenzyme A transferase 1 has been linked to the use of ketones as flight fuel in another dispersing insect (Jones et al. 2015). In males, such genes may be related to the production of *exo*-brevicommin, an aggregation pheromone (Song et al. 2014), but this pheromone is not produced by females (Pierce et al. 1987). More work is needed on potential ketone bodies in these tissues in *D. ponderosae*.

Now that candidate genes have been identified, it is possible to validate and test effects of specific genes. I verified the differential expression analysis results with supporting GO trends and KEGG pathways. However, qPCR validation of some of the more independent genes would further verify the results and allow more in-depth focus of specific genes and their functions. To then test the effects of these genes in mountain pine beetle would be a challenge; they are difficult

to breed and rear in the laboratory, and they spend the majority of their lives below the bark of a host tree, making them difficult to access during development. Other model organisms such as *Tribolium* or *Drosophila* may be a plausible next step in investigating these genes through RNAi or CRISPR (Wu et al. 2020; Song et al. 2020).

For Chapter 3, I focused on total flight distance as a measure for flight capacity, but it has been argued that flight propensity is actually more translatable to realized dispersal in a natural environment (Steyn et al. 2016; Minter et al. 2018), and my association study results also support the importance of flight propensity. In future, an RNA-seq experiment using propensity as a measure to define dispersal phenotype could be informative.

During alignment to the mountain pine beetle genome for RNA-seq, millions of reads are lost either due to poor quality or because they are not represented in the draft genome. These reads are normally considered contaminants and are ignored; however, *D. ponderosae* has many known symbionts (Six and Bracewell 2015) and these unaligned reads may be from symbiotic organisms linked to flight capacity. This can be tested using a differential expression analysis. I am currently exploring this with other researchers, and we have had mixed results. This is an ongoing investigation.

5.2.3 Future work on landscape-scale dispersal (Chapter 4)

My sampling for Chapter 4 involved many samples from several locations collected over the course of 4 years. For increased detail on the population dynamics of mountain pine beetle, a more robust annual sampling regimen would be required, but would provide an excellent snapshot of the current state of infection. If this were to be achieved over several years, it would provide

relatively detailed information on population movement, mixing, and the prevalence of long-distance dispersal events.

Extensive, recent dispersal and high rates of admixture in mountain pine beetle are preventing the development of strong population structure (Janes et al. 2018); however, this provides an exceptional opportunity to watch selection and adaptation in real time. Mountain pine beetle in Grande Prairie are in different ecological conditions than those in Lac La Biche, but, due to high rates of dispersal, they are currently genetically homogenous. Once the current outbreak is over and dispersal slows, these populations can be observed and assessed for adaptation in their respective environments and host trees (assuming the populations persist in an endemic state). Identifying these adaptations, and the time it takes for them to develop, could help us understand genetic mechanisms and adaptations associated with insect-plant evolutionary relationships, and how these contribute to the success of this tree-killing bark beetle.

In conclusion, I hope that I have contributed to our understanding of several correlates of dispersal by flight. I now understand this is a Sisyphean pursuit, as the web of factors contributing to realized dispersal is potentially endless. Regardless, the study of dispersal is an enlightening challenge. I believe that this research has filled some gaps in the literature, but also, more importantly, shown others we didn't know existed.

Biography

I was born in Timmins, Ontario on March 17, 1986, to Henrietta and Roy Shegelski. I was a middle child, having an older brother, older sister, younger brother and younger sister. Needless to say, I learned to navigate the politics of life in a moderately large family. My parents always had a deep appreciation for nature, and they made sure we, the children, also saw the beauty in the natural world and its uncountable wonders, even when we had to move several times to accommodate my father's work. In time, I found I too enjoyed the changing scenery and the thrill of discovering "new lands".

When I finished high school, I joined the Canadian Armed Forces. As a young adult I had a sense that spending some time serving my country was appropriate, but I also wanted to experience the world as it *really* is. Canada is an amazing country, but you can't truly appreciate it until you've seen just how rough the world can be. I became an armored crewman and trained on various vehicles, but I spent most of my time on the leopard tanks (C2 & A6M), which I used in my two deployments to Afghanistan (winter '06 and summer '08). In that time, I got more life experience than I bargained for, but I also gained a profound appreciation for my home country and the security that so many of its citizens take for granted. While overseas, however, I also began to recognize just how diverse and amazing the "bug" world can be. Scorpions, sun spiders, praying mantises, and the weird, giant, spiny thing I caught, and subsequently lost right beside my sleeping space one evening (needless to say, "sleeping" space was not an appropriate term that night) all contributed to my growing interest for what my mother would call "creepy crawlies" (aka invertebrates).

Once I finished my contract with the army, I was relatively content with my life, doing mundane things at mundane jobs, but I eventually met my first wife, Michelle. She was a brilliant, philosophical woman that constantly challenged me, eventually convincing me to pursue a post-secondary education. After she passed away, with the much-appreciated support of friends and family I was able to see my education through. I spent a term after my undergrad teaching labs at Concordia University of Edmonton, and that is when I realized I have a passion for teaching. I then contacted Dr. Felix Sperling, an interesting professor at the University of Alberta, that happens to enjoy betting on students with odd histories. And so, I began my foray into the thick of the academic realm. My Master's project with mountain pine beetle eventually developed into a PhD, and during this time I got married to Kyla, an amazing, beautiful and strong-willed woman. Together we have two children, a brilliant boy named Isaac, and a new baby girl, Hazel, that was born only hours after this thesis was written.

Works Cited

- Abdellaoui A, Hottenga J, de Knijff P, Nivard MG, Xiao X, Scheet P, Brooks A, Ehli EA, Hu Y, Davies GE, Hudziak JJ, Sullivan PF, van Beijsterveldt T, Willemsen G, de Geus EJ, Penninx BWJH, Boomsma DI. 2013. Population structure, migration, and diversifying selection in the Netherlands. *European Journal of Human Genetics*, **21**: 1277-1285.
- Ainslie B, Jackson PL. 2011. Investigation into mountain pine beetles above canopy dispersion using weather radar and an atmospheric dispersion model. *Aerobiologia*, **27**: 51-65.
- Alberta Agriculture and Forestry. 2016. Mountain pine beetle detection and management in Alberta (Blue Book). Government of Alberta. Available at:
<[https://www1.agric.gov.ab.ca/\\$department/deptdocs.nsf/all/formain15619/\\$FILE/MPB%20Blue%20Book%20-%20Complete%20Guide%202016.pdf](https://www1.agric.gov.ab.ca/$department/deptdocs.nsf/all/formain15619/$FILE/MPB%20Blue%20Book%20-%20Complete%20Guide%202016.pdf)> [Accessed 17 April 2018]
- Alfaro RI, Campbell E, Hawkes BC. 2010. Historical frequency, intensity and extent of mountain pine beetle disturbance in British Columbia. Natural Resources Canada, Canadian Forest Service, Pacific Forestry Centre, Victoria, BC. Mountain Pine Beetle Working Paper. 52 p
- Armstrong JD, Texada MJ, Munjaal R, Baker DA, Beckingham KM. 2006. Gravitaxis in *Drosophila melanogaster*: a forward genetic screen. *Genes, Brain and Behavior*, **5**: 222-239.

- Atkins MD. 1959. A study of the flight of the Douglas-fir beetle, *Dendroctonus pseudotsugae*.
Hopk. (Coleoptera: Scolytidae). I. Flight preparation and response. The Canadian
Entomologist **91**: 283-291.
- Atkins MD. 1961. A study of the flight of the douglas-fir beetle *Dendroctonus pseudotsugae*
Hopk. (Coleoptera: Scolytidae). III. Flight Capacity. The Canadian Entomologist, **93**:
467-474.
- Atkins MD. 1966. Laboratory Studies on the Behaviour of the Douglas-fir Beetle, *Dendroctonus*
pseudotsugae Hopkins. The Canadian Entomologist, **98**: 953-991.
- Atkins MD. 1960. A study on the flight of the Douglas-fir beetle, *Dendroctonus pseudotsugae*
Hopk. (Scolytidae). University of British Columbia.
- Atkins MD, Farris SH. 1962. A contribution to the knowledge of flight muscle changes in the
Scolytidae (Coleoptera). The Canadian Entomologist, **94**: 25-32.
- Augspurger, CK. 1986. Morphology and Dispersal Potential of Wind-Dispersed Diaspores of
Neotropical Trees. American Journal of Botany, **73**: 353-363.
- Aukema BH, Carroll AL, Zheng Y, Zhu J, Raffa KF, Moore RD, Stahl K, Taylor SW. 2008.
Movement of outbreak populations of mountain pine beetle: influences of spatiotemporal
patterns of climate. Ecography, **31**: 348-358.
- Aw T, Schlauch K, Keeling CI, Young S, Bearfield JC, Blomquist GJ, Tittiger C. 2010.
Functional genomics of mountain pine beetle (*Dendroctonus ponderosae*) midguts and
fat bodies. BMC Genomics, **11**: 1165-1188.

- Axelsson JN, Alfaro RI, Hawkes B. 2009. Influence of fire and mountain pine beetle on the dynamics of lodgepole pine stands in British Columbia, Canada. *Forest Ecology and Management*, **257**: 1874-1882.
- Azevedo RBR, James AC, McCabe J, Partridge L. 1998. Latitudinal variation of wing: thorax size ratio and wing-aspect ratio in *Drosophila melanogaster*. *Evolution*, **52**: 1353-1362.
- Bailey E, Horne JA, Izatt MEG, Hill L. 1972. Role of ketone bodies in the metabolism of the adult desert locust. *Biochemical Journal*, **128**: 79.
- Bateman AJ. 1950. Is gene dispersion normal? *Heredity*, **4**: 353–363.
- Bates D, Maechler M, Bolker B, Walker S. 2015. Fitting Linear Mixed Effects Models Using lme4. *Journal of Statistical Software*, **67**: 1-48.
- Batista PD, Janes JK, Boone CK, Murray BW, Sperling FAH. 2016. Adaptive and neutral markers both show continent-wide population structure of mountain pine beetle (*Dendroctonus ponderosae*). *Ecology and Evolution*, **6**: 6292–6300.
- Bäumler F, Büsse S. 2019. Resilin in the flight apparatus of Odonata (Insecta)-cap tendons and their biomechanical importance for flight. *Biology Letters*, **15**: 20190127.
- Bennett RB, Borden JH. 1971. Flight Arrestment of Tethered *Dendroctonus pseudotsugae* and *Trypodendron lineatum* (Coleoptera: Scolytidae) in Response to Olfactory Stimuli. *Annals of the Entomological Society of America*, **64**: 1273-1286.

- Betts CR, Wootton RJ. 1988. Wing shape and flight behaviour in butterflies (Lepidoptera: Papilionoidea and Hesperioidea): A preliminary analysis. *Journal of Experimental Biology*, **138**: 271-288.
- Bhakthan NMG, Borden JH, Nair KK. 1970. Fine structure of degenerating and regenerating flight muscles in a bark beetle, *Ips confusus*. *Journal of Cell Science*, **6**: 807–819.
- Bleiker KP, Smith GD, Humble LM. 2017. Cold tolerance of mountain pine beetle (Coleoptera: Curculionidae) eggs from historic and expanded ranges. *Environmental Entomology*, **46**: 1165-1170.
- Bleiker KP, Smith GD. 2019. Cold tolerance of mountain pine beetle (Coleoptera: Curculionidae) Pupae. *Environmental Entomology*, **48**: 1412-1417.
- Bleiker K, Six DL. 2007. Dietary benefits of fungal associates to an eruptive herbivore: potential implications of multiple associates on host population dynamics. *Environmental Entomology*, **36**: 1384–1396.
- Bleiker KP. 2019. Risk assessment of the threat of mountain pine beetle to Canada’s boreal and eastern pine forests. *In* Canadian Council of Forest Ministers Report Fo79-14/2014E-PDF.
- Bleiker KP, O’Brien MR, Smith GD, Carroll AL. 2014. Characterisation of attacks made by the mountain pine beetle (Coleoptera: Curculionidae) during its endemic population phase. *The Canadian Entomologist*, **146**: 271–284.

- Bleiker KP, Potter SE, Lauzon CR, Six DL. 2009. Transport of fungal symbionts by mountain pine beetle. *The Canadian Entomologist*, **141**: 503–514.
- Blomquist GJ, Figueroa-Teran R, Aw M, Song M, Gorzalski A, Abbott NL, Chang E, Tittiger C. 2010. Pheromone production in bark beetles. *Insect Biochemistry and Molecular Biology*, **40**: 699-712.
- Boggs CL. 1992. Resource Allocation: exploring connections between foraging and life history. *Functional Ecology*, **6**: 508-518.
- Borden JH, Slater CE. 1969. Flight muscle volume changes in *Ips confuses* (Coleoptera: Scolytidae). *Canadian Journal of Zoology*, **47**: 29–32.
- Bowler DE, Benton TG. 2005. Causes and consequences of animal dispersal strategies: Relating individual behaviour to special dynamics. *Biological Reviews of the Cambridge Philosophical Society*, **80**: 205-22.
- Bradbury PJ, Zhang Z, Kroon DE, Casstevens TM, Ramdoss Y, Buckler ES. 2007. TASSEL: software for association mapping of complex traits in diverse samples. *Bioinformatics*, **23**: 2633-2635.
- Bridges JR, 1982. Effects of juvenile hormone on pheromone synthesis in *Dendroctonus frontalis*. *Environmental Entomology*, **11**: 417e420.
- Burke JL, Carroll AL. 2017. Breeding matters: natal experience influences population state-dependent host acceptance by an eruptive insect herbivore. *PLoS ONE*, **12**: e0172448.

- Campbell EO, Davis CS, Dupuis JR, Muirhead K, Sperling FAH. 2017. Cross-platform compatibility of de novo-aligned SNPs in a nonmodel butterfly genus. *Molecular Ecology Resources*, **17**: e84-e93.
- Candy DJ, Becker A, Wegener G. 1997. Coordination and integration of metabolism in insect flight. *Comparative Biochemistry & Physiology B*, **117**: 497-512
- Carroll AL, Taylor SW, Régnière J, Safranyik L. 2004. Effects of climate and climate change on the mountain pine beetle (pp 221-230) in Shore TL, Brooks JE, Stone JE (eds) *Challenges and Solutions: Proceedings of the Mountain Pine Beetle Symposium*. Kelowna, British Columbia, Canada October 30 - 31, 2003. Canadian Forest Services.
- Catchen JM, Amores A, Hohenlohe P, Cresko W, Postlethwait JH. 2011. Stacks: building and genotyping loci de novo from short-read sequences. *G3: Genes, Genomes, Genetics*, **1**: 171-182.
- Cerezke HF. 1989. Mountain pine beetle aggregation semiochemical use in Alberta and Saskatchewan, 1983-1987. In Amman GD. (Compiler). *Proceedings-Symposium on the management of lodgepole pine to minimize losses to the mountain pine beetle, July 12-14, 1988, Kalispell, Montana* (pp 108-113). Ogden, Utah: USDA Forest Service, Intermountain Research Station.
- Chai P, Srygley RB. 1990. Predation and the flight, morphology, and temperature of neotropical rain-forest butterflies. *American Naturalist*. **135**: 748-765.

- Chapman DS, Dytham C, Oxford GS. 2006. Modelling population redistribution in a leaf beetle: an evaluation of alternative dispersal functions. *Journal of Animal Ecology*, **76**: 36-44.
- Chapman RF. 1998. *The Insects: Structure and function* (4th ed.). Cambridge: Cambridge University Press.
- Che R, Jack JR, Motsinger-Reif AA, Brown CC. 2014. An adaptive permutation approach for genome-wide association study: evaluation and recommendations for use. *BioData Mining*, **7**: 9.
- Chen H, Walton A. 2011. Mountain pine beetle dispersal: spatiotemporal patterns and role in the spread and expansion of the present outbreak. *Ecosphere*, **2**: 1-17.
- Chiu CC, Keeling CI, Bohlmann J. 2018. Cytochromes P450 preferentially expressed in antennae of the mountain pine beetle. *Journal of Chemical Ecology*. **45**:178-186.
- Chiu CC, Keeling CI, Bohlmann J. 2019. The cytochrome P450 CYP6DE1 catalyzes the conversion of α -pinene into the mountain pine beetle aggregation pheromone *trans*-verbenol. *Scientific Reports*, **9**: 1477.
- Chubaty AM, Hart M, Rotenberg D. 2014. ‘To tree or not to tree’: the role of energy limitation on host tree acceptance in a bark beetle. *Evolutionary Ecology Research*, **16**: 337-349.
- Clark JS. 1998. Why trees migrate so fast: confronting theory with dispersal biology and the paleorecord. *American Naturalist*, **152**: 204–224.

- Conn JE, Borden JH, Hunt DW, Holman J, Whittney HS, Spanier OJ, Pierce HD Jr, Oehlschlager AC. 1984. Pheromone production by axenically reared *Dendroctonus ponderosae* and *Ips paraconfusus* (Coleoptera: Scolytidae). *Journal of Chemical Ecology*, **10**: 281-290.
- Cooke BJ. 2009. Forecasting mountain pine beetle-overwintering mortality in a variable environment. Natural Resources Canada, Canadian Forest Service, Pacific Forestry Centre, Victoria, BC. Mountain Pine Beetle Working Paper 2009-03.
- Corbett LJ, Withey P, Lantz VA, Ochuodho TO. 2015. The economic impact of the mountain pine beetle infestation in British Columbia: provincial estimates from a CGE analysis. *Forestry*, **89**: 100-105.
- Crawley MJ. 2013. Regression (Chapter 10). In *The R book* (2nd ed) (pp 449-497). West Sussex, United Kingdom: John Wiley & Sons, Ltd.
- Cullingham, CI, Cooke JEK, Dang S, Cooke BJ, Coltman DW. 2011. Mountain Pine Beetle host-range expansion threatens the boreal forest. *Molecular Ecology*, **20**: 2157-2171.
- Cullingham CI, Janes JK, Hamelin RC, James PMA, Murray BW, Sperling FAH. 2019. The contribution of genetics and genomics to understanding the ecology of the mountain pine beetle system. *Canadian Journal of Forest Research*. **49**: 721–730.
- Cullingham CI, Roe AD, Sperling FAH, Coltman DW. 2012. Phylogeographic insights into an irruptive pest outbreak. *Ecology and Evolution*, **2**: 908–919.

- Danchin E, Charmantier A, Champagne FA, Mesoudi A, Pujol B, Blanchet S. 2011. Beyond DNA: integrating inclusive inheritance into an extended theory of evolution. *Nature Reviews Genetics*, **12**: 475-486.
- Danecek P, Auton A, Abecasis G, Albers CA, Banks E, DePristo MA, Handsaker R, Lunter G, Marth G, Sherry ST, McVean G, Durbin R, 1000 Genomes Project Analysis Group. 2011. The variant call format and VCFtools. *Bioinformatics*, **27**: 2156-2158.
- de la Giroday HC, Carroll AL, Aukema BH. 2012. Breach of the northern Rocky Mountain geoclimatic barrier: initiation of range expansion by the mountain pine beetle. *Biogeography*, **39**: 1112-1123.
- de la Giroday HMC, Carroll AL, Lindgren BS, Aukema BH. 2011. Incoming! Association of landscape features with dispersing mountain pine beetle populations during a range expansion event in western Canada. *Landscape Ecology*. **26**: 1097–1110.
- Dempster JP, King ML, Lakhani KH. 1976. The status of the swallowtail butterfly in Britain. *Ecological Entomology*, **1**: 71-84.
- Dominguez E, Abdala V. 2019. Morphology and evolution of the wing bullae in South American Leptophlebiidae (Ephemeroptera). *Journal of Morphology*, **280**: 95-102.
- Dudley R. 1990. Biomechanics of flight in neotropical butterflies: morphometrics and kinematics. *Journal of Experimental biology*, **150**: 37-53.

- Eidson EL, Mock KE, Bentz BJ. 2017. Mountain pine beetle host selection behavior confirms high resistance in Great Basin bristlecone pine. *Forest Ecology and Management*, **402**: 12-20.
- Elkin CM, Reid ML. 2004. Attack and reproductive success of mountain pine beetles (Coleoptera: Scolytidae) in fire-damaged lodgepole pines. *Environmental Entomology*, **33**: 1070-1080.
- Elkin CM, Reid ML. 2005. Low energy reserves and energy allocation decisions affect reproduction by mountain pine beetles, *Dendroctonus ponderosae*. *Functional Ecology*, **19**: 102-109.
- Erion R., Sehgal A. 2013. Regulation of insect behavior via the insulin-signaling pathway. *Frontiers in Physiology*, **4**: 353.
- Esch ED, Langor DW, Spence JR. 2016. Gallery success, brood production, and condition of mountain pine beetle (Coleoptera: Curculionidae) reared in whitebark and lodgepole pine from Alberta, Canada. *Canadian Journal of Forest Research*, **46**: 557-563.
- Eveleigh ES, Lucarotti CJ, McCarthy PC, Morin B, Royama T, Thomas AW. 2007. Occurrence and effects of *Nosema fumiferanae* infections on adult spruce budworm caught above and within the forest canopy. *Agriculture and Forest Entomology*, **9**: 247-258.
- Evenden ML, Whitehouse CM, Sykes J. 2014. Factors influencing flight capacity of the mountain pine beetle (Coleoptera: Curculionidae: Scolytinae). *Environmental Entomology*, **43**: 187-196.

- Fairbairn DJ, Roff DA. 1990. Genetic correlations among traits determining migratory tendency in sand cricket *Gryllus firmus*. *Evolution*, **44**: 1787-1795.
- Falush D, Stephens M, Pritchard JK. 2003. Inference of population structure using multilocus genotype data: linked loci and correlated allele frequencies. *Genetics*, **164**: 1567-1587.
- Falush D, Stephens M, Pritchard JK. 2007. Inference of population structure using multilocus genotype data: dominant markers and null alleles. *Molecular Ecology Notes*, **7**: 574-578.
- Fettig CJ, Steed BE, Munson AS, Progar RA, Mafra-Neto A. 2020. Evaluating doses of SPLAT®verb to protect lodgepole pine trees and stands from mountain pine beetle. *Crop Protection*, **136**: 105228.
- Fettig CJ. 2016. Native bark beetles and wood borers in Mediterranean forests of California. *In* *Insects and Diseases of Mediterranean Forest Systems*. Edited by Paine T, Lieutier F. Springer, Cham.
- Fraser JD, Bonnett TR, Keeling CI, Huber DPW. 2017. Seasonal shifts in accumulation of glycerol biosynthetic gene transcripts in mountain pine beetle, *Dendroctonus ponderosae* Hopkins (Coleoptera: Curculionidae), larvae. *PeerJ*. **5**: e3284.
- Frazier MR, Harrison JF, Kirkton SD, Roberts SP. 2008. Cold rearing improves cold-flight performance in *Drosophila* via changes in wing morphology. *The Journal of Experimental Biology*, **211**: 2116-2122.

- Gao X, Lee K, Reid MA, Sanderson SM, Qiu C, Li S, Liu J, Locasale J. 2018. Serine Availability influences mitochondrial dynamics and function through lipid metabolism. *Cell Reports*, **22**: 3507-3520.
- Gatehouse AG. 1997. Behavior and ecological genetics of wind-borne migration by insects. *Annual Review of Entomology* **42**: 475–502.
- Godefroid M, Meseguer AS, Sauné L, Genson G, Streito, J-C, Rossi J-P, Riverón AZ, Mayer F, Cruaud A, Rasplus J-Y. 2019. *Molecular Phylogenetics and Evolution*, **139**: 106528.
- Goodsman DW, Koch D, Whitehouse C, Evenden ML, Cooke BJ, Lewis MA. 2016. Aggregation and a strong Allee effect in a cooperative outbreak insect. *Ecological Applications*, **26**: 2623-2636.
- Götz S, Garcia-Gomez JM, Terol J, Williams TD, Nagaraj SH, Nueda MJ, Robles M, Talon M, Dopazo J, Conesa A. 2008. High-throughput functional annotation and data mining with the Blast2GO suite. *Nucleic Acids Research*, **36**: 3420-3435.
- Gruber B, Georges A. 2019. dartR: Importing and analysing SNP and silicodart data generated by genome-wide restriction fragment analysis. R package version 1.1.11 [online]. Available from <https://CRAN.R-project.org/package=dartR> [accessed 27 November 2019]
- Gruntenko NE, Rauschenbach IY . 2008. Interplay of JH, 20E and biogenic amines under normal and stress conditions and its effect on reproduction. *Journal of Insect Physiology*, **54**: 902-908.

- Haas F, Gorb S, Blickhan R. 2000. The function of resilin in beetle wings. Proceedings of the Royal Society of London B, **267**: 1375-1381.
- Hart SJ, Schoennagel T, Veblen TT, Chapman TB. 2015. Area burned in the western United States is unaffected by recent mountain pine beetle outbreaks. Proceedings of the National Academy of Sciences of the United States of America, **112**: 4375-4380.
- Hassall C, Thompson DJ, Harvey IF. 2009. Variation in morphology between core and marginal populations of three British damselflies. International Journal of Freshwater Entomology, **31**: 187-197.
- Hassall C. 2015. Strong geographical variation in wing aspect ratio of a damselfly, *Calopteryx maculate* (Odonata: Zygoptera). PeerJ, **3**: e1219.
- Hijmans RJ. 2019. geosphere: Spherical Trigonometry. R package version 1.5-10 [online]. Available from <https://CRAN.R-project.org/package=geosphere> [accessed 16 August 2019]
- Hill JK, Thomas CD, Blakeley DS. 1999a. Evolution of flight morphology in a butterfly that has recently expanded its geographic range. Oecologia, **121**: 165-170.
- Hill JK, Thomas CD, Lewis OT. 1999b. Flight morphology in fragmented populations of a rare British butterfly, *Hesperia comma*. Biological Conservation, **87**: 277-283.
- Hopping GR, Mathers WG. 1945. Observations on outbreaks and control of the mountain pine beetle in the lodge-pole pine stands of western Canada. The Forestry Chronicle, **21**: 98-108.

- Huang Y, Gu X, Peng X, Tao M, Chen G, Zhang X. 2020. Effect of short-term high-temperatures on the growth, development and reproduction in the fruit fly, *Bactrocera tau* (Diptera: Tephritidae). *Scientific Reports*, **10**: 6418.
- Hubbard RM, Rhoades CC, Elder K, Negron J. 2013. Changes in transpiration and foliage growth in lodgepole pine trees following mountain pine beetle attack and mechanical girdling. *Forest Ecology and Management*, **289**: 312-317.
- Huber DPW, Robert JA. 2016. The proteomics and transcriptomics of early host colonization and overwintering physiology in the mountain pine beetle, *Dendroctonus ponderosae* Hopkins (Coleoptera: Curculionidae). *Advances in Insect Physiology*, **50**: 101-128.
- Hubisz MJ, Falush D, Stephens M, Pritchard JK. 2009. Inferring weak population structure with the assistance of sample group information. *Molecular Ecology Resources*, **9**: 1322-1332.
- Hulcr J, Atkinson TH, Cognato AI, Jordal BH, McKenna DD. 2015. Morphology, taxonomy, and phylogenetics of bark beetles. In *Bark Beetles: Biology and Ecology of Native and Invasive Species*. Edited by Vega FE, Hofstetter RW. Academic Press, Elsevier. pp. 41–81.
- Hulm PE. 2017. Climate change and biological invasions: evidence, expectations, and response options. *Biological reviews*, **92**: 1297-1313.
- Iga M, Kataoka H. 2012. Recent studies on insect hormone metabolic pathways mediated by cytochrome P450 enzymes. *Biological and Pharmaceutical Bulletin*, **35**: 838-843.

- Jackson PL, Straussfogel D, Lindgren BS, Mitchell S, Murphy B. 2008. Radar observation and aerial capture of mountain pine beetle, *Dendroctonus ponderosae* Hopk. (Coleoptera: Scolytidae) above the forest canopy. Canadian Journal of Forest Research, **38**: 2313-2327.
- Jactel H. 1993. Individual variability of the flight potential of *Ips sexdentatus* Boern. (Coleoptera: Scolytidae) in relation to day of emergence, sex, size, and lipid content. Can. Entomol. **125**: 919–930.
- Janes JK, Roe AD, Rice AV, Gorrell JC, Coltman DW, Langor DW, Sperling FAH. 2016. Polygamy and an absence of fine-scale structure in *Dendroctonus ponderosae* (Hopk.) (Coleoptera: Curculionidae) confirmed using molecular markers. Heredity, **116**: 68–74.
- Janes JK, Li Y, Keeling CI, Yuen MMS, Boone CK, Cooke JEK, Bohlmann J, Huber DPW, Murray BW, Coltman DW, Sperling FAH. 2014. How the mountain pine beetle (*Dendroctonus ponderosae*) breached the Canadian Rocky Mountains. Molecular Biology and Evolution, **31**: 1803–1815.
- Janes JK, Worth JRP, Batista PD, Sperling FAH. 2018. Inferring ancestry and divergence events in a forest pest using low-density single-nucleotide polymorphisms. Insect Systematics and Diversity, **2**: 1-9.
- Johnson P, Rees HH. 1977. The mechanism of C-20 hydroxylation of alpha-ecdysone in the desert locust, *Schistocerca gregaria*. Biochemical Journal, **168**: 513–520.

- Johnson PCD. 2014. Extension of Nakagawa Schielzeth's R^2_{GLMM} to random slopes models. *Methods in Ecology and Evolution*, **5**: 944-946.
- Jombart T. 2008. adegenet: a R package for the multivariate analysis of genetic markers. *Bioinformatics*, **24**: 1403-1405.
- Jombart T, Ahmed I. 2011. adegenet 1.3-1: new tools for the analysis of genome-wide SNP data. *Bioinformatics*, **27**: 3070-3071.
- Jombart T, Devillard S, Balloux F. 2010. Discriminant analysis of principle components: a new method for the analysis of genetically structured populations. *BMC Genetics*, **11**: 94.
- Jones CM, Papanicolaou A, Mironidis GK, Vontas J, Yang Y, Lim KS, Oakshott JG, Bass C, Chapman JW. 2015. Genomewide transcriptional signatures of migratory flight activity in a globally invasive insect pest. *Molecular Ecology*, **24**: 4901-4911.
- Jones KL, Rajabzadeh R, Ishangulyyeva G, Erbilgin N, Evenden ML. 2020. Mechanisms and consequences of flight polyphenisms in an outbreaking bark beetle species. *Journal of Experimental Biology*, **223**: jeb219642.
- Jones KL, Shegelski VA, Marculis NG, Wijerathna AN, Evenden ML. 2019. Factors influencing dispersal by flight in bark beetles (Coleoptera: Curculionidae: Scolytinae): from genes to landscapes. *Canadian Journal of Forest Research*, **49**: 1024-1041.
- Jones KL. 2019. Influence of semiochemical cues on mountain pine beetle flight and subsequent effect of flight on host colonization process [Master's Thesis]. Edmonton (AB): University of Alberta. 110p.

- Jordal BH, Cognato AI. 2012. Molecular phylogeny of bark and ambrosia beetles reveals multiple origins of fungus and farming during periods of global warming. *BMC Evolutionary Biology*, **12**: 133.
- Kaitala V, Kaitala A, Getz W. 1989. Evolutionary stable dispersal of a waterstrider in a temporally and spatially heterogeneous environment. *Evolutionary Ecology*, **3**: 283-298.
- Kanehisa M, Goto S. 2000. KEGG: Kyoto Encyclopedia of Genes and Genomes. *Nucleic Acids Research*, **28**: 27-30.
- Kautz M, Imron MA, Dworschak K, Schopf R. 2016. Dispersal variability and associated population-level consequences in tree-killing bark beetles. *Movement Ecology*, **4**: 9.
- Keeling CI, Chiu CC, Aw T, Li M, Henderson H, Tittiger C, Weng H-B, Blomquist GJ, Bohlman J. 2013a. Frontalin pheromone biosynthesis in the mountain pine beetle, *Dendroctonus ponderosae*, and the role of isoprenyl diphosphate synthases. *PNAS*, **110**: 18838-18843.
- Keeling CI, Yuen MM, Liao NY, et al. 2013b. Draft genome of the mountain pine beetle, *Dendroctonus ponderosae* Hopkins, a major forest pest. *Genome Biology*, **14**: R27
- Kim D, Pertea G, Trapnell C, Pimentel H, Kelley R, Salzberg S. 2013. Tophat2: accurate alignment of transcriptomes in the presence of insertions, deletions and gene fusions. *Genome Biology*, **14**: R36.

- Klutsch JG, Najar A, Cale JA, Erbilgin N. 2016. Direction of interaction between mountain pine beetle (*Dendroctonus ponderosae*) and resource-sharing wood-boring beetles depends on plant parasite infection. *Oecologia*, **182**: 1-12.
- Koenker R. 2017. Quantreg: Quantile Regression. R package version 5.29. URL <https://CRAN.R-project.org/package=quantreg>
- Kopelman NM, Mayzel J, Jakobsson M, Rosenberg NA, Mayrose I. 2015. CLUMPAK: a program for identifying clustering models and packaging population structure inferences across K. *Molecular Ecology Resources*, **15**: 1179-1191.
- Kristensen NP, De Barro PJ, Schellhorn. 2013. The initial dispersal and spread of an international invader at three spatial scales. *PLoS ONE*, **8**: e62407.
- Kumar S, Chen D, Jang C, Nall A, Zheng X, Sehgal A. 2014 An ecdysone-responsive nuclear receptor regulates circadian rhythms in *Drosophila*. *Nature Communications*, **5**: 5697.
- Kurz WA, Dymond CC, Stinson G, Rampley GJ, Neilson ET, Carroll AL, Ebata T, Safranyik L. 2008. Mountain pine beetle and forest carbon feedback to climate change. *Nature*, **452**: 987-990.
- Langmead B, Salzberg S. 2012. Fast gapped-read alignment with Bowtie 2. *Nature Methods*, **9**: 357-359.
- Langor DW, Spence JR. 1991. Host effects on allozyme and morphological variation of the mountain pine beetle, *Dendroctonus ponderosae* Hopkins (Coleoptera: Scolytidae). *The Canadian Entomologist*, **123**: 395-410.

- Laporte J, Blondeau F, Buj-Bello A, Mandel JL. 2001. The myotubularin family: from genetic disease to phosphoinositide metabolism. *Trends in Genetics*, **17**: 221-228.
- Larroque J, Johns R, Canape J, Morin B, James PMA. 2020. Spatial genetic structure at the leading edge of a spruce budworm outbreak: the role of dispersal in outbreak spread. *Forest Ecology and Management*, **461**: 117965.
- Latty TM, Reid ML. 2010. Who goes first? Condition and danger dependent pioneering in a group-killing bark beetle (*Dendroctonus ponderosae*). *Behavioral Ecology and Sociobiology*, **64**: 639-646.
- Lawrence M, Huber W, Pagés H, Aboyoun P, Carlson M, Gentleman R, Morgan MT, Carey VJ. 2013. Software for computing and annotating genomic ranges. *PLoS Comput Biol*, **9**: e1003118.
- Lee S, Hamelin RC, Six DL, Breuil C. 2007. Genetic diversity and the presence of two distinct groups in *Ophiostom clavigerum* associated with *Dendroctonus ponderosae* in BC and the northern Rocky Mountains. *Phytopathology*, **97**: 1177–1185.
- Lefcheck JS. 2015 piecewiseSEM: Piecewise structural equation modeling in R for ecology, evolution, and systematics. *Methods in Ecology and Evolution*, **7**: 573-579.
- Lenormand T. 2002. Gene flow and the limits to natural selection. *Trends in Ecology & Evolution*. **17**: 183-189.
- Lewis MA, Nelson W, Xu C. 2009. A structured threshold model for mountain pine beetle outbreak. *Bulletin of Mathematical Biology*, **72**: 565-589.

- Li H, Durbin R. 2009. Fast and accurate short read alignment with Burrows-Wheeler Transform. *Bioinformatics*, **25**: 1754-60.
- Li H, Handsaker B, Wysoker A, Fennell T, Ruan J, Homer N, Marth G, Abecasis G, Durbin R, 1000 Genome Project Data Processing Subgroup. 2009. The Sequence Alignment/Map format and SAMtools. *Bioinformatics*, **25**: 2078-2079.
- Lindgren BS, Raffa KF. 2013. Evolution of tree-killing in bark beetles (Coleoptera, Curculionidae): trade-offs between the maddening crowds and a sticky situation. *The Canadian Entomologist*, **145**: 471–495.
- Liu H, Mardahl-Dumesnil M, Sweeney ST, O’Kane CJ, Bernstein SI. 2003. *Drosophila* paramyosin is important for myoblast fusion and essential for myofibril formation. *Journal of Cell Biology*, **160**: 899-908.
- Lorenz LJ, Hall JC, Rosbash M. 1989. Expression of a *Drosophila* mRNA is under circadian clock control during pupation. *Development*, **107**: 869-880.
- Love MI, Huber W, Anders S. 2014. Moderated estimation of fold change and dispersion for RNA-Seq data with DESeq2. *Genome Biology*, **15**: 550.
- Mac Cormick J. 2020. Spread management action collaborative. *Bugs and Diseases*, **31**: 6.
- Machado DN, Costa EC, Guedes JVC, Barbosa LR, Martínez G, Mayorga SI, Ramos SO, Branco M, Garcia A, Vanegas-Rico JM, Jiménez-Quiroz E, Laudonia S, Novoselsky T, Hodel DR, Arakelin G, Silva H, Perini CR, Valmorbidia I, Ugalde GA, Arnemann JA. 2020. One maternal lineage leads the expansion of *Thaumastocoris peregrinus*

- (Hemiptera: Thaumastocoridae) in the New and Old Worlds. *Scientific Reports*, **10**: 3487.
- Manning CG, Reid ML. 2013. Sub-lethal effects of monoterpenes on reproduction by mountain pine beetles. *Agriculture and Forest Entomology*, **15**: 262-271.
- Marden JH, Fescemyer HW, Schilder RJ, Doerfler WR, Vera JC, Wheat CW. 2012. Genetic variation in HIF signalling underlies quantitative variation in physiological and life-history traits within lowland butterfly populations. *Evolution*, **67**: 1105-1115.
- Martin M. 2011. Cutadapt removed adapter sequences from high-throughput sequencing reads. *EMBnet.journal*, **17**: 10-11.
- McCambridge WF, Mata SA Jr. 1969. Flight muscle changes in black hills beetles, *Dendroctonus ponderosae* (Coleoptera: Scolytidae), during emergence and egg laying. *The Canadian Entomologist*, **101**: 507–512.
- Miller DR, Lindgren BS, Borden JH. 2005. Dose-dependent pheromone responses of mountain pine beetle in stands of lodgepole pine. *Environmental Entomology*. **34**: 1019–1027.
- Minter M, Pearson A, Lim KS, Wilson K, Chapman JW, Jones CM. 2018. The tethered flight technique as a tool for studying life-history strategies associated with migration in insects. *Ecological Entomology*, **43**: 397-411
- Mock KE, Bentz BJ, O’Neill EM, Chong JP, Orwin J, Pfrender ME. 2007. Landscape-scale genetic variation in a forest outbreak species, the mountain pine beetle (*Dendroctonus ponderosae*). *Molecular Ecology*, **16**: 553–568.

- Morgan M, Pagées H, Obenchain V, Hayden N. 2017. Rsamtools: Binary alignment (BAM), FASTA, variant call (BCF), and tabix file import. R package version 1.26.2.
<http://bioconductor.org/packages/release/bioc/html/Rsamtools.html>
- Mountcastle AM, Combes SA. 2013. Wing flexibility enhances load-lifting capacity in bumblebees. *Proceedings of the Royal Society B*, **280**: 23536604.
- Nadeau JA, Petereit J, Tillett RL, Jung K, Fotoohi M, MacLean M, Young S, Schlauch K, Blomquist GJ, Tittiger C. 2017. Comparative transcriptomics of mountain pine beetle pheromone-biosynthetic tissues and functional analysis of CYP6DE3. *BMC Genomics*, **18**: 311.
- Nagoshi E., Sugino K., Kula E., Okazaki E., Tachibana T., Nelson S., Rosbash M. 2010. Dissecting differential gene expression within the circadian neuronal circuit of *Drosophila*. *Nature Neuroscience*, **13**: 60-68.
- Nakagawa S, Schielzeth H. 2013. A general and simple method for obtaining R^2 from generalized linear mixed-effects models. *Methods in Ecology and Evolution*, **4**: 133-142.
- Nakazawa M. 2017. fmsb: Functions for Medical Statistics Book with some Demographic Data. R package version 0.6.1. URL <https://cran.r-project.org/web/packages/fmsb/index.html>
- Naranjo SE. 2019. Assessing insect flight behavior in the laboratory: a primer on flight mill methodology and what can be learned. *Annals of the Entomological Society of America*, **112**: 182-199.

- Nässel DR, Liuy Y, Luo J. 2015. Insulin/IGF signaling and its regulation in *Drosophila*. *General and Comparative Endocrinology*, **221**: 255-266.
- Nathan R, Klein E, Robledo-Arnuncio JJ, Revilla E. Chapter 15 Dispersal kernels: review. *In* Dispersal Ecology and Evolution. Edited by Clobert J, Baguette M, Benton TG, Bullock JM. Oxford University Press, Oxford. pp. 187-210.
- Nazif A, Partridge L. 2008. Stage debut for the elusive *Drosophila* insulin-like growth factor binding protein. *Journal of Biology*, **7**: 18.
- Nigg HN, Svoboda JA, Thompson MJ, Dutky SR, Kaplanis JN, Robbins WE. 1976. Ecdysome 20-hydroxylase from the midgut of the tobacco hornworm (*Manduca sexta* L.). *Experientia*, **32**: 438–439.
- Niitepold K, Smith AD, Osborne JL, Reynolds DR, Carreck NL, Martin AP, Marden JH, Ovaskainen O, Hanski I. 2009. Flight metabolic rate and *Pgi* genotype influence butterfly dispersal rate in the field. *Ecology*. **90**: 2223-2232.
- Norberg RÅ. 1972. The pterostigma of insect wings an inertial regulator of wing pitch. *Journal of Comparative Physiology*, **81**: 9-22.
- NRCan (Natural Resources Canada). (2017, February 21). Mountain pine beetle (factsheet). Retrieved from <http://www.nrcan.gc.ca/forests/fire-insects-disturbances/top-insects/13397>

- NRCan (Natural Resources Canada). 2017 [accessed February 21]. Mountain pine beetle (factsheet). Retrieved from <http://www.nrcan.gc.ca/forests/fire-insects-disturbances/top-insects/13397>
- Ohms HA, Mohapatra A, Lytle DA, De Leenheer P. 2019. The evolutionary stability of partial migration under different forms of competition. *Theoretical Ecology*, **12**: 347-363.
- Oikonomopoulos S, Wang YC, Djambazian H, Badescu D, Ragoussis J. 2016. Benchmarking of the Oxford Nanopore MinION sequencing for quantitative and qualitative assessment of cDNA populations. *Scientific Reports*, **6**: 31602 (2016).
- Olivieri I, Gouyon P-H. 1997. Evolution of migration rate and other traits: the metapopulation effect (pp 293–323) In Hanski IA, Gilpin ME. (eds), *Metapopulation biology: ecology, genetics, and evolution*. San Diego, California: Academic Press.
- Paine TD, Millar JG, Hanlon CC, Hwang J-S. 1999. Identification of semiochemicals associated with Jeffrey pine beetle, *Dendroctonus jeffreyi*. *Journal of Chemical Ecology*, **25**: 433-453.
- Palmer JO, Dingle H. 1989. Responses of selection on flight behaviour in a migratory population of milkweed bugs (*Oncopeltus fasciatus*). *Evolution*, **43**: 1805-1808.
- Paris JR, Stevens JR, Catchen JM. 2017. Lost in parameter space: a road map for STACKS. *Methods in Ecology and Evolution*, **8**: 1360-1373.

- Peterson BK, Weber JN, Kay EH, Fisher HS, Hoekstra HE. 2012. Double Digest RADseq: An inexpensive method for de novo SNP discovery and genotyping in model and non-model species. *PLoS ONE*, **7**: e37135.
- Pierce HD Jr, Conn JE, Oehlschlager AC, Borden JH. 1987. Monoterpene metabolism in female mountain pine beetles, *Dendroctonus ponderosae* Hopkins, attacking ponderosa pine. *Journal of Chemical Ecology*, **13**: 1455-1480.
- Pinheiro J, Bates D, DebRoy S, Sarkar D, R Core Team. 2017. nlme: Linear and Nonlinear Mixed Effects Models. R package version 3.1-131. URL: <https://CRAN.R-project.org/package=nlme>
- Pistone D, Gohli J, Jordal BH. 2018. Molecular phylogeny of bark and ambrosia beetles (Curculionidae: Scolytinae) based on 18 molecular markers. *Systematic Entomology*, **43**: 387-406.
- Poland JA, Brown PJ, Sorrells ME, Jannink JL. 2012. Development of high-density genetic maps for barley and wheat using a novel two-enzyme genotyping-by-sequencing approach. *PLoS ONE*, **7**: e32253.
- Pompella A, Visvikis A, Paolicchi A, De Tata V, Casini AF. 2003. The changing faces of glutathione, a cellular protagonist. *Biochemical Pharmacology*, **66**: 1499–503.
- Pritchard JK, Stephens M, Donnelly P. 2000. Inference of population structure using multilocus genotype data. *Genetics*, **155**: 945-959.

- R Core Team. 2017. R: A Language and Environment for Statistical Computing. R Foundation for Statistical Computing, Austria [online]. Available from <https://www.R-project.org/> [accessed 3 October 2017]
- R Core Team. 2018. R: A Language and Environment for Statistical Computing. R Foundation for Statistical Computing, Austria [online]. Available from <https://www.R-project.org/> [accessed 13 September 2018]
- Raffa KF, Grégoire J-C, Lindgren BS. 2015. Natural history and ecology of bark beetles. *In* Bark Beetles: Biology and Ecology of Native and Invasive Species. Edited by Vega FE, Hofstetter RW. Academic Press, Elsevier. pp. 1–40.
- Rajkumar AP, Qvist P, Lazarus R, Lescai F, Ju J, Nyegaard M, Mors O, Børglum D, Li Q, Christensen JH. 2015. Experimental validation of methods for differential gene expression analysis and sample pooling in RNA-seq. *BMC Genomics*, **16**: 548.
- Raymond M, Rousset F. 1995. GENEPOP (version 1.2): population genetics software for exact tests and ecumenicism. *Journal of Heredity*, **86**: 248-249.
- Reeve JD, Anderson FE, Kelley ST. 2012. Ancestral state reconstruction for *Dendroctonus* bark beetles: evolution of a tree killer. *Environmental Entomology*, **41**: 723-730.
- Reid ML, Purcell JRC. 2011. Condition-dependent tolerance of monoterpenes in an insect herbivore. *Arthropod-Plant Interactions*, **5**: 331-337.
- Reid RW. 1958. Internal changes in female mountain pine beetle *Dendroctonus monticolae* Hopk., Associated with Egg Laying and Flight. *The Canadian Entomologist*, **90**: 464-468.

- Reynolds AM, Reynolds DR, Sanjay PS, Gao H, Chapman JW. 2016. Orientation in high-flying migrant insects in relation to flows: mechanisms and strategies. *Philosophical Transactions of the Royal Society B*, **371**: 20150392.
- Ribak G, Barkan S, Soroker V. 2017. The aerodynamics of flight in an insect flight-mill. *PLoS ONE*, **12**: e0186441.
- Rice AV, Thormann MN, Langor DW. 2008. Mountain pine beetle-associated blue-stain fungi are differentially adapted to boreal temperatures. *Forest Pathology*, **38**: 113–123.
- Rieux A, Soubeyrand S, Bonnot F, Klein EK, Ngando JE, Mehl A, et al. 2014. Long-distance wind-dispersal of spores in a fungal plant pathogen: estimation of anisotropic dispersal kernels from an extensive field experiment. *PLoS ONE*, **9**: e103225.
- Robert JA, Bonnett T, Pitt C, Spooner LJ, Fraser J, Yuen MMS, Keeling CI, Bohlmann J, Huber DPW. 2016. Gene expression analysis of overwintering mountain pine beetle larvae suggests multiple systems involved in overwintering stress, cold hardiness, and preparation for spring development. *PeerJ*, **4**: e2109.
- Robert JA, Pitt C, Bonnett TR, Yuen MMS, Keeling CI, Bohlmann J, Huber DPW. 2013. Disentangling detoxification: gene expression analysis of feeding mountain pine beetle illuminates molecular-level host chemical defense detoxification mechanisms. *PLoS ONE*, **8**: e77777.
- Robertson C, Nelson TA, Boots B. 2007. Mountain pine beetle dispersal: the spatial-temporal interaction of infestations. *Forest Science*, **53**: 395-405.

- Robertson IC. 1998. Flight muscle changes in male pine engraver beetles during reproduction: the effects of body size, mating status and breeding failure. *Physiological Entomology*, **23**: 75-80.
- Robertson IC, Roitberg BD. 1998. Duration of paternal care in pine engraver beetles: Why do larger males care less? *Behav. Ecol. Sociobiol.* **43**: 379–386.
- Rochette NC, Rivera-Colón AG, Catchen, JM. 2019. Stacks 2: Analytical methods for paired-end sequencing improve RADseq-based population genomics. *Molecular Ecology*, **28**: 4737-4754.
- Roff DA, Fairbairn DJ. 2007. The evolution and genetics of migration in insects. *BioScience*, **57**: 155–164.
- Rogulja D, Rauskolb C, Irvine KD. 2008. Morphogen Control of wing growth through the Fat signalling pathway. *Developmental Cell*, **15**: 309-321.
- Rosenberger DW, Venette RC, Aukema BH. 2016. Sexing live mountain pine beetles *Dendroctonus ponderosae*: refinement of a behavioral method for *Dendroctonus* spp.. *Entomologia Experimentalis et Applicata*, **160**: 195-199.
- Rousset F. 2008. Genepop'007: a complete reimplementation of the Genepop software for Windows and Linux. *Molecular Ecology Resources*, **8**: 103-106.
- Royama T. 1984. Population dynamics of the spruce budworm *Choristoneura fumiferana*. *Ecological Monographs*, **54**: 429-462.

- Rueden CT, Schindelin J, Hiner MC, DeZonia BE, Walter AE, Arena ET, Eliceiri KW. 2017. ImageJ2: ImageJ for the next generation of scientific image data. *BMC Bioinformatics*, **18**: 529.
- Saastamoinen M, Bocedi G, Cote J, Legrand D, Guillaume F, Wheat CW, Fronhofer EA, Garcia C, Henry R, Husby A, Baguette M, Bonte D, Coulon A, Kokko H, Matthysen E, Niitepõld, Nonaka E, Stevens VM, Travis JM, Donohue K, Bullock JM, Delgado MM. 2018. Genetics of dispersal. *Biological Reviews*, **93**: 574-599.
- Safranyik L, Carroll AL, Régnière J, Langor DW, Riel WG, Shore TL, Peter B, Cooke BJ, Nealis VG, Taylor SW. 2010. Potential for range expansion of mountain pine beetle into the boreal forest of North America. *The Canadian Entomologist*, **142**: 415-442.
- Safranyik L, Silversides R, McMullen LH, Linton DA. 1989. An empirical approach to modeling the local dispersal of the mountain pine beetle (*Dendroctonus ponderosae* Hopk.) (Col., Scolytidae) in relation to sources of attraction, wind direction and speed. *Journal of Applied Entomology*, **108**: 498-511.
- Safranyik L. 1998. Mortality of mountain pine beetle larvae, *Dendroctonus ponderosae* (Coleoptera: Scolytidae) in logs of lodgepole pine (*Pinus contorta* var. *latifolia*) at constant low temperatures. *Journal of the Entomological Society of British Columbia*. **95**: 81-87.
- Safranyik L. Carroll AL. 2006. The biology and epidemiology of the mountain pine beetle in lodgepole pine forests (Chapter 1). In Safranyik, L. Wilson, W.R. (Eds.), *The mountain pine beetle: a synthesis of biology, management, and impacts on lodgepole pine* (pp. 3-

- 66). Victoria, British Columbia: Natural Resources Canada, Canadian Forest Service, Pacific Forestry Centre.
- Sahota TS. 1975. Effect of juvenile hormone on acid phosphatases in the degenerating flight muscles of the Douglas-fir beetle, *Dendroctonus pseudotsugae*. *Journal of Insect Physiology*, 21: 471-475, 477-478.
- Samarasekera GDNG, Bartell NV, Lindgren BS, Cooke JEK, Davis CS, James PMA, Coltman, DW, Mock KE, Murray BW. 2012. Spatial genetic structure of the mountain pine beetle (*Dendroctonus ponderosae*) outbreak in western Canada: Historical patterns and contemporary dispersal. *Molecular Ecology*, 21: 2931–2948.
- Sandstrom P, Welch WH, Blomquist GJ, Tittiger C. 2006. Functional expression of a bark beetle cytochrome P450 that hydroxylates myrcene to ipsdienol. *Insect Biochemistry and Molecular Biology*, 36: 835-845.
- Schneider CA, Rasband WS, Eliceiri KW. 2012. NIH Image to ImageJ: 25 years of image analysis. *Nature Methods*, 9: 671-675.
- Segraves WA, Hogness DS. 1990. The E75 ecdysone-inducible gene responsible for the 75B early puff in *Drosophila* encodes two new members of the steroid receptor superfamily. *Genes & Development*, 4: 204-219.
- Seybold SJ, Huber DPW, Lee JC, Graves AD, Bohlmann J. 2006. Pine monoterpenes and pine bark beetles: a marriage of convenience for defense and chemical communication. *Phytochemistry Reviews*, 5: 143-178.

- Sheehan D, Meade G, Foley VM, Dowd CA. 2001. Structure, function and evolution of glutathione transferases: implications for classification of non-mammalian members of an ancient enzyme superfamily. *Biochemical Journal*, **360**: 1-16.
- Shegelski VA, Evenden ML, Sperling FAH. 2019. Morphological variation associated with dispersal capacity in a tree-killing bark beetle *Dendroctonus ponderosae* Hopkins. *Agriculture and Forest Entomology*, **21**: 79-97.
- Shepherd RF. 1966. Factors influencing the orientation and rates of activity of *Dendroctonus ponderosae* Hopkins (Coleoptera: Scolytidae). *The Canadian Entomologist*, **98**: 507-518.
- Sieber MH, Spradling AC. 2015. Steroid signaling establishes a female metabolic state and regulates SREBP to control oocyte lipid accumulation. *Current Biology*, **25**: 993-1004.
- Singh SP, Coronella JA, Benes H, Cochrane BJ, Zimniak P. 2001. Catalytic function of *Drosophila melanogaster* glutathione S-transferase DmGSTS1-1 (GST-2) in conjugation of lipid peroxidation end products. *European Journal of Biochemistry*, **268**: 2912–2923.
- Six DL, Bracewell R. 2015. *Dendroctonus*. In *Bark Beetles: Biology and Ecology of Native and Invasive Species*. Edited by Vega FE, Hofstetter RW. Academic Press, Elsevier. pp. 305–350.
- Six DL. 2020. A major symbiont shift supports a major niche shift in a clade of tree-killing bark beetles. *Ecological Entomology*, **45**: 190-201.
- Six DL, Bentz BJ. 2007. Temperature determines the relative abundance of symbionts in a multipartite bark beetle-fungus symbiosis. *Microbial Ecology*, **54**: 112–118.

- Song M, Gorzalski A, Nguyen TT, Liu X, Jeffrey C, Blomquist GJ, Tittiger C. 2014. *Exo-brevicommin biosynthesis in the fat body of the mountain pine beetle, Dendroctonus ponderosae*. *Journal of Chemical Ecology*, **40**: 181-189.
- Song X, Zhang Y, Zhong Q, Zhan, Bi J, Tang J, Xie J, Li B. 2020. Identification and functional characterization of methyl-CpG binding domain protein from *Tribolium castaneum*. *Genomics*, **112**: 2223-2232.
- Stark R, Grzelak M, Hadfield J. 2019. RNA sequencing: the teenage years. *Nature Reviews Genetics*, **20**: 631-656.
- Steyn VM, Mitchell KA, Terblanche JS. 2016. Dispersal propensity, but not flight performance, explains variation in dispersal ability. *Proceedings of the Royal Society B*, **283**: 20160905.
- Stinner RE, Barfield CS, Stimac JL, Dohse L. 1983. Dispersal and movement of insect pests. *Annual Review of Entomology*, **28**: 319-335.
- Taft S, Najar A, Erbilgin N. 2015. Pheromone production by an invasive bark beetle varies with monoterpene composition of its naïve host. *Journal of Chemical Ecology*, **41**: 540–549.
- Taylor PD, Merriam G. 1995. Wing morphology of a forest damselfly is related to landscape structure. *Oikos*, **73**: 43-48.
- Taylor S, Carroll AL. 2004. Disturbance, forest age, and mountain pine beetle outbreak dynamics in BC: A historical perspective (pp 41-51). In Shore, T.L., Brooks, J.E. Stone, J.E. (eds). *Mountain Pine Beetle Symposium: Challenges and Solutions*. Kelowna, British

Columbia: Natural Resources Canada, Canadian Forest Service, Pacific Forestry Centre, Information Report BC-X-399, Victoria, BC. 298 p.

- Taylor RAJ, Bauer LS, Poland TM, Windell KN. 2010. Flight performance of *Agrilus planipennis* (Coleoptera: Buprestidae) on a flight mill and in free flight. *Journal of Insect Behavior*, **23**: 128–148.
- Thompson KM, Huber DPW, Murray BW. 2020. Autumn shifts in cold tolerance metabolites in overwintering mountain pine beetles. *PLoS ONE*, **15**: e0227203.
- Thompson SN, Bennett RB. 1971. Oxidation of fat during flight of male Douglas-fir beetles, *Dendroctonus pseudotsugae*. *Journal of Insect Physiology*, **17**: 1555–1563.
- Tillman JA, Lu F, Goodard LM, Donaldson Z, Dwinell SC, Tittiger C, Hall GM, Storer AJ, Blomquist GJ, Seybold SJ. 2004. Juvenile hormone regulates de novo isoprenoid aggregation pheromone biosynthesis in pine bark beetles, *Ips* spp. (Coleoptera: Scolytidae), through transcriptional control of HMG-CoA reductase. *Journal of Chemical Ecology*, **30**: 2459-2494.
- Town of Hinton. [date unknown]. Program work updates: mountain pine beetle [accessed 2020 Jun 03]. <https://www.hinton.ca/898/Mountain-Pine-Beetle>
- Trevoy SAL, Janes JK, Muirhead K, Sperling FAH. 2018a. Repurposing population genetics data to discern genomic architecture: a case study of linkage cohort detection in mountain pine beetle (*Dendroctonus ponderosae*). *Ecology and Evolution*, **9**: 1147-1159.

- Trevoy SAL, Janes JK, Sperling FAH. 2018b. Where did mountain pine beetle populations in Jasper Park come from? Tracking beetles with genetics. *The Forestry Chronicle*, **94**: 20-24.
- Victor J, Zúñiga G. 2016. Phylogeny of *Dendroctonus* bark beetles (Coleoptera: Curculionidae: Scolytinae) inferred from morphological and molecular data. *Systematic Entomology*, **41**: 162-177.
- Visscher PM, Wray NR, Zhang Q, Sklar P, McCarthy MI, Brown MA, Yang J. 2017. 10 years of GWAS discovery: biology, function, and translation. *The American Journal of Human Genetics*, **101**: 5-22.
- Wang S, Liu S, Wang J, Zhou S, Jiang RJ, Bendena WG, Li S. 2010. 20-hydroxyecdysone reduces insect food consumption resulting in fat body lipolysis during molting and pupation. *Journal of Molecular Cell Biology*, **2**: 128-138.
- Ward SF, Fei S, Liebhold AM. 2020. Temporal dynamics and drivers of landscape-level spread by emerald ash borer. *Journal of Applied Ecology*, **57**: 1020-1030.
- Wegener G. 1996. Flying insects: Model systems in exercise physiology. *Experientia*, **52**: 404-412.
- Wertman DL, Bleiker KP, Perlman SJ. 2018. The light at the end of the tunnel: Photosensitivity in larvae of the mountain pine beetle (Coleoptera: Curculionidae: Scolytinae). *The Canadian Entomologist*, **150**: 622-631.

- Wertman DL, Bleiker KP. 2019. Shedding new light upon circadian emergence rhythmicity in the mountain pine beetle (Coleoptera: Curculionidae: Scolytinae). *The Canadian Entomologist*, **151**: 273-277.
- Wheat CW, Haag CR, Marden JH, Hanski I, Frilander MJ. 2010. Nucleotide polymorphism at a gene (Pgi) under balancing selection in a butterfly metapopulation. *Molecular Biology Evolution*, **27**: 267-281.
- Whittaker P. 2018. Federal government must act on national pine beetle problem [online]. *CBC News*. Available from: <https://www.cbc.ca/news/canada/edmonton/pine-beetle-column-alberta-forest-products-association-1.4895576> [accessed 24 February 2020]
- Wickham H. 2016. *ggplot2: Elegant Graphics for Data Analysis*. Springer-Verlag New York [online]. Available from <https://CRAN.R-project.org/package=ggplot2> [accessed 13 August 2019].
- Wijerathna A, Evenden M. 2019. Energy use by the mountain pine beetle (Coleoptera: Curculionidae: Scolytinae) for dispersal by flight. *Physiological Entomology*, **44**: 200-208.
- Wijerathna A, Whitehouse C, Proctor H, Evenden M. 2019. Testing for trade-offs between flight and reproduction in the mountain pine beetle (Coleoptera: Curculionidae) on two pine (Pinacea) hosts. *The Canadian Entomologist*, **151**: 298-310.

- Williams WI, Robertson IC. 2008. Using automated flight mills to manipulate fat reserves in Douglas-fir beetles (Coleoptera: Curculionidae). *Environmental Entomology*, **37**: 850-856.
- Wood SL. 1982. The bark and ambrosia beetles of North and Central America (Coleoptera: Scolytidae), a taxonomic monograph. *Great Basin Naturalist Memoirs*, **6**: 1–1359.
- Wootton RJ. 1992. Functional morphology of insect wings. *Annual Review of Entomology*, **37**: 113-140.
- Wu M, Zhang X, Wei W, Long L, An S, Gao G. 2020. CRISPR/Cas9 mediated genetic resource for unknown kinase and phosphatase genes in *Drosophila*. *Scientific Reports*, **10**: 7383.
- Yamamoto K, Hirowatari A, Shiotsuki T, Yamada N. 2016. Biochemical characterization of an unclassified glutathione S-transferase of *Plutella xylostella*. *Journal of Pesticide Science*, **41**: 145-151.
- Yamamoto K, Ichinose H, Aso Y, Banno Y, Kimura M, Nakashima T. 2011. Molecular characterization of an insecticide-induced novel glutathione transferase in silkworm. *Biochimica et Biophysica Acta – General Subjects*, **1810**: 420-426.
- Zhan S, Zhang W, Niitepold K, Hsu J, Haeger JF, Zalucki MP, Altizer S, de Roode JC, Reppert SM, Kronforst MR. 2014. The genetics of monarch butterfly migration and warning colouration. *Nature*, **514**: 317–321.

Zhang R, Gao G, Chen, H. 2016. Silencing of the olfactory co-receptor gene in *Dendroctonus armandi* leads to EAG response declining to major host volatiles. Scientific Reports, **6**: 23136.

Zhang R-J, Chen J, Jiang L-Y, Qiao G-X. 2019. The genes expression difference between winged and wingless bird cherry-oat aphid *Rhopalosiphum padi* based on transcriptomic data. Scientific Reports, **9**: 4754.

Zhang S, Clark R, Huang Y. 2020. Frequency-dependent strategy selection in a hunting game with a finite population. Applied Mathematics and Computation, **382**: 125355.

Zhou C, Wang L, Price M, Li J, Meng Y, Yue B-S. 2020. Genomic features of the fall armyworm (*Spodoptera frugiperda*) (J.E. Smith) yield insights into its defense system and flight capability. Entomological Research, **50**: 100-112.

Appendices

Appendix 2.1 Measured morphology and data collected from flight mills, as well as data on number of days specimens were stored after emergence before being flown, mill number for flight, emergence bolt, and natal tree. Dashes indicate specimens that did not have muscle measurements taken.

ID	preflight weight (mg)	postflight weight (mg)	wing area (mm ²)	wing length (mm)	wing chord (mm)	pronotal width (mm)	body length (mm)	muscle volume (mm ³)	total flight duration (s)	rotations	days stored before flight	flight mill #	Tree #	Emergence bolt #
G253	9.86	9.27	8.97	5.69	1.8	2.17	4.96	16.17	7.27	11	5	18	1	18
G260	15.66	13.44	11.74	6.7	2.07	2.5	5.92	-	9.09	12	5	17	1	16
G300	11.58	9.04	10.1	6.24	1.84	2.1	5.1	-	14.75	12	3	22	1	16
G388	10.42	9.67	9.2	6.1	1.77	2.17	5.15	-	29.06	18	4	7	1	18
G350	16.28	15.43	13.4	6.98	2.15	2.6	5.99	-	10.34	25	4	8	1	18
G298	15.94	14.24	12.05	6.75	2.15	2.3	5.65	-	40.84	40	3	21	2	20
G306	19.84	18.45	14.44	7.26	2.26	2.38	6.41	-	22.23	43	5	17	2	20
G418	11.69	11.1	10.91	6.35	1.99	2.03	5.45	-	75.91	45	4	21	1	18
G375	12.87	11.54	11.35	6.72	2.04	2.35	5.82	19.99	72.61	59	5	8	1	18
G377	11.16	10	9.09	6.14	1.75	2.15	5.05	-	112.34	60	5	22	1	18
G293	17.12	16.06	14.26	7.24	2.24	2.44	5.85	-	97.83	97	3	8	2	20
G246	12.4	12	10.47	6.34	1.96	2.13	5.41	25.64	236.59	104	5	2	3	14
G254	11.76	10.78	10.04	6.27	1.91	2.52	5.18	-	129.58	104	5	2	3	14
G404	10.09	9.51	8.88	5.82	1.83	1.9	4.88	-	91.75	106	4	2	1	16
G328	17.3	15.66	12.88	7.12	2.08	2.37	5.85	-	177.06	127	4	23	1	16
G338	14.02	13.91	10.53	6.28	1.98	2.38	5.25	-	468.56	273	3	6	2	21
G289	18.89	16.24	12.36	6.65	2.2	2.43	5.88	-	562.2	292	3	12	2	20
G259	17.22	14.97	13.1	6.99	2.12	2.58	6.19	27.37	828.73	317	5	16	1	16

G332	9.58	8.49	9.44	6.01	1.77	2	5.24	-	1035.91	387	4	14	1	16
G386	13.97	12.88	11.31	6.6	1.96	2.32	5.45	-	324.42	414	4	5	1	18
G271	17.83	15.61	13.61	6.9	2.29	2.52	5.96	-	917.88	418	5	17	1	18
G335	19.91	18.73	13.87	6.94	2.32	2.38	6.66	23.74	578.27	451	3	2	2	20
G359	13.1	12.38	11	6.43	2.06	2.15	5.59	-	861.52	510	5	16	1	16
G407	16.03	14.55	10.85	6.37	1.95	2.39	5.62	-	1133.58	632	4	16	1	18
G358	10.65	9.8	9.64	5.92	1.91	2.01	5.3	-	1148.72	732	5	17	1	16
G376	11.8	10.92	9.43	6.3	1.75	2.26	5.29	-	1313.83	767	5	23	1	18
G414	12.81	11.44	11.48	6.69	1.98	2.29	5.41	-	2501.19	871	4	11	1	18
G285	11.3	10.36	10.39	6.12	1.95	1.8	5.05	19.74	1810.47	895	3	2	2	20
G400	16.6	15.72	12	6.58	2.02	2.51	5.68	-	1222.81	902	4	4	1	18
G362	15.81	14.71	12.55	6.54	2.09	2.41	5.63	-	1377.73	911	5	8	1	16
G302	14.8	13.02	12.63	6.88	2.16	2.43	5.67	18.35	1722.45	1055	3	23	2	21
G401	16.97	15.9	13.28	7.07	2.14	2.43	5.76	23.8	1519	1135	4	2	1	18
G284	19.47	17.41	12.7	6.98	2.13	2.25	5.93	24.12	1368.33	1201	3	1	2	20
G257	10.48	9.97	9.4	5.86	1.87	2.19	4.95	18.9	5613.41	1637	5	10	3	14
G360	15.76	14.63	12.86	6.82	2.18	2.42	5.87	26.41	3389.52	1666	5	11	1	16
G268	11.96	11.89	9.92	6.19	1.92	2.23	5.45	24.02	2628.5	1920	5	11	4	19
G272	18.22	14.03	13.09	6.77	2.21	2.39	5.78	22.2	5082.89	2101	5	18	1	18
G331	17.08	15.12	12.54	6.87	2.12	2.04	5.75	29.91	4775.78	2877	4	20	1	16
G327	14.86	13.4	12.16	6.74	2.11	2.23	5.41	23.89	56434.8	3358	4	10	2	20
G261	16.81	14	12.7	6.92	2.11	2.57	6.12	23.67	7182.95	3702	5	18	1	16
G356	18.86	17.15	13.95	7.16	2.24	2.54	5.92	17.01	5924.8	3767	5	19	2	20
G398	14.66	12.51	11.99	6.81	1.99	2.25	5.31	24.91	9098.3	3867	4	21	1	18
G363	17.4	16.42	12.08	6.71	2.08	2.24	5.75	24.8	4073.81	3892	5	23	1	18
G389	11.65	10.51	9.94	6.27	1.83	2.07	5.18	25.02	5252.27	3900	4	19	1	16
G408	10.43	9.05	9.35	5.91	1.91	2.09	5.08	22.11	6968.92	3969	4	17	1	18
G264	18.84	16.92	13.85	6.9	2.4	2.36	5.93	21.44	5626.88	4086	5	2	2	20
G344	10.26	9.42	9.88	5.85	1.91	2.22	5.1	20.87	8126.41	4618	4	23	1	16
G361	17.26	15.08	12.59	6.94	2.14	2.31	5.81	21	7071.78	5040	5	10	1	16
G336	17.69	16.4	13.21	6.91	2.24	2.64	5.97	26.59	10276.1	5171	3	1	2	20

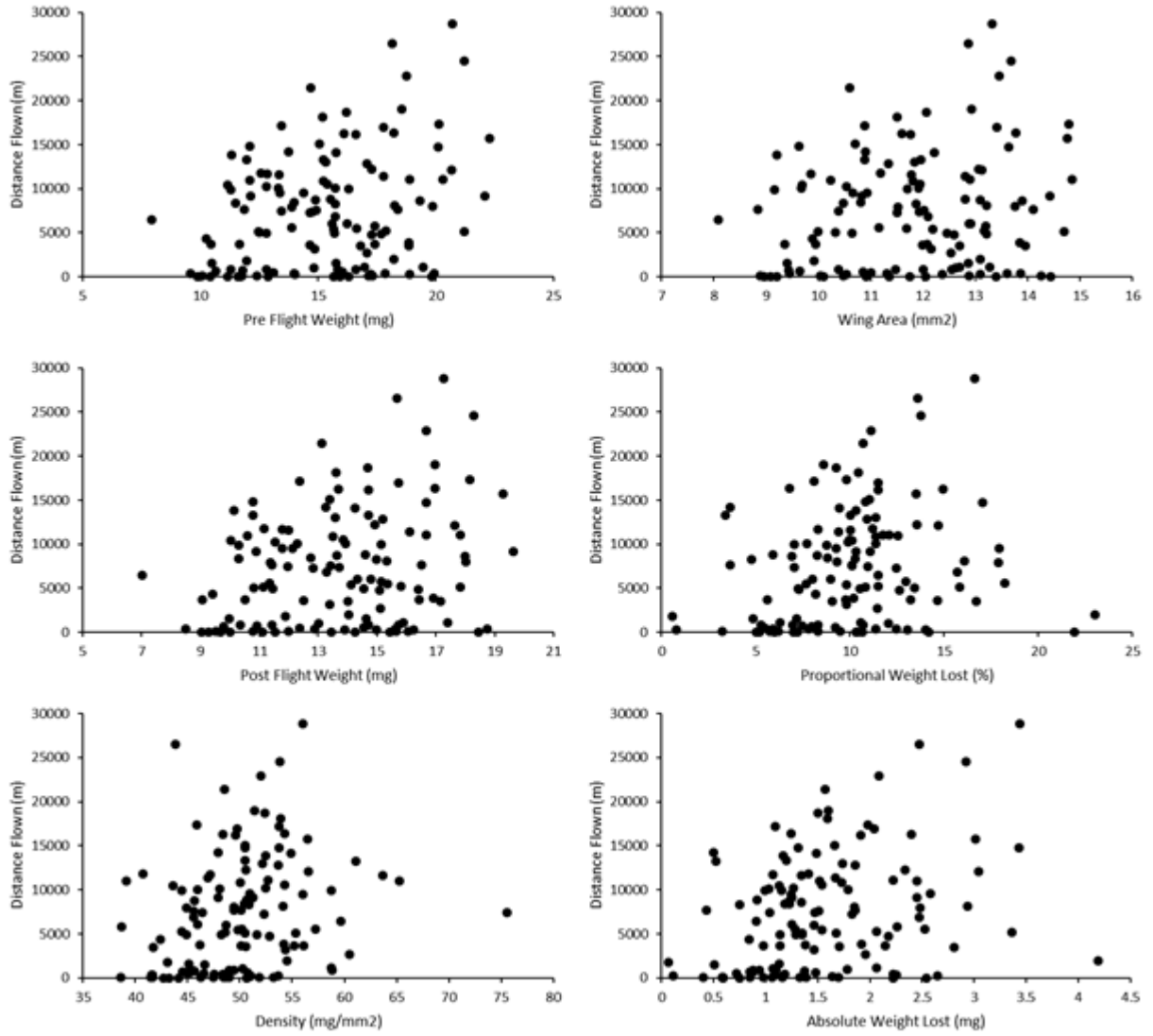
G266	12.8	11.45	10.64	6.21	1.93	2.19	5.2	21.11	14791.9	5215	5	8	3	14
G343	15.7	14.56	12.46	6.78	2.08	2.24	5.89	24.12	8375.3	5256	4	16	1	16
G364	12.5	10.82	10.32	6.24	1.93	2.13	5.27	20.49	14374.5	5381	5	22	1	18
G369	12.47	11.12	9.99	6.28	1.88	2.03	5.15	18.92	8187.84	5432	5	19	1	16
G307	21.2	17.84	14.7	7.41	2.28	2.51	6.44	30.34	8498	5484	5	16	2	20
G290	17.88	15.82	13.17	6.96	2.16	2.59	6.09	26.89	13268.7	5551	3	13	2	20
G251	15.65	14.11	12.18	6.71	2.08	2.35	5.65	26.06	10845.5	5748	5	16	4	19
G417	16.63	15.35	11.68	6.84	2.03	2.22	5.59	21.58	9585.47	5869	4	16	1	18
G301	13.87	11.34	11.16	6.52	1.91	2.28	5.38	20.75	12055.2	5901	3	18	1	16
G326	17.4	15.14	13.2	6.87	2.09	2.32	6.8	25.11	10939.3	6148	4	11	2	20
G373	16.24	14.78	12.91	6.96	2.17	2.4	5.76	19.55	8682.27	6362	5	11	1	18
G419	15.59	14.34	12.88	6.85	2.18	2.35	5.87	19.5	14344.4	6421	4	20	1	18
G250	7.92	7.01	8.08	5.62	1.69	1.7	4.32	15.01	13556.3	6868	5	11	4	15
G315	15.74	13.27	12.1	6.63	2.1	2.46	5.79	25.73	15583.1	7268	4	22	1	18
G371	14.66	12.83	11.5	6.57	2.02	2.26	5.44	19.32	17752.5	7705	5	17	1	18
G416	14.75	13.71	11.93	6.78	2.04	2.37	5.66	18.33	12202.8	7870	4	23	1	18
G368	13.44	11.97	10.39	6.25	1.94	1.86	4.78	14.12	17734.8	7897	5	2	1	18
G263	14.93	13.42	12.02	6.72	2.08	2.46	5.64	26.55	13967.3	8034	1	17	1	18
G287	18.37	16.51	14.1	7.21	2.34	2.74	5.69	33.06	10926.6	8120	3	6	2	20
G247	11.86	11.43	8.84	5.88	1.76	2.13	5.15	22.47	11774.2	8126	5	4	3	14
G329	13.86	11.38	11.52	6.45	2.05	2.5	5.43	17.85	17326.1	8435	4	22	1	16
G308	19.86	18.01	13.76	7.12	2.26	2.51	6.18	26.41	12983.6	8516	5	11	2	20
G391	18.26	15.32	13.22	7.08	2.2	2.41	5.78	27.97	13874.9	8612	4	17	1	18
G255	15.73	14.98	11.86	6.67	2.06	2.33	5.63	20.18	11551.7	8803	5	4	3	14
G382	11.48	10.3	10.48	6.22	1.95	2.1	5.08	19.55	17246	8892	4	12	2	20
G340	13.97	12.74	10.81	6.25	2.01	2.41	5.24	17.63	17829.4	8955	4	19	2	21
G322	19.32	17.98	13.89	7.19	2.22	2.47	6.06	23.28	11245	9147	4	19	2	20
G383	14.87	13.64	13.1	6.94	2.23	2.33	5.78	18.9	11303.3	9296	4	4	1	16
G323	15.51	14.59	12.81	6.89	2.19	2.25	5.7	22.79	10752.4	9359	4	18	2	20
G381	12.13	10.88	10.83	6.51	1.95	2.16	5.29	17.13	15743	9712	4	13	2	20
G305	22.09	19.64	14.42	7.26	2.23	2.53	6.38	27.14	11501.6	9721	5	18	2	20

G396	13.38	12.14	10.66	6.29	2.01	2.11	5.2	-	21868.7	1007 7	4	10	1	18
G310	14.37	11.79	10.93	6.38	1.96	2.18	5.56	-	13120.6	1012 7	5	8	2	21
G387	11.3	10.31	9.16	5.78	1.75	2.16	5.3	-	20369.3	1053 6	4	6	1	18
G248	16.28	15.13	11.7	6.56	2.13	2.11	5.6	25.78	16395.9	1054 6	5	8	4	15
G252	15.73	13.94	11.91	6.65	2.01	2.39	5.85	22.45	16781.8	1067 5	5	19	1	18
G249	13.31	12.28	9.67	6.28	1.8	2.25	5.42	20.6	19074.5	1072 1	5	10	4	15
G258	12.81	11.54	10.54	6.23	1.97	2.14	5.22	17.93	16511.2	1085 2	5	11	3	14
G267	11.15	10.02	9.69	6.09	1.89	2.24	5.22	-	24680.7	1107 7	5	10	3	14
G321	15.4	13.86	11.95	6.75	2.07	2.35	5.37	-	16651.1	1119 5	4	7	2	21
G314	15.23	13.5	11.81	6.75	2.05	2.36	5.55	-	18776.7	1150 2	4	23	1	16
G412	12.11	10.59	10.24	6.26	1.94	1.81	4.95	-	18161.6	1167 0	4	18	1	16
G304	20.28	17.83	14.84	7.36	2.27	2.63	6.86	26.16	17271.5	1170 9	5	19	2	20
G318	18.88	16.66	12.9	6.95	2.09	2.4	5.97	-	13806.4	1173 5	4	13	2	20
G317	17.79	16.12	12.81	6.87	2.16	2.45	6.08	-	18884.4	1206 6	4	20	1	18
G337	13.33	11.99	11.78	6.37	2.08	1.93	5.09	-	21620.1	1232 2	3	5	2	20
G256	12.84	11.77	9.85	6.36	1.88	2.29	5.33	-	21630.2	1242 0	5	8	3	14

G380	12.56	11.15	11.18	6.52	2	2.46	5.47	-	28012.7	1250 2	5	14	1	18
G324	20.67	17.63	13.13	6.85	2.21	2.5	5.91	-	21772.7	1282 8	4	17	2	20
G291	17.26	14.92	13.06	6.76	2.14	2.34	5.9	-	52462.5	1301 3	3	14	2	20
G365	17.06	15.2	11.34	6.49	2.15	2.52	5.49	-	28923.4	1359 4	5	21	1	18
G399	15.32	13.58	11.84	6.57	2.07	2.32	5.5	-	24624.4	1380 2	4	20	1	18
G411	15.23	14.71	11.96	6.67	2.13	2.08	5.35	-	17229.1	1406 4	4	19	1	16
G370	11.97	10.77	10.88	6.27	2.03	2.11	5.18	-	18781.8	1412 6	5	18	1	16
G405	11.31	10.14	9.2	5.93	1.76	1.94	5.15	-	33874.5	1472 7	4	10	1	18
G334	15.75	14.26	12.22	6.74	2.15	2.21	5.57	-	18135.1	1497 1	3	4	2	20
G372	13.75	13.25	10.9	6.55	1.96	2.17	5.62	-	22569.8	1507 3	5	16	1	18
G299	20.1	16.67	13.64	7.21	2.16	2.48	6	-	21212.2	1565 0	3	17	2	20
G406	12.1	10.79	9.63	6	1.86	2.06	5.27	-	32096	1569 2	4	11	1	18
G342	15.05	13.39	10.71	6.3	1.97	2.37	5.48	-	24240.3	1598 5	4	17	1	16
G319	22.28	19.27	14.76	7.51	2.28	2.5	6.14	-	19725.2	1670 4	4	5	2	20
G384	16.61	14.7	11.76	6.68	2.01	2.41	5.76	-	24584.6	1717 9	4	2	1	16
G262	16.08	13.68	11.6	6.62	2.04	2.4	5.75	-	25984.3	1729 0	5	19	1	18

G409	18.2	16.96	13.78	7.06	2.25	2.5	5.66	-	29481.5	1738 6	4	18	1	18
G295	17.76	15.72	13.41	6.93	2.2	2.51	5.83	27.33	31798.2	1800 0	3	11	2	20
G346	13.45	12.36	10.89	6.24	1.95	2.11	5.32	-	29751	1822 2	4	21	1	18
G385	20.12	18.14	14.79	7.43	2.34	2.58	6.37	-	26066.5	1843 1	4	1	1	18
G390	15.2	13.61	11.5	6.51	2.04	2.26	5.46	-	31295.1	1924 6	4	18	1	16
G357	16.18	14.68	12.07	6.77	2.09	2.44	5.5	-	23038.2	1985 7	5	18	1	16
G345	18.56	16.96	12.92	7.16	2.09	2.41	5.98	-	27914.1	2018 6	4	22	1	16
G393	14.69	13.12	10.6	6.29	2.01	2.28	5.63	-	31962	2276 8	4	11	1	18
G286	18.76	16.67	13.45	7.2	2.19	2.51	5.86	-	30457.7	2434 3	3	4	2	20
G297	21.2	18.28	13.68	7.07	2.26	2.52	6.11	-	37807.4	2608 1	3	16	2	20
G311	18.15	15.68	12.86	6.67	2.16	2.73	6.02	-	34651.8	2815 8	5	4	2	21
G320	20.71	17.27	13.32	7.02	2.18	2.35	6.13	-	37560.7	3058 3	4	6	2	20

Appendix 2.2 Plots showing all 124 specimens relating morphological features to the distance flown (m), as measured on 22-h computer-linked flight mill bioassays.



Appendix 3.1 Table containing the results of the differential expression analysis, including Genbank accession #, scaffold, mean number of reads, log2 fold change, adjusted p-value, and annotation.

Accession	Scaffold	baseMean	log2Fold Change	B-H adjusted p-value	Gene Annotation
XM_019901506.1	NW_017844745.1	535.1	0.37	0.007	melanization protease 1-like
XM_019897720.1	NW_017851231.1	449.6	0.86	0.000	DNA mismatch repair protein Msh2-like
XM_019897721.1	NW_017851231.1	934.4	0.29	0.005	leucine--tRNA ligase%2C cytoplasmic
XR_002171432.1	NW_017851232.1	25.1	-0.97	0.001	uncharacterized LOC109532710
XR_002171435.1	NW_017851236.1	153.0	0.93	0.006	uncharacterized LOC109532713
XM_019897734.1	NW_017851239.1	1789.4	-0.99	0.001	uncharacterized LOC109532725
XM_019897741.1	NW_017851239.1	1052.1	0.53	0.009	metaxin-2-like
XM_019897749.1	NW_017846330.1	972.8	-0.86	0.000	REST corepressor 2-like
XM_019897755.1	NW_017851239.1	1452.1	0.52	0.001	protein prune homolog 2
XM_019897760.1	NW_017851239.1	6744.2	-0.52	0.002	phosphatidylinositol 4-phosphate 5-kinase type-1 alpha%2C transcript variant X1
XM_019897778.1	NW_017851239.1	870.0	0.61	0.000	poly(A) RNA polymerase%2C mitochondrial
XM_019897779.1	NW_017851239.1	4859.2	0.41	0.005	thioredoxin-like protein 1
XM_019897781.1	NW_017851239.1	4161.8	-0.38	0.009	myb-related protein B%2C transcript variant X1
XM_019897788.1	NW_017851239.1	3800.5	1.91	0.000	senecionine N-oxygenase-like%2C transcript variant X1
XM_019897792.1	NW_017851239.1	193.8	1.43	0.000	uracil-DNA glycosylase-like
XM_019897797.1	NW_017851239.1	1705.8	0.74	0.002	uncharacterized LOC109532756
XM_019897816.1	NW_017851241.1	2851.2	-0.32	0.008	phosphatidylinositol 4-kinase beta
XM_019897824.1	NW_017851241.1	137.8	-1.45	0.001	homeotic protein proboscipedia-like%2C transcript variant X1
XM_019897828.1	NW_017851242.1	2150.0	-0.45	0.000	probable ATP-dependent RNA helicase DDX56
XM_019897848.1	NW_017851256.1	10612.6	-0.53	0.008	microtubule-associated serine/threonine-protein kinase 3%2C transcript variant X1
XM_019897867.1	NW_017851256.1	155.1	-0.61	0.009	gamma-1-syntrophin
XM_019897872.1	NW_017851260.1	1441.6	0.27	0.001	uncharacterized LOC109532808
XM_019897904.1	NW_017845006.1	1677.9	0.60	0.000	acylglycerol kinase%2C mitochondrial
XM_019897882.1	NW_017846400.1	1004.0	-0.69	0.002	ATP-sensitive inward rectifier potassium channel 11-like
XM_019897880.1	NW_017851268.1	1990.2	-0.52	0.000	ras-related protein Rab-39B-like
XM_019897898.1	NW_017851276.1	320.3	1.54	0.000	probable beta-hexosaminidase fdl
XM_019897909.1	NW_017851281.1	5221.5	-0.64	0.000	WD repeat and FYVE domain-containing protein 3

XM_019897932.1	NW_017851282.1	5615.4	0.29	0.004	small glutamine-rich tetratricopeptide repeat-containing protein beta-like%2C transcript variant X1
XM_019897937.1	NW_017846420.1	1257.2	-0.67	0.003	uncharacterized LOC109532859
XM_019897947.1	NW_017851282.1	1558.8	-0.26	0.002	guanylate kinase-like putative Dol-P-Glc:Glc(2)Man(9)GlcNAc(2)-PP-Dol alpha-1%2C2-glucosyltransferase
XM_019897951.1	NW_017851282.1	744.2	-0.35	0.001	protein MON2 homolog
XM_019897952.1	NW_017851282.1	3631.2	-0.23	0.002	rho GTPase-activating protein 28-like%2C transcript variant X1
XM_019897953.1	NW_017851282.1	8584.4	-0.56	0.000	epidermal growth factor receptor kinase substrate 8-like protein 2%2C transcript variant X1
XM_019897963.1	NW_017851282.1	9892.2	0.71	0.000	uncharacterized LOC109532875%2C transcript variant X1
XM_019897977.1	NW_017851282.1	11920.7	1.00	0.000	putative tyrosine-protein kinase Wsck%2C transcript variant X1
XM_019898011.1	NW_017851282.1	1708.6	0.50	0.000	insulin receptor-like
XM_019898016.1	NW_017846438.1	239.9	0.99	0.000	5'-nucleotidase domain-containing protein 3%2C transcript variant X1
XM_019898017.1	NW_017851282.1	3592.8	0.54	0.002	chromodomain-helicase-DNA-binding protein 1%2C transcript variant X1
XM_019898021.1	NW_017851282.1	4921.2	-0.47	0.007	SHC-transforming protein 4%2C transcript variant X1
XM_019898023.1	NW_017851282.1	6762.2	-0.68	0.000	neurofibromin%2C transcript variant X1
XM_019898035.1	NW_017851282.1	1079.4	0.47	0.006	uncharacterized LOC109532906
XM_019898044.1	NW_017851282.1	2610.2	-0.29	0.003	tyrosine-protein kinase shark%2C transcript variant X1
XM_019898051.1	NW_017851282.1	7889.7	-0.84	0.005	DNA repair protein complementing XP-A cells homolog
XM_019898056.1	NW_017851282.1	1152.6	0.40	0.000	exonuclease 1
XM_019898066.1	NW_017851282.1	320.5	0.68	0.002	uncharacterized LOC109532926
XM_019898073.1	NW_017846446.1	1331.7	0.38	0.000	tyrosine-protein kinase RYK-like%2C transcript variant X1
XM_019898084.1	NW_017851282.1	195.4	-0.76	0.002	RNA pseudouridylate synthase domain-containing protein 1-like prion-like-(Q/N-rich) domain-bearing protein 25%2C transcript variant X1
XM_019898096.1	NW_017851282.1	475.9	-0.58	0.000	alanine--glyoxylate aminotransferase 2-like
XM_019898098.1	NW_017851282.1	7496.8	1.09	0.000	kinesin-like protein CG14535
XM_019898113.1	NW_017851283.1	3602.2	1.38	0.000	cyclin-K-like
XM_019898114.1	NW_017851287.1	127.9	-0.85	0.000	monocarboxylate transporter 7-like%2C transcript variant X1
XM_019898118.1	NW_017851291.1	2811.1	-0.31	0.007	zinc finger protein 287-like%2C transcript variant X1
XM_019898129.1	NW_017851291.1	1209.6	-0.85	0.006	uncharacterized LOC109532980
XM_019898138.1	NW_017851300.1	776.7	0.24	0.005	ikaros family zinc finger protein%2C transcript variant X1
XR_002171474.1	NW_017851300.1	199.6	-0.63	0.007	uncharacterized LOC109532994
XM_019898151.1	NW_017851313.1	3370.9	-0.50	0.000	platelet-derived growth factor receptor alpha-like
XR_002171476.1	NW_017851315.1	1010.2	-0.89	0.000	vascular endothelial growth factor receptor kdr-like
XM_019898188.1	NW_017851322.1	770.3	-0.80	0.001	
XM_019898189.1	NW_017851322.1	2771.1	-0.77	0.002	

XM_019898191.1	NW_017851322.1	3906.0	-0.98	0.000	ATP-binding cassette sub-family G member 1-like%2C transcript variant X1
XM_019898194.1	NW_017851323.1	718.5	0.47	0.002	probable DNA-directed RNA polymerases I and III subunit RPAC2
XM_019898202.1	NW_017851323.1	1890.6	1.11	0.000	45 kDa calcium-binding protein%2C transcript variant X1
XM_019898213.1	NW_017851326.1	6.4	1.37	0.000	keratin%2C type II cytoskeletal 1-like
XR_002171477.1	NW_017846491.1	177.0	-0.55	0.002	uncharacterized LOC109533025%2C transcript variant X1
XM_019898225.1	NW_017851351.1	729.4	-0.74	0.000	zinc finger SWIM domain-containing protein 8-like
XM_019898226.1	NW_017851351.1	632.3	-0.71	0.000	zinc finger SWIM domain-containing protein 8-like
XR_002171480.1	NW_017851351.1	155.9	-0.67	0.002	uncharacterized LOC109533040
XM_019898234.1	NW_017851365.1	21.4	-0.87	0.005	uncharacterized LOC109533048%2C transcript variant X1
XR_002171482.1	NW_017851368.1	533.7	-2.04	0.000	uncharacterized LOC109533050
XM_019898241.1	NW_017851370.1	764.8	-0.58	0.003	uncharacterized LOC109533051
XM_019898245.1	NW_017851375.1	742.0	0.57	0.002	uncharacterized protein C7orf50 homolog
XM_019898252.1	NW_017851379.1	829.8	0.37	0.000	TATA-box-binding protein
XM_019898320.1	NW_017851382.1	662.7	0.52	0.005	uncharacterized LOC109533090
XM_019898321.1	NW_017851382.1	498.4	0.96	0.000	uncharacterized LOC109533091%2C transcript variant X1
XR_002171484.1	NW_017851388.1	543.0	0.25	0.003	uncharacterized LOC109533097
XM_019898338.1	NW_017846528.1	2032.0	-0.38	0.000	uncharacterized LOC109533104%2C transcript variant X1
XR_002171486.1	NW_017851395.1	121.6	-0.75	0.007	uncharacterized LOC109533105
XM_019898353.1	NW_017851403.1	640.8	0.40	0.000	cell division cycle protein 23 homolog
XM_019898358.1	NW_017846528.1	1041.7	-0.64	0.000	DNA mismatch repair protein Mlh1-like%2C transcript variant X1
XM_019898356.1	NW_017851403.1	10041.2	-0.31	0.005	repressor of RNA polymerase III transcription MAF1 homolog
XM_019898375.1	NW_017851403.1	1003.7	0.60	0.000	condensin complex subunit 1
XM_019898377.1	NW_017851403.1	1455.7	0.40	0.000	RNA-binding protein 45
XM_019898395.1	NW_017851403.1	1059.3	0.56	0.001	uncharacterized LOC109533145%2C transcript variant X1
XM_019898408.1	NW_017851407.1	141.9	0.92	0.000	carboxy-terminal kinesin 2-like
XM_019898410.1	NW_017851410.1	7595.1	-0.79	0.000	protein FAM46C
XM_019898415.1	NW_017851411.1	1620.7	-0.50	0.009	SCY1-like protein 2
XM_019898418.1	NW_017851413.1	2462.1	-0.85	0.000	acyl-CoA:lysophosphatidylglycerol acyltransferase 1-like
XR_002171495.1	NW_017851413.1	348.0	-1.02	0.000	uncharacterized LOC109533169
XM_019898423.1	NW_017851422.1	981.0	0.53	0.002	protein lethal(2)denticleless-like
XM_019898427.1	NW_017851424.1	8815.1	-1.23	0.000	melanization protease 1-like
XM_019898432.1	NW_017846541.1	75.0	-0.77	0.000	rap guanine nucleotide exchange factor 4-like
XM_019898436.1	NW_017851434.1	310.6	0.95	0.000	bombesin receptor subtype-3-like
XM_019898437.1	NW_017851434.1	1369.1	1.12	0.000	endothelin-converting enzyme 1-like
XM_019898438.1	NW_017851435.1	61.8	0.85	0.004	helix-loop-helix protein delilah-like

XM_019898453.1	NW_017851439.1	3512.3	0.22	0.006	ubiquitin carboxyl-terminal hydrolase 5
XM_019898463.1	NW_017851439.1	9671.1	-0.65	0.000	heterogeneous nuclear ribonucleoprotein U-like protein 2
XM_019898468.1	NW_017851439.1	810.8	-0.95	0.000	uncharacterized LOC109533208%2C transcript variant X1
XM_019898479.1	NW_017851439.1	39.9	-1.10	0.001	cytosol aminopeptidase-like
NW_017851442.1_c3724-1145	NW_017851442.1	6172.3	1.40	0.001	#N/A
XM_019898489.1	NW_017851445.1	2608.4	-0.42	0.000	vacuolar protein sorting-associated protein 18 homolog%2C transcript variant X1
XM_019898493.1	NW_017851445.1	777.9	0.35	0.009	translation initiation factor eIF-2B subunit epsilon%2C transcript variant X1
XM_019898502.1	NW_017851452.1	1842.5	-0.33	0.001	negative elongation factor D%2C transcript variant X1
XM_019898506.1	NW_017851452.1	917.6	0.49	0.000	mediator of RNA polymerase II transcription subunit 22
XM_019898509.1	NW_017851452.1	376.6	0.41	0.000	protein UXT homolog%2C transcript variant X1
XM_019898511.1	NW_017851452.1	923.8	-1.04	0.001	toll-like receptor 7
XM_019898542.1	NW_017851453.1	177.9	-1.68	0.000	uncharacterized LOC109533259
XM_019898544.1	NW_017851453.1	908.4	-0.85	0.001	uncharacterized LOC109533262%2C transcript variant X1
XM_019898547.1	NW_017851453.1	939.9	0.32	0.002	uncharacterized LOC109533264
XM_019898552.1	NW_017851453.1	157.3	0.79	0.004	cytochrome P450 4g15-like
XM_019898553.1	NW_017851453.1	876.3	-0.68	0.001	zinc finger protein Elbow
XM_019898558.1	NW_017851465.1	38081.7	1.89	0.000	cytochrome P450 6A1-like
XM_019898560.1	NW_017851465.1	7664.5	1.71	0.000	cytochrome P450 6a2-like
XM_019898565.1	NW_017851470.1	1152.7	1.35	0.000	mitochondrial ornithine transporter 1%2C transcript variant X1
XM_019898568.1	NW_017851470.1	374.4	0.81	0.000	THAP domain-containing protein 2-like%2C transcript variant X1
XM_019898581.1	NW_017846595.1	158.9	-0.85	0.005	piggyBac transposable element-derived protein 3-like
XR_002171509.1	NW_017851481.1	8404.9	0.85	0.003	aldose reductase-like
XM_019898613.1	NW_017851488.1	557.0	0.41	0.008	transforming growth factor beta regulator 1-like
XM_019898615.1	NW_017851488.1	1039.0	0.20	0.009	actin-related protein 10-like
XM_019898619.1	NW_017851489.1	8013.2	-1.19	0.000	uncharacterized LOC109533325
XM_019898630.1	NW_017851504.1	951.5	0.63	0.002	RNA-binding protein MEX3B-like
XM_019898631.1	NW_017851505.1	6571.5	-0.48	0.000	serine/threonine-protein kinase 10-like
XM_019898632.1	NW_017851505.1	2559.3	0.57	0.000	ecdysone 20-monooxygenase%2C transcript variant X1
XM_019898650.1	NW_017851509.1	7236.0	0.89	0.001	uncharacterized LOC109533356
XM_019898666.1	NW_017851513.1	1889.6	-1.54	0.000	kielin/chordin-like protein
XM_019898685.1	NW_017851515.1	417.7	-0.64	0.007	1-phosphatidylinositol 4%2C5-bisphosphate phosphodiesterase classes I and II-like
XM_019898689.1	NW_017851515.1	5198.3	-1.22	0.000	nose resistant to fluoxetine protein 6-like%2C transcript variant X1
XM_019898694.1	NW_017851515.1	5627.7	-1.17	0.000	nose resistant to fluoxetine protein 6-like
XM_019898697.1	NW_017851516.1	3482.0	-0.22	0.007	glycogen synthase kinase-3 beta-like

XM_019898703.1	NW_017851520.1	970.7	-0.58	0.007	B-cell lymphoma/leukemia 11A
XM_019898705.1	NW_017851522.1	40066.2	-1.50	0.000	ATP-binding cassette sub-family G member 4-like
XM_019898706.1	NW_017851523.1	24765.2	1.40	0.001	uncharacterized LOC109533401
XM_019898720.1	NW_017851525.1	1274.7	0.47	0.000	39S ribosomal protein L22%2C mitochondrial
NW_017846633.1_2849-3465	NW_017846633.1	299.1	0.97	0.000	#N/A
XM_019898727.1	NW_017851531.1	572.3	0.75	0.003	anillin%2C transcript variant X1
XM_019898730.1	NW_017851531.1	6012.3	-1.52	0.000	calcium/calmodulin-dependent protein kinase kinase 1%2C transcript variant X1
XM_019898733.1	NW_017851531.1	1800.4	0.48	0.001	uncharacterized LOC109533418
XM_019898735.1	NW_017851531.1	11779.9	0.96	0.001	protein I'm not dead yet%2C transcript variant X1
XM_019898741.1	NW_017851531.1	1479.3	0.67	0.001	disks large-associated protein 5%2C transcript variant X1
XM_019898747.1	NW_017851531.1	842.4	0.55	0.000	mitochondrial import inner membrane translocase subunit Tim22
XM_019898758.1	NW_017846640.1	2471.4	-1.01	0.001	L-lactate dehydrogenase-like
XM_019898760.1	NW_017851538.1	27493.5	-0.48	0.005	AN1-type zinc finger protein 6%2C transcript variant X1
XM_019898780.1	NW_017851546.1	4240.0	-1.20	0.000	uncharacterized LOC109533453
XM_019898786.1	NW_017851551.1	372.6	-0.53	0.000	myotubularin-related protein 13-like
XM_019898787.1	NW_017851551.1	90.8	-0.49	0.008	myotubularin-related protein 13-like
XM_019898807.1	NW_017851552.1	1917.0	-1.00	0.001	probable multidrug resistance-associated protein lethal(2)03659
XM_019898808.1	NW_017851552.1	196.5	0.98	0.008	soluble guanylate cyclase 89Db-like
XM_019898811.1	NW_017851554.1	2665.3	1.05	0.000	chorion peroxidase
XM_019898840.1	NW_017851564.1	283.7	-1.41	0.000	uncharacterized LOC109533501
XM_019898842.1	NW_017851565.1	166.1	1.38	0.001	uncharacterized LOC109533505%2C transcript variant X1
XR_002171531.1	NW_017851565.1	34.5	1.38	0.004	uncharacterized LOC109533508
XM_019898846.1	NW_017851569.1	40305.1	1.28	0.001	pectinesterase B-like
XM_019898853.1	NW_017851570.1	3614.0	-1.81	0.000	hemicentin-2-like
XM_019898861.1	NW_017851577.1	3018.2	0.35	0.005	caprin homolog%2C transcript variant X1
XM_019898868.1	NW_017851577.1	1491.1	-0.61	0.002	protein shuttle craft-like
XM_019898875.1	NW_017851578.1	105.3	0.79	0.009	uncharacterized LOC109533536%2C transcript variant X1
XM_019898879.1	NW_017851583.1	544.0	0.77	0.004	uncharacterized LOC109533542
XM_019898885.1	NW_017851587.1	1065.1	1.00	0.000	E3 ubiquitin-protein ligase SINAT2-like%2C transcript variant X1
XM_019898897.1	NW_017851590.1	1945.3	0.90	0.001	mitochondrial amidoxime reducing component 2-like%2C transcript variant X1
XM_019898910.1	NW_017851598.1	2029.5	-0.61	0.004	uncharacterized LOC109533567
XM_019898912.1	NW_017851599.1	2018.4	-0.34	0.002	tyrosine-protein kinase PR2%2C transcript variant X1
XM_019898920.1	NW_017851599.1	1163.3	0.81	0.000	39S ribosomal protein L20%2C mitochondrial
XM_019898925.1	NW_017851601.1	906.9	-0.94	0.000	DNA-binding protein D-ETS-4%2C transcript variant X1

XM_019898928.1	NW_017851601.1	2173.3	-0.54	0.001	tumor necrosis factor receptor superfamily member wengen-like%2C transcript variant X1
XM_019898936.1	NW_017851601.1	1262.9	0.41	0.006	mitochondrial import inner membrane translocase subunit TIM44
XM_019898945.1	NW_017851604.1	56.1	-0.74	0.008	uncharacterized LOC109533590
XM_019898950.1	NW_017851605.1	113.2	-0.64	0.001	serum response factor homolog
XM_019898952.1	NW_017851611.1	416.2	-0.36	0.007	tetratricopeptide repeat protein 5-like
XM_019898956.1	NW_017851612.1	76.2	-0.80	0.000	rap guanine nucleotide exchange factor 4-like
XM_019898962.1	NW_017851612.1	2763.4	-0.37	0.003	multidrug resistance-associated protein 1%2C transcript variant X1 facilitated trehalose transporter Tret1-like%2C transcript variant X1
XM_019898967.1	NW_017851612.1	14259.5	-2.05	0.000	uncharacterized LOC109533612
XM_019898970.1	NW_017851612.1	14.4	-1.50	0.001	superkiller viralicidic activity 2-like 2
XM_019898982.1	NW_017851612.1	2880.7	-0.38	0.000	ankyrin-3-like
XM_019898995.1	NW_017851612.1	709.1	0.91	0.002	putative ankyrin repeat protein RF_0381
XM_019898996.1	NW_017851612.1	582.8	1.02	0.000	troponin C-like
XM_019898999.1	NW_017851612.1	5225.8	0.47	0.000	cuticle protein 18.7-like
XM_019899002.1	NW_017851612.1	80.2	-1.26	0.002	REST corepressor 3-like
XM_019899013.1	NW_017851617.1	1152.2	-0.81	0.000	glutathione S-transferase-like%2C transcript variant X1
XM_019899020.1	NW_017851618.1	4541.3	0.99	0.003	venom carboxylesterase-6-like
XM_019899033.1	NW_017851618.1	45.4	1.11	0.002	uncharacterized LOC109533654
XM_019899035.1	NW_017851619.1	1042.2	0.78	0.000	DNA-directed RNA polymerase III subunit RPC2-like
XM_019899036.1	NW_017851619.1	796.0	0.25	0.006	phosphoenolpyruvate carboxykinase [GTP]-like
XM_019899042.1	NW_017851628.1	30059.8	0.88	0.005	threonine aspartase 1
XM_019899063.1	NW_017851632.1	645.8	-0.41	0.000	uncharacterized LOC109533687
XM_019899064.1	NW_017851632.1	182.7	0.69	0.000	histone-lysine N-methyltransferase NSD2
XM_019899066.1	NW_017851632.1	1117.6	0.65	0.000	bifunctional purine biosynthesis protein PURH%2C transcript variant X1
XM_019899073.1	NW_017851633.1	35936.2	0.96	0.002	protein diaphanous
XM_019899085.1	NW_017851633.1	7437.4	-0.48	0.010	uncharacterized LOC109533701%2C transcript variant X1
XM_019899086.1	NW_017851633.1	1789.8	0.84	0.000	estrogen sulfotransferase-like
XM_019899095.1	NW_017851633.1	39.0	-1.01	0.003	uncharacterized LOC109533709%2C transcript variant X1
XM_019899101.1	NW_017851633.1	16931.3	0.85	0.002	apoptosis-stimulating of p53 protein 2-like
XM_019899117.1	NW_017851637.1	916.3	0.56	0.002	vacuolar ATPase assembly integral membrane protein VMA21 homolog
XM_019899118.1	NW_017851637.1	2078.0	0.49	0.000	muscarinic acetylcholine receptor DM1%2C transcript variant X1
XM_019899120.1	NW_017851638.1	247.3	-1.04	0.000	gastrula zinc finger protein XICGF57.1-like
XM_019899123.1	NW_017851640.1	2737.3	-0.29	0.000	kinesin-like protein KIF11-B
XM_019899130.1	NW_017851640.1	1001.7	0.74	0.000	putative glutathione-specific gamma-glutamylcyclotransferase 2
XM_019899143.1	NW_017851644.1	829.1	0.50	0.007	

XM_019899155.1	NW_017851647.1	5088.3	-0.47	0.001	myosin-VIIa%2C transcript variant X1
XM_019899163.1	NW_017851647.1	2030.6	-0.38	0.000	uncharacterized LOC109533758%2C transcript variant X1
XM_019899165.1	NW_017851647.1	1041.5	-0.64	0.000	DNA mismatch repair protein Mlh1-like%2C transcript variant X1
XM_019899169.1	NW_017846795.1	350.9	-1.04	0.000	protein dachsous-like
XM_019899182.1	NW_017851649.1	796.2	1.00	0.000	uncharacterized LOC109533777
XM_019899188.1	NW_017846800.1	17.7	-0.86	0.005	gamma-aminobutyric acid receptor subunit beta-like
XM_019899191.1	NW_017851651.1	82.5	-1.35	0.000	zinc finger protein 423 homolog plasma membrane calcium-transporting ATPase 1%2C transcript variant X1
XM_019899194.1	NW_017851651.1	14648.2	-0.52	0.000	
XM_019899207.1	NW_017851651.1	17035.0	-0.39	0.003	E3 ubiquitin-protein ligase HUWE1%2C transcript variant X1
XM_019899212.1	NW_017851651.1	3588.4	-0.37	0.007	latrophilin Cirl%2C transcript variant X1
XM_019899222.1	NW_017851651.1	4873.4	-0.29	0.003	uncharacterized LOC109533799%2C transcript variant X1
XM_019899225.1	NW_017851651.1	702.2	0.80	0.000	heat shock 70 kDa protein-like%2C transcript variant X1
XM_019899241.1	NW_017851651.1	3107.4	0.45	0.002	uroporphyrinogen decarboxylase
XM_019899246.1	NW_017851651.1	4308.9	-0.95	0.000	leucine-rich repeats and immunoglobulin-like domains protein 3
XM_019899247.1	NW_017851651.1	5500.8	0.55	0.008	glucose-6-phosphate 1-dehydrogenase%2C transcript variant X1
XM_019899282.1	NW_017851651.1	35813.6	1.03	0.000	SEC23-interacting protein%2C transcript variant X1
XM_019899286.1	NW_017851651.1	7801.1	-0.99	0.010	uncharacterized LOC109533822
XM_019899299.1	NW_017851651.1	6426.5	1.82	0.000	pancreatic triacylglycerol lipase-like
XM_019899310.1	NW_017846821.1	1198.6	-1.23	0.000	G-protein coupled receptor moody-like
XM_019899316.1	NW_017851651.1	18069.9	0.79	0.000	cytokine receptor%2C transcript variant X1
XM_019899321.1	NW_017851651.1	2334.6	-0.57	0.001	uncharacterized LOC109533839
XM_019899330.1	NW_017851651.1	52.0	-0.85	0.007	protein tyrosine phosphatase domain-containing protein 1-like
XM_019899335.1	NW_017846824.1	5786.8	-1.43	0.000	uncharacterized LOC109533846%2C transcript variant X1
XM_019899333.1	NW_017851651.1	2125.1	0.29	0.008	5'-nucleotidase domain-containing protein 1
XM_019899346.1	NW_017851651.1	3793.0	-0.32	0.000	potential E3 ubiquitin-protein ligase ariadne-1-like
XM_019899377.1	NW_017851651.1	1358.0	1.18	0.002	lipoprotein lipase-like
XM_019899378.1	NW_017851651.1	403.0	-0.60	0.003	protein trachealess%2C transcript variant X1
XM_019899382.1	NW_017851651.1	1071.2	0.51	0.002	putative GTP-binding protein 6%2C transcript variant X1
XM_019899385.1	NW_017851651.1	9580.3	1.09	0.003	transmembrane protein 205
XM_019899393.1	NW_017851651.1	4000.8	0.52	0.001	cytochrome c oxidase subunit 5A%2C mitochondrial-like
XM_019899394.1	NW_017851651.1	1583.2	-0.58	0.002	uncharacterized LOC109533886 mono [ADP-ribose] polymerase PARP16-like%2C transcript variant X1
XM_019899395.1	NW_017851651.1	585.3	0.48	0.007	
XM_019899407.1	NW_017851651.1	362.6	0.89	0.000	M-phase inducer phosphatase-like%2C transcript variant X1
XM_019899415.1	NW_017851654.1	2857.3	0.43	0.001	glucosamine-6-phosphate isomerase-like
XM_019899427.1	NW_017851655.1	549.5	0.80	0.003	gamma-interferon-inducible-lysosomal thiol reductase-like

XM_019899433.1	NW_017851656.1	95.5	0.72	0.001	uncharacterized LOC109533920
XM_019899438.1	NW_017846838.1	308.9	1.04	0.000	uncharacterized LOC109533922
XM_019899446.1	NW_017851659.1	583.1	-0.46	0.000	ras-related protein Rab-27A
XM_019899448.1	NW_017851661.1	19.6	-1.14	0.001	uncharacterized LOC109533935
XM_019899451.1	NW_017851662.1	40231.0	-1.50	0.000	ATP-binding cassette sub-family G member 4-like
XM_019899452.1	NW_017851662.1	2752.1	-0.66	0.000	monocarboxylate transporter 9-like%2C transcript variant X1
XM_019899455.1	NW_017851662.1	1183.7	0.56	0.000	single-stranded DNA-binding protein%2C mitochondrial-like
XM_019899458.1	NW_017851662.1	843.6	-1.19	0.004	cytochrome b5-like
XM_019899459.1	NW_017851662.1	317.0	-0.64	0.004	prothoracicostatic peptide
XM_019899461.1	NW_017851663.1	113.2	-0.64	0.001	serum response factor homolog
XM_019899473.1	NW_017846850.1	156.6	0.49	0.004	zinc finger protein OZF-like
XM_019899477.1	NW_017851666.1	2314.3	0.22	0.002	uncharacterized LOC109533955%2C transcript variant X1
XM_019899479.1	NW_017851666.1	852.5	0.52	0.009	condensin complex subunit 2%2C transcript variant X1
XM_019899497.1	NW_017851666.1	1331.7	0.38	0.000	uncharacterized LOC109533968
XM_019899515.1	NW_017851675.1	1160.2	-0.64	0.001	uncharacterized LOC109533983
XM_019899568.1	NW_017845104.1	373.8	0.60	0.000	deoxycytidylate deaminase coiled-coil domain-containing protein 28A%2C transcript variant X1
XM_019899528.1	NW_017851680.1	1468.9	0.32	0.001	partner of xrn-2 protein 1-like
XM_019899535.1	NW_017851680.1	964.9	0.42	0.000	heat shock 70 kDa protein II-like%2C transcript variant X1
XM_019899536.1	NW_017851680.1	970.4	-0.68	0.002	uncharacterized LOC109534003%2C transcript variant X1
XM_019899539.1	NW_017851680.1	2046.3	-0.27	0.000	tryptophan--tRNA ligase%2C mitochondrial
XM_019899542.1	NW_017851680.1	522.1	0.44	0.001	uncharacterized LOC109534009
XM_019899551.1	NW_017851680.1	214.6	0.76	0.005	zinc finger protein 43-like%2C transcript variant X1
XM_019899559.1	NW_017851680.1	1042.2	0.91	0.000	uncharacterized LOC109534019
XM_019899564.1	NW_017851680.1	221.0	0.69	0.008	farnesol dehydrogenase-like
XM_019899567.1	NW_017851683.1	68.0	1.16	0.002	glutathione S-transferase 1-like%2C transcript variant X1
XM_019899571.1	NW_017851683.1	3564.2	0.53	0.000	farnesol dehydrogenase-like
XM_019899575.1	NW_017851683.1	397.7	1.76	0.000	zinc finger protein 569%2C transcript variant X1
XM_019899593.1	NW_017851689.1	1611.8	-0.38	0.000	uncharacterized LOC109534057
XM_019899610.1	NW_017851689.1	61.6	-1.60	0.000	uncharacterized LOC109534073
XM_019899628.1	NW_017851689.1	575.2	0.47	0.000	uncharacterized LOC109534077
XM_019899633.1	NW_017851689.1	1766.5	-1.37	0.000	tyrosine-protein phosphatase 10D
XM_019899638.1	NW_017851690.1	4316.9	-0.65	0.000	RNA cytidine acetyltransferase%2C transcript variant X1
XM_019899639.1	NW_017851690.1	1696.4	0.31	0.007	protein mab-21
XM_019899652.1	NW_017851693.1	126.6	-0.62	0.001	uncharacterized LOC109534097
XR_002171597.1	NW_017846910.1	6.4	-1.27	0.009	

XM_019899663.1	NW_017851694.1	1326.4	0.60	0.000	39S ribosomal protein L37%2C mitochondrial two pore potassium channel protein sup-9%2C transcript variant X1
XM_019899664.1	NW_017851694.1	185.4	-0.66	0.000	
XM_019899668.1	NW_017851694.1	2823.4	0.63	0.007	isopentenyl-diphosphate Delta-isomerase 1
XM_019899670.1	NW_017851694.1	7782.3	-0.41	0.000	ran-binding protein 9
XM_019899671.1	NW_017851694.1	3553.2	0.21	0.007	28S ribosomal protein S5%2C mitochondrial transient receptor potential cation channel trpm%2C transcript variant X1
XM_019899677.1	NW_017851694.1	4904.2	0.40	0.000	
XM_019899689.1	NW_017851694.1	981.9	0.24	0.007	WD repeat-containing protein 20
XM_019899698.1	NW_017851694.1	1366.5	0.39	0.008	retinol dehydrogenase 12-like%2C transcript variant X1
XM_019899706.1	NW_017851694.1	1083.4	0.39	0.001	39S ribosomal protein L39%2C mitochondrial
XM_019899742.1	NW_017851697.1	139.8	1.13	0.000	UDP-glucuronosyltransferase 2B15-like
XM_019899743.1	NW_017851699.1	1089.7	1.10	0.000	angiotensin-converting enzyme-like
XM_019899744.1	NW_017851699.1	763.2	1.08	0.000	angiotensin-converting enzyme-like
XM_019899749.1	NW_017846929.1	1638.2	-0.67	0.000	activating transcription factor 3-like
XM_019899763.1	NW_017851702.1	12058.3	1.05	0.000	uncharacterized LOC109534191
XM_019899772.1	NW_017851704.1	5617.0	0.27	0.001	CDGSH iron-sulfur domain-containing protein 2 homolog major facilitator superfamily domain-containing protein 9-like%2C transcript variant X1
XM_019899773.1	NW_017851704.1	2192.9	0.70	0.003	
XM_019899775.1	NW_017851704.1	457.8	0.55	0.002	protein PET100 homolog%2C mitochondrial PH and SEC7 domain-containing protein 1%2C transcript variant X1
XM_019899779.1	NW_017851704.1	3951.2	-0.51	0.000	
XR_002171612.1	NW_017846932.1	407.1	-1.13	0.000	uncharacterized LOC109534206
XM_019899787.1	NW_017851704.1	3092.4	1.29	0.000	acyl-CoA Delta(11) desaturase
XM_019899788.1	NW_017851704.1	328.1	1.08	0.003	UDP-glucuronosyltransferase 2B10-like
XM_019899789.1	NW_017851704.1	62.4	1.03	0.000	UDP-glucuronosyltransferase 2B10-like
XM_019899791.1	NW_017851704.1	4700.0	-0.53	0.005	uncharacterized LOC109534210
XM_019899794.1	NW_017851704.1	2209.1	0.54	0.000	J domain-containing protein CG6693
XM_019899802.1	NW_017851710.1	3628.5	0.24	0.001	uncharacterized LOC109534221
XM_019899806.1	NW_017851711.1	329.1	-0.61	0.000	angiotensin-converting enzyme-like
XM_019899814.1	NW_017851713.1	1524.3	0.34	0.002	probable small nuclear ribonucleoprotein Sm D2 zinc finger CCCH domain-containing protein 10-like%2C transcript variant X1
XM_019899821.1	NW_017851713.1	2891.3	-0.19	0.005	
XM_019899835.1	NW_017851713.1	771.7	0.35	0.007	pyridoxal phosphate phosphatase PHOSPHO2-like schwannomin-interacting protein 1 homolog%2C transcript variant X1
XM_019899836.1	NW_017851713.1	2462.0	-0.46	0.001	
XM_019899842.1	NW_017851713.1	255.0	-1.52	0.000	facilitated trehalose transporter Tret1-like
XM_019899859.1	NW_017851716.1	718.7	0.35	0.003	ubiquinol-cytochrome-c reductase complex assembly factor 1-like
XM_019899878.1	NW_017851723.1	4292.8	2.53	0.000	tryptophan 2%2C3-dioxygenase-like

XM_019899880.1	NW_017851724.1	344.0	0.88	0.000	uncharacterized LOC109534281
XM_019899885.1	NW_017846956.1	473.7	0.67	0.005	neutral and basic amino acid transport protein rBAT-like
XM_019899900.1	NW_017851724.1	62782.0	-0.65	0.002	gelsolin
XM_019899904.1	NW_017851724.1	3255.5	-0.36	0.001	putative leucine-rich repeat-containing protein DDB_G0290503
XM_019899906.1	NW_017851724.1	3497.6	1.26	0.000	4-coumarate--CoA ligase 1-like
XM_019899913.1	NW_017851724.1	2990.3	1.19	0.000	4-coumarate--CoA ligase 1-like
XM_019899917.1	NW_017851724.1	20763.3	-1.00	0.000	uncharacterized LOC109534306
XM_019899921.1	NW_017851724.1	2620.4	0.39	0.000	AFG3-like protein 2
XM_019899926.1	NW_017851724.1	14361.6	-0.66	0.000	proton-coupled amino acid transporter-like protein pathetic%2C transcript variant X1
XM_019899941.1	NW_017851724.1	11039.0	-0.46	0.000	rho guanine nucleotide exchange factor 12%2C transcript variant X1
XM_019899961.1	NW_017851724.1	644.6	-1.08	0.000	potassium channel subfamily T member 1
XM_019899968.1	NW_017851724.1	24667.0	-0.33	0.006	serine/threonine-protein kinase MARK2-like%2C transcript variant X1
XM_019899997.1	NW_017851724.1	3617.7	-0.62	0.004	pyrimidodiazepine synthase-like
XM_019900002.1	NW_017846981.1	791.4	-0.58	0.007	B-cell lymphoma/leukemia 11A-like
XM_019900000.1	NW_017851724.1	1253.4	0.91	0.000	targeting protein for Xk1p2%2C transcript variant X1
XM_019900015.1	NW_017851724.1	562.8	0.45	0.001	origin recognition complex subunit 2
XM_019900021.1	NW_017851724.1	963.3	0.50	0.000	WASH complex subunit strumpellin%2C transcript variant X1
XM_019900030.1	NW_017851724.1	380.5	-0.52	0.004	uncharacterized LOC109534372
XM_019900031.1	NW_017851724.1	3925.8	-0.34	0.008	rap guanine nucleotide exchange factor 6
XR_002171627.1	NW_017846997.1	5.2	1.46	0.001	uncharacterized LOC109534375
XM_019900045.1	NW_017851724.1	8445.8	-1.49	0.001	cathepsin L-like proteinase
XM_019900049.1	NW_017851724.1	1041.0	0.44	0.000	retinoblastoma-binding protein 5 homolog%2C transcript variant X1
XM_019900053.1	NW_017851724.1	211.7	1.16	0.000	angiotensin-2
XM_019900059.1	NW_017851724.1	492.8	0.46	0.003	uncharacterized LOC109534392
XM_019900060.1	NW_017851724.1	3365.4	0.48	0.000	NADH dehydrogenase [ubiquinone] 1 alpha subcomplex assembly factor 8-like%2C transcript variant X1
XM_019900063.1	NW_017851724.1	1381.9	0.50	0.000	transmembrane protein 70 homolog%2C mitochondrial
XM_019900064.1	NW_017851724.1	1285.0	0.61	0.008	protein abnormal spindle-like
XM_019900075.1	NW_017851724.1	434.1	-0.56	0.002	cathepsin B-like%2C transcript variant X1
XM_019900077.1	NW_017851724.1	927.4	1.00	0.000	histone-lysine N-methyltransferase SMYD3-like
XM_019900078.1	NW_017851724.1	394.3	1.00	0.000	uncharacterized LOC109534405
XR_002171629.1	NW_017851724.1	70.5	1.07	0.000	uncharacterized LOC109534406
XR_002171630.1	NW_017851724.1	67.2	1.05	0.000	uncharacterized LOC109534407
XM_019900082.1	NW_017851724.1	1286.9	0.55	0.000	surfeit locus protein 1

XM_019900097.1	NW_017851729.1	898.6	0.60	0.000	TELO2-interacting protein 1 homolog%2C transcript variant X1
XM_019900100.1	NW_017851729.1	615.2	-0.36	0.006	zinc finger protein 678-like
XM_019900102.1	NW_017851731.1	220.8	2.09	0.000	protein cycle
XM_019900106.1	NW_017851731.1	922.6	-1.03	0.000	propionyl-CoA carboxylase beta chain%2C mitochondrial-like%2C transcript variant X1
XM_019900126.1	NW_017851737.1	10395.7	-0.49	0.000	transmembrane protein 184B%2C transcript variant X1
XM_019900136.1	NW_017851737.1	3981.2	1.49	0.001	lysozyme C-1-like
XM_019900149.1	NW_017851737.1	1613.7	0.42	0.003	uridine diphosphate glucose pyrophosphatase-like
XM_019900150.1	NW_017851737.1	1445.5	-0.42	0.000	bladder cancer-associated protein CCR4-NOT transcription complex subunit 1%2C transcript variant X1
XM_019900152.1	NW_017851737.1	10067.6	-0.30	0.002	
XM_019900159.1	NW_017851737.1	6312.7	-0.56	0.006	heparan-alpha-glucosaminide N-acetyltransferase-like
XM_019900167.1	NW_017851737.1	3604.1	-0.86	0.000	uncharacterized LOC109534480%2C transcript variant X1
XM_019900192.1	NW_017851737.1	2037.4	-0.61	0.009	ankyrin-3-like%2C transcript variant X1
XM_019900201.1	NW_017851737.1	799.0	0.37	0.001	nuclear nucleic acid-binding protein C1D-like
XM_019900202.1	NW_017851737.1	1702.0	-0.53	0.000	NF-X1-type zinc finger protein NFXL1 ras-specific guanine nucleotide-releasing factor RalGPS1-like%2C transcript variant X1
XM_019900205.1	NW_017851737.1	5547.5	0.65	0.000	
XM_019900228.1	NW_017851737.1	914.4	0.93	0.000	small ubiquitin-related modifier 3-like
XM_019900229.1	NW_017851737.1	638.8	-0.68	0.003	leukocyte tyrosine kinase receptor%2C transcript variant X1
XM_019900232.1	NW_017851737.1	1505.8	0.57	0.004	inactive peptidyl-prolyl cis-trans isomerase shutdown
XR_002171640.1	NW_017851737.1	113.0	-1.43	0.001	uncharacterized LOC109534517
XM_019900254.1	NW_017851737.1	279.8	1.04	0.000	tRNA-specific adenosine deaminase 1%2C transcript variant X1 cyclic AMP response element-binding protein A-like%2C transcript variant X1
XM_019900262.1	NW_017847028.1	541.7	-0.46	0.003	
XM_019900263.1	NW_017851737.1	486.0	0.42	0.003	probable ATP-dependent RNA helicase DDX20
XM_019900265.1	NW_017851737.1	1408.1	0.45	0.001	immunoglobulin-binding protein 1
XM_019900280.1	NW_017851743.1	1131.5	1.04	0.000	putative molluscan insulin-related peptide(s) receptor
XM_019900281.1	NW_017851743.1	2999.2	1.02	0.000	insulin receptor-like
NW_017851743.1_c628-13	NW_017851743.1	299.1	0.97	0.000	#N/A
XM_019900285.1	NW_017851743.1	800.4	0.63	0.003	gephyrin%2C transcript variant X1
XM_019900299.1	NW_017851748.1	625.5	0.55	0.002	PCI domain-containing protein 2 homolog
XM_019900300.1	NW_017851749.1	2405.3	0.47	0.000	eukaryotic translation initiation factor 3 subunit K-like
XM_019900301.1	NW_017851749.1	1524.9	0.26	0.008	polyphosphoinositide phosphatase-like
XM_019900302.1	NW_017851749.1	15.6	-1.55	0.000	uncharacterized LOC109534583
XM_019900304.1	NW_017851751.1	5479.3	-0.40	0.003	dmX-like protein 2
XM_019900305.1	NW_017851751.1	27654.9	1.26	0.007	sorbitol dehydrogenase-like
XM_019900306.1	NW_017851751.1	2082.3	-0.57	0.000	U11/U12 small nuclear ribonucleoprotein 48 kDa protein-like

XM_019900307.1	NW_017851751.1	1255.2	-0.65	0.000	uncharacterized LOC109534589%2C transcript variant X1
XM_019900311.1	NW_017851751.1	191.8	1.05	0.001	uncharacterized LOC109534591
XM_019900317.1	NW_017851753.1	5508.7	-0.43	0.000	maternal protein tudor-like%2C transcript variant X1
XR_002171650.1	NW_017851753.1	352.8	1.67	0.000	uncharacterized LOC109534601
XM_019900326.1	NW_017851754.1	16370.9	-0.63	0.000	baculoviral IAP repeat-containing protein 2-like baculoviral IAP repeat-containing protein 7-B-like%2C transcript variant X1
XM_019900327.1	NW_017851754.1	2715.7	0.31	0.000	
XM_019900332.1	NW_017851755.1	4957.0	-0.42	0.004	ubiquitin-like protein 3
XM_019900345.1	NW_017851758.1	23848.5	0.96	0.008	myosinase 1-like
XM_019900363.1	NW_017851758.1	2212.7	0.59	0.000	cystathionine beta-synthase%2C transcript variant X1
XM_019900378.1	NW_017847130.1	72.4	1.74	0.000	farnesol dehydrogenase-like
XM_019900381.1	NW_017851760.1	1990.0	0.47	0.002	acyl-CoA dehydrogenase family member 9%2C mitochondrial
XM_019900395.1	NW_017851760.1	28370.9	1.07	0.001	venom acid phosphatase Acph-1-like
XM_019900404.1	NW_017851760.1	2289.9	0.90	0.005	venom carboxylesterase-6-like
XM_019900418.1	NW_017851768.1	353.9	-1.03	0.000	protein dachsous
XM_019900421.1	NW_017847141.1	2137.6	0.97	0.000	anaphase-promoting complex subunit 4-like
XM_019900424.1	NW_017851769.1	10443.3	-0.31	0.001	spectrin beta chain-like
XM_019900426.1	NW_017851769.1	698.2	1.04	0.000	uncharacterized LOC109534680
XM_019900427.1	NW_017851769.1	1040.2	1.06	0.000	monocarboxylate transporter 3-like
XM_019900435.1	NW_017851773.1	1324.3	0.35	0.007	nucleoporin Nup37
XM_019900441.1	NW_017851775.1	3120.6	-0.98	0.000	protein hunchback-like
XM_019900463.1	NW_017851775.1	2000.1	-0.87	0.000	UPF0598 protein CG30010
XM_019900466.1	NW_017851775.1	1968.9	0.79	0.000	uncharacterized LOC109534711%2C transcript variant X1
XM_019900474.1	NW_017851775.1	2590.1	0.48	0.000	probable RNA polymerase II nuclear localization protein SLC7A6OS
XM_019900479.1	NW_017851775.1	2041.7	0.28	0.006	RE1-silencing transcription factor-like
XM_019900487.1	NW_017851775.1	3225.6	0.23	0.006	small nuclear ribonucleoprotein-associated protein B
XM_019900493.1	NW_017851775.1	4748.3	-1.24	0.000	RNA binding protein fox-1 homolog 3
XM_019900500.1	NW_017847165.1	10092.8	-0.30	0.002	spectrin beta chain-like
XM_019900501.1	NW_017851775.1	4356.5	-0.87	0.000	protein unzipped%2C transcript variant X1
XM_019900503.1	NW_017851775.1	966.6	0.42	0.000	probable dimethyladenosine transferase
XM_019900513.1	NW_017847169.1	246.0	1.31	0.000	regucalcin-like
XM_019900512.1	NW_017851775.1	701.9	0.81	0.000	hydroxysteroid dehydrogenase-like protein 1
XM_019900516.1	NW_017851775.1	966.9	0.52	0.001	rRNA methyltransferase 3%2C mitochondrial
XM_019900520.1	NW_017851775.1	12.1	-1.99	0.000	uncharacterized LOC109534747
XM_019900527.1	NW_017851775.1	1845.7	0.73	0.000	uncharacterized LOC109534753%2C transcript variant X1
XM_019900531.1	NW_017851775.1	11836.7	-0.70	0.001	protein slowmo

XM_019900533.1	NW_017851775.1	13885.1	-0.34	0.000	tetratricopeptide repeat protein 14 homolog%2C transcript variant X1
XM_019900554.1	NW_017851775.1	22620.8	-1.25	0.000	protein hunchback-like
XM_019900555.1	NW_017851775.1	667.8	-0.67	0.000	MPN domain-containing protein CG4751-like%2C transcript variant X1
XM_019900562.1	NW_017851775.1	2783.6	-0.89	0.000	POU domain protein CF1A
XM_019900563.1	NW_017851775.1	3445.8	-0.83	0.000	uncharacterized LOC109534775%2C transcript variant X1
XM_019900571.1	NW_017851775.1	338.5	0.93	0.005	endocuticle structural glycoprotein SgAbd-4-like
XR_002171663.1	NW_017851775.1	6012.7	0.81	0.000	uncharacterized LOC109534782
XM_019900574.1	NW_017851775.1	1264.3	-0.33	0.004	sphingomyelin synthase-related 1-like
XR_002171666.1	NW_017847180.1	188.0	-0.65	0.000	uncharacterized LOC109534798
XM_019900587.1	NW_017851776.1	575.0	-0.56	0.007	uncharacterized LOC109534805%2C transcript variant X1
XM_019900605.1	NW_017851783.1	749.2	-0.52	0.002	uncharacterized LOC109534826
XR_002171668.1	NW_017851783.1	941.9	-0.87	0.000	uncharacterized LOC109534842
XM_019900626.1	NW_017851783.1	2273.2	0.48	0.000	cyclin-related protein FAM58A
XM_019900633.1	NW_017851783.1	6238.1	-0.63	0.000	adipocyte plasma membrane-associated protein-like
XM_019900637.1	NW_017851783.1	93.7	-0.50	0.001	cilia- and flagella-associated protein 36 serine/threonine-protein phosphatase 4 regulatory subunit 3%2C transcript variant X1
XM_019900638.1	NW_017851783.1	2069.1	-0.37	0.000	uncharacterized LOC109534862
XR_002171670.1	NW_017851783.1	6260.1	-0.66	0.001	uncharacterized LOC109534862
XM_019900648.1	NW_017851783.1	800.4	0.96	0.000	bone morphogenetic protein 7-like
XM_019900663.1	NW_017851783.1	864.7	0.37	0.009	ATP-dependent RNA helicase Ddx1
XM_019900695.1	NW_017851783.1	1676.1	-1.36	0.003	uncharacterized LOC109534899
NW_017851802.1_c28234-24	NW_017851802.1	35062.3	-1.07	0.000	#N/A
XM_019900731.1	NW_017851809.1	41.3	-0.92	0.003	protein ovo-like
XM_019900746.1	NW_017851813.1	1810.4	0.52	0.005	probable nucleoporin Nup58%2C transcript variant X1
XM_019900770.1	NW_017851813.1	9465.9	-0.90	0.000	activating transcription factor 3-like
NW_017847245.1_c782-7	NW_017847245.1	61.6	1.83	0.000	#N/A
XM_019900783.1	NW_017851814.1	11425.1	-0.47	0.000	E3 ubiquitin-protein ligase UBR2
XM_019900795.1	NW_017851815.1	231.6	0.52	0.003	apoptosis-stimulating of p53 protein 2-like
XM_019900797.1	NW_017851815.1	226.7	0.52	0.002	apoptosis-stimulating of p53 protein 2-like
XM_019900816.1	NW_017851816.1	1715.9	0.48	0.002	surfeit locus protein 6 homolog
XM_019900820.1	NW_017851816.1	146.3	-0.54	0.001	uncharacterized LOC109535008
XM_019900821.1	NW_017851816.1	26386.9	-0.59	0.010	transferrin-like%2C transcript variant X1 von Willebrand factor D and EGF domain-containing protein-like%2C transcript variant X1
XM_019900823.1	NW_017851816.1	4535.2	-0.83	0.000	uncharacterized LOC109535015%2C transcript variant X1
XM_019900825.1	NW_017851816.1	148.8	-1.46	0.000	uncharacterized LOC109535015%2C transcript variant X1
NW_017847275.1_1312-2163	NW_017847275.1	100.1	0.52	0.001	#N/A

XM_019900850.1	NW_017851819.1	3600.4	-0.52	0.000	liprin-beta-1%2C transcript variant X1
XM_019900860.1	NW_017847278.1	2531.4	-1.14	0.001	uncharacterized LOC109535044
XM_019900862.1	NW_017851820.1	1121.3	0.54	0.003	OTU domain-containing protein 6B
XM_019900869.1	NW_017851820.1	2641.8	0.44	0.000	bystin
XM_019900888.1	NW_017851821.1	3445.2	-0.99	0.002	probable multidrug resistance-associated protein lethal(2)03659
XM_019900889.1	NW_017851821.1	143.5	-1.24	0.000	uncharacterized LOC109535069%2C transcript variant X1
XM_019900899.1	NW_017851823.1	1292.5	0.38	0.001	protein AATF
XM_019900918.1	NW_017851823.1	487.8	0.41	0.002	putative transferase CAF17 homolog%2C mitochondrial
XM_019900921.1	NW_017851823.1	1128.8	0.36	0.002	tubulin--tyrosine ligase-like protein 12
XM_019900922.1	NW_017851823.1	1272.8	0.47	0.001	trafficking protein particle complex subunit 13
XM_019900926.1	NW_017851823.1	2445.0	-0.42	0.007	protein fork head
XM_019900930.1	NW_017847288.1	1116.6	-0.66	0.009	uncharacterized LOC109535102
XM_019900929.1	NW_017851823.1	2231.4	-0.37	0.000	high mobility group protein 20A-like acyl-CoA synthetase family member 2%2C mitochondrial-like%2C transcript variant X1
XM_019900941.1	NW_017847288.1	838.8	1.53	0.000	WD repeat-containing protein mio
XM_019900951.1	NW_017851824.1	1134.4	0.28	0.006	WD repeat-containing protein 24
XM_019900952.1	NW_017851824.1	774.8	0.42	0.000	WD repeat-containing protein 24
XM_019900953.1	NW_017851824.1	500.7	-0.84	0.001	somatostatin receptor type 2-like%2C transcript variant X1
XM_019900961.1	NW_017851824.1	999.7	-1.14	0.000	uncharacterized LOC109535133%2C transcript variant X1
XM_019901011.1	NW_017851824.1	2991.6	-0.26	0.001	cell cycle control protein 50A%2C transcript variant X1
XM_019901016.1	NW_017851824.1	5047.2	-0.77	0.005	transmembrane protein 47%2C transcript variant X1
XM_019901048.1	NW_017851824.1	1199.0	0.95	0.000	protein aurora borealis
XM_019901049.1	NW_017851824.1	1010.8	0.45	0.001	E3 ubiquitin-protein ligase Hakai
XM_019901062.1	NW_017851824.1	12137.6	1.22	0.003	alcohol dehydrogenase [acceptor]-like%2C transcript variant X1
XM_019901074.1	NW_017851824.1	6137.6	0.92	0.000	uncharacterized LOC109535199
XM_019901075.1	NW_017851824.1	1172.3	0.30	0.001	protein MTO1 homolog%2C mitochondrial%2C transcript variant X1
XM_019901084.1	NW_017847344.1	43.3	-1.07	0.007	uncharacterized LOC109535205
XM_019901094.1	NW_017851824.1	36.9	-1.05	0.004	WD repeat-containing protein on Y chromosome%2C transcript variant X1
XM_019901101.1	NW_017851824.1	227.2	1.01	0.001	uncharacterized LOC109535222
XM_019901106.1	NW_017851824.1	9930.1	3.79	0.000	phosphoglycolate phosphatase 2-like
XM_019901108.1	NW_017851824.1	376.5	0.54	0.000	methionine--tRNA ligase%2C mitochondrial
XM_019901118.1	NW_017851824.1	602.0	-0.99	0.003	tyrosine decarboxylase-like
XM_019901120.1	NW_017851824.1	289.3	-0.70	0.004	neuropeptide F receptor%2C transcript variant X1
XM_019901126.1	NW_017851824.1	716.3	1.32	0.000	cytochrome P450 4g1-like
XM_019901134.1	NW_017851824.1	473.7	0.67	0.005	neutral and basic amino acid transport protein rBAT-like

XM_019901139.1	NW_017851824.1	20.1	-1.66	0.000	alpha-amylase-like
XR_002171690.1	NW_017851824.1	27.4	1.15	0.003	uncharacterized LOC109535258%2C transcript variant X1
XM_019901144.1	NW_017851824.1	3.6	1.31	0.006	uncharacterized LOC109535259
XM_019901157.1	NW_017851827.1	1254.4	0.87	0.002	uncharacterized LOC109535268
XM_019901159.1	NW_017851827.1	178.7	0.87	0.000	probable cytochrome P450 4aa1
XM_019901171.1	NW_017851830.1	1137.3	0.46	0.000	cleavage stimulation factor subunit 2 tau variant
XM_019901196.1	NW_017851837.1	27.9	1.37	0.000	lipase 3-like
XM_019901207.1	NW_017851841.1	257.3	0.57	0.009	uncharacterized LOC109535320
XM_019901208.1	NW_017851842.1	473.4	0.62	0.000	tetraspanin-7-like
XM_019901211.1	NW_017851842.1	52.5	-1.88	0.000	cuticle protein 21-like
XM_019901213.1	NW_017851842.1	1739.0	-0.36	0.003	uncharacterized LOC109535327%2C transcript variant X1
XM_019901218.1	NW_017851842.1	931.1	0.32	0.002	histone deacetylase complex subunit SAP30 homolog
XM_019901227.1	NW_017851843.1	4.6	-2.02	0.000	uncharacterized LOC109535337
XM_019901230.1	NW_017851843.1	8424.7	-0.60	0.000	serine protease 42-like%2C transcript variant X1
XM_019901232.1	NW_017851843.1	23077.0	-1.12	0.000	tryptase-2
XR_002171702.1	NW_017851843.1	306.4	-0.68	0.004	uncharacterized LOC109535343
XR_002171703.1	NW_017851843.1	205.7	-0.76	0.004	uncharacterized LOC109535344
XM_019901242.1	NW_017851850.1	11967.5	-0.49	0.001	heat shock 70 kDa protein 4%2C transcript variant X1
XM_019901275.1	NW_017851853.1	2539.3	-0.37	0.007	zinc finger protein 587-like
XM_019901281.1	NW_017851856.1	878.6	0.34	0.001	centromere/kinetochore protein zw10 homolog
XM_019901295.1	NW_017851859.1	3981.7	-0.42	0.000	protein pangolin%2C isoforms A/H/I/S%2C transcript variant X1 pyruvate dehydrogenase E1 component subunit alpha%2C mitochondrial-like%2C transcript variant X1
XM_019901306.1	NW_017851859.1	6575.8	0.59	0.000	
XM_019901308.1	NW_017851859.1	72322.3	-1.38	0.000	annexin B9%2C transcript variant X1
XM_019901312.1	NW_017851859.1	3082.7	-3.46	0.000	uncharacterized LOC109535405
XM_019901314.1	NW_017851859.1	1272.4	0.30	0.002	histone acetyltransferase KAT8 queuine tRNA-ribosyltransferase accessory subunit 2%2C transcript variant X1
XM_019901316.1	NW_017851859.1	1454.4	-0.52	0.001	
XM_019901324.1	NW_017851859.1	1899.8	-2.72	0.000	uncharacterized LOC109535412
XM_019901327.1	NW_017851859.1	1836.0	-1.89	0.000	uncharacterized LOC109535416%2C transcript variant X1
XR_002171716.1	NW_017851859.1	28.3	-2.55	0.000	uncharacterized LOC109535417
XM_019901336.1	NW_017851860.1	7626.0	-0.61	0.001	carbonic anhydrase 2%2C transcript variant X1
XM_019901340.1	NW_017851860.1	1464.6	0.42	0.000	putative RNA exonuclease NEF-sp
XM_019901341.1	NW_017851860.1	8660.0	-0.81	0.001	fructose-1%2C6-bisphosphatase 1
XM_019901344.1	NW_017851860.1	6861.2	0.28	0.007	T-complex protein 1 subunit eta-like
XM_019901345.1	NW_017851860.1	951.1	0.63	0.002	RNA-binding protein MEX3B-like
XM_019901356.1	NW_017851863.1	266.3	1.28	0.000	transmembrane and TPR repeat-containing protein CG4341-like

XM_019901359.1	NW_017851866.1	4524.8	2.54	0.000	tryptophan 2%2C3-dioxygenase-like
XM_019901369.1	NW_017851870.1	3173.6	-1.40	0.000	glycine-rich cell wall structural protein-like
XM_019901378.1	NW_017851876.1	2636.3	-0.38	0.003	phosphatidylinositol phosphatase PTPRQ-like%2C transcript variant X1
XM_019901386.1	NW_017851876.1	446.2	0.53	0.000	centrosomal protein of 135 kDa-like
XM_019901387.1	NW_017851876.1	125.6	-1.22	0.001	uncharacterized LOC109535470
XM_019901388.1	NW_017851876.1	1179.0	-0.45	0.001	protein lap4-like
XM_019901389.1	NW_017851876.1	98.5	-0.77	0.000	odorant receptor 67c-like%2C transcript variant X1
XM_019901398.1	NW_017851876.1	2327.9	0.52	0.001	zinc finger CCCH domain-containing protein 11A-like
XM_019901400.1	NW_017851876.1	206.9	1.07	0.000	separin
NW_017851876.1_c115857-112911	NW_017851876.1	141.4	0.77	0.001	#N/A
XM_019901410.1	NW_017851882.1	281.7	-1.20	0.009	bombyxin B-8-like
XM_019901411.1	NW_017851883.1	697.8	0.46	0.000	glycerol-3-phosphate phosphatase-like
XM_019901412.1	NW_017851883.1	6844.4	-0.27	0.005	CREB-binding protein%2C transcript variant X1
XM_019901418.1	NW_017851883.1	2098.5	-0.38	0.002	probable phospholipid-transporting ATPase VD
XM_019901419.1	NW_017851883.1	651.0	0.40	0.001	probable asparagine--tRNA ligase%2C mitochondrial
XM_019901420.1	NW_017851883.1	1847.7	0.43	0.000	glycerol-3-phosphate phosphatase
XM_019901421.1	NW_017851883.1	883.7	-0.73	0.000	polyprenol reductase-like
XR_002171728.1	NW_017847442.1	618.6	-1.37	0.001	uncharacterized LOC109535518
XM_019901431.1	NW_017851888.1	4737.5	-0.41	0.002	sorting nexin lst-4%2C transcript variant X1
XM_019901433.1	NW_017851888.1	632.3	0.52	0.007	CD151 antigen-like
XM_019901438.1	NW_017851889.1	79.5	-0.77	0.001	kinesin-like protein CG14535
XR_002171729.1	NW_017847443.1	605.7	-1.39	0.001	uncharacterized LOC109535524
XM_019901444.1	NW_017851893.1	920.8	1.14	0.001	retinol dehydrogenase 14-like
XM_019901456.1	NW_017851898.1	7359.9	-0.50	0.000	oxysterol-binding protein 1%2C transcript variant X1
XM_019901458.1	NW_017851898.1	2299.0	-0.75	0.007	putative fatty acyl-CoA reductase CG5065
XM_019901462.1	NW_017851898.1	121.2	0.99	0.000	CUE domain-containing protein 2
NW_017851903.1_c17061-2059	NW_017851903.1	1092.1	0.46	0.002	#N/A
XM_019901475.1	NW_017851907.1	2648.0	0.62	0.000	replication protein A 70 kDa DNA-binding subunit-like
XM_019901488.1	NW_017851909.1	133.4	-0.86	0.003	vang-like protein 2-B
XM_019901492.1	NW_017851912.1	3723.4	-0.57	0.008	uncharacterized LOC109535575%2C transcript variant X1
XM_019901503.1	NW_017851913.1	774.1	0.38	0.003	UPF0415 protein C7orf25 homolog
XM_019901504.1	NW_017851913.1	504.1	0.62	0.000	tRNA (adenine(58)-N(1))-methyltransferase catalytic subunit TRMT61A-like
XM_019901512.1	NW_017851914.1	1357.7	0.96	0.000	anaphase-promoting complex subunit 4-like
XM_019901525.1	NW_017851920.1	929.0	0.37	0.001	uncharacterized LOC109535608

XM_019901534.1	NW_017851921.1	1651.1	-0.70	0.009	15-hydroxyprostaglandin dehydrogenase [NAD(+)]-like
XM_019901536.1	NW_017851923.1	4670.5	-0.49	0.000	striatin-3 putative ATP-dependent RNA helicase me31b%2C transcript variant X1
XM_019901540.1	NW_017851923.1	24431.3	0.64	0.000	tryptophan 2%2C3-dioxygenase-like
XM_019901548.1	NW_017851923.1	5255.0	2.52	0.000	tryptophan 2%2C3-dioxygenase-like
XM_019901549.1	NW_017851923.1	287.7	2.41	0.000	tryptophan 2%2C3-dioxygenase-like
XM_019901552.1	NW_017851924.1	689.4	0.58	0.000	uncharacterized LOC109535627
XM_019901555.1	NW_017851924.1	7259.1	-0.47	0.001	eukaryotic translation initiation factor 4 gamma 2-like 7-methylguanosine phosphate-specific 5'-nucleotidase%2C transcript variant X1
XM_019901561.1	NW_017851924.1	755.8	0.43	0.000	SH3 and multiple ankyrin repeat domains protein 3-like
XM_019901566.1	NW_017851926.1	1491.0	0.50	0.009	anoctamin-1-like%2C transcript variant X1
XM_019901568.1	NW_017851926.1	4128.0	-0.57	0.003	sphingomyelin phosphodiesterase-like
XM_019901577.1	NW_017851926.1	2196.2	0.73	0.000	uncharacterized LOC109535649
XR_002171740.1	NW_017851926.1	10986.6	1.03	0.000	esterase FE4-like
XM_019901595.1	NW_017851928.1	1725.3	-1.40	0.002	sodium/hydrogen exchanger 9B1-like%2C transcript variant X1
XM_019901598.1	NW_017851928.1	887.6	0.61	0.004	tubulin-specific chaperone cofactor E-like protein
XM_019901617.1	NW_017851930.1	3593.7	-0.40	0.006	TBC1 domain family member 23
XM_019901626.1	NW_017851931.1	3265.6	-0.31	0.003	transmembrane protein 87A
XM_019901632.1	NW_017851931.1	1909.2	-0.29	0.006	general transcription factor IIH subunit 1
XM_019901633.1	NW_017851931.1	973.1	0.31	0.002	tyrosine-protein kinase Fer-like
XM_019901635.1	NW_017851932.1	167.1	-0.44	0.007	uncharacterized LOC109535706%2C transcript variant X1
XR_002171745.1	NW_017851936.1	786.7	-1.02	0.000	uncharacterized LOC109535711%2C transcript variant X1
XR_002171748.1	NW_017851937.1	430.2	1.02	0.000	dosage compensation regulator
XM_019901645.1	NW_017851937.1	1470.9	-0.41	0.003	protein SMG8 NADH dehydrogenase [ubiquinone] 1 alpha subcomplex assembly factor 3%2C transcript variant X1
XM_019901655.1	NW_017851937.1	1256.4	0.45	0.002	pre-mRNA-splicing factor CWC25 homolog
XM_019901676.1	NW_017851937.1	755.3	0.62	0.000	protein patched homolog 1-like
XM_019901678.1	NW_017851937.1	1854.7	-0.59	0.004	zinc finger protein 569-like%2C transcript variant X1
XM_019901682.1	NW_017851937.1	1999.6	-0.43	0.005	zinc finger protein 2 homolog
XM_019901684.1	NW_017851937.1	2641.6	-0.30	0.000	uncharacterized LOC109535742%2C transcript variant X1
XM_019901688.1	NW_017851937.1	1564.8	-0.34	0.000	39S ribosomal protein L10%2C mitochondrial
XM_019901696.1	NW_017851937.1	366.1	-0.63	0.000	ankyrin-3%2C transcript variant X1
XM_019901700.1	NW_017851937.1	2318.9	0.34	0.006	rho GTPase-activating protein 190
XM_019901716.1	NW_017851937.1	6624.2	0.89	0.000	kidney mitochondrial carrier protein 1%2C transcript variant X1
XM_019901737.1	NW_017851937.1	2431.9	-0.40	0.000	toll-like receptor 3
XM_019901742.1	NW_017851937.1	5344.6	1.01	0.000	
XM_019901766.1	NW_017851937.1	190.5	1.29	0.001	

XM_019901776.1	NW_017851937.1	3736.0	0.48	0.001	sodium/potassium-transporting ATPase subunit beta-1-like
XM_019901802.1	NW_017851937.1	17.0	0.98	0.004	cuticle protein CP14.6-like
XM_019901807.1	NW_017851937.1	24.0	-0.88	0.000	twist-related protein 2-like
XM_019901812.1	NW_017851939.1	3480.7	-0.57	0.001	uncharacterized LOC109535807
XM_019901816.1	NW_017847550.1	676.0	-1.16	0.005	cytochrome b5-like
XM_019901817.1	NW_017851939.1	13940.4	-0.68	0.000	WD repeat-containing protein 26%2C transcript variant X1
XR_002171764.1	NW_017851940.1	395.2	1.14	0.000	uncharacterized LOC109535821
XM_019901830.1	NW_017851943.1	7.7	1.61	0.001	uncharacterized LOC109535823
XM_019901868.1	NW_017851946.1	651.7	-0.72	0.000	E3 SUMO-protein ligase RanBP2-like
XR_002171770.1	NW_017851948.1	53.4	-1.13	0.000	uncharacterized LOC109535854
XM_019901903.1	NW_017851949.1	443.7	-0.74	0.007	uncharacterized LOC109535883
XM_019901906.1	NW_017851949.1	1988.8	-0.32	0.000	GRAM domain-containing protein 1B-like
XM_019901913.1	NW_017851949.1	1921.1	0.34	0.000	28S ribosomal protein S2%2C mitochondrial
XM_019901914.1	NW_017851949.1	7126.2	-0.33	0.002	E3 ubiquitin-protein ligase znr1%2C transcript variant X1
XM_019901916.1	NW_017851949.1	2775.2	-0.55	0.003	uncharacterized LOC109535893%2C transcript variant X1
XM_019901929.1	NW_017851949.1	2610.9	-0.25	0.007	brain protein I3-like
XM_019901941.1	NW_017851949.1	213.5	-1.19	0.001	myosinase 1-like
XM_019901944.1	NW_017851949.1	291.7	0.61	0.000	probable RNA helicase armi
XM_019901965.1	NW_017851951.1	18568.9	-1.01	0.000	ATP-binding cassette sub-family G member 1-like
XM_019901970.1	NW_017847637.1	39.8	-1.09	0.002	cytosol aminopeptidase-like
XM_019901968.1	NW_017851952.1	90.5	-0.58	0.007	uncharacterized LOC109535928
XM_019901972.1	NW_017851955.1	1119.9	-0.43	0.001	uncharacterized LOC109535930
XM_019901973.1	NW_017851955.1	615.8	-0.36	0.007	zinc finger protein 678-like
XM_019901974.1	NW_017851955.1	1053.3	0.62	0.000	TELO2-interacting protein 1 homolog
XM_019901981.1	NW_017847637.1	824.8	-0.94	0.000	uncharacterized LOC109535936%2C transcript variant X1
XM_019901986.1	NW_017851962.1	300.4	-1.08	0.000	cathepsin B-like
XM_019901991.1	NW_017851963.1	15208.4	1.14	0.000	cytosolic purine 5'-nucleotidase
XM_019902018.1	NW_017851975.1	15666.3	-0.88	0.000	uncharacterized LOC109535974
XR_002171783.1	NW_017851975.1	4176.1	-0.95	0.000	uncharacterized LOC109535975
XM_019902034.1	NW_017847645.1	1530.1	-0.43	0.000	probable phospholipid-transporting ATPase VD
XM_019902050.1	NW_017851980.1	1663.1	1.15	0.000	uncharacterized LOC109535989%2C transcript variant X1
XM_019902060.1	NW_017851984.1	2770.3	1.06	0.000	uncharacterized LOC109535998
XM_019902070.1	NW_017851984.1	2632.5	0.98	0.001	endothelin-converting enzyme 1-like
XM_019902072.1	NW_017851984.1	792.6	0.81	0.006	neprilysin-1-like
XM_019902073.1	NW_017851984.1	3963.7	1.12	0.000	uncharacterized LOC109536009%2C transcript variant X1
XM_019902075.1	NW_017851984.1	3551.2	1.08	0.000	neprilysin-2-like

XM_019902076.1	NW_017851984.1	1227.0	1.31	0.000	membrane metallo-endopeptidase-like 1
XM_019902078.1	NW_017851987.1	53.1	0.82	0.000	protein timeless homolog
XM_019902079.1	NW_017851987.1	138.7	0.77	0.000	protein timeless homolog
XM_019902081.1	NW_017851988.1	1590.0	0.35	0.000	centromere/kinetochore protein zw10 homolog
XM_019902086.1	NW_017851990.1	153048.5	0.94	0.010	pectinesterase B-like
XM_019902087.1	NW_017851990.1	65308.7	1.23	0.002	pectinesterase B-like
XM_019902095.1	NW_017851993.1	3195.0	-1.07	0.000	tyrosine-protein kinase transmembrane receptor Ror-like
XM_019902097.1	NW_017851993.1	2155.7	1.06	0.000	serine/threonine-protein kinase polo%2C transcript variant X1
NW_017847678.1_12805-15631	NW_017847678.1	7.1	-1.32	0.005	#N/A
XM_019902101.1	NW_017851993.1	2515.3	0.39	0.002	28S ribosomal protein S22%2C mitochondrial
XM_019902102.1	NW_017851993.1	18447.5	1.89	0.000	D-3-phosphoglycerate dehydrogenase
XM_019902117.1	NW_017851993.1	672.2	0.45	0.000	peptidyl-prolyl cis-trans isomerase NIMA-interacting 4
XM_019902119.1	NW_017851993.1	8020.6	0.37	0.001	extracellular sulfatase SULF-1 homolog
XM_019902177.1	NW_017852003.1	3947.9	0.64	0.007	kinesin-like protein KIN-7L
XR_002171794.1	NW_017852003.1	49.7	-0.92	0.001	uncharacterized LOC109536101
XM_019902191.1	NW_017847728.1	3574.4	1.38	0.001	lysosomal aspartic protease-like
XM_019902198.1	NW_017852003.1	1917.7	0.24	0.009	nurim homolog
XR_002171799.1	NW_017852003.1	97.1	-0.39	0.008	uncharacterized LOC109536116
XM_019902203.1	NW_017852003.1	554.9	0.50	0.003	ribonuclease H2 subunit C
XM_019902208.1	NW_017852003.1	5320.5	-0.57	0.001	protein dopey-1 homolog%2C transcript variant X1
XR_002171801.1	NW_017847728.1	2910.6	1.42	0.001	uncharacterized LOC109536127
XM_019902210.1	NW_017852003.1	6660.1	-0.36	0.002	pre-mRNA-processing-splicing factor 8
XM_019902211.1	NW_017852003.1	9221.6	-0.70	0.000	protein transport protein Sec24C
XM_019902215.1	NW_017852003.1	4143.4	-0.56	0.000	suppressor of cytokine signaling 5%2C transcript variant X1
XM_019902229.1	NW_017852003.1	3123.9	-0.53	0.002	transcription initiation factor TFIIID subunit 1%2C transcript variant X1
XM_019902234.1	NW_017852003.1	1771.7	0.26	0.009	protein FAM98A
XM_019902237.1	NW_017852003.1	15.1	-1.52	0.001	sphingomyelin phosphodiesterase-like%2C transcript variant X1
XM_019902243.1	NW_017852003.1	668.9	0.45	0.003	anaphase-promoting complex subunit 2
XM_019902244.1	NW_017852003.1	497.7	0.77	0.000	spindle pole body component 110-like
XM_019902258.1	NW_017852003.1	934.0	0.32	0.006	dr1-associated corepressor
XM_019902259.1	NW_017852003.1	490.8	0.61	0.000	condensin complex subunit 3-like
XM_019902261.1	NW_017852003.1	1375.7	0.49	0.000	proteasome assembly chaperone 2
XM_019902271.1	NW_017852003.1	1246.4	-0.62	0.000	thyroid hormone receptor-associated protein 3-like
XM_019902282.1	NW_017852003.1	690.8	-0.68	0.000	zinc finger BED domain-containing protein 1-like%2C transcript variant X1
XM_019902287.1	NW_017847751.1	235.6	0.80	0.008	proclotting enzyme-like

XM_019902286.1	NW_017852003.1	924.1	0.60	0.000	threonylcarbamoyladenosine tRNA methyltransferase%2C transcript variant X1
XM_019902289.1	NW_017852003.1	1163.3	0.45	0.000	uncharacterized LOC109536182%2C transcript variant X1
XM_019902293.1	NW_017852003.1	367.3	-0.53	0.006	protein lines%2C transcript variant X1
XM_019902296.1	NW_017852003.1	915.0	0.57	0.005	borealin%2C transcript variant X1
XM_019902304.1	NW_017852003.1	712.9	0.51	0.002	DNA-directed RNA polymerase III subunit RPC8
XM_019902313.1	NW_017852003.1	5513.4	1.56	0.000	uncharacterized LOC109536201
XM_019902322.1	NW_017852007.1	519.9	0.46	0.008	meiosis-specific nuclear structural protein 1-like
XM_019902334.1	NW_017852008.1	694.0	-1.01	0.000	uncharacterized LOC109536219%2C transcript variant X1
XM_019902336.1	NW_017852008.1	1133.2	-1.00	0.000	uncharacterized LOC109536220
XM_019902337.1	NW_017852009.1	2025.4	0.47	0.009	protein ELYS
XM_019902338.1	NW_017852009.1	1349.9	0.30	0.002	DNA-directed RNA polymerase III subunit RPC2
XM_019902339.1	NW_017852009.1	887.9	0.49	0.000	uncharacterized LOC109536224
XM_019902352.1	NW_017852012.1	40.9	-1.76	0.000	RNA polymerase II degradation factor 1-like
XM_019902360.1	NW_017852012.1	1420.5	-0.37	0.002	uncharacterized LOC109536244%2C transcript variant X1
XM_019902369.1	NW_017852012.1	5758.7	-0.57	0.001	protein phosphatase 1A-like%2C transcript variant X1
XM_019902392.1	NW_017852012.1	902.2	0.80	0.000	suppressor protein of bem1/bed5 double mutants-like
XM_019902400.1	NW_017847751.1	2280.4	0.31	0.001	gametocyte-specific factor 1 homolog
XM_019902403.1	NW_017852012.1	232.5	0.80	0.000	uncharacterized LOC109536268%2C transcript variant X1
XM_019902406.1	NW_017852012.1	1014.6	0.33	0.002	protoheme IX farnesyltransferase%2C mitochondrial%2C transcript variant X1
XM_019902409.1	NW_017852012.1	5740.9	-0.68	0.000	uncharacterized LOC109536273%2C transcript variant X1
XM_019902425.1	NW_017852012.1	2643.4	-1.17	0.000	ejaculatory bulb-specific protein 3-like
XM_019902427.1	NW_017852012.1	3315.5	-0.35	0.003	bromodomain adjacent to zinc finger domain protein 2B%2C transcript variant X1
XM_019902432.1	NW_017852012.1	3483.6	-0.51	0.005	WD repeat%2C SAM and U-box domain-containing protein 1-like%2C transcript variant X1
XM_019902436.1	NW_017852012.1	3940.7	0.61	0.003	nucleolin 1-like
XM_019902437.1	NW_017852012.1	3178.6	0.51	0.002	transcription initiation factor TFIID subunit 11-like
XM_019902438.1	NW_017852012.1	6608.8	1.07	0.000	deoxyuridine 5'-triphosphate nucleotidohydrolase
XM_019902444.1	NW_017852012.1	4156.2	-0.38	0.001	uncharacterized LOC109536289
XM_019902453.1	NW_017852012.1	745.7	0.43	0.001	asparagine synthetase domain-containing protein CG17486
XM_019902478.1	NW_017852012.1	3776.0	0.27	0.001	armadillo repeat-containing protein 6 homolog
XM_019902481.1	NW_017852012.1	250.3	0.96	0.000	paired box protein Pax-5
XM_019902483.1	NW_017852012.1	1483.5	0.31	0.000	HD domain-containing protein 2
XR_002171826.1	NW_017852012.1	282.6	1.42	0.001	histidine decarboxylase%2C transcript variant X1
XM_019902489.1	NW_017847776.1	5127.0	-0.59	0.006	ATP-binding cassette sub-family G member 1-like
XM_019902486.1	NW_017852012.1	253.6	-1.00	0.006	uncharacterized LOC109536320

XM_019902487.1	NW_017852012.1	1325.2	-0.61	0.000	calbindin-32%2C transcript variant X1
XM_019902493.1	NW_017852012.1	575369.6	-0.88	0.008	uncharacterized LOC109536324
XM_019902494.1	NW_017852012.1	86.7	-1.22	0.000	B2 protein-like
XR_002171828.1	NW_017852012.1	30.5	-1.63	0.000	uncharacterized LOC109536330
XM_019902506.1	NW_017852012.1	11125.8	-0.29	0.001	RNA-binding protein Nova-1%2C transcript variant X1
XM_019902540.1	NW_017852012.1	66.8	-1.09	0.000	intracellular protein transport protein USO1-like
XM_019902546.1	NW_017852012.1	1312.9	0.47	0.001	sulfide:quinone oxidoreductase%2C mitochondrial
XM_019902550.1	NW_017852012.1	681.9	0.41	0.000	neuralized-like protein 2
XM_019902551.1	NW_017852012.1	13875.3	0.36	0.000	nascent polypeptide-associated complex subunit alpha
XM_019902553.1	NW_017852012.1	2461.1	-0.33	0.009	RE1-silencing transcription factor-like
XM_019902555.1	NW_017852012.1	671.8	0.48	0.000	nucleoporin seh1
XM_019902566.1	NW_017852012.1	898.1	0.33	0.003	uncharacterized LOC109536378%2C transcript variant X1
XM_019902569.1	NW_017852012.1	2357.2	0.21	0.003	TM2 domain-containing protein almondex
XM_019902573.1	NW_017852012.1	32570.3	-1.91	0.000	putative transcription factor SOX-14
XM_019902585.1	NW_017852012.1	5297.6	-0.34	0.008	atlastin
XM_019902592.1	NW_017852012.1	3980.6	-0.79	0.000	glutathione S-transferase theta-1-like%2C transcript variant X1
XM_019902595.1	NW_017852012.1	3521.2	-0.33	0.002	transmembrane protein 192
XM_019902598.1	NW_017852012.1	244.8	-0.70	0.003	sodium/calcium exchanger 3
XM_019902608.1	NW_017852012.1	475.3	-1.49	0.000	ninjurin-2-like%2C transcript variant X1
XM_019902615.1	NW_017847812.1	222.0	-0.64	0.008	1-phosphatidylinositol 4%2C5-bisphosphate phosphodiesterase classes I and II-like
XM_019902616.1	NW_017852012.1	1071.4	-0.54	0.004	trichohyalin
XM_019902627.1	NW_017847815.1	34861.1	-1.06	0.000	ATP-binding cassette sub-family G member 1-like
XM_019902624.1	NW_017852012.1	416.7	0.54	0.000	dnaJ homolog subfamily C member 17
XM_019902625.1	NW_017852012.1	933.9	-1.50	0.000	integrin alpha-PS5-like
XM_019902653.1	NW_017852012.1	115.4	0.48	0.000	uncharacterized LOC109536437
XM_019902667.1	NW_017852012.1	1903.6	0.56	0.001	DNA repair protein RAD51 homolog 1
XM_019902668.1	NW_017852012.1	1753.5	-0.51	0.000	RNA polymerase II subunit A C-terminal domain phosphatase
XM_019902669.1	NW_017852012.1	1110.9	0.41	0.005	28S ribosomal protein S17%2C mitochondrial
XM_019902670.1	NW_017852012.1	99.9	-1.04	0.002	uncharacterized LOC109536446
XM_019902676.1	NW_017852012.1	672.0	0.44	0.003	vesicle transport protein USE1
XM_019902677.1	NW_017852012.1	2244.8	0.57	0.000	protein NEDD1%2C transcript variant X1
XM_019902685.1	NW_017852012.1	904.6	0.47	0.000	nuclear transcription factor Y subunit gamma%2C transcript variant X1
XM_019902692.1	NW_017852012.1	534.7	0.76	0.000	serine/threonine-protein kinase VRK1-like
XM_019902696.1	NW_017852012.1	10676.2	1.11	0.000	putative vitellogenin receptor%2C transcript variant X1
XR_002171838.1	NW_017852012.1	224.9	-1.33	0.001	uncharacterized LOC109536482

XM_019902740.1	NW_017852013.1	3574.5	0.27	0.005	serine/threonine-protein kinase RIO1
XM_019902741.1	NW_017852013.1	702.0	0.73	0.000	protein SMG9%2C transcript variant X1
XM_019902768.1	NW_017847848.1	873.3	0.60	0.000	DNA replication licensing factor Mcm7-like
XM_019902797.1	NW_017847848.1	903.8	0.38	0.001	mitotic checkpoint protein BUB3-like
XR_002171851.1	NW_017852014.1	99.5	0.88	0.007	uncharacterized LOC109536532
XM_019902798.1	NW_017852014.1	3034.0	-0.58	0.001	phosphoinositide 3-kinase adapter protein 1%2C transcript variant X1
XM_019902809.1	NW_017852014.1	572.3	0.65	0.000	prolyl 4-hydroxylase subunit alpha-1-like
XM_019902815.1	NW_017852015.1	151.2	-0.89	0.006	A disintegrin and metalloproteinase with thrombospondin motifs 7-like
XM_019902817.1	NW_017852015.1	3391.1	-0.84	0.001	zinc metalloproteinase-disintegrin-like EoMP06
XM_019902818.1	NW_017852015.1	4191.2	-0.73	0.007	glucose-6-phosphate exchanger SLC37A2
XM_019902845.1	NW_017852016.1	4999.6	-0.52	0.000	tyrosine-protein phosphatase non-receptor type 9
XM_019902867.1	NW_017852016.1	1320.3	0.51	0.000	39S ribosomal protein L51%2C mitochondrial
XM_019902876.1	NW_017852016.1	695.5	0.56	0.001	centromere/kinetochore protein zw10-like
XM_019902880.1	NW_017852017.1	20.3	-1.52	0.000	FACT complex subunit SSRP1-like
XM_019902882.1	NW_017852017.1	54.9	1.68	0.000	choline dehydrogenase%2C mitochondrial-like
XM_019902883.1	NW_017852017.1	83.1	1.60	0.000	uncharacterized LOC109536598
XR_002171855.1	NW_017852017.1	439.6	0.79	0.007	uncharacterized LOC109536604
XM_019902891.1	NW_017852017.1	2479.7	0.26	0.000	rab GTPase-binding effector protein 1%2C transcript variant X1
XM_019902895.1	NW_017852017.1	6745.2	-0.54	0.000	autophagy-related protein 101%2C transcript variant X1
XM_019902898.1	NW_017852017.1	5119.3	-0.61	0.001	fibrous sheath CABYR-binding protein-like
XM_019902900.1	NW_017852017.1	395.8	0.54	0.000	nucleoside diphosphate-linked moiety X motif 8
XM_019902903.1	NW_017852017.1	1027.9	1.09	0.005	uncharacterized LOC109536617
XM_019902923.1	NW_017852017.1	2974.8	-0.45	0.000	synaptogyrin-1
XM_019902925.1	NW_017852017.1	1154.1	-0.73	0.005	sarcoplasmic calcium-binding protein 1
XM_019902935.1	NW_017852017.1	853.0	0.47	0.000	cytosolic Fe-S cluster assembly factor NUBP2 homolog
XM_019902937.1	NW_017852017.1	2042.7	-0.71	0.000	cytokine-inducible SH2-containing protein-like
XM_019902938.1	NW_017852017.1	214.0	-0.70	0.008	uncharacterized LOC109536639%2C transcript variant X1
XM_019902961.1	NW_017852017.1	690.0	0.50	0.001	caseinolytic peptidase B protein homolog%2C transcript variant X1
XM_019902972.1	NW_017852017.1	4105.5	0.69	0.000	superoxide dismutase [Mn] 1%2C mitochondrial
XM_019902974.1	NW_017852017.1	799.7	0.41	0.002	anaphase-promoting complex subunit 15-like%2C transcript variant X1
XM_019902981.1	NW_017852017.1	618.7	0.42	0.010	uncharacterized LOC109536667
XM_019902991.1	NW_017852017.1	1632.5	0.79	0.001	uncharacterized LOC109536676
XM_019902994.1	NW_017852017.1	5747.2	-0.36	0.006	transcription elongation factor SPT6
XM_019903002.1	NW_017852017.1	239.3	1.75	0.000	glucose dehydrogenase [FAD%2C quinone]-like

XM_019903029.1	NW_017852017.1	827.4	0.74	0.002	uncharacterized LOC109536707%2C transcript variant X1
XM_019903042.1	NW_017852017.1	3229.0	-0.44	0.005	zinc finger protein 665-like%2C transcript variant X1
XM_019903047.1	NW_017852017.1	3002.3	-0.61	0.002	uncharacterized LOC109536715%2C transcript variant X1
XM_019903054.1	NW_017852017.1	22692.1	-0.53	0.005	6-phosphofructo-2-kinase/fructose-2%2C6-bisphosphatase-like
XM_019903078.1	NW_017852017.1	2010.5	0.37	0.001	28S ribosomal protein S33%2C mitochondrial
XM_019903086.1	NW_017852017.1	487.6	-0.70	0.003	neo-calmodulin-like%2C transcript variant X1
XM_019903093.1	NW_017852017.1	297.4	0.85	0.007	uncharacterized LOC109536742
XM_019903104.1	NW_017852017.1	1106.7	0.63	0.002	innexin inx2-like
XR_002171863.1	NW_017852017.1	343.3	-0.85	0.000	uncharacterized LOC109536754
XM_019903132.1	NW_017852021.1	2166.0	0.34	0.000	uncharacterized LOC109536774
XM_019903153.1	NW_017847924.1	2280.3	0.31	0.001	gametocyte-specific factor 1 homolog enoyl-CoA hydratase domain-containing protein 3%2C mitochondrial%2C transcript variant X1
XM_019903151.1	NW_017852021.1	383.3	0.66	0.000	
XM_019903155.1	NW_017852021.1	872.1	0.39	0.006	COX assembly mitochondrial protein homolog
XM_019903157.1	NW_017852021.1	4180.2	-1.14	0.001	broad-complex core protein%2C transcript variant X1
XM_019903168.1	NW_017847924.1	235.4	0.80	0.008	proclotting enzyme-like
XM_019903192.1	NW_017852021.1	6360.1	-0.39	0.003	derlin-2
XM_019903196.1	NW_017852021.1	3008.2	-1.37	0.000	uncharacterized LOC109536806%2C transcript variant X1
XM_019903205.1	NW_017852021.1	11214.6	-0.52	0.000	fatty aldehyde dehydrogenase-like%2C transcript variant X1
XM_019903221.1	NW_017852021.1	1103.1	0.66	0.000	NFU1 iron-sulfur cluster scaffold homolog%2C mitochondrial-like
XM_019903229.1	NW_017852021.1	379.3	0.42	0.003	rRNA methyltransferase 2%2C mitochondrial serine/threonine-protein phosphatase 2A 56 kDa regulatory subunit epsilon isoform%2C transcript variant X1
XM_019903247.1	NW_017852026.1	4726.7	0.29	0.006	
XM_019903259.1	NW_017852026.1	450.5	0.35	0.007	uncharacterized LOC109536846
XM_019903260.1	NW_017852026.1	893.9	-0.87	0.000	diacylglycerol kinase 1%2C transcript variant X1
XM_019903274.1	NW_017852026.1	26.8	0.81	0.006	NEDD8-like
XM_019903277.1	NW_017852026.1	11389.2	-0.23	0.002	protein transport protein Sec23A%2C transcript variant X1
XM_019903284.1	NW_017852026.1	8503.1	-0.83	0.000	hepatocyte nuclear factor 4-gamma%2C transcript variant X1
XM_019903313.1	NW_017852026.1	2773.9	0.35	0.009	tudor domain-containing protein 1-like%2C transcript variant X1
XM_019903320.1	NW_017852026.1	1240.4	0.45	0.006	uncharacterized LOC109536876%2C transcript variant X1
XM_019903326.1	NW_017852026.1	10.3	1.65	0.000	uncharacterized LOC109536879
XM_019903327.1	NW_017852026.1	102.8	-1.24	0.000	patj homolog
XM_019903332.1	NW_017852026.1	383.2	0.41	0.007	D-beta-hydroxybutyrate dehydrogenase%2C mitochondrial-like
XM_019903334.1	NW_017852026.1	183.7	-0.97	0.006	uncharacterized LOC109536887
XM_019903336.1	NW_017852028.1	66.0	-1.64	0.000	perlucin-like
XM_019903342.1	NW_017852028.1	759.6	0.74	0.004	2-hydroxyacyl-CoA lyase 1

XM_019903347.1	NW_017852028.1	5788.6	-1.26	0.002	putative inorganic phosphate cotransporter%2C transcript variant X1
XM_019903350.1	NW_017852028.1	353.2	1.88	0.000	putative inorganic phosphate cotransporter putative inorganic phosphate cotransporter%2C transcript variant X1
XM_019903352.1	NW_017852028.1	4.5	-1.46	0.001	
XM_019903357.1	NW_017852028.1	7298.4	1.10	0.000	transducin beta-like protein 2%2C transcript variant X1
XR_002171879.1	NW_017852028.1	3757.4	-0.57	0.001	uncharacterized LOC109536905
XM_019903366.1	NW_017852028.1	8732.8	0.59	0.000	protein gustavus%2C transcript variant X1
XM_019903374.1	NW_017852028.1	539.6	0.45	0.004	target of rapamycin complex subunit Ist8%2C transcript variant X1
XM_019903393.1	NW_017852028.1	8113.5	-0.97	0.000	sorting nexin-8-like%2C transcript variant X1
XM_019903413.1	NW_017852028.1	347.4	1.44	0.000	uncharacterized LOC109536931
XM_019903414.1	NW_017852028.1	6913.1	1.88	0.000	cytoglobin-1-like
XM_019903416.1	NW_017852028.1	1090.7	0.30	0.000	nuclear pore complex protein Nup85
XM_019903417.1	NW_017852028.1	500.2	0.37	0.002	deoxyhypusine hydroxylase
XM_019903419.1	NW_017852028.1	321.4	0.94	0.000	G1/S-specific cyclin-E
XM_019903422.1	NW_017852028.1	1369.8	-0.48	0.003	nudC domain-containing protein 3 polypeptide N-acetylgalactosaminyltransferase 3-like%2C transcript variant X1
XM_019903429.1	NW_017852028.1	913.9	1.25	0.000	
XM_019903435.1	NW_017852028.1	440.2	-1.03	0.006	cyclin-dependent kinase 5 activator 1
XM_019903443.1	NW_017852028.1	1191.3	1.02	0.000	bone morphogenetic protein receptor type-1B-like
XM_019903464.1	NW_017848006.1	93.2	-0.56	0.001	uncharacterized G-patch domain protein DDB_G0278987-like
XM_019903460.1	NW_017852029.1	1967.8	0.36	0.002	H/ACA ribonucleoprotein complex subunit 3
XM_019903473.1	NW_017852029.1	20.5	-0.99	0.006	uncharacterized LOC109536973
XM_019903474.1	NW_017852029.1	4268.1	0.27	0.002	DNA damage-binding protein 1%2C transcript variant X1
XM_019903476.1	NW_017852029.1	1550.4	0.30	0.001	complex I intermediate-associated protein 30%2C mitochondrial
XM_019903480.1	NW_017852029.1	1047.8	-1.67	0.000	gonadotropin-releasing hormone II receptor-like
XM_019903487.1	NW_017848008.1	1638.5	-0.41	0.001	probable phospholipid-transporting ATPase VA potassium/sodium hyperpolarization-activated cyclic nucleotide-gated channel 1-like
XM_019903489.1	NW_017852030.1	29.1	-1.39	0.001	
XM_019903491.1	NW_017852030.1	33.2	-1.15	0.004	uncharacterized LOC109536990
XM_019903499.1	NW_017848011.1	627.3	-0.26	0.010	putative U5 small nuclear ribonucleoprotein 200 kDa helicase
XM_019903501.1	NW_017852030.1	9088.9	0.63	0.001	phosphoglucomutase
XR_002171888.1	NW_017848018.1	77.0	-0.68	0.000	uncharacterized LOC109537014
XM_019903520.1	NW_017852030.1	9218.1	-1.44	0.001	protein lethal(2)essential for life-like
XM_019903523.1	NW_017852030.1	1797.9	-0.47	0.000	intersectin-1-like%2C transcript variant X1
XM_019903544.1	NW_017848023.1	1122.6	-0.46	0.000	probable cation-transporting ATPase 13A3
XM_019903551.1	NW_017852030.1	2348.3	0.77	0.000	macrophage migration inhibitory factor homolog
XR_002171890.1	NW_017848033.1	157.6	-0.83	0.001	uncharacterized LOC109537034

XM_019903556.1	NW_017852030.1	579.6	0.32	0.008	protein arginine methyltransferase NDUFAF7 homolog%2C mitochondrial
XM_019903564.1	NW_017852030.1	3286.9	0.23	0.003	mitochondrial import inner membrane translocase subunit Tim23%2C transcript variant X1
XM_019903569.1	NW_017852030.1	4685.6	-0.55	0.000	myelin regulatory factor-like protein%2C transcript variant X1
XM_019903581.1	NW_017852030.1	2018.6	0.51	0.001	39S ribosomal protein L12%2C mitochondrial
XM_019903590.1	NW_017852030.1	2222.0	0.26	0.003	uncharacterized protein C6orf136 homolog
XM_019903625.1	NW_017852030.1	6840.9	0.75	0.004	acetyl-CoA carboxylase%2C transcript variant X1
XM_019903627.1	NW_017852030.1	184.0	-0.61	0.001	hyaluronidase-like
XM_019903632.1	NW_017852030.1	1294.0	0.66	0.001	uncharacterized LOC109537078%2C transcript variant X1
XM_019903644.1	NW_017852030.1	2615.0	-1.26	0.000	zinc finger protein 761-like uncharacterized aarF domain-containing protein kinase 5%2C transcript variant X1
XM_019903654.1	NW_017852030.1	1699.2	0.72	0.000	
XM_019903665.1	NW_017852030.1	2898.8	-0.50	0.001	golgin subfamily A member 4%2C transcript variant X1
XM_019903684.1	NW_017852030.1	1619.9	0.27	0.002	zinc finger HIT domain-containing protein 2 ankyrin repeat domain-containing protein 50%2C transcript variant X1
XM_019903693.1	NW_017852030.1	1847.7	-0.35	0.000	
XM_019903700.1	NW_017852030.1	3322.3	-0.39	0.000	protein PAT1 homolog 1 breast cancer anti-estrogen resistance protein 1%2C transcript variant X1
XM_019903710.1	NW_017852030.1	3831.8	-0.76	0.000	
XM_019903713.1	NW_017852030.1	2249.7	-0.75	0.000	uncharacterized LOC109537128%2C transcript variant X1
XM_019903720.1	NW_017852030.1	1467.6	-0.45	0.004	homeobox protein cut%2C transcript variant X1
XM_019903731.1	NW_017852030.1	1456.1	-0.45	0.001	kelch-like protein 5%2C transcript variant X1 neural/ectodermal development factor IMP-L2%2C transcript variant X1
XM_019903737.1	NW_017852030.1	8746.3	2.01	0.000	
XM_019903741.1	NW_017848127.1	210.2	-1.97	0.000	uncharacterized LOC109537138 potassium/sodium hyperpolarization-activated cyclic nucleotide-gated channel 2-like
XM_019903739.1	NW_017852030.1	66.3	-1.30	0.002	
XM_019903766.1	NW_017852032.1	14956.0	1.17	0.000	myotubularin-related protein 14%2C transcript variant X1
XM_019903768.1	NW_017852032.1	17328.6	1.69	0.000	calcium/calmodulin-dependent protein kinase type 1-like coiled-coil domain-containing protein R3HCC1L-like%2C transcript variant X1
XM_019903769.1	NW_017852032.1	1948.7	0.36	0.002	
XM_019903772.1	NW_017852032.1	972.0	0.63	0.000	elongation factor-like GTPase 1%2C transcript variant X1
XM_019903775.1	NW_017852032.1	677.1	2.93	0.000	protein giant-lens
XM_019903777.1	NW_017852032.1	1260.8	0.82	0.000	ATP-dependent Clp protease proteolytic subunit
XR_002171902.1	NW_017848143.1	41.8	1.09	0.006	uncharacterized LOC109537179
XM_019903783.1	NW_017852032.1	988.7	0.43	0.001	NEDD8-conjugating enzyme UBE2F-like%2C transcript variant X1 uncharacterized protein DDB_G0283697-like%2C transcript variant X1
XM_019903789.1	NW_017848143.1	1195.0	-0.90	0.000	
XM_019903785.1	NW_017852032.1	2063.6	0.41	0.000	protein phosphatase methylesterase 1%2C transcript variant X1

XM_019903790.1	NW_017852032.1	2334.8	-0.33	0.003	G protein alpha i subunit
XM_019903794.1	NW_017852032.1	229.3	-0.89	0.003	hemicentin-2-like
XR_002171904.1	NW_017852033.1	54.2	1.63	0.000	uncharacterized LOC109537196
XM_019903805.1	NW_017852034.1	422.6	0.89	0.003	uncharacterized LOC109537199
XM_019903834.1	NW_017848150.1	1600.2	0.97	0.000	anaphase-promoting complex subunit 4-like AT-rich interactive domain-containing protein 4B%2C transcript variant X1
XM_019903841.1	NW_017852034.1	3027.8	-0.42	0.000	uncharacterized LOC109537224
XR_002171905.1	NW_017852034.1	48.4	-1.10	0.004	uncharacterized LOC109537224
XM_019903844.1	NW_017852034.1	318.1	-1.29	0.000	protein FAM161A-like%2C transcript variant X1
XM_019903853.1	NW_017852034.1	2729.2	0.27	0.002	ATP-dependent RNA helicase DHX36-like conserved oligomeric Golgi complex subunit 1%2C transcript variant X1
XM_019903865.1	NW_017852034.1	1007.4	0.34	0.003	uncharacterized LOC109537246
XR_002171908.1	NW_017845339.1	70.7	-0.70	0.001	uncharacterized LOC109537246
XM_019903903.1	NW_017852037.1	9300.8	-0.66	0.000	long-chain-fatty-acid--CoA ligase 4%2C transcript variant X1
XM_019903917.1	NW_017852037.1	1642.7	0.59	0.001	uncharacterized LOC109537282%2C transcript variant X1
XM_019903925.1	NW_017852037.1	2259.7	0.36	0.000	39S ribosomal protein L15%2C mitochondrial
XM_019903931.1	NW_017852037.1	1351.2	0.36	0.000	cleavage stimulation factor subunit 1
XM_019903935.1	NW_017852037.1	429.3	0.69	0.000	GPI transamidase component PIG-S
XM_019903951.1	NW_017852037.1	2933.1	0.34	0.006	28S ribosomal protein S15%2C mitochondrial
XM_019903982.1	NW_017852037.1	5759.3	0.33	0.005	eukaryotic translation initiation factor 4E-1A-like
XM_019903984.1	NW_017852037.1	3153.0	-0.57	0.000	GTPase-activating protein%2C transcript variant X1
XM_019904001.1	NW_017852037.1	5330.9	-0.74	0.000	piezo-type mechanosensitive ion channel component
XM_019904002.1	NW_017852037.1	4874.8	-0.81	0.000	acyl-coenzyme A thioesterase 9%2C mitochondrial-like piezo-type mechanosensitive ion channel component-like%2C transcript variant X1
XM_019904003.1	NW_017852037.1	260.8	-0.80	0.000	dolichyldiphosphatase 1-like
XM_019904007.1	NW_017852037.1	10705.7	-0.80	0.000	zinc finger protein 665-like
XM_019904008.1	NW_017852037.1	1654.8	-0.46	0.000	uncharacterized LOC109537347%2C transcript variant X1
XM_019904010.1	NW_017852037.1	1835.4	-0.36	0.004	uncharacterized LOC109537347%2C transcript variant X1
XM_019904015.1	NW_017852037.1	2825.9	0.41	0.001	ubiquitin-like-conjugating enzyme ATG3
XM_019904030.1	NW_017852037.1	450.1	0.41	0.001	phosphatidate cytidyltransferase%2C mitochondrial
XM_019904049.1	NW_017852037.1	1671.2	-1.77	0.000	alpha-tocopherol transfer protein-like%2C transcript variant X1
XM_019904062.1	NW_017852037.1	10743.9	-1.48	0.000	clavesin-1
XM_019904063.1	NW_017852037.1	1847.2	-0.92	0.000	annulin-like
XM_019904068.1	NW_017852037.1	1924.8	0.43	0.000	uncharacterized protein C18orf19 homolog A
XM_019904085.1	NW_017848199.1	697.0	0.46	0.000	glycerol-3-phosphate phosphatase-like
XM_019904099.1	NW_017848199.1	56.8	-0.85	0.000	polyprenol reductase-like%2C transcript variant X1
XM_019904111.1	NW_017852037.1	65.3	-0.84	0.001	uncharacterized LOC109537401

XM_019904114.1	NW_017852037.1	21.6	-1.17	0.001	coiled-coil domain-containing protein 39%2C transcript variant X1 serine/threonine-protein phosphatase 2A regulatory subunit B''
XM_019904133.1	NW_017852037.1	2331.7	-0.51	0.001	subunit beta-like%2C transcript variant X1
XM_019904139.1	NW_017852037.1	1232.6	-0.55	0.000	histone acetyltransferase KAT2B
XM_019904140.1	NW_017852037.1	4678.4	-0.25	0.003	multiple epidermal growth factor-like domains protein 8
XM_019904141.1	NW_017852037.1	8538.0	-0.57	0.001	uncharacterized LOC109537418%2C transcript variant X1
XM_019904144.1	NW_017852037.1	1542.4	0.73	0.000	plexin domain-containing protein 2-like
XM_019904146.1	NW_017852037.1	1663.2	0.40	0.001	39S ribosomal protein L47%2C mitochondrial
XM_019904154.1	NW_017852037.1	2631.8	-0.18	0.002	F-box/WD repeat-containing protein 5%2C transcript variant X1
XM_019904167.1	NW_017852037.1	1050.9	-1.26	0.000	protein vein-like%2C transcript variant X1
XM_019904174.1	NW_017852037.1	313.9	0.93	0.001	mitotic spindle assembly checkpoint protein MAD2A
XM_019904175.1	NW_017852037.1	5276.7	-0.37	0.009	tyrosine-protein phosphatase non-receptor type 23
XM_019904176.1	NW_017852037.1	610.7	1.07	0.006	clavesin-2-like
XM_019904178.1	NW_017852037.1	3069.0	0.36	0.000	kelch-like protein diablo
XM_019904181.1	NW_017852037.1	94572.6	-0.51	0.001	heat shock protein 83
XM_019904215.1	NW_017852037.1	160.4	1.06	0.003	calcitonin receptor-like%2C transcript variant X1
XM_019904219.1	NW_017852037.1	1992.5	-0.31	0.002	sorting nexin-20%2C transcript variant X1
XM_019904232.1	NW_017852037.1	814.5	0.27	0.006	presenilins-associated rhomboid-like protein%2C mitochondrial
XM_019904236.1	NW_017852037.1	36.7	1.38	0.000	uncharacterized LOC109537474%2C transcript variant X1
XM_019904255.1	NW_017852037.1	1477.6	0.43	0.000	DCN1-like protein 1 F-box-like/WD repeat-containing protein TBL1XR1%2C transcript variant X1
XM_019904265.1	NW_017852037.1	2478.2	0.27	0.000	
XM_019904272.1	NW_017852037.1	153.3	1.24	0.001	uncharacterized LOC109537499
XM_019904292.1	NW_017852037.1	2210.8	0.35	0.003	uncharacterized LOC109537517%2C transcript variant X1
XM_019904300.1	NW_017852037.1	2065.4	0.68	0.001	kinesin-like protein KIF18A%2C transcript variant X1 probable multidrug resistance-associated protein lethal(2)03659%2C transcript variant X1
XM_019904305.1	NW_017852037.1	680.7	1.12	0.000	
XM_019904308.1	NW_017852037.1	102.6	-0.52	0.009	T-box transcription factor TBX20-like
XM_019904354.1	NW_017845362.1	88.7	-0.53	0.004	uncharacterized LOC109537537
XM_019904342.1	NW_017852038.1	2607.7	0.53	0.008	uncharacterized LOC109537562
XM_019904358.1	NW_017848296.1	12292.4	-1.36	0.000	lipid storage droplets surface-binding protein 1-like
XM_019904359.1	NW_017852038.1	26929.1	-0.25	0.002	profilin%2C transcript variant X1
XM_019904372.1	NW_017852038.1	2151.5	0.42	0.006	ubiquitin-conjugating enzyme E2 N-like
XM_019904387.1	NW_017852038.1	4330.4	-0.59	0.000	protein tramtrack%2C alpha isoform-like%2C transcript variant X1
XM_019904398.1	NW_017852038.1	3594.6	-0.53	0.004	uncharacterized LOC109537597%2C transcript variant X1
XM_019904417.1	NW_017852038.1	716.7	1.03	0.005	follicle cell protein 3C-1
XM_019904427.1	NW_017848330.1	881.2	-0.71	0.000	beta-1%2C4-glucuronyltransferase 1-like

XM_019904429.1	NW_017852040.1	1301.1	0.28	0.001	golgin-45%2C transcript variant X1
XM_019904514.1	NW_017848363.1	48.0	-0.84	0.008	cytochrome P450 307a1-like
XM_019904512.1	NW_017852043.1	994.6	0.38	0.002	zinc finger and SCAN domain-containing protein 12-like
XM_019904515.1	NW_017852043.1	2438.3	0.33	0.004	chromobox protein homolog 5
XM_019904524.1	NW_017852043.1	18685.4	-0.34	0.002	puromycin-sensitive aminopeptidase
XM_019904538.1	NW_017852043.1	602.1	0.34	0.001	THUMP domain-containing protein 1 homolog
XM_019904540.1	NW_017852043.1	2258.1	-1.04	0.000	zinc finger protein 2 homolog%2C transcript variant X1
XM_019904543.1	NW_017852043.1	46.4	-1.38	0.001	enkurin
XM_019904553.1	NW_017852043.1	550.8	0.41	0.001	U6 snRNA-associated Sm-like protein LSm5%2C transcript variant X1
XM_019904572.1	NW_017852046.1	3329.1	-1.43	0.000	proton-coupled amino acid transporter-like protein pathetic%2C transcript variant X1
XM_019904602.1	NW_017848364.1	47.6	-0.83	0.009	cytochrome P450 307a1-like
XM_019904601.1	NW_017852049.1	2531.5	0.31	0.003	leucine-rich repeat-containing protein 40-like%2C transcript variant X1
XM_019904604.1	NW_017852049.1	20250.4	-0.64	0.001	alcohol dehydrogenase class-3%2C transcript variant X1
XM_019904606.1	NW_017852049.1	6798.8	-0.46	0.003	SH3 domain-binding protein 5 homolog%2C transcript variant X1
XM_019904608.1	NW_017852049.1	4502.3	0.36	0.006	protein I(2)37Cc
XM_019904612.1	NW_017852049.1	3129.6	0.53	0.009	dnaJ homolog subfamily C member 8
XM_019904616.1	NW_017852049.1	173.2	0.72	0.001	uncharacterized LOC109537746%2C transcript variant X1
XM_019904632.1	NW_017852049.1	13392.5	0.98	0.000	ornithine aminotransferase%2C mitochondrial%2C transcript variant X1
XM_019904647.1	NW_017852049.1	5975.3	-0.50	0.000	phosphoacetylglucosamine mutase
XM_019904703.1	NW_017845370.1	1440.7	1.35	0.001	prostaglandin reductase 1-like
XM_019904670.1	NW_017852052.1	1388.2	-0.49	0.003	protein son of sevenless
XM_019904671.1	NW_017852052.1	1280.0	0.67	0.000	116 kDa U5 small nuclear ribonucleoprotein component
XM_019904674.1	NW_017852052.1	414.3	0.74	0.000	zinc finger protein rotund-like%2C transcript variant X1
XM_019904682.1	NW_017852052.1	189.1	0.77	0.001	flocculation protein FLO11-like
XM_019904683.1	NW_017852052.1	9450.6	0.40	0.004	46 kDa FK506-binding nuclear protein
XM_019904698.1	NW_017852055.1	711.5	1.00	0.000	uncharacterized LOC109537806
XM_019904704.1	NW_017852055.1	65.7	-1.49	0.000	histidine-rich glycoprotein-like
XM_019904715.1	NW_017852055.1	1213.1	0.65	0.000	uncharacterized LOC109537816%2C transcript variant X1
XM_019904733.1	NW_017852055.1	7958.9	-0.37	0.002	dyslexia-associated protein KIAA0319-like protein
XM_019904734.1	NW_017852055.1	780.5	0.55	0.000	erlin-1-like
XM_019904743.1	NW_017852055.1	9998.8	-1.13	0.000	uncharacterized LOC109537831%2C transcript variant X1
XR_002171975.1	NW_017852055.1	11.4	-1.24	0.001	uncharacterized LOC109537834
XM_019904761.1	NW_017852055.1	771.6	-0.94	0.002	calcium-activated chloride channel regulator 4-like
XM_019904767.1	NW_017852055.1	6380.6	-0.48	0.007	dihydropteridine reductase

XM_019904781.1	NW_017852055.1	1324.6	0.41	0.001	cyclin-dependent kinase 2-associated protein 1-like%2C transcript variant X1
XM_019904790.1	NW_017852055.1	55.5	-0.88	0.003	uncharacterized LOC109537861
XR_002171981.1	NW_017852056.1	1677.0	0.98	0.000	uncharacterized LOC109537880
XM_019904804.1	NW_017852056.1	10149.9	-1.01	0.001	DE-cadherin transforming acidic coiled-coil-containing protein 1%2C transcript variant X1
XM_019904809.1	NW_017852056.1	5036.9	-1.02	0.000	
XM_019904814.1	NW_017852056.1	3301.3	-0.51	0.001	HEAT repeat-containing protein 5B%2C transcript variant X1
XM_019904822.1	NW_017848453.1	348.5	0.34	0.009	WD and tetratricopeptide repeats protein 1-like
XM_019904826.1	NW_017852056.1	4916.1	-0.47	0.007	solute carrier family 12 member 8
XM_019904827.1	NW_017852056.1	8285.3	-0.89	0.000	rab11 family-interacting protein 1%2C transcript variant X1 lipoamide acyltransferase component of branched-chain alpha-keto acid dehydrogenase complex%2C mitochondrial%2C transcript variant X1
XM_019904829.1	NW_017852056.1	2276.8	0.81	0.009	
XM_019904838.1	NW_017852056.1	4587.8	-0.49	0.008	endophilin-A%2C transcript variant X1
XM_019904849.1	NW_017848457.1	3082.2	-0.64	0.004	serine protease 7-like
XM_019904883.1	NW_017852056.1	1174.5	0.32	0.002	leishmanolysin-like peptidase
XM_019904896.1	NW_017852056.1	7453.4	-0.61	0.000	transcriptional coactivator YAP1-A%2C transcript variant X1
XM_019904902.1	NW_017852056.1	7523.8	-0.81	0.000	neuroglian%2C transcript variant X1 dual specificity tyrosine-phosphorylation-regulated kinase 2%2C transcript variant X1
XM_019904930.1	NW_017852056.1	3391.8	-0.56	0.000	
XM_019904932.1	NW_017852056.1	1146.8	0.30	0.009	protein SHQ1 homolog
XM_019904933.1	NW_017852056.1	975.7	-0.55	0.001	BTB/POZ domain-containing protein 7%2C transcript variant X1
XM_019904937.1	NW_017848485.1	775.0	0.36	0.002	N-alpha-acetyltransferase 15%2C NatA auxiliary subunit-like steroid receptor seven-up%2C isoforms B/C%2C transcript variant X1
XM_019904944.1	NW_017852056.1	2680.1	-0.74	0.002	
XM_019904951.1	NW_017848485.1	591.8	0.34	0.001	DNA-directed RNA polymerase III subunit RPC3-like
XM_019904949.1	NW_017852056.1	5017.8	-1.61	0.000	protein windpipe 5-aminolevulinate synthase%2C erythroid-specific%2C mitochondrial
XM_019904956.1	NW_017852056.1	6662.2	0.70	0.004	
XR_002171987.1	NW_017852056.1	1153.7	-0.55	0.000	uncharacterized LOC109537964%2C transcript variant X1
XM_019904971.1	NW_017852056.1	5315.4	-0.45	0.000	PRA1 family protein 3
XM_019904979.1	NW_017852056.1	935.3	1.04	0.000	uncharacterized LOC109537971
XM_019904980.1	NW_017852056.1	646.7	1.06	0.000	actin-like protein 6B%2C transcript variant X1
XM_019904982.1	NW_017852056.1	1431.3	0.51	0.005	battenin%2C transcript variant X1
XM_019904987.1	NW_017852056.1	764.5	0.54	0.001	protein patched
XM_019904991.1	NW_017852056.1	5139.1	-0.36	0.000	ubiquitin-conjugating enzyme E2 H%2C transcript variant X1
XM_019905003.1	NW_017852056.1	681.9	-0.43	0.001	mothers against decapentaplegic homolog 4
XM_019905005.1	NW_017852056.1	12831.0	-0.51	0.002	translocon-associated protein subunit gamma

XM_019905006.1	NW_017852056.1	28073.7	1.02	0.001	uncharacterized LOC109537989
XM_019905013.1	NW_017852056.1	3552.1	-0.82	0.000	caspase-3-like%2C transcript variant X1
XM_019905021.1	NW_017852056.1	1010.2	-0.81	0.001	protein limb expression 1 homolog%2C transcript variant X1 UDP-xylose and UDP-N-acetylglucosamine transporter-like%2C transcript variant X1
XM_019905038.1	NW_017852056.1	2588.1	0.40	0.000	
XM_019905050.1	NW_017852056.1	928.3	0.84	0.003	very-long-chain 3-oxoacyl-CoA reductase
XM_019905052.1	NW_017852056.1	1242.4	1.03	0.001	protein eiger
XM_019905062.1	NW_017852056.1	444.7	1.00	0.000	protein rolling stone-like%2C transcript variant X1
XR_002171995.1	NW_017852056.1	31.2	1.38	0.000	uncharacterized LOC109538034
XM_019905074.1	NW_017852056.1	325.1	0.45	0.006	protein RRNAD1-like
XM_019905077.1	NW_017852056.1	99.8	-0.68	0.001	uncharacterized LOC109538037
XM_019905078.1	NW_017852056.1	11.1	-1.12	0.001	uncharacterized LOC109538038
XM_019905080.1	NW_017852057.1	580.9	1.01	0.000	uncharacterized LOC109538041
XM_019905081.1	NW_017852057.1	1368.1	1.01	0.000	uncharacterized LOC109538042%2C transcript variant X1
XM_019905083.1	NW_017852058.1	114.8	0.49	0.002	zinc finger protein 878-like
XM_019905084.1	NW_017852058.1	72.3	0.70	0.001	zinc finger protein OZF-like
XM_019905085.1	NW_017852058.1	115.3	0.42	0.008	zinc finger protein 268-like
XM_019905086.1	NW_017852058.1	120.1	0.61	0.000	zinc finger protein 184-like
XM_019905088.1	NW_017852058.1	100.4	0.50	0.006	zinc finger protein 678-like
XM_019905089.1	NW_017852058.1	44.0	0.68	0.001	zinc finger protein 883-like
XM_019905090.1	NW_017852058.1	205.4	0.71	0.000	zinc finger protein 37-like
XM_019905094.1	NW_017852058.1	9171.2	0.27	0.000	uncharacterized LOC109538054
XM_019905096.1	NW_017852058.1	1105.6	0.52	0.000	protein arginine N-methyltransferase 7%2C transcript variant X1
XM_019905101.1	NW_017852058.1	15237.1	-1.02	0.004	heat shock protein 68-like
XM_019905105.1	NW_017852058.1	6958.2	-1.39	0.000	heat shock protein 70 A1-like%2C transcript variant X1
XM_019905107.1	NW_017852058.1	90.9	0.53	0.009	zinc finger protein OZF-like
XM_019905108.1	NW_017852058.1	279.1	0.34	0.005	zinc finger protein 182-like
XM_019905109.1	NW_017852058.1	57.8	0.59	0.001	zinc finger protein 62-like
XM_019905111.1	NW_017852058.1	274.7	0.40	0.001	zinc finger protein OZF-like
XM_019905112.1	NW_017852058.1	116.6	0.72	0.002	zinc finger protein 525-like
XM_019905113.1	NW_017852058.1	34703.9	0.91	0.000	actin%2C muscle-like
XM_019905114.1	NW_017852058.1	190.5	0.45	0.006	gastrula zinc finger protein XICGF8.2DB-like
XM_019905116.1	NW_017852058.1	93.6	0.54	0.000	oocyte zinc finger protein XICOF19-like
XM_019905117.1	NW_017852058.1	45.5	0.73	0.001	zinc finger protein 525-like
XM_019905119.1	NW_017852058.1	13.0	1.21	0.001	zinc finger protein 660-like
XM_019905136.1	NW_017852058.1	2174.6	-0.37	0.003	RING finger and SPRY domain-containing protein 1-like

XM_019905138.1	NW_017852058.1	1165.0	-0.39	0.005	nuclear hormone receptor FTZ-F1%2C transcript variant X1
XM_019905147.1	NW_017848551.1	438.6	0.64	0.001	uncharacterized LOC109538087
XR_002171997.1	NW_017845408.1	21235.4	-1.92	0.000	uncharacterized LOC109538091
XM_019905168.1	NW_017852058.1	2649.3	0.89	0.000	glutathione S-transferase-like
XM_019905169.1	NW_017852058.1	10186.5	-0.29	0.009	glutathione S-transferase-like
XM_019905177.1	NW_017852058.1	1047.8	0.33	0.003	serine/threonine-protein phosphatase 4 regulatory subunit 4-like%2C transcript variant X1
XM_019905183.1	NW_017852058.1	331.3	0.91	0.000	haloacid dehalogenase-like hydrolase domain-containing protein 2
XM_019905191.1	NW_017852058.1	2469.0	0.40	0.001	DNA topoisomerase 2
XM_019905198.1	NW_017848559.1	1705.3	-1.80	0.000	uncharacterized LOC109538113
XM_019905206.1	NW_017852058.1	724.0	0.47	0.000	tctex1 domain-containing protein 2-like
XM_019905209.1	NW_017852059.1	275.5	-0.92	0.001	paired box protein Pax-6-like
XM_019905217.1	NW_017848565.1	3261.8	-0.57	0.000	fasciculation and elongation protein zeta-2-like
XM_019905270.1	NW_017845415.1	56.4	-1.32	0.001	E3 ubiquitin-protein ligase MARCH3-like
XM_019905236.1	NW_017852059.1	10378.3	1.07	0.000	alcohol dehydrogenase [NADP(+)]-like
XM_019905252.1	NW_017852059.1	338.0	2.03	0.000	rhamnogalacturonate lyase-like
XM_019905254.1	NW_017852059.1	5787.3	-0.45	0.000	heat shock protein 75 kDa%2C mitochondrial
XM_019905260.1	NW_017852060.1	11601.3	0.60	0.004	prostaglandin reductase 1-like
XM_019905264.1	NW_017852060.1	1584.5	-1.29	0.000	leucine-zipper-like transcriptional regulator 1%2C transcript variant X1
XM_019905280.1	NW_017852061.1	2201.1	-0.41	0.002	rap1 GTPase-GDP dissociation stimulator 1-B
XM_019905295.1	NW_017852061.1	2460.2	-0.32	0.000	uncharacterized protein CG5098%2C transcript variant X1
XM_019905303.1	NW_017852061.1	1356.7	1.41	0.000	protein bfr2-like%2C transcript variant X1
XM_019905321.1	NW_017852061.1	4177.1	1.24	0.002	sodium-independent sulfate anion transporter-like%2C transcript variant X1
XM_019905327.1	NW_017852061.1	493.3	0.29	0.006	lethal(3)malignant brain tumor-like protein 3%2C transcript variant X1
XR_002172008.1	NW_017852061.1	29.1	-1.02	0.002	uncharacterized LOC109538197
XM_019905347.1	NW_017852061.1	27.2	-0.81	0.003	uncharacterized LOC109538205
XM_019905350.1	NW_017852062.1	27.0	-1.49	0.000	homeotic protein proboscipedia-like
XM_019905351.1	NW_017852062.1	4511.3	1.00	0.000	homeobox protein Hox-B3a-like%2C transcript variant X1
XM_019905353.1	NW_017852062.1	279.6	-0.96	0.000	homeotic protein antennapedia-like%2C transcript variant X1
XM_019905375.1	NW_017852064.1	407.4	0.57	0.001	diphthine methyltransferase
XM_019905381.1	NW_017852064.1	24.9	1.24	0.002	uncharacterized LOC109538238
XM_019905387.1	NW_017852064.1	7102.8	-0.29	0.008	ubiquitin carboxyl-terminal hydrolase 7
XM_019905389.1	NW_017852064.1	2361.5	-0.90	0.000	protein asunder%2C transcript variant X1
XR_002172015.1	NW_017848626.1	86.7	0.65	0.001	uncharacterized LOC109538248
XM_019905398.1	NW_017852064.1	1622.4	0.37	0.006	dynein assembly factor 5%2C axonemal%2C transcript variant X1

XM_019905402.1	NW_017852064.1	208.9	0.75	0.000	PI-PLC X domain-containing protein 3-like%2C transcript variant X1
XM_019905407.1	NW_017852064.1	8648.1	0.61	0.000	GMP synthase [glutamine-hydrolyzing]%2C transcript variant X1
XM_019905415.1	NW_017852064.1	502.1	2.00	0.000	uncharacterized LOC109538260
XM_019905416.1	NW_017852064.1	480.8	0.39	0.008	centrosomal protein of 162 kDa%2C transcript variant X1 serine hydroxymethyltransferase%2C cytosolic%2C transcript variant X1
XM_019905419.1	NW_017852064.1	22013.6	1.95	0.000	
XM_019905421.1	NW_017852064.1	175.7	-0.73	0.000	carboxypeptidase B-like
XR_002172018.1	NW_017852064.1	831.3	1.99	0.000	protein KIAA0556-like%2C transcript variant X1 class A basic helix-loop-helix protein 15-like%2C transcript variant X1
XM_019905427.1	NW_017852064.1	3005.5	-0.56	0.000	
XM_019905459.1	NW_017852064.1	13883.3	1.09	0.000	galactokinase-like
XM_019905461.1	NW_017852064.1	19096.8	1.13	0.002	trifunctional purine biosynthetic protein adenosine-3
XM_019905473.1	NW_017852064.1	481.6	-0.27	0.000	triokinase/FMN cyclase-like
XM_019905483.1	NW_017848653.1	931.0	0.39	0.000	N-alpha-acetyltransferase 15%2C NatA auxiliary subunit-like
XM_019905485.1	NW_017852064.1	257.7	-1.11	0.006	perlucin-like protein
XM_019905486.1	NW_017852064.1	1951.1	0.28	0.004	monocarboxylate transporter 10-like%2C transcript variant X1 dual specificity mitogen-activated protein kinase kinase 4%2C transcript variant X1
XM_019905490.1	NW_017852064.1	10248.2	-0.88	0.000	ankyrin repeat domain-containing protein 13D%2C transcript variant X1
XM_019905493.1	NW_017852064.1	2399.2	-0.74	0.000	
XM_019905500.1	NW_017852064.1	24447.5	0.20	0.007	eukaryotic translation initiation factor 5A%2C transcript variant X1
XM_019905512.1	NW_017852064.1	1866.2	1.00	0.000	tolloid-like protein 1%2C transcript variant X1
XM_019905515.1	NW_017852064.1	574.1	-1.09	0.000	glycine receptor subunit alpha-2-like
XM_019905525.1	NW_017852064.1	1202.0	0.44	0.003	septin-2%2C transcript variant X1
XM_019905531.1	NW_017852064.1	44.5	-1.09	0.007	uncharacterized LOC109538333
XM_019905539.1	NW_017852064.1	1556.2	0.29	0.006	E3 ubiquitin-protein ligase CHIP
XM_019905542.1	NW_017852064.1	4372.4	-0.63	0.000	retinal dehydrogenase 1
XM_019905553.1	NW_017852064.1	664.9	0.97	0.000	ovarian-specific serine/threonine-protein kinase Lok-like
XM_019905567.1	NW_017852064.1	9.4	1.40	0.003	uncharacterized LOC109538355%2C transcript variant X1 putative inorganic phosphate cotransporter%2C transcript variant X1
XM_019905572.1	NW_017852064.1	1156.7	-0.79	0.000	
XM_019905586.1	NW_017852064.1	1435.4	0.34	0.006	GTP-binding protein 128up
XM_019905589.1	NW_017852064.1	412.9	-0.50	0.000	polycomb group protein Pc-like
XM_019905599.1	NW_017848681.1	463.5	0.83	0.001	retinol dehydrogenase 13-like
NW_017852067.1_75595-89820	NW_017852067.1	31.9	1.10	0.005	#N/A
XM_019905610.1	NW_017852067.1	3196.9	-0.33	0.004	uncharacterized LOC109538396%2C transcript variant X1
XM_019905621.1	NW_017852067.1	541.2	0.40	0.002	translation initiation factor IF-3%2C mitochondrial
XM_019905629.1	NW_017852068.1	2326.0	-0.46	0.000	sex determination protein fruitless%2C transcript variant X1

XM_019905645.1	NW_017852068.1	7744.1	-0.79	0.000	vacuolar protein sorting-associated protein 13C%2C transcript variant X1
XM_019905653.1	NW_017852068.1	5320.3	0.37	0.001	T-complex protein 1 subunit beta
XM_019905658.1	NW_017848706.1	18.7	-1.44	0.000	iodotyrosine deiodinase 1-like
XR_002172040.1	NW_017852068.1	1462.8	0.24	0.009	pleiotropic regulator 1%2C transcript variant X1
XM_019905672.1	NW_017852068.1	701.5	0.49	0.000	peptidyl-prolyl cis-trans isomerase-like 3%2C transcript variant X1
XM_019905679.1	NW_017852068.1	873.3	0.60	0.000	DNA replication licensing factor Mcm7-like
XM_019905682.1	NW_017852068.1	951.1	0.36	0.001	mitotic checkpoint protein BUB3-like
XM_019905688.1	NW_017852068.1	1447.2	0.33	0.003	probable ATP-dependent RNA helicase YTHDC2%2C transcript variant X1
XM_019905691.1	NW_017852068.1	597.3	0.55	0.000	uncharacterized LOC109538449%2C transcript variant X1
XM_019905694.1	NW_017852068.1	1305.3	0.51	0.001	nucleoporin NDC1
XM_019905706.1	NW_017852070.1	980.8	0.56	0.009	polyamine-modulated factor 1-binding protein 1-like
XM_019905707.1	NW_017852070.1	874.9	1.10	0.004	prostaglandin reductase 1-like
XM_019905708.1	NW_017852070.1	3895.4	-0.56	0.005	charged multivesicular body protein 2a
XM_019905709.1	NW_017852070.1	2519.7	0.84	0.000	protein Smaug homolog 1
XM_019905719.1	NW_017852070.1	3456.4	-0.32	0.001	DENN domain-containing protein 5B
XM_019905720.1	NW_017852070.1	510.5	1.08	0.003	UDP-glucuronosyltransferase 2B17-like
XM_019905723.1	NW_017852070.1	666.6	-1.12	0.000	uncharacterized LOC109538479
XM_019905724.1	NW_017852070.1	184.6	-0.85	0.004	uncharacterized LOC109538480
XM_019905728.1	NW_017852070.1	1233.4	0.93	0.000	lysoplasmalogenase-like protein TMEM86A
XM_019905730.1	NW_017852070.1	141.7	-0.95	0.001	uncharacterized LOC109538486%2C transcript variant X1
XM_019905734.1	NW_017852071.1	53.5	0.79	0.004	uncharacterized LOC109538489
XM_019905736.1	NW_017852071.1	384.7	0.80	0.000	carboxy-terminal kinesin 2-like
XM_019905739.1	NW_017852071.1	1147.3	0.45	0.003	tail-anchored protein insertion receptor WRB-like
XM_019905740.1	NW_017852071.1	2215.6	0.95	0.000	kinesin-like protein subito%2C transcript variant X1
XM_019905744.1	NW_017852072.1	4595.4	0.44	0.000	modifier of mdg4-like%2C transcript variant X1
XM_019905758.1	NW_017848723.1	695.4	0.35	0.000	death-associated inhibitor of apoptosis 2-like
XM_019905755.1	NW_017852072.1	1186.9	0.25	0.001	cyclin-dependent kinase 2-like
XM_019905761.1	NW_017852072.1	4767.4	1.37	0.000	alanine--glyoxylate aminotransferase 2-like
XM_019905774.1	NW_017852073.1	136.2	1.01	0.002	uncharacterized LOC109538522
XM_019905782.1	NW_017848744.1	951.1	0.63	0.002	RNA-binding protein MEX3B-like
XM_019905796.1	NW_017852073.1	2783.9	0.29	0.000	cysteine protease ATG4B
XM_019905798.1	NW_017852073.1	1505.7	0.28	0.001	protein CWC15 homolog%2C transcript variant X1
XM_019905800.1	NW_017852073.1	5779.2	-0.19	0.004	ras-related protein Rab-14%2C transcript variant X1
NW_017848745.1_5706-7006	NW_017848745.1	457.4	0.35	0.008	#N/A
XM_019905803.1	NW_017852073.1	1392.5	1.86	0.000	cytochrome b5-like

XM_019905804.1	NW_017852073.1	432.1	1.03	0.007	acyl-CoA synthetase family member 2%2C mitochondrial-like
XM_019905808.1	NW_017852073.1	2884.9	0.40	0.008	probable histone-lysine N-methyltransferase CG1716
XM_019905814.1	NW_017852073.1	474.3	0.92	0.000	kinesin-like protein KIF14
XM_019905827.1	NW_017852073.1	567.8	0.45	0.002	N-terminal Xaa-Pro-Lys N-methyltransferase 1
XM_019905833.1	NW_017852073.1	952.5	0.55	0.001	H/ACA ribonucleoprotein complex subunit 2-like protein
XM_019905837.1	NW_017848746.1	951.1	0.63	0.002	RNA-binding protein MEX3B-like
XM_019905845.1	NW_017852073.1	1136.6	1.52	0.000	acyl-CoA synthetase family member 2%2C mitochondrial-like%2C transcript variant X1
XM_019905869.1	NW_017852073.1	1347.6	-0.66	0.007	uncharacterized LOC109538578%2C transcript variant X1
XM_019905900.1	NW_017852073.1	1451.4	0.37	0.000	pre-mRNA 3' end processing protein WDR33
XM_019905910.1	NW_017852073.1	9652.5	-0.61	0.000	serine/threonine-protein kinase mig-15%2C transcript variant X1
XM_019905923.1	NW_017852073.1	1264.7	0.48	0.000	probable 28S ribosomal protein S25%2C mitochondrial%2C transcript variant X1
XM_019905926.1	NW_017852073.1	11973.5	0.80	0.001	collagen alpha-5(IV) chain
XM_019905945.1	NW_017852073.1	106424.2	0.50	0.000	Y-box factor homolog%2C transcript variant X1
XM_019905948.1	NW_017852073.1	368.9	0.36	0.000	uncharacterized LOC109538628
XM_019905954.1	NW_017852073.1	1725.9	0.72	0.001	uncharacterized LOC109538632
XM_019905971.1	NW_017852073.1	478.3	0.43	0.006	WD repeat domain-containing protein 83
XR_002172056.1	NW_017848758.1	69.7	-1.36	0.000	uncharacterized LOC109538642
XM_019905988.1	NW_017852073.1	1589.8	-0.47	0.001	putative Polycomb group protein ASXL3%2C transcript variant X1
XM_019905992.1	NW_017852073.1	489.3	0.54	0.001	phosphatidylinositol N-acetylglucosaminyltransferase subunit C
XM_019906012.1	NW_017852073.1	1661.8	-0.74	0.001	aromatic-L-amino-acid decarboxylase%2C transcript variant X1
XM_019906018.1	NW_017852073.1	2776.9	0.38	0.000	calcium uptake protein 1 homolog%2C mitochondrial-like%2C transcript variant X1
XM_019906021.1	NW_017852073.1	14311.2	-1.23	0.000	ras-associated and pleckstrin homology domains-containing protein 1
XR_002172059.1	NW_017852073.1	209.8	-0.95	0.000	uncharacterized LOC109538667
XM_019906030.1	NW_017852073.1	49.3	-1.09	0.010	protein artichoke
XM_019906033.1	NW_017852073.1	1992.7	-0.63	0.000	uncharacterized LOC109538678
XM_019906037.1	NW_017852073.1	2802.7	-0.30	0.004	division abnormally delayed protein
XM_019906049.1	NW_017852073.1	1984.4	0.43	0.000	COP9 signalosome complex subunit 6
XM_019906085.1	NW_017852073.1	1102.1	1.04	0.000	E3 ubiquitin-protein ligase SINAT2-like%2C transcript variant X1
XM_019906098.1	NW_017852074.1	2709.0	-0.41	0.003	zinc/cadmium resistance protein-like
XM_019906099.1	NW_017852074.1	3885.6	-0.37	0.001	zinc/cadmium resistance protein-like
XM_019906110.1	NW_017852075.1	24.6	-1.50	0.000	MORN repeat-containing protein 3-like
XM_019906113.1	NW_017852075.1	388.0	-0.38	0.008	uncharacterized LOC109538740
XM_019906123.1	NW_017852075.1	3206.4	-0.75	0.001	inositol hexakisphosphate kinase 1%2C transcript variant X1
XM_019906136.1	NW_017852075.1	435.7	1.17	0.000	growth/differentiation factor 11

XM_019906149.1	NW_017852076.1	547.5	-1.76	0.000	GTPase-activating Rap/Ran-GAP domain-like protein 3%2C transcript variant X1
XM_019906151.1	NW_017852076.1	1282.7	1.03	0.000	lipase 3-like
XM_019906154.1	NW_017852076.1	1909.4	-0.82	0.000	uncharacterized LOC109538775%2C transcript variant X1
XM_019906162.1	NW_017852076.1	99.3	-0.87	0.001	bromodomain-containing protein DDB_G0280777-like%2C transcript variant X1
XM_019906164.1	NW_017852076.1	1526.6	-1.29	0.000	innexin shaking-B%2C transcript variant X1
XM_019906166.1	NW_017852076.1	4106.6	-0.50	0.000	protein SMG5
XM_019906172.1	NW_017852076.1	315.3	-1.11	0.000	actin cytoskeleton-regulatory complex protein PAN1
XM_019906180.1	NW_017852077.1	216.1	-1.26	0.002	cytochrome P450 9e2-like
XM_019906184.1	NW_017848797.1	90.1	-1.23	0.001	pupal cuticle protein-like
XR_002172066.1	NW_017852077.1	179.9	0.89	0.000	uncharacterized LOC109538798
XM_019906192.1	NW_017848797.1	545.9	0.45	0.000	D-beta-hydroxybutyrate dehydrogenase%2C mitochondrial-like
XM_019906197.1	NW_017852080.1	34.2	1.39	0.000	homeobox protein OTX2-like
XM_019906204.1	NW_017848797.1	1806.5	0.94	0.000	probable phospholipid hydroperoxide glutathione peroxidase%2C transcript variant X1
XM_019906207.1	NW_017852080.1	919.5	0.99	0.000	juvenile hormone epoxide hydrolase 1-like
XM_019906210.1	NW_017852081.1	1191.9	0.38	0.001	N-alpha-acetyltransferase 15%2C NatA auxiliary subunit-like
XM_019906211.1	NW_017852081.1	928.9	0.34	0.002	DNA-directed RNA polymerase III subunit RPC3-like
XM_019906231.1	NW_017852082.1	276.9	-0.89	0.000	uncharacterized LOC109538832%2C transcript variant X1
XM_019906236.1	NW_017852082.1	1702.9	0.35	0.002	DNA-directed RNA polymerase III subunit RPC5
XM_019906243.1	NW_017852082.1	1249.9	-0.42	0.002	dedicator of cytokinesis protein 7-like
XM_019906250.1	NW_017848797.1	1480.3	0.46	0.006	39S ribosomal protein L11%2C mitochondrial-like
XM_019906254.1	NW_017852082.1	3744.1	-0.57	0.003	transmembrane protein 208
XM_019906259.1	NW_017852082.1	13559.6	-0.25	0.008	uncharacterized LOC109538855%2C transcript variant X1
XM_019906277.1	NW_017852082.1	3304.3	0.42	0.000	uncharacterized LOC109538862%2C transcript variant X1
XM_019906285.1	NW_017852082.1	4621.9	-0.49	0.007	adenylyl cyclase-associated protein 1-like
XM_019906286.1	NW_017852082.1	2968.6	0.47	0.002	NADH dehydrogenase [ubiquinone] flavoprotein 2%2C mitochondrial%2C transcript variant X1
XM_019906299.1	NW_017852082.1	71.3	-1.11	0.000	carcinine transporter%2C transcript variant X1
XM_019906315.1	NW_017852082.1	3294.2	0.69	0.000	uncharacterized LOC109538888
XM_019906322.1	NW_017852082.1	3172.5	2.33	0.000	uncharacterized LOC109538892%2C transcript variant X1
XM_019906327.1	NW_017852082.1	2669.9	-0.51	0.004	uncharacterized LOC109538897%2C transcript variant X1
XM_019906342.1	NW_017852082.1	5164.1	-0.76	0.006	GTP-binding protein REM 1
XM_019906347.1	NW_017852082.1	1167.0	0.62	0.000	28S ribosomal protein S31%2C mitochondrial
XM_019906352.1	NW_017852082.1	10594.8	-0.99	0.000	translocating chain-associated membrane protein 1
XM_019906353.1	NW_017852082.1	96.3	-1.12	0.000	tektin-3-like%2C transcript variant X1
XM_019906362.1	NW_017852082.1	2328.0	-0.62	0.000	sphingosine-1-phosphate lyase

XM_019906367.1	NW_017848819.1	379.5	0.38	0.009	post-GPI attachment to proteins factor 2-like
XM_019906385.1	NW_017852083.1	104.8	1.72	0.000	SUN domain-containing protein 3-like
XM_019906390.1	NW_017848840.1	9832.9	-1.16	0.000	nose resistant to fluoxetine protein 6-like%2C transcript variant X1
XM_019906403.1	NW_017852083.1	13561.7	-0.49	0.002	myosin heavy chain%2C non-muscle%2C transcript variant X1
XM_019906406.1	NW_017852083.1	2646.1	-0.58	0.001	mediator of RNA polymerase II transcription subunit 13%2C transcript variant X1
XM_019906437.1	NW_017852083.1	2716.2	-0.40	0.001	uncharacterized protein CG7065-like%2C transcript variant X1
XM_019906458.1	NW_017852083.1	1129.4	-0.88	0.000	switch-associated protein 70-like%2C transcript variant X1
XM_019906460.1	NW_017852083.1	560.5	0.52	0.005	tRNA (cytosine-5-)-methyltransferase%2C transcript variant X1
XM_019906467.1	NW_017852083.1	17582.2	1.80	0.000	bifunctional methylenetetrahydrofolate dehydrogenase/cyclohydrolase%2C mitochondrial%2C transcript variant X1
XM_019906479.1	NW_017848844.1	265.1	-0.89	0.000	sine oculis-binding protein homolog
XM_019906487.1	NW_017852083.1	2145.8	-0.64	0.007	sodium-independent sulfate anion transporter-like%2C transcript variant X1
XM_019906498.1	NW_017852083.1	922.0	-0.85	0.005	sialin%2C transcript variant X1
XM_019906503.1	NW_017852083.1	2156.5	1.21	0.002	uncharacterized LOC109539000
XM_019906507.1	NW_017852083.1	733.7	1.11	0.000	uncharacterized LOC109539002
XM_019906512.1	NW_017852083.1	3495.6	0.83	0.002	alkaline phosphatase%2C tissue-nonspecific isozyme-like%2C transcript variant X1
XM_019906522.1	NW_017852083.1	798.1	0.47	0.000	uncharacterized LOC109539013
XM_019906527.1	NW_017852083.1	1266.7	0.44	0.001	coiled-coil domain-containing protein 115
XM_019906531.1	NW_017852083.1	2571.1	1.05	0.000	cyclin-A2-like
XM_019906532.1	NW_017852083.1	130.1	-1.14	0.000	uncharacterized LOC109539021%2C transcript variant X1
XM_019906540.1	NW_017852084.1	352.4	-0.39	0.007	rho GTPase-activating protein 26-like
XM_019906541.1	NW_017852085.1	851.9	0.88	0.000	anoctamin-5
XM_019906546.1	NW_017852085.1	2069.3	0.49	0.000	NFX1-type zinc finger-containing protein 1-like
XM_019906564.1	NW_017852085.1	1908.9	0.43	0.007	platelet-activating factor acetylhydrolase IB subunit beta homolog
XM_019906568.1	NW_017852085.1	313.3	0.84	0.000	xyloside xylosyltransferase 1-like
XM_019906570.1	NW_017852085.1	101.9	-1.13	0.000	transmembrane protein 189
XM_019906574.1	NW_017852086.1	35.3	-0.85	0.002	protein glass-like
XM_019906639.1	NW_017852086.1	28125.2	-0.64	0.001	CAP-Gly domain-containing linker protein 2%2C transcript variant X1
XM_019906660.1	NW_017852086.1	4590.2	-0.29	0.001	cyclin-G-associated kinase%2C transcript variant X1
XM_019906683.1	NW_017852086.1	678.6	0.59	0.010	lymphokine-activated killer T-cell-originated protein kinase
XM_019906686.1	NW_017852086.1	7506.5	0.58	0.000	proteasome activator complex subunit 3%2C transcript variant X1
XM_019906689.1	NW_017852086.1	9065.4	0.37	0.007	nucleoplasmin-like protein%2C transcript variant X1
XM_019906696.1	NW_017852086.1	3279.9	-0.40	0.001	regulator of G-protein signaling 11%2C transcript variant X1

XM_019906708.1	NW_017852086.1	1627.9	0.26	0.002	mitochondrial assembly of ribosomal large subunit protein 1
XM_019906710.1	NW_017852086.1	7080.8	0.52	0.000	cyclic AMP-dependent transcription factor ATF-1
XM_019906711.1	NW_017852086.1	2909.7	0.39	0.001	histone H2A deubiquitinase MYSM1-like%2C transcript variant X1
XM_019906720.1	NW_017852086.1	196.6	1.25	0.000	argininosuccinate lyase
XM_019906737.1	NW_017852087.1	1692.2	0.34	0.006	DNA-directed RNA polymerase I subunit RPA43
XM_019906739.1	NW_017852087.1	678.4	0.79	0.000	protein gone early
XM_019906753.1	NW_017852087.1	84.7	-0.56	0.002	fork head domain-containing protein crocodile
XM_019906761.1	NW_017852088.1	1663.9	0.22	0.008	probable peroxisomal membrane protein PEX13
XM_019906769.1	NW_017852088.1	5510.7	1.25	0.000	zinc finger protein 385B-like
XM_019906771.1	NW_017852089.1	2409.4	-0.45	0.002	nuclear factor related to kappa-B-binding protein
XM_019906776.1	NW_017848892.1	4485.6	-0.89	0.000	uncharacterized LOC109539164
XM_019906783.1	NW_017852091.1	355.6	-0.70	0.001	roundabout homolog 1-like
XM_019906786.1	NW_017852091.1	710.8	0.64	0.002	uncharacterized LOC109539177%2C transcript variant X1
XM_019906803.1	NW_017852091.1	977.1	0.34	0.009	polycomb protein EED
XM_019906808.1	NW_017852091.1	1141.6	0.26	0.005	mitochondrial folate transporter/carrier-like
XM_019906814.1	NW_017852091.1	1575.5	0.63	0.000	PHD finger protein 19%2C transcript variant X1
XM_019906826.1	NW_017852091.1	829.9	0.37	0.002	nuclear pore complex protein Nup160 homolog
XM_019906840.1	NW_017852091.1	502.5	-0.69	0.002	uncharacterized LOC109539220
XM_019906853.1	NW_017852091.1	642.0	-0.91	0.000	UPF0565 protein C2orf69 homolog%2C transcript variant X1
XM_019906856.1	NW_017852091.1	1085.6	1.71	0.000	beta-galactosidase-1-like protein 3
XM_019906859.1	NW_017852091.1	3046.0	1.61	0.000	probable U2 small nuclear ribonucleoprotein A'%2C transcript variant X1
XM_019906875.1	NW_017848910.1	418.5	0.42	0.002	protein arginine N-methyltransferase 3-like
XM_019906871.1	NW_017852091.1	577.8	0.37	0.004	DNA replication complex GINS protein PSF1-like
XM_019906876.1	NW_017852091.1	8503.0	-0.70	0.000	probable JmjC domain-containing histone demethylation protein 2C
XM_019906883.1	NW_017852091.1	15441.2	1.03	0.001	protein henna%2C transcript variant X1
XM_019906885.1	NW_017852091.1	39.1	1.04	0.005	tryptase beta-2-like
XM_019906894.1	NW_017852091.1	2286.7	-0.34	0.002	pre-mRNA-splicing factor 38B%2C transcript variant X1
XM_019906902.1	NW_017852091.1	1885.5	-0.37	0.007	D-glucuronyl C5-epimerase%2C transcript variant X1
XM_019906903.1	NW_017852091.1	1218.0	0.32	0.002	nuclear envelope integral membrane protein 1
XM_019906916.1	NW_017852091.1	1665.8	0.28	0.004	stomatin-like protein 2%2C mitochondrial
XM_019906918.1	NW_017852091.1	2361.7	0.35	0.000	39S ribosomal protein L9%2C mitochondrial
XM_019906924.1	NW_017852091.1	110.0	0.47	0.009	zinc finger protein 239-like
XM_019906934.1	NW_017852091.1	2939.0	-0.62	0.000	uncharacterized LOC109539281%2C transcript variant X1
XM_019906948.1	NW_017852091.1	797.1	0.71	0.005	single-minded homolog 1
XR_002172104.1	NW_017852091.1	66.1	-0.97	0.001	uncharacterized LOC109539300

XM_019906962.1	NW_017852092.1	272.4	0.41	0.000	transducin-like enhancer protein 4
XM_019906965.1	NW_017852093.1	991.0	0.62	0.000	collagen alpha chain CG42342-like%2C transcript variant X1
XM_019906987.1	NW_017852094.1	7748.6	2.67	0.000	lysosome membrane protein 2-like%2C transcript variant X1
XM_019906992.1	NW_017852095.1	1143.9	-0.63	0.000	rho GTPase-activating protein 21-like
XM_019906993.1	NW_017852095.1	371.2	-0.77	0.001	uncharacterized LOC109539319%2C transcript variant X1
XM_019906998.1	NW_017852095.1	5038.9	-0.45	0.006	X-box-binding protein 1%2C transcript variant X1
XM_019907014.1	NW_017848912.1	791.6	-0.58	0.006	B-cell lymphoma/leukemia 11A-like
XM_019907015.1	NW_017852096.1	678.6	0.60	0.007	dnaJ homolog subfamily C member 22
XM_019907028.1	NW_017852096.1	841.0	0.49	0.002	28S ribosomal protein S9%2C mitochondrial
XM_019907029.1	NW_017852096.1	2828.5	0.85	0.006	diphosphomevalonate decarboxylase%2C transcript variant X1
XM_019907049.1	NW_017852096.1	500.8	0.43	0.009	TFIIH basal transcription factor complex helicase XPD subunit
XM_019907053.1	NW_017852096.1	528.1	0.61	0.000	RNA-binding protein 40
XM_019907058.1	NW_017852096.1	8157.2	1.02	0.009	uncharacterized LOC109539363%2C transcript variant X1
XR_002172109.1	NW_017848915.1	465.1	-0.70	0.001	uncharacterized LOC109539364
XM_019907065.1	NW_017852096.1	1552.4	0.61	0.000	uncharacterized LOC109539367
XM_019907066.1	NW_017852096.1	1225.5	-0.59	0.001	coiled-coil domain-containing protein 102A%2C transcript variant X1
XM_019907069.1	NW_017852096.1	9115.0	-0.46	0.002	protein lifeguard 1-like%2C transcript variant X1
XM_019907074.1	NW_017852096.1	54.6	-1.14	0.000	cingulin-like protein 1
XM_019907086.1	NW_017852096.1	25348.4	0.37	0.007	protein disulfide-isomerase
XM_019907088.1	NW_017852096.1	922.9	0.33	0.009	epimerase family protein SDR39U1%2C transcript variant X1
XM_019907093.1	NW_017852096.1	733.1	0.57	0.000	ankyrin repeat domain-containing protein SOWAHC%2C transcript variant X1
XM_019907095.1	NW_017852096.1	3078.6	-0.54	0.002	arf-GAP with Rho-GAP domain%2C ANK repeat and PH domain-containing protein 1%2C transcript variant X1
XM_019907107.1	NW_017852096.1	1375.2	0.48	0.006	enoyl-CoA delta isomerase 2%2C mitochondrial
XM_019907112.1	NW_017848922.1	1378.6	-0.46	0.002	ras-related protein Rab-39B-like
XM_019907109.1	NW_017852096.1	967.0	-0.51	0.007	dual specificity protein phosphatase 22-like%2C transcript variant X1
XM_019907118.1	NW_017852096.1	968.5	-0.93	0.002	ankyrin repeat and SAM domain-containing protein 4B-like
XM_019907119.1	NW_017852097.1	545.5	1.23	0.000	coiled-coil domain-containing protein 8 homolog
XR_002172113.1	NW_017852097.1	164.1	1.03	0.000	uncharacterized LOC109539402
XM_019907129.1	NW_017852098.1	6176.2	2.04	0.000	serine hydrolase-like protein
XM_019907157.1	NW_017852099.1	612.4	0.74	0.001	pro-interleukin-16-like%2C transcript variant X1
XM_019907170.1	NW_017852100.1	2656.4	-0.72	0.000	F-actin-uncapping protein LRRC16A%2C transcript variant X1
XM_019907191.1	NW_017852100.1	2303.6	0.33	0.001	DNA/RNA-binding protein KIN17
XM_019907193.1	NW_017852100.1	1072.8	0.35	0.000	adenylate kinase isoenzyme 6
XR_002172124.1	NW_017852100.1	82.7	-1.36	0.000	uncharacterized LOC109539449

XM_019907230.1	NW_017852100.1	15052.4	-1.20	0.000	nocturnin%2C transcript variant X1
XM_019907237.1	NW_017848929.1	958.9	-0.70	0.000	zinc finger protein 143-like
XM_019907259.1	NW_017852100.1	6974.4	-0.69	0.000	MOG interacting and ectopic P-granules protein 1
XM_019907274.1	NW_017848929.1	1321.3	-1.43	0.000	ferritin%2C heavy subunit-like
XM_019907271.1	NW_017852100.1	629.9	0.47	0.001	lariat debranching enzyme
NW_017852100.1_920979-921493	NW_017852100.1	19.8	-1.46	0.001	#N/A
XM_019907278.1	NW_017852100.1	857.7	-1.01	0.000	uncharacterized LOC109539499%2C transcript variant X1
XM_019907281.1	NW_017852100.1	3080.0	0.23	0.002	protein IWS1 homolog
XM_019907285.1	NW_017848929.1	4009.3	-0.75	0.005	soma ferritin-like
XM_019907283.1	NW_017852100.1	26.2	-0.93	0.002	pro-resilin-like
XM_019907284.1	NW_017852100.1	1676.7	-2.22	0.000	keratin-associated protein 5-11-like
XM_019907288.1	NW_017852100.1	43.7	-1.13	0.000	uncharacterized LOC109539509
XM_019907295.1	NW_017852102.1	1939.7	-0.30	0.003	CD82 antigen-like%2C transcript variant X1
XM_019907299.1	NW_017852102.1	204.9	-0.61	0.000	progesterin and adipoQ receptor family member 4%2C transcript variant X1
XM_019907321.1	NW_017848930.1	273.0	0.49	0.002	DNA polymerase delta catalytic subunit-like
XM_019907325.1	NW_017852103.1	4229.0	-0.82	0.000	uncharacterized LOC109539534%2C transcript variant X1
XM_019907330.1	NW_017852103.1	1282.4	0.56	0.002	uncharacterized LOC109539537%2C transcript variant X1
XM_019907333.1	NW_017848930.1	1521.6	-0.66	0.000	zinc finger protein 143-like
XM_019907335.1	NW_017852103.1	321.9	0.70	0.001	UPF0545 protein C22orf39 homolog
XM_019907338.1	NW_017852103.1	10543.4	-0.33	0.000	kinesin heavy chain%2C transcript variant X1
XM_019907350.1	NW_017852103.1	6138.9	-0.37	0.003	histone-lysine N-methyltransferase 2E%2C transcript variant X1
XM_019907367.1	NW_017852103.1	4060.8	0.22	0.004	aminoacyl tRNA synthase complex-interacting multifunctional protein 2%2C transcript variant X1
XM_019907369.1	NW_017852103.1	712.3	-0.75	0.004	cullin-4-like%2C transcript variant X1
XM_019907373.1	NW_017848930.1	1298.0	-1.42	0.000	ferritin%2C heavy subunit-like%2C transcript variant X1
XM_019907372.1	NW_017852103.1	5729.3	-0.98	0.000	nuclear receptor-binding protein homolog%2C transcript variant X1
XM_019907393.1	NW_017852103.1	3876.7	0.47	0.000	RNA-binding protein cabeza-like%2C transcript variant X1
NW_017848930.1_c12289-10686	NW_017848930.1	4122.3	-0.76	0.005	#N/A
XM_019907407.1	NW_017852103.1	2601.2	-1.21	0.000	uncharacterized LOC109539575%2C transcript variant X1
XM_019907414.1	NW_017852103.1	2177.8	0.29	0.006	importin-13
XM_019907422.1	NW_017852103.1	900.6	0.49	0.000	pre-mRNA-splicing factor ISY1 homolog
XM_019907423.1	NW_017852103.1	13295.4	-0.80	0.000	ecdysone-inducible protein E75%2C transcript variant X1
XM_019907429.1	NW_017852103.1	3938.8	-0.76	0.002	integrin alpha-PS2-like%2C transcript variant X1
XM_019907445.1	NW_017852103.1	39.0	-0.82	0.010	venom allergen 3-like%2C transcript variant X1
XM_019907453.1	NW_017852103.1	3801.1	-0.38	0.003	dnaj homolog dnj-5

XM_019907456.1	NW_017852103.1	538.5	0.36	0.004	DNA polymerase epsilon subunit 4
XM_019907458.1	NW_017852103.1	45994.0	-0.71	0.000	uncharacterized LOC109539606
XM_019907477.1	NW_017852103.1	3748.3	-0.43	0.004	TBC1 domain family member 9
XM_019907481.1	NW_017852103.1	10963.2	1.11	0.000	alpha-aminoadipic semialdehyde synthase%2C mitochondrial
XM_019907483.1	NW_017852103.1	1068.7	-0.64	0.000	rap guanine nucleotide exchange factor 4%2C transcript variant X1
XM_019907486.1	NW_017852103.1	5607.0	0.41	0.000	elongation factor Tu-like
XM_019907496.1	NW_017848934.1	790.9	0.49	0.008	39S ribosomal protein L14%2C mitochondrial
XM_019907492.1	NW_017852103.1	1386.5	1.03	0.000	phosphoglucomutase-2-like%2C transcript variant X1
XM_019907504.1	NW_017852103.1	23344.3	0.76	0.001	mitochondrial enolase superfamily member 1-like
XM_019907509.1	NW_017852103.1	3238.3	-0.45	0.000	sorting nexin-29-like
XM_019907511.1	NW_017852103.1	1090.6	0.47	0.007	transcription factor RFX3%2C transcript variant X1
XM_019907520.1	NW_017852103.1	685.6	0.83	0.000	paramyosin-like zinc finger BED domain-containing protein 1-like%2C transcript variant X1
XM_019907522.1	NW_017852103.1	1221.0	-0.50	0.001	
XM_019907536.1	NW_017852103.1	74.1	-1.33	0.004	ras-related protein Rab-34-like
XM_019907538.1	NW_017852103.1	1879.7	0.65	0.000	cytochrome c-type heme lyase
XM_019907545.1	NW_017852103.1	558.2	0.71	0.000	uncharacterized LOC109539658
XM_019907549.1	NW_017852104.1	210.8	-2.48	0.000	glutamate receptor U1-like
XM_019907603.1	NW_017852104.1	1108.9	0.34	0.003	ribosomal RNA small subunit methyltransferase NEP1
XM_019907610.1	NW_017852104.1	928.9	0.58	0.000	coiled-coil domain-containing protein 58
XM_019907615.1	NW_017852104.1	89.0	-0.82	0.001	ionotropic receptor 25a
XM_019907635.1	NW_017852104.1	7235.3	-0.34	0.008	WD repeat-containing protein 44%2C transcript variant X1
XM_019907649.1	NW_017852104.1	32.4	1.31	0.006	aminopeptidase N-like%2C transcript variant X1
XM_019907652.1	NW_017852104.1	32570.8	-0.77	0.003	membrane alanyl aminopeptidase-like POU domain%2C class 6%2C transcription factor 1-like%2C transcript variant X1
XM_019907689.1	NW_017852104.1	233.2	-0.75	0.004	
XM_019907693.1	NW_017852104.1	646.1	-0.88	0.006	cystinosin homolog ATP-dependent RNA helicase SUV3 homolog%2C mitochondrial%2C transcript variant X1
XM_019907695.1	NW_017852104.1	1009.6	0.53	0.000	
XM_019907701.1	NW_017852104.1	840.5	0.80	0.000	centrobin%2C transcript variant X1
XM_019907707.1	NW_017852104.1	928.7	-0.42	0.000	splicing regulator RBM11
XM_019907717.1	NW_017852104.1	5639.7	-1.00	0.000	lysophospholipid acyltransferase 1%2C transcript variant X1
XM_019907722.1	NW_017852104.1	2354.3	0.28	0.004	serine-arginine protein 55-like%2C transcript variant X1
XM_019907734.1	NW_017852104.1	1671.2	0.60	0.003	aminopeptidase N-like
XM_019907741.1	NW_017852104.1	1836.1	0.48	0.004	NADH dehydrogenase [ubiquinone] 1 beta subcomplex subunit 7
XM_019907750.1	NW_017852104.1	160.6	-1.52	0.001	uncharacterized LOC109539770
XM_019907754.1	NW_017852104.1	679.5	0.76	0.003	T-box-containing protein TBX6L-like%2C transcript variant X1

XM_019907771.1	NW_017852106.1	5361.9	-0.37	0.003	protein crumbs%2C transcript variant X1
XM_019907774.1	NW_017852106.1	9959.9	-0.25	0.008	regulator of nonsense transcripts 1 homolog
XM_019907777.1	NW_017852106.1	1509.8	0.40	0.000	39S ribosomal protein L30%2C mitochondrial
XM_019907778.1	NW_017852106.1	49.2	-0.80	0.001	TPPP family protein CG45057-like
XM_019907782.1	NW_017852106.1	1203.4	0.40	0.001	nuclear pore complex protein Nup107%2C transcript variant X1
XM_019907793.1	NW_017852106.1	832.7	0.50	0.000	uncharacterized LOC109539802
XM_019907802.1	NW_017852106.1	1354.6	0.33	0.000	RING finger protein 37
XM_019907806.1	NW_017848968.1	58.5	-1.12	0.001	uncharacterized LOC109539807%2C transcript variant X1
XM_019907805.1	NW_017852106.1	1048.3	0.64	0.000	prolyl 4-hydroxylase subunit alpha-1-like%2C transcript variant X1
XM_019907814.1	NW_017852106.1	4674.4	-0.52	0.000	serine/threonine-protein kinase Warts%2C transcript variant X1
XM_019907820.1	NW_017852106.1	17140.9	0.95	0.000	synaptic vesicle glycoprotein 2B-like%2C transcript variant X1
XM_019907834.1	NW_017852107.1	133.5	1.70	0.000	cuticle protein 7-like
XM_019907835.1	NW_017852107.1	786.4	1.55	0.001	multidrug resistance-associated protein 4-like%2C transcript variant X1
XM_019907858.1	NW_017852107.1	3293.5	0.54	0.001	neuroguidin
XM_019907860.1	NW_017852107.1	596.9	-0.51	0.008	inosine triphosphate pyrophosphatase
XM_019907874.1	NW_017852107.1	10010.0	-0.42	0.000	FERM%2C RhoGEF and pleckstrin domain-containing protein 2%2C transcript variant X1
XM_019907878.1	NW_017852107.1	29270.8	-0.67	0.000	5'-AMP-activated protein kinase subunit gamma-2%2C transcript variant X1
XM_019907889.1	NW_017852107.1	2430.0	0.52	0.000	SUN domain-containing ossification factor
XM_019907891.1	NW_017852107.1	1743.1	0.27	0.007	methyltransferase-like protein 13
XM_019907898.1	NW_017852107.1	547.5	0.38	0.001	probable RNA methyltransferase CG11342
XM_019907910.1	NW_017852107.1	2641.2	-0.38	0.008	zinc finger protein OZF-like%2C transcript variant X1
XM_019907922.1	NW_017852107.1	1497.2	-0.49	0.000	zinc finger protein 335-like
XM_019907933.1	NW_017852107.1	634.4	-1.10	0.002	probable nuclear hormone receptor HR38%2C transcript variant X1
XM_019907949.1	NW_017852107.1	1376.4	0.86	0.001	T-related protein
XM_019907950.1	NW_017852107.1	1663.1	0.46	0.000	SUMO-activating enzyme subunit 1
XM_019907994.1	NW_017849008.1	1667.0	-0.63	0.006	1-phosphatidylinositol 4%2C5-bisphosphate phosphodiesterase classes I and II-like
XM_019907992.1	NW_017852108.1	2677.4	-0.58	0.001	peptidoglycan-recognition protein SC2-like%2C transcript variant X1
XM_019908004.1	NW_017852108.1	2999.5	-0.39	0.005	uncharacterized LOC109539922%2C transcript variant X1
XM_019908014.1	NW_017849009.1	1526.9	-0.62	0.006	1-phosphatidylinositol 4%2C5-bisphosphate phosphodiesterase classes I and II-like
XM_019908017.1	NW_017852108.1	743.7	0.43	0.008	forkhead box protein F2-like
XM_019908018.1	NW_017852108.1	1407.9	0.45	0.006	U1 small nuclear ribonucleoprotein A
XR_002172151.1	NW_017852108.1	1895.7	-1.49	0.001	uncharacterized LOC109539940

XM_019908034.1	NW_017852109.1	1968.4	1.07	0.000	L-galactose dehydrogenase-like%2C transcript variant X1
XM_019908037.1	NW_017852109.1	4100.5	0.63	0.002	stress response protein NST1%2C transcript variant X1
XM_019908046.1	NW_017852109.1	1972.1	1.32	0.000	multidrug resistance-associated protein 4-like
XM_019908049.1	NW_017852109.1	3112.4	-0.23	0.008	calcium channel flower%2C transcript variant X1
XM_019908055.1	NW_017852109.1	120.3	-0.84	0.007	protein commissureless 2 homolog%2C transcript variant X1
XM_019908090.1	NW_017852110.1	970.6	0.77	0.000	chymotrypsin-C-like%2C transcript variant X1
XM_019908103.1	NW_017852110.1	1382.2	-0.81	0.003	rhomboid-related protein 2-like
XM_019908107.1	NW_017852110.1	339.1	0.31	0.000	uncharacterized LOC109539997
XM_019908117.1	NW_017852110.1	2299.0	-0.49	0.009	Krueppel-like factor 3%2C transcript variant X1
XM_019908130.1	NW_017852110.1	1415.6	0.27	0.007	low molecular weight phosphotyrosine protein phosphatase 1-like
XM_019908142.1	NW_017849021.1	506.4	0.35	0.001	N-alpha-acetyltransferase 15%2C NatA auxiliary subunit-like
XM_019908169.1	NW_017852110.1	666.5	0.28	0.008	DNA replication licensing factor Mcm6
XM_019908207.1	NW_017852110.1	9541.1	-0.44	0.008	uncharacterized LOC109540050
XM_019908212.1	NW_017852110.1	333.0	0.59	0.005	uncharacterized LOC109540053%2C transcript variant X1
XM_019908216.1	NW_017852110.1	878.8	0.28	0.005	6-pyruvoyl tetrahydrobiopterin synthase%2C transcript variant X1
XM_019908219.1	NW_017852110.1	2132.8	0.81	0.000	citron Rho-interacting kinase-like%2C transcript variant X1
XM_019908237.1	NW_017852110.1	544.0	-0.60	0.000	alpha-tocopherol transfer protein-like
XM_019908247.1	NW_017852110.1	8071.0	-0.61	0.005	programmed cell death protein 10-like%2C transcript variant X1
XM_019908265.1	NW_017852110.1	7379.1	-0.67	0.008	uncharacterized LOC109540078%2C transcript variant X1
XM_019908288.1	NW_017852110.1	160.4	0.96	0.000	phospholipase B1%2C membrane-associated-like
XM_019908289.1	NW_017852110.1	383.1	0.81	0.001	purine nucleoside phosphorylase-like
XM_019908294.1	NW_017849039.1	627.5	0.58	0.001	tetraspanin-7-like%2C transcript variant X1
XM_019908312.1	NW_017852111.1	2486.7	0.53	0.001	fork-head transcriptional regulator FHL1-like
XM_019908331.1	NW_017852111.1	1370.3	1.08	0.001	fatty acyl-CoA reductase wat-like
XR_002172161.1	NW_017849039.1	1104.7	-0.46	0.000	uncharacterized LOC109540124
XM_019908357.1	NW_017849040.1	808.7	1.52	0.000	aldose reductase-like
					potassium/sodium hyperpolarization-activated cyclic nucleotide-gated channel 4-like
XM_019908372.1	NW_017852115.1	10.3	-1.19	0.003	uncharacterized LOC109540154
XM_019908374.1	NW_017852115.1	2368.8	0.54	0.001	uncharacterized LOC109540154
XM_019908376.1	NW_017852115.1	3014.7	0.58	0.000	uncharacterized LOC109540156
NW_017849041.1_6-3419	NW_017849041.1	430.9	1.57	0.000	#N/A
XM_019908402.1	NW_017852115.1	3136.6	-0.50	0.003	ARF GTPase-activating protein GIT2
XM_019908406.1	NW_017852115.1	1854.8	0.53	0.000	uncharacterized LOC109540174%2C transcript variant X1
XM_019908408.1	NW_017852115.1	1389.4	-0.86	0.002	octopamine receptor-like%2C transcript variant X1
XR_002172168.1	NW_017852115.1	106.5	0.66	0.000	uncharacterized LOC109540178
XM_019908414.1	NW_017852115.1	329.7	-0.55	0.008	ATP-binding cassette sub-family G member 8

XM_019908415.1	NW_017852115.1	1382.9	-0.61	0.000	syntaxin-binding protein 5-like%2C transcript variant X1
XR_002172169.1	NW_017852115.1	36.7	-0.82	0.005	uncharacterized LOC109540186
XM_019908438.1	NW_017852115.1	959.8	0.35	0.003	transcription initiation factor TFIIID subunit 13
XM_019908442.1	NW_017852115.1	3747.5	-0.82	0.004	peptide methionine sulfoxide reductase%2C transcript variant X1
XM_019908456.1	NW_017852115.1	1592.7	0.74	0.000	serine/threonine-protein kinase haspin-like
XM_019908457.1	NW_017852115.1	1229.8	0.65	0.002	UPF0562 protein C7orf55
XM_019908458.1	NW_017852115.1	11490.0	-0.69	0.000	forkhead box protein O%2C transcript variant X1
XM_019908475.1	NW_017852115.1	2261.5	0.71	0.009	innexin inx3
XM_019908476.1	NW_017852115.1	11635.9	-0.48	0.000	metal transporter CNNM4
XM_019908477.1	NW_017852115.1	2668.8	0.50	0.001	SUMO-conjugating enzyme UBC9-B
XM_019908480.1	NW_017852115.1	1685.7	0.34	0.001	vesicle transport protein SEC20
XM_019908482.1	NW_017852115.1	1006.9	0.38	0.004	U1 small nuclear ribonucleoprotein C short/branched chain specific acyl-CoA dehydrogenase%2C mitochondrial
XM_019908494.1	NW_017852115.1	52167.2	0.87	0.000	myotubularin-related protein 10-A
XM_019908500.1	NW_017852115.1	1486.0	0.40	0.000	polynucleotide 5'-hydroxyl-kinase NOL9%2C transcript variant X1
XM_019908517.1	NW_017852115.1	1441.8	0.67	0.000	ATP-binding cassette sub-family G member 5
XM_019908521.1	NW_017852115.1	625.3	-0.50	0.002	H/ACA ribonucleoprotein complex non-core subunit NAF1%2C transcript variant X1
XM_019908540.1	NW_017852116.1	3729.9	0.63	0.001	cytosolic purine 5'-nucleotidase-like
XM_019908546.1	NW_017849094.1	3311.2	1.12	0.000	calpain-9-like%2C transcript variant X1
XM_019908542.1	NW_017852116.1	609.8	0.72	0.005	maf-like protein Amet_2288
XM_019908554.1	NW_017852117.1	287.3	0.55	0.009	U4/U6.U5 small nuclear ribonucleoprotein 27 kDa protein-like%2C transcript variant X1
XM_019908597.1	NW_017852117.1	827.1	-0.50	0.000	signal transducer and activator of transcription 5B%2C transcript variant X1
XM_019908616.1	NW_017852117.1	3440.5	-0.35	0.000	tribbles homolog 2
XM_019908618.1	NW_017852117.1	6180.1	-0.76	0.005	rho-associated protein kinase 1%2C transcript variant X1
XM_019908619.1	NW_017852117.1	3110.8	-0.60	0.000	E3 ubiquitin-protein ligase complex SLX5-SLX8 subunit SLX8-like%2C transcript variant X1
XM_019908632.1	NW_017852117.1	1893.2	0.57	0.001	chromobox protein homolog 3-like
XM_019908636.1	NW_017852117.1	3634.1	0.43	0.002	leucine-rich repeat-containing protein 51-like%2C transcript variant X1
XM_019908637.1	NW_017852117.1	5.2	1.39	0.003	BTB/POZ domain-containing protein 6-like%2C transcript variant X1
XM_019908647.1	NW_017852117.1	2325.7	0.46	0.000	nuclear cap-binding protein subunit 2-like
XM_019908653.1	NW_017852117.1	1336.3	0.24	0.007	G2/mitotic-specific cyclin-B3%2C transcript variant X1
XM_019908658.1	NW_017852117.1	1070.2	0.89	0.000	uncharacterized LOC109540323
XM_019908662.1	NW_017852117.1	741.5	0.71	0.001	nose resistant to fluoxetine protein 6-like%2C transcript variant X1
XM_019908670.1	NW_017852117.1	17.5	0.86	0.006	

XM_019908674.1	NW_017852117.1	2829.0	-0.23	0.001	uncharacterized LOC109540328%2C transcript variant X1
XM_019908686.1	NW_017852117.1	385.3	0.82	0.004	transcription factor sox-2
XM_019908687.1	NW_017852117.1	14484.9	0.80	0.000	uncharacterized LOC109540339%2C transcript variant X1
XM_019908689.1	NW_017852117.1	50465.2	0.98	0.000	uncharacterized LOC109540340%2C transcript variant X1
XM_019908696.1	NW_017852117.1	1402.5	0.64	0.000	elongation factor Ts%2C mitochondrial
XM_019908700.1	NW_017852117.1	31.0	-0.80	0.002	uncharacterized LOC109540350%2C transcript variant X1
XM_019908702.1	NW_017852117.1	1177.7	1.05	0.000	transcription factor Sox-14
XM_019908711.1	NW_017852117.1	4226.3	1.24	0.000	uncharacterized LOC109540358
XM_019908715.1	NW_017852117.1	2276.9	1.25	0.000	uncharacterized LOC109540361%2C transcript variant X1
XM_019908718.1	NW_017852117.1	4019.7	1.16	0.000	uncharacterized LOC109540362
XM_019908722.1	NW_017852117.1	3803.8	1.18	0.000	ankyrin-2-like
XM_019908725.1	NW_017852118.1	342.0	0.66	0.001	RNA-binding protein Musashi homolog 2-like
XM_019908726.1	NW_017852118.1	1759.6	0.38	0.003	WD and tetratricopeptide repeats protein 1-like 5-demethoxyubiquinone hydroxylase%2C mitochondrial%2C transcript variant X1
XM_019908728.1	NW_017852118.1	289.8	0.53	0.001	autophagy-related protein 9A%2C transcript variant X1
XM_019908731.1	NW_017852120.1	7389.8	-0.39	0.001	DNA replication ATP-dependent helicase/nuclease DNA2
XM_019908751.1	NW_017852121.1	324.7	0.59	0.008	myotubularin-related protein 8
XM_019908753.1	NW_017852121.1	2476.5	-0.40	0.007	39S ribosomal protein L19%2C mitochondrial
XM_019908755.1	NW_017852121.1	1368.0	0.51	0.000	39S ribosomal protein L48%2C mitochondrial
XM_019908756.1	NW_017852121.1	623.3	0.32	0.001	basic salivary proline-rich protein 1-like
XM_019908768.1	NW_017852122.1	2264.0	0.35	0.000	alpha-soluble NSF attachment protein-like
XM_019908774.1	NW_017852122.1	16.0	1.35	0.001	uncharacterized LOC109540417
XM_019908782.1	NW_017849146.1	7900.4	-1.08	0.008	poly(ADP-ribose) glycohydrolase
XM_019908780.1	NW_017852123.1	923.6	0.40	0.000	microtubule-actin cross-linking factor 1%2C transcript variant X1
XM_019908802.1	NW_017852126.1	44181.8	-0.55	0.001	venom serine protease-like
XM_019908829.1	NW_017852126.1	73.7	0.86	0.002	venom serine protease-like
XM_019908831.1	NW_017852126.1	377.4	1.42	0.001	polyadenylate-binding protein 2%2C transcript variant X1
XM_019908838.1	NW_017852126.1	3011.1	0.31	0.004	CCAAT/enhancer-binding protein gamma
XM_019908855.1	NW_017852126.1	3690.2	-0.56	0.000	polyribonucleotide nucleotidyltransferase 1%2C mitochondrial
XM_019908857.1	NW_017852126.1	694.2	0.41	0.003	dynein heavy chain%2C cytoplasmic%2C transcript variant X1
XM_019908859.1	NW_017852126.1	7998.2	-0.29	0.009	dystrophin-like
XM_019908862.1	NW_017852126.1	372.1	0.62	0.002	lysM and putative peptidoglycan-binding domain-containing protein 3
XM_019908873.1	NW_017852126.1	1074.9	-0.36	0.000	uncharacterized LOC109540475%2C transcript variant X1
XM_019908882.1	NW_017852126.1	72195.0	-1.80	0.000	uncharacterized LOC109540477
XR_002172198.1	NW_017852126.1	323.7	-3.32	0.000	DNA-directed RNA polymerase II subunit RPB1
XM_019908900.1	NW_017852126.1	6121.7	-0.47	0.001	

XM_019908911.1	NW_017852126.1	653.2	0.45	0.004	kaptin-like
XM_019908912.1	NW_017852126.1	296.8	1.30	0.002	uncharacterized LOC109540501
XM_019908915.1	NW_017852126.1	3521.8	-0.22	0.009	DAZ-associated protein 2-like%2C transcript variant X1 oxysterol-binding protein-related protein 9%2C transcript variant X1
XM_019908920.1	NW_017852126.1	2819.2	-0.39	0.005	
XM_019908931.1	NW_017852126.1	142.7	-0.71	0.008	synaptogenesis protein syg-2%2C transcript variant X1
XM_019908948.1	NW_017852126.1	1064.9	0.40	0.000	nuclear pore membrane glycoprotein 210
XM_019908951.1	NW_017852126.1	17467.9	-0.28	0.001	abhydrolase domain-containing protein 2
XR_002172207.1	NW_017852126.1	307.1	0.39	0.001	uncharacterized LOC109540534%2C transcript variant X1
XM_019908963.1	NW_017852126.1	5179.8	0.82	0.006	uncharacterized LOC109540536
XM_019908967.1	NW_017852126.1	501.4	-0.37	0.000	synaptic vesicle 2-related protein mothers against decapentaplegic homolog 4-like%2C transcript variant X1
XM_019908969.1	NW_017852126.1	1225.3	-0.82	0.004	
XM_019908977.1	NW_017849169.1	9061.1	0.82	0.000	ATP-dependent RNA helicase p62-like
XM_019908982.1	NW_017852126.1	269.0	0.55	0.001	growth arrest-specific protein 1-like%2C transcript variant X1
XM_019909009.1	NW_017852127.1	246.0	1.31	0.000	regucalcin-like
XM_019909034.1	NW_017852128.1	1713.8	-0.53	0.004	stromal membrane-associated protein 1-like
XM_019909039.1	NW_017852128.1	678.4	0.89	0.000	peroxiredoxin-6
XM_019909046.1	NW_017852128.1	845.2	0.48	0.006	mitochondrial GTPase 1
XM_019909077.1	NW_017852128.1	2752.6	-0.49	0.000	TIMELESS-interacting protein mitochondrial tRNA-specific 2-thiouridylase 1%2C transcript variant X1
XM_019909092.1	NW_017852128.1	963.9	0.60	0.000	
XM_019909096.1	NW_017852128.1	1125.3	-0.41	0.000	INO80 complex subunit D
XM_019909114.1	NW_017852128.1	637.8	0.73	0.000	kinetochore protein NDC80 homolog
XM_019909121.1	NW_017852128.1	292.1	-0.78	0.005	uncharacterized LOC109540676
XR_002172228.1	NW_017852138.1	529.3	-0.83	0.000	uncharacterized LOC109540686
XM_019909130.1	NW_017852139.1	1024.4	-0.29	0.010	exocyst complex component 6-like
XM_019909138.1	NW_017852139.1	4110.7	-0.75	0.001	protein OPI10 homolog
XM_019909139.1	NW_017852139.1	90055.5	-1.10	0.000	uncharacterized LOC109540696
XM_019909147.1	NW_017852139.1	2874.3	-0.43	0.006	sorting nexin-4-like%2C transcript variant X1
XM_019909162.1	NW_017852139.1	1671.7	0.31	0.001	translation initiation factor eIF-2B subunit beta
XM_019909164.1	NW_017852139.1	1597.0	0.51	0.000	protein mago nashi
XM_019909170.1	NW_017852139.1	734.0	0.36	0.006	uncharacterized LOC109540715
XM_019909183.1	NW_017852143.1	3028.9	0.29	0.004	histone H2A.V
XR_002172238.1	NW_017852143.1	37.6	-0.78	0.008	uncharacterized LOC109540731%2C transcript variant X1
XM_019909186.1	NW_017852145.1	2592.1	0.21	0.004	set1/Ash2 histone methyltransferase complex subunit ASH2
XR_002172244.1	NW_017852145.1	81.8	-0.88	0.000	uncharacterized LOC109540737

XM_019909190.1	NW_017852148.1	28.5	-0.97	0.007	uncharacterized LOC109540740
XM_019909217.1	NW_017852154.1	4683.8	0.53	0.006	galectin-8-like%2C transcript variant X1
XR_002172245.1	NW_017852155.1	476.9	-0.69	0.001	uncharacterized LOC109540766
XM_019909243.1	NW_017852156.1	1579.9	0.40	0.001	ribosome biogenesis protein WDR12 homolog
XM_019909244.1	NW_017852156.1	11096.9	0.66	0.000	6-phosphogluconate dehydrogenase%2C decarboxylating
XM_019909252.1	NW_017852156.1	2360.8	0.61	0.000	serine/threonine-protein kinase OSR1%2C transcript variant X1
XM_019909259.1	NW_017852156.1	1001.8	0.41	0.007	COP9 signalosome complex subunit 8
XM_019909271.1	NW_017852156.1	1004.2	-0.38	0.002	gamma-secretase subunit Aph-1
XM_019909275.1	NW_017852158.1	49433.8	-0.91	0.000	ATP-binding cassette sub-family G member 4
XM_019909282.1	NW_017852158.1	36.0	-1.22	0.001	uncharacterized LOC109540799%2C transcript variant X1
XR_002172250.1	NW_017852158.1	302.5	-1.31	0.000	uncharacterized LOC109540801%2C transcript variant X1
XM_019909294.1	NW_017852160.1	512.1	-0.87	0.000	angiotensin-converting enzyme-like
XM_019909307.1	NW_017852160.1	925.8	-0.45	0.001	uncharacterized LOC109540816
XM_019909311.1	NW_017852162.1	20057.7	-0.51	0.002	sortilin-related receptor-like
XM_019909329.1	NW_017852162.1	1338.5	-0.54	0.000	uncharacterized LOC109540838
XM_019909337.1	NW_017849221.1	292.2	0.83	0.000	sodium channel protein 60E-like
XM_019909346.1	NW_017849221.1	7925.3	0.94	0.000	uncharacterized LOC109540853
XM_019909347.1	NW_017852166.1	1719.4	0.99	0.000	uncharacterized LOC109540857
XM_019909348.1	NW_017852166.1	398.8	-0.63	0.002	major facilitator superfamily domain-containing protein 6-like
XM_019909350.1	NW_017852166.1	8600.8	-0.55	0.001	kinesin-like protein KIF13A pyruvate dehydrogenase phosphatase regulatory subunit%2C mitochondrial-like%2C transcript variant X1
XM_019909360.1	NW_017852166.1	1149.8	-0.26	0.001	
XM_019909367.1	NW_017852166.1	3363.5	-0.41	0.000	SAFB-like transcription modulator
XM_019909368.1	NW_017852166.1	4772.0	0.35	0.009	uncharacterized LOC109540869
XM_019909370.1	NW_017852166.1	35.6	-0.73	0.003	NGFI-A-binding protein homolog%2C transcript variant X1
XM_019909373.1	NW_017852166.1	1046.8	-0.41	0.000	protein DENND6A%2C transcript variant X1
XM_019909399.1	NW_017852166.1	4583.1	-0.66	0.001	venom protease-like
XM_019909401.1	NW_017852166.1	213.8	1.13	0.001	cathepsin L1%2C transcript variant X1
XM_019909421.1	NW_017852166.1	971.2	-0.62	0.002	uncharacterized LOC109540896%2C transcript variant X1
XR_002172263.1	NW_017852166.1	6522.1	-0.77	0.002	uncharacterized LOC109540898
XM_019909426.1	NW_017852166.1	3945.6	-0.45	0.000	trafficking protein particle complex subunit 8
XM_019909439.1	NW_017849234.1	2373.1	-0.45	0.007	tubulin-specific chaperone cofactor E-like protein
XM_019909453.1	NW_017852166.1	124.1	-0.87	0.000	protein tipE
XM_019909454.1	NW_017852166.1	3054.9	1.09	0.000	uncharacterized LOC109540914%2C transcript variant X1
XR_002172266.1	NW_017852166.1	1171.1	1.11	0.000	uncharacterized LOC109540917
XM_019909474.1	NW_017852166.1	4168.0	-0.34	0.000	uncharacterized LOC109540928%2C transcript variant X1

XM_019909478.1	NW_017852166.1	4403.3	-0.32	0.002	cytoplasmic FMR1-interacting protein
XM_019909488.1	NW_017849248.1	270.5	-0.81	0.000	uncharacterized LOC109540933
XM_019909493.1	NW_017852166.1	485.7	0.89	0.006	uncharacterized LOC109540938
XM_019909494.1	NW_017852166.1	4056.6	-0.52	0.000	tetratricopeptide repeat protein 39B-like%2C transcript variant X1
XM_019909498.1	NW_017852166.1	276.3	0.71	0.001	uncharacterized LOC109540942%2C transcript variant X1
NW_017852166.1_1751943-1753407	NW_017852166.1	271.6	0.80	0.004	#N/A
XM_019909505.1	NW_017852166.1	4980.8	-0.42	0.004	plexin A3%2C transcript variant X1
XM_019909534.1	NW_017852166.1	9675.1	-0.83	0.000	mid1-interacting protein 1-like%2C transcript variant X1
XM_019909550.1	NW_017852166.1	1993.2	-0.68	0.003	dual serine/threonine and tyrosine protein kinase-like%2C transcript variant X1
XM_019909552.1	NW_017852166.1	2872.3	-1.27	0.000	membrane-associated guanylate kinase%2C WW and PDZ domain-containing protein 1
XM_019909553.1	NW_017852166.1	11256.4	-0.44	0.005	dnaj protein homolog 1
XM_019909555.1	NW_017852166.1	3996.0	-0.46	0.002	histone-lysine N-methyltransferase%2C H3 lysine-79 specific-like%2C transcript variant X1
XM_019909560.1	NW_017852166.1	4773.5	-0.68	0.000	CSC1-like protein 2
XM_019909576.1	NW_017852166.1	8529.1	-0.70	0.000	UPF0518 protein GK23746%2C transcript variant X1
XM_019909578.1	NW_017852166.1	3849.6	-0.53	0.000	GTP-binding protein 2%2C transcript variant X1
XM_019909582.1	NW_017852166.1	3483.5	-0.35	0.000	ADP-ribosylation factor 6
XM_019909585.1	NW_017852166.1	1682.0	-0.69	0.004	uncharacterized LOC109540977
XM_019909587.1	NW_017852166.1	1627.2	-1.28	0.000	formin-like protein 20
XM_019909588.1	NW_017852166.1	959.7	-1.38	0.000	uncharacterized LOC109540979%2C transcript variant X1
XM_019909590.1	NW_017852166.1	4438.3	-0.30	0.004	lysine-specific demethylase lid%2C transcript variant X1
XM_019909637.1	NW_017852166.1	5604.8	-0.44	0.000	phospholipid scramblase 2%2C transcript variant X1
XM_019909660.1	NW_017852166.1	6404.6	-0.35	0.000	IQ motif and SEC7 domain-containing protein 1%2C transcript variant X1
XM_019909690.1	NW_017852166.1	2464.0	-0.64	0.001	uncharacterized LOC109541025%2C transcript variant X1
XM_019909700.1	NW_017849275.1	325.4	0.74	0.007	retinol dehydrogenase 13-like
XM_019909702.1	NW_017852166.1	15547.7	-1.10	0.000	dual specificity protein phosphatase 10-like%2C transcript variant X1
XM_019909706.1	NW_017852166.1	15117.8	-0.68	0.000	RING finger protein 11
XM_019909709.1	NW_017852166.1	1284.9	0.65	0.000	uncharacterized LOC109541038
XM_019909710.1	NW_017852166.1	8367.0	-0.80	0.001	serine protease inhibitor 77Ba
XM_019909712.1	NW_017852166.1	5356.2	-0.57	0.000	alpha-soluble NSF attachment protein%2C transcript variant X1
XM_019909736.1	NW_017852166.1	17333.1	-0.71	0.000	23 kDa integral membrane protein-like
XM_019909743.1	NW_017852166.1	12736.1	-0.63	0.000	syndecan%2C transcript variant X1
XM_019909746.1	NW_017852166.1	4919.8	-0.27	0.000	AP-2 complex subunit alpha%2C transcript variant X1
XM_019909754.1	NW_017852166.1	1918.4	-0.79	0.000	muscle calcium channel subunit alpha-1%2C transcript variant X1

XM_019909766.1	NW_017852166.1	13804.6	-1.04	0.000	monocarboxylate transporter 13-like
XM_019909777.1	NW_017849286.1	1386.4	-0.75	0.000	zinc finger SWIM domain-containing protein 8-like
XM_019909779.1	NW_017852166.1	2919.8	-0.76	0.000	nuclear factor 1 C-type%2C transcript variant X1
XM_019909801.1	NW_017852166.1	31543.2	-0.44	0.000	BCL2/adenovirus E1B 19 kDa protein-interacting protein 3%2C transcript variant X1
XM_019909805.1	NW_017852166.1	237.9	-0.76	0.001	potassium voltage-gated channel protein Shal
XM_019909811.1	NW_017852166.1	981.5	0.40	0.002	facilitated trehalose transporter Tret1-like
XM_019909818.1	NW_017852166.1	2273.9	-0.70	0.003	semaphorin-5B
XM_019909851.1	NW_017852166.1	3385.1	-0.35	0.001	uncharacterized LOC109541114
XM_019909857.1	NW_017852166.1	343.6	-0.80	0.001	zinc finger protein 449-like
XM_019909860.1	NW_017852166.1	3227.3	0.33	0.004	mitochondrial import inner membrane translocase subunit TIM50-C-like
XM_019909868.1	NW_017852166.1	5001.3	0.96	0.000	protein-serine O-palmitoleoyltransferase porcupine%2C transcript variant X1
XM_019909872.1	NW_017852166.1	2297.5	-1.53	0.000	zinc finger protein basonuclin-2-like%2C transcript variant X1
XM_019909877.1	NW_017852166.1	2500.6	0.34	0.001	sodium/hydrogen exchanger 7%2C transcript variant X1
XM_019909886.1	NW_017852166.1	2573.7	-0.65	0.005	neuroligin-2%2C transcript variant X1
XM_019909889.1	NW_017852166.1	2101.3	-0.51	0.000	vinexin-like
XM_019909891.1	NW_017852166.1	19986.2	-0.66	0.000	translocon-associated protein subunit beta
XM_019909896.1	NW_017852166.1	455.5	-0.68	0.006	SRSF protein kinase 3-like
XM_019909908.1	NW_017852166.1	1115.0	-1.26	0.000	uncharacterized LOC109541144
XM_019909909.1	NW_017852166.1	91.8	-2.11	0.000	bone morphogenetic protein 2
XM_019909916.1	NW_017852166.1	299.8	-0.47	0.002	uncharacterized LOC109541150%2C transcript variant X1
XM_019909918.1	NW_017852166.1	2015.9	-0.25	0.006	mesoderm induction early response protein 1-like
XM_019909923.1	NW_017852166.1	115.8	-0.70	0.007	atrial natriuretic peptide-converting enzyme%2C transcript variant X1
XM_019909936.1	NW_017852166.1	474.3	0.77	0.001	F-box/LRR-repeat protein 7-like
XM_019909939.1	NW_017852166.1	71.8	-0.77	0.005	bone morphogenetic protein 2%2C transcript variant X1
XM_019909955.1	NW_017852166.1	553.8	-0.77	0.000	transcription initiation factor IIA subunit 1-like
XM_019909956.1	NW_017852166.1	1319.7	1.09	0.000	protein cortex-like
XM_019909966.1	NW_017852166.1	301.8	-0.65	0.006	protein bunched%2C class 2/F/G isoform-like
XM_019909968.1	NW_017852166.1	2078.6	1.03	0.002	uncharacterized LOC109541182%2C transcript variant X1
XM_019909970.1	NW_017852166.1	1776.3	0.89	0.002	trichohyalin-like
XM_019910013.1	NW_017845629.1	1326.2	-1.43	0.000	ferritin%2C heavy subunit-like%2C transcript variant X1
XM_019909979.1	NW_017852166.1	13.5	-1.15	0.004	uncharacterized LOC109541192
XM_019909980.1	NW_017852166.1	1851.8	1.17	0.000	uncharacterized LOC109541194
XM_019909983.1	NW_017852167.1	968.3	-1.39	0.001	cytochrome P450 9e2-like
XM_019909987.1	NW_017852167.1	1047.8	-1.55	0.000	cytochrome P450 9e2-like

XR_002172288.1	NW_017852168.1	5621.2	0.48	0.003	alpha-aminoadipic semialdehyde dehydrogenase%2C transcript variant X1
XM_019909998.1	NW_017852168.1	12570.1	-0.32	0.001	thymosin beta%2C transcript variant X1
XM_019910016.1	NW_017852168.1	1266.0	-0.74	0.000	zinc finger SWIM domain-containing protein 8-like
XR_002172291.1	NW_017852168.1	1261.4	-0.67	0.000	uncharacterized LOC109541218
XM_019910017.1	NW_017852168.1	60133.2	0.29	0.004	60S ribosomal protein L5-like
XM_019910019.1	NW_017852168.1	3081.2	1.14	0.000	angiotensin-converting enzyme-like
XM_019910021.1	NW_017852168.1	1065.5	0.29	0.003	oligoribonuclease-like
XM_019910027.1	NW_017852168.1	1844.4	0.27	0.002	ribosomal protein S6 kinase 2 beta
XM_019910029.1	NW_017852168.1	2855.0	0.40	0.000	RISC-loading complex subunit tarbp2-like
XM_019910030.1	NW_017852168.1	23375.4	0.27	0.003	60S ribosomal protein L18a
XM_019910042.1	NW_017852170.1	174.9	0.97	0.000	neurotrimin-like%2C transcript variant X1
XM_019910044.1	NW_017852171.1	271.9	1.53	0.000	cytochrome P450 6k1-like
XM_019910046.1	NW_017852172.1	447.6	-0.45	0.004	uncharacterized LOC109541246
XM_019910050.1	NW_017852172.1	21190.4	-0.96	0.000	NADP-dependent malic enzyme-like
XM_019910054.1	NW_017852173.1	606.5	0.45	0.000	COMM domain-containing protein 3%2C transcript variant X1
XM_019910090.1	NW_017852173.1	5677.7	-0.88	0.000	brachyurin-like ankyrin repeat domain-containing protein 12%2C transcript variant X1
XM_019910109.1	NW_017852173.1	4947.0	-0.39	0.000	transcriptional repressor protein YY1-like%2C transcript variant X1
XM_019910115.1	NW_017852173.1	860.0	-0.47	0.000	transcriptional repressor protein YY1-like%2C transcript variant X1
XM_019910121.1	NW_017849321.1	1137.1	0.39	0.004	prefoldin subunit 3-like
XM_019910119.1	NW_017852173.1	654.0	0.76	0.000	spindle assembly abnormal protein 6 homolog
XM_019910123.1	NW_017852175.1	9489.7	-0.42	0.001	protein TIS11-like%2C transcript variant X1
XM_019910125.1	NW_017852175.1	898.0	0.35	0.002	probable asparagine--tRNA ligase%2C mitochondrial
XM_019910130.1	NW_017852176.1	9686.6	-0.46	0.002	dnaj homolog subfamily B member 6%2C transcript variant X1
XM_019910140.1	NW_017852176.1	4240.7	-0.71	0.000	formin-like protein CG32138
XM_019910148.1	NW_017852176.1	68.2	-1.25	0.007	retinol dehydrogenase 13-like
XM_019910150.1	NW_017852176.1	260.4	0.69	0.001	uncharacterized LOC109541323%2C transcript variant X1 Golgi-specific brefeldin A-resistance guanine nucleotide exchange factor 1%2C transcript variant X1
XM_019910159.1	NW_017852178.1	3451.7	-0.46	0.000	uncharacterized LOC109541334
XR_002172312.1	NW_017852178.1	464.3	-0.81	0.000	uncharacterized LOC109541334
XM_019910175.1	NW_017852178.1	10539.4	0.94	0.002	spermatogenesis-associated protein 20%2C transcript variant X1
XM_019910188.1	NW_017852178.1	2267.3	-0.33	0.002	uncharacterized LOC109541342%2C transcript variant X1
XM_019910206.1	NW_017852178.1	534.4	0.58	0.000	uncharacterized LOC109541353
XM_019910208.1	NW_017852178.1	2001.6	-0.49	0.001	zinc finger protein 878-like
XM_019910213.1	NW_017852179.1	599.7	0.74	0.000	disheveled-associated activator of morphogenesis 1
XM_019910214.1	NW_017852179.1	570.0	-0.79	0.000	ras association domain-containing protein 10-like

XM_019910219.1	NW_017852180.1	258.8	-0.46	0.002	myotubularin-related protein 13-like
XM_019910220.1	NW_017852180.1	5920.8	0.68	0.001	2-oxoisovalerate dehydrogenase subunit alpha%2C mitochondrial
XR_002172317.1	NW_017852180.1	2580.7	-0.46	0.001	uncharacterized LOC109541368
XM_019910225.1	NW_017852181.1	110.0	-0.72	0.000	gamma-aminobutyric acid receptor subunit alpha-2-like
XM_019910226.1	NW_017852181.1	8124.3	-0.23	0.006	programmed cell death 6-interacting protein
XM_019910236.1	NW_017852181.1	2257.8	0.86	0.000	geranylgeranyl pyrophosphate synthase%2C transcript variant X1
NW_017845629.1_c12910-11307	NW_017845629.1	4124.0	-0.76	0.004	#N/A
XM_019910281.1	NW_017852190.1	6649.8	-1.05	0.000	uncharacterized LOC109541423
XM_019910282.1	NW_017852190.1	3759.2	-0.80	0.000	vacuolar protein sorting-associated protein 16 homolog
XM_019910290.1	NW_017852191.1	5210.7	-0.30	0.001	putative U5 small nuclear ribonucleoprotein 200 kDa helicase glutaredoxin domain-containing cysteine-rich protein CG31559- like
XM_019910292.1	NW_017852191.1	412.0	0.69	0.001	
XM_019910296.1	NW_017852192.1	3.2	-1.45	0.002	odorant receptor 49b-like
XR_002172334.1	NW_017852192.1	593.8	-0.74	0.000	uncharacterized LOC109541445%2C transcript variant X1
XM_019910316.1	NW_017852192.1	1161.4	1.66	0.000	putative protein TPRXL%2C transcript variant X1
XM_019910318.1	NW_017852192.1	1995.6	-0.97	0.000	D-amino-acid oxidase-like%2C transcript variant X1
XR_002172338.1	NW_017852198.1	24.0	-0.69	0.009	uncharacterized LOC109541480
XM_019910340.1	NW_017852199.1	979.6	-1.15	0.000	organic cation transporter protein-like%2C transcript variant X1
XM_019910343.1	NW_017852199.1	2194.4	-0.28	0.001	ras association domain-containing protein 4-like
XM_019910353.1	NW_017852201.1	2378.0	-0.59	0.009	proto-oncogene tyrosine-protein kinase ROS
XM_019910355.1	NW_017852201.1	1790.4	-0.39	0.001	histone-lysine N-methyltransferase 2C-like
XM_019910361.1	NW_017852201.1	1652.3	0.59	0.001	cell division cycle protein 20 homolog
XR_002172340.1	NW_017852201.1	83.8	-0.75	0.000	uncharacterized LOC109541503%2C transcript variant X1
XM_019910375.1	NW_017852201.1	13496.8	-0.55	0.004	monocarboxylate transporter 3-like
XM_019910396.1	NW_017852201.1	1141.7	2.30	0.000	argininosuccinate synthase
XM_019910397.1	NW_017852201.1	347.1	0.96	0.000	ribonuclease H2 subunit A
XM_019910403.1	NW_017852201.1	241.6	-0.65	0.000	toll-like receptor Tollo
XM_019910423.1	NW_017852214.1	27.5	1.04	0.001	uncharacterized LOC109541546
XM_019910424.1	NW_017852214.1	1646.7	-0.45	0.006	acyl-CoA Delta(11) desaturase-like%2C transcript variant X1
XM_019910446.1	NW_017852220.1	1719.2	-0.41	0.000	slit homolog 3 protein-like
XR_002172348.1	NW_017852224.1	647.0	-0.79	0.001	uncharacterized LOC109541576%2C transcript variant X1
XR_002172350.1	NW_017852224.1	99.4	-0.51	0.007	uncharacterized LOC109541578
XM_019910464.1	NW_017852228.1	1597.1	0.40	0.000	prefoldin subunit 3-like
XM_019910470.1	NW_017852228.1	1932.6	0.38	0.000	prefoldin subunit 3-like
XM_019910492.1	NW_017852233.1	379.3	0.38	0.009	post-GPI attachment to proteins factor 2-like
XM_019910493.1	NW_017852233.1	379.4	0.38	0.009	post-GPI attachment to proteins factor 2-like

XR_002172359.1	NW_017852234.1	143.7	-0.86	0.005	uncharacterized LOC109541625
XM_019910525.1	NW_017852235.1	1050.5	0.56	0.000	protein maelstrom 1
XM_019910545.1	NW_017852238.1	713.4	1.29	0.001	phosphoglycolate phosphatase 1B%2C chloroplastic-like 1-acyl-sn-glycerol-3-phosphate acyltransferase alpha-like%2C transcript variant X1
XM_019910552.1	NW_017852238.1	2413.8	-0.83	0.007	zinc finger protein 358-like
XM_019910557.1	NW_017852238.1	2357.9	-0.26	0.001	biotinidase-like
XM_019910559.1	NW_017852239.1	812.7	-0.65	0.006	uncharacterized LOC109541671%2C transcript variant X1
XM_019910569.1	NW_017852239.1	151.0	0.63	0.009	transmembrane protein 53%2C transcript variant X1
XM_019910584.1	NW_017849390.1	10561.9	-0.55	0.000	apoptosis-inducing factor 1%2C mitochondrial%2C transcript variant X1
XM_019910581.1	NW_017852241.1	2600.3	0.34	0.004	synaptotagmin-11-like
XM_019910589.1	NW_017852242.1	514.0	1.01	0.003	voltage-gated potassium channel subunit beta-2%2C transcript variant X1
XM_019910598.1	NW_017852243.1	445.3	-0.80	0.000	39S ribosomal protein L21%2C mitochondrial%2C transcript variant X1
XM_019910626.1	NW_017849390.1	1256.0	0.43	0.000	longitudinals lacking protein%2C isoforms J/P/Q/S/Z%2C transcript variant X1
XM_019910627.1	NW_017852245.1	36470.0	0.29	0.006	FGFR1 oncogene partner 2 homolog
XM_019910644.1	NW_017849390.1	1992.7	0.28	0.001	
NW_017852245.1_c576586- 566924	NW_017852245.1	468.4	-1.60	0.000	#N/A
XM_019910647.1	NW_017852245.1	207.4	-0.85	0.008	uncharacterized LOC109541719
XR_002172365.1	NW_017852245.1	2598.2	-0.81	0.002	uncharacterized LOC109541720%2C transcript variant X1
XM_019910664.1	NW_017852245.1	489.2	1.11	0.001	zinc finger and SCAN domain-containing protein 10-like
XM_019910667.1	NW_017852245.1	1560.3	0.43	0.001	PQ-loop repeat-containing protein 3
XM_019910679.1	NW_017852245.1	5128.1	-0.45	0.000	cyclin-dependent kinase 14%2C transcript variant X1
XR_002172373.1	NW_017852245.1	2.8	-1.25	0.009	uncharacterized LOC109541754
XM_019910689.1	NW_017852245.1	14297.1	-0.65	0.003	triple functional domain protein-like%2C transcript variant X1
XM_019910723.1	NW_017852245.1	29.7	0.73	0.003	uncharacterized LOC109541766
XM_019910731.1	NW_017852245.1	5654.3	0.23	0.004	ras-related protein Rac1
XM_019910733.1	NW_017852245.1	1802.5	-0.61	0.000	trimethylguanosine synthase
XM_019910737.1	NW_017852245.1	465.5	0.80	0.001	serine/threonine-protein kinase greatwall
XM_019910738.1	NW_017852245.1	633.7	0.87	0.000	mini-chromosome maintenance complex-binding protein
XM_019910751.1	NW_017852245.1	1930.4	0.32	0.009	beta-parvin
XM_019910769.1	NW_017852245.1	184.4	-0.58	0.005	Krueppel-like factor luna
XM_019910770.1	NW_017852245.1	902.4	0.65	0.000	uncharacterized LOC109541803%2C transcript variant X1
XM_019910773.1	NW_017852245.1	354.6	0.47	0.000	methyltransferase-like protein 22%2C transcript variant X1
XM_019910777.1	NW_017852245.1	565.8	0.56	0.000	uncharacterized LOC109541809%2C transcript variant X1

XM_019910783.1	NW_017852245.1	3867.1	-0.79	0.000	sodium- and chloride-dependent neutral and basic amino acid transporter B(0+)-like%2C transcript variant X1
XM_019910787.1	NW_017852245.1	794.8	0.35	0.001	probable malonyl-CoA-acyl carrier protein transacylase%2C mitochondrial
XM_019910790.1	NW_017852245.1	9024.3	-0.48	0.000	phosphatidylinositol-binding clathrin assembly protein LAP%2C transcript variant X1
XM_019910793.1	NW_017852245.1	844.7	0.97	0.000	COP9 signalosome complex subunit 1-like%2C transcript variant X1
XM_019910795.1	NW_017852245.1	1556.7	0.56	0.000	retinol dehydrogenase 11-like
XM_019910798.1	NW_017852245.1	4138.6	-0.55	0.001	transcriptional repressor CTCF-like%2C transcript variant X1
XM_019910807.1	NW_017852245.1	14799.1	-0.62	0.000	aryl hydrocarbon receptor nuclear translocator-like protein 1
XM_019910817.1	NW_017852245.1	1716.9	0.43	0.000	ran GTPase-activating protein 1
XM_019910818.1	NW_017852245.1	311.3	0.67	0.000	uncharacterized LOC109541831
XM_019910821.1	NW_017852245.1	3750.7	0.80	0.000	glycine cleavage system H protein%2C mitochondrial
XM_019910832.1	NW_017852245.1	1057.2	0.43	0.001	prostaglandin E synthase 2
XM_019910844.1	NW_017849417.1	7177.7	-0.39	0.003	protein TIS11-like
XM_019910841.1	NW_017852245.1	1575.4	-0.93	0.000	putative uncharacterized protein DDB_G0277255%2C transcript variant X1
XM_019910845.1	NW_017852245.1	136.9	-1.24	0.002	uncharacterized LOC109541849
XM_019910846.1	NW_017852245.1	27806.1	-0.45	0.007	stress-associated endoplasmic reticulum protein 2
XM_019910851.1	NW_017852245.1	1284.3	0.37	0.005	probable small nuclear ribonucleoprotein Sm D1
XM_019910855.1	NW_017849418.1	1495.5	-0.86	0.000	uncharacterized LOC109541856
XM_019910863.1	NW_017852247.1	999.8	0.40	0.002	ribonucleases P/MRP protein subunit POP1
XM_019910868.1	NW_017852247.1	1025.7	0.98	0.000	uncharacterized LOC109541875%2C transcript variant X1
XM_019910875.1	NW_017849423.1	1743.0	-0.55	0.000	E3 ubiquitin-protein ligase UBR1-like
XM_019910874.1	NW_017852247.1	422.5	-1.16	0.001	superoxide dismutase [Cu-Zn]%2C chloroplastic-like
XM_019910877.1	NW_017852247.1	2358.7	0.55	0.005	glucose 1-dehydrogenase-like
XM_019910884.1	NW_017849431.1	277.0	0.85	0.000	sodium channel protein 60E-like
XR_002172380.1	NW_017852248.1	103.0	-0.70	0.000	uncharacterized LOC109541893
XM_019910887.1	NW_017852248.1	2365.2	0.79	0.007	putative sodium-dependent multivitamin transporter%2C transcript variant X1
XM_019910894.1	NW_017849431.1	7924.3	0.94	0.000	uncharacterized LOC109541897
XR_002172385.1	NW_017849433.1	23.5	-1.52	0.000	uncharacterized LOC109541917
XM_019910917.1	NW_017852254.1	5109.5	0.73	0.007	ATP-binding cassette sub-family A member 3-like
XM_019910918.1	NW_017852254.1	2750.9	-0.73	0.003	uncharacterized LOC109541922%2C transcript variant X1
XM_019910922.1	NW_017852254.1	837.7	0.74	0.000	protein MMS22-like
XM_019910936.1	NW_017852254.1	9649.8	0.75	0.001	glycerol kinase-like%2C transcript variant X1
XR_002172388.1	NW_017849443.1	125.9	0.56	0.002	uncharacterized LOC109541938
XM_019910941.1	NW_017852254.1	86.9	-0.57	0.004	protein FAM234B-like

XM_019910947.1	NW_017852254.1	11730.2	0.94	0.005	ATP-binding cassette sub-family A member 3-like
XM_019910962.1	NW_017852254.1	455.8	0.70	0.000	V-type proton ATPase 21 kDa proteolipid subunit%2C transcript variant X1
XR_002172389.1	NW_017852254.1	1051.5	1.01	0.000	uncharacterized LOC109541959
XM_019910984.1	NW_017849449.1	114.4	0.82	0.000	RNA-binding protein Musashi homolog Rbp6-like
XM_019910980.1	NW_017852254.1	32272.0	-0.43	0.000	activating transcription factor of chaperone%2C transcript variant X1
XM_019910983.1	NW_017852254.1	89.4	-0.92	0.008	EF-hand calcium-binding domain-containing protein 2-like%2C transcript variant X1
XM_019910995.1	NW_017852254.1	12008.6	-0.69	0.001	C3 and PZP-like alpha-2-macroglobulin domain-containing protein 8
XM_019911002.1	NW_017852254.1	100.8	-1.52	0.000	uncharacterized LOC109541982
XM_019911003.1	NW_017852255.1	4015.8	-0.50	0.001	coiled-coil and C2 domain-containing protein 1-like
XM_019911033.1	NW_017852256.1	1597.5	0.41	0.000	ubiquitin-conjugating enzyme E2 S
XM_019911037.1	NW_017852257.1	917.9	-0.87	0.000	low-density lipoprotein receptor-related protein 1-like
XM_019911038.1	NW_017852257.1	918.5	-0.99	0.000	prolow-density lipoprotein receptor-related protein 1-like
XM_019911045.1	NW_017849453.1	1299.3	1.04	0.000	uncharacterized LOC109542017
XM_019911047.1	NW_017852257.1	1460.0	-0.92	0.000	prolow-density lipoprotein receptor-related protein 1-like
XM_019911056.1	NW_017849455.1	1800.4	0.53	0.004	probable nucleoporin Nup58
XM_019911053.1	NW_017852257.1	276.2	-1.01	0.000	low-density lipoprotein receptor-related protein 1B-like
XM_019911059.1	NW_017852257.1	388.1	-0.90	0.000	prolow-density lipoprotein receptor-related protein 1-like
XM_019911064.1	NW_017852258.1	411.4	-0.98	0.006	uncharacterized LOC109542038
XM_019911089.1	NW_017852258.1	1964.7	0.52	0.000	sorting nexin-7-like
XM_019911105.1	NW_017852258.1	3317.1	0.27	0.010	zinc finger Ran-binding domain-containing protein 2%2C transcript variant X1
XM_019911107.1	NW_017852258.1	1236.9	0.53	0.000	probable small nuclear ribonucleoprotein G
XM_019911108.1	NW_017852258.1	9938.8	1.02	0.001	zinc transporter ZIP13-like
XM_019911119.1	NW_017852258.1	1306.3	0.37	0.003	treacle protein-like%2C transcript variant X1
XM_019911125.1	NW_017852258.1	864.6	0.27	0.010	mitochondrial ubiquitin ligase activator of NFKB 1
XM_019911132.1	NW_017852258.1	39363.9	0.88	0.001	sterol O-acyltransferase 1
XM_019911143.1	NW_017852258.1	7453.0	0.94	0.000	equilibrative nucleoside transporter 1%2C transcript variant X1
XM_019911149.1	NW_017852258.1	1841.8	-1.21	0.000	muscle segmentation homeobox
XM_019911152.1	NW_017852258.1	3218.1	-1.21	0.000	homeobox protein MSX-3-like
XM_019911158.1	NW_017852259.1	5153.0	-0.30	0.001	uncharacterized LOC109542101
XM_019911163.1	NW_017852260.1	181.8	-0.92	0.004	uncharacterized LOC109542105
XM_019911166.1	NW_017852262.1	1854.2	-0.60	0.002	protein-methionine sulfoxide oxidase Mical-like
XM_019911167.1	NW_017852262.1	714.2	-0.61	0.001	protein-methionine sulfoxide oxidase MICAL2-like
XM_019911171.1	NW_017852263.1	1147.0	-0.71	0.005	uncharacterized LOC109542113

XM_019911185.1	NW_017852263.1	208.1	-0.61	0.008	putative metabolite transport protein HI_1104
XM_019911204.1	NW_017852263.1	916.6	0.46	0.001	uncharacterized LOC109542133%2C transcript variant X1
XM_019911214.1	NW_017852263.1	1822.0	1.30	0.002	uncharacterized LOC109542137
XM_019911217.1	NW_017852263.1	2632.4	-0.59	0.001	uncharacterized LOC109542141
XM_019911219.1	NW_017852263.1	1236.1	0.84	0.000	voltage-dependent calcium channel subunit alpha-2/delta-3%2C transcript variant X1
XM_019911244.1	NW_017852263.1	11715.0	0.57	0.001	eukaryotic translation initiation factor 4E transporter-like%2C transcript variant X1
XM_019911261.1	NW_017852263.1	3962.3	-0.30	0.001	septin-1
XM_019911268.1	NW_017852263.1	649.4	-1.46	0.000	farnesol dehydrogenase-like
XM_019911269.1	NW_017852263.1	366.1	0.40	0.010	DNA repair and recombination protein RAD54-like
XM_019911274.1	NW_017852264.1	1102.0	0.54	0.000	YEATS domain-containing protein 4%2C transcript variant X1
XR_002172401.1	NW_017852264.1	1641.2	-0.49	0.007	uncharacterized LOC109542172
XM_019911277.1	NW_017852265.1	1602.7	0.37	0.003	evolutionarily conserved signaling intermediate in Toll pathway%2C mitochondrial-like
XM_019911281.1	NW_017852265.1	5796.9	-0.48	0.000	WW domain-binding protein 2
XM_019911287.1	NW_017852265.1	1769.9	0.47	0.005	S-adenosylmethionine mitochondrial carrier protein homolog%2C transcript variant X1
XM_019911300.1	NW_017852265.1	824.5	-0.48	0.001	phosphatidylinositol 3%2C4%2C5-trisphosphate 3-phosphatase and dual-specificity protein phosphatase PTEN%2C transcript variant X1
XM_019911320.1	NW_017852265.1	401.6	0.81	0.000	deoxynucleoside kinase-like
XM_019911327.1	NW_017852267.1	2617.4	-0.71	0.000	uncharacterized LOC109542202
XM_019911354.1	NW_017852267.1	872.1	-1.16	0.000	glycine-rich protein 5-like
XM_019911358.1	NW_017852267.1	9071.6	-0.56	0.000	supervillin-like%2C transcript variant X1
XM_019911362.1	NW_017852267.1	467.4	0.45	0.006	leukocyte receptor cluster member 1 homolog
XM_019911369.1	NW_017852267.1	1948.0	-0.53	0.002	ubiquitin-conjugating enzyme E2 J1-like
XM_019911389.1	NW_017852267.1	1053.4	0.67	0.001	zinc finger homeobox protein 3
XM_019911417.1	NW_017852269.1	1830.9	0.35	0.004	mediator of RNA polymerase II transcription subunit 23
XM_019911424.1	NW_017852269.1	364.0	0.53	0.000	mismatch repair endonuclease PMS2
XM_019911438.1	NW_017852269.1	4319.3	0.85	0.002	juvenile hormone epoxide hydrolase 1-like
XM_019911441.1	NW_017852269.1	1698.1	0.38	0.001	28S ribosomal protein S35%2C mitochondrial
XM_019911463.1	NW_017852269.1	1842.8	0.72	0.000	protein FAM60A%2C transcript variant X1
XM_019911481.1	NW_017852269.1	279.3	-0.77	0.004	BAI1-associated protein 3
XM_019911482.1	NW_017852269.1	405.0	0.79	0.000	mitochondrial inner membrane protease ATP23 homolog
XM_019911498.1	NW_017852270.1	1496.8	0.75	0.000	uncharacterized LOC109542314
XM_019911499.1	NW_017852270.1	862.6	-0.51	0.002	activating signal cointegrator 1
XM_019911517.1	NW_017852270.1	1497.0	0.67	0.003	lipase member H-A-like

XM_019911546.1	NW_017852272.1	967.9	0.47	0.001	PRKR-interacting protein 1 homolog
XM_019911556.1	NW_017852278.1	2006.6	0.38	0.002	protein mini spindles
XM_019911563.1	NW_017852278.1	2641.5	-0.48	0.001	RNA polymerase II elongation factor EII
XM_019911592.1	NW_017852279.1	4315.2	-0.96	0.000	protein ECT2%2C transcript variant X1
XM_019911595.1	NW_017852279.1	4406.0	-0.74	0.000	GATA-binding factor 5-B-like%2C transcript variant X1
XM_019911597.1	NW_017852279.1	1580.5	-0.46	0.000	sorting nexin-13-like%2C transcript variant X1
XM_019911599.1	NW_017852279.1	10630.7	-0.68	0.000	MLX-interacting protein%2C transcript variant X1
XM_019911605.1	NW_017852279.1	2939.5	0.29	0.000	nuclear migration protein nudC
XM_019911614.1	NW_017852279.1	13336.3	0.20	0.005	importin subunit alpha-3
XM_019911620.1	NW_017852279.1	3244.4	-0.82	0.001	matrix metalloproteinase-14
XM_019911623.1	NW_017852279.1	37.2	-0.86	0.001	beta-galactoside alpha-2%2C6-sialyltransferase 1
XM_019911627.1	NW_017849532.1	201.7	0.77	0.003	kinesin-like protein 2
XM_019911631.1	NW_017852279.1	1363.1	0.50	0.002	nuclear pore complex protein Nup93-like
XM_019911633.1	NW_017852279.1	1139.8	-0.68	0.001	MAGUK p55 subfamily member 6%2C transcript variant X1
XM_019911640.1	NW_017852279.1	675.2	0.53	0.000	uncharacterized LOC109542416%2C transcript variant X1
XM_019911646.1	NW_017852279.1	3554.1	1.28	0.000	protein bicaudal C homolog 1-B
XM_019911654.1	NW_017852283.1	2685.3	-0.46	0.003	cell surface glycoprotein 1-like
XM_019911663.1	NW_017852286.1	1173.6	0.80	0.000	translation factor GUF1 homolog%2C mitochondrial
XM_019911686.1	NW_017852287.1	1708.9	0.35	0.003	serine/threonine-protein kinase D1%2C transcript variant X1
XM_019911688.1	NW_017852287.1	2628.4	-0.45	0.007	low-density lipoprotein receptor-related protein 2-like
XM_019911690.1	NW_017852287.1	385.0	0.53	0.009	origin recognition complex subunit 4%2C transcript variant X1
XM_019911704.1	NW_017852288.1	720.7	0.38	0.001	tudor domain-containing protein 3-like
XM_019911716.1	NW_017852289.1	2484.0	-0.47	0.003	uncharacterized LOC109542474
XM_019911719.1	NW_017852290.1	4.6	-1.93	0.000	uncharacterized LOC109542478
XM_019911720.1	NW_017852290.1	2617.2	-0.97	0.000	mitogen-activated protein kinase kinase kinase 4
XM_019911727.1	NW_017852290.1	3147.6	-0.55	0.001	probable enoyl-CoA hydratase echA8%2C transcript variant X1
XM_019911734.1	NW_017852291.1	2633.5	-0.48	0.002	dynamamin-like
XM_019911745.1	NW_017852294.1	799.5	-0.38	0.000	transient receptor potential channel pyrexia GDP-fucose protein O-fucosyltransferase 1%2C transcript variant X1
XM_019911758.1	NW_017852296.1	380.6	0.76	0.000	
XM_019911761.1	NW_017852296.1	12706.4	-0.85	0.001	immediate early response gene 5-like protein
XM_019911776.1	NW_017852296.1	4716.9	-0.64	0.000	uncharacterized LOC109542526%2C transcript variant X1
XM_019911781.1	NW_017852296.1	3587.0	-0.85	0.000	uncharacterized LOC109542527%2C transcript variant X1
XM_019911783.1	NW_017852296.1	2958.9	0.30	0.004	uncharacterized LOC109542528
XM_019911787.1	NW_017852296.1	967.5	0.39	0.001	serine/threonine-protein phosphatase 2A activator-like
XM_019911792.1	NW_017849548.1	71.8	0.70	0.002	protein lethal(2)denticleless-like%2C transcript variant X1

XM_019911790.1	NW_017852296.1	3584.9	-0.41	0.001	uncharacterized LOC109542535%2C transcript variant X1
XM_019911799.1	NW_017852296.1	5416.4	-0.29	0.010	arf-GAP domain and FG repeat-containing protein 1 mannose-P-dolichol utilization defect 1 protein homolog%2C transcript variant X1
XM_019911800.1	NW_017852296.1	1218.4	0.68	0.000	uncharacterized LOC109542545
XR_002172436.1	NW_017852296.1	3679.4	-2.01	0.000	dnaj homolog subfamily C member 11
XM_019911810.1	NW_017852296.1	2257.3	0.27	0.000	protein FAM122A-like%2C transcript variant X1
XM_019911814.1	NW_017852296.1	2039.8	0.40	0.010	protein phosphatase 1 regulatory subunit 12A%2C transcript variant X1
XM_019911828.1	NW_017852296.1	571.4	1.04	0.000	pantothenate kinase 4
XM_019911832.1	NW_017852296.1	7358.0	0.86	0.000	replication factor C subunit 5
XM_019911835.1	NW_017852296.1	961.9	0.46	0.006	uncharacterized LOC109542565
XM_019911837.1	NW_017852296.1	490.1	0.36	0.008	circadian clock-controlled protein-like
XM_019911839.1	NW_017852296.1	90.2	1.99	0.000	beta-hexosaminidase subunit alpha-like
XM_019911849.1	NW_017852297.1	1062.7	1.16	0.000	beta-hexosaminidase subunit alpha-like
XM_019911852.1	NW_017852297.1	4703.4	1.49	0.000	C-1-tetrahydrofolate synthase%2C cytoplasmic
XM_019911869.1	NW_017852297.1	88903.5	1.18	0.001	THO complex subunit 2%2C transcript variant X1
XM_019911879.1	NW_017852298.1	4316.7	-0.26	0.000	fasciculation and elongation protein zeta-2-like
XM_019911897.1	NW_017852299.1	4319.8	-0.57	0.000	retinol dehydrogenase 13-like
XM_019911904.1	NW_017852299.1	775.2	0.73	0.003	serine/threonine/tyrosine-interacting protein-like%2C transcript variant X1
XM_019911906.1	NW_017852299.1	1099.4	0.65	0.007	iron-sulfur cluster assembly 2 homolog%2C mitochondrial
XM_019911910.1	NW_017852300.1	305.6	0.56	0.001	cullin-1
XM_019911936.1	NW_017852300.1	4302.9	0.23	0.000	potassium/sodium hyperpolarization-activated cyclic nucleotide- gated channel 1-like%2C transcript variant X1
XM_019911950.1	NW_017852300.1	155.8	-0.54	0.003	UTP--glucose-1-phosphate uridylyltransferase%2C transcript variant X1
XM_019911961.1	NW_017852300.1	15312.1	0.47	0.003	DNA-directed RNA polymerases I and III subunit RPAC1
XM_019911975.1	NW_017852300.1	1263.0	0.33	0.007	T-complex protein 1 subunit eta pseudogene
XR_002172448.1	NW_017849571.1	4311.2	0.30	0.007	cyclin-H
XM_019911980.1	NW_017852300.1	449.0	0.52	0.000	LIM and SH3 domain protein Lasp
XM_019911985.1	NW_017852300.1	7608.2	-0.78	0.000	tRNA selenocysteine 1-associated protein 1
XM_019911986.1	NW_017852300.1	1033.4	0.23	0.008	REST corepressor-like
XM_019911990.1	NW_017849573.1	283.7	-0.85	0.001	uncharacterized protein C1orf43 homolog%2C transcript variant X1
XM_019911987.1	NW_017852300.1	345.8	0.37	0.006	REST corepressor-like
XM_019912002.1	NW_017849574.1	588.8	-0.85	0.001	probable pterin-4-alpha-carbinolamine dehydratase
XM_019912014.1	NW_017852300.1	2726.7	0.40	0.006	riboflavin kinase%2C transcript variant X1
XM_019912018.1	NW_017852300.1	2032.9	-0.56	0.010	uncharacterized LOC109542699
XM_019912033.1	NW_017852300.1	8850.6	0.40	0.007	

XM_019912044.1	NW_017852300.1	1278.2	0.52	0.000	protein will die slowly
XM_019912052.1	NW_017849592.1	279.8	0.38	0.007	uncharacterized LOC109542713
XM_019912059.1	NW_017852300.1	1380.8	0.73	0.000	flap endonuclease 1
XM_019912062.1	NW_017849592.1	2024.4	0.35	0.000	periodic tryptophan protein 1 homolog
XM_019912086.1	NW_017852301.1	17.5	-1.66	0.000	uncharacterized LOC109542737%2C transcript variant X1
XM_019912109.1	NW_017852301.1	1161.3	0.63	0.000	pre-rRNA-processing protein ESF2-like
XM_019912147.1	NW_017852302.1	558.7	1.78	0.000	nuclear receptor subfamily 2 group E member 1
XM_019912148.1	NW_017852302.1	261.3	-0.63	0.003	protein unc-13 homolog C
XM_019912155.1	NW_017852302.1	565.1	0.96	0.000	serine/threonine-protein kinase mos
XM_019912158.1	NW_017852302.1	1241.6	0.50	0.001	modifier of mdg4-like%2C transcript variant X1
XM_019912170.1	NW_017849621.1	909.5	0.36	0.006	putative E3 ubiquitin-protein ligase UBR7
XM_019912174.1	NW_017852302.1	2032.2	2.90	0.000	kynurenine formamidase-like
XM_019912184.1	NW_017852302.1	6062.2	-0.44	0.001	cytoplasmic dynein 1 intermediate chain%2C transcript variant X1
XM_019912205.1	NW_017852302.1	6627.8	-0.48	0.002	formin-binding protein 1-like%2C transcript variant X1 cytochrome c oxidase assembly protein COX15 homolog%2C transcript variant X1
XM_019912227.1	NW_017852302.1	674.4	0.51	0.004	protein spindle-F%2C transcript variant X1
XM_019912230.1	NW_017852302.1	1231.3	-0.54	0.000	uncharacterized LOC109542828
XM_019912238.1	NW_017852302.1	5955.4	-0.56	0.004	protein Malvolio-like
XM_019912274.1	NW_017852302.1	5592.2	-0.95	0.007	beta-1%2C4-glucuronyltransferase 1%2C transcript variant X1
XM_019912275.1	NW_017852302.1	395.4	-1.38	0.000	spore wall protein 2-like
XM_019912285.1	NW_017852302.1	189.1	-1.43	0.001	insulin-like growth factor 1 receptor
XM_019912320.1	NW_017849639.1	289.1	0.96	0.000	receptor-type tyrosine-protein phosphatase gamma
XM_019912321.1	NW_017852302.1	9178.7	-0.66	0.000	protein prenyltransferase alpha subunit repeat-containing protein 1
XM_019912325.1	NW_017852302.1	1834.7	0.62	0.001	synaptic vesicle glycoprotein 2B-like
XM_019912327.1	NW_017852302.1	2138.9	1.07	0.007	glutaredoxin-3
XM_019912330.1	NW_017852302.1	1829.9	0.47	0.000	integrator complex subunit 10
XM_019912339.1	NW_017852302.1	617.4	0.39	0.009	uncharacterized LOC109542887
XR_002172463.1	NW_017852302.1	73.1	-1.14	0.000	protein NRDE2 homolog
XM_019912344.1	NW_017852302.1	651.2	-0.43	0.000	uncharacterized LOC109542891
XR_002172464.1	NW_017852302.1	52.1	-1.20	0.003	GPI mannosyltransferase 3
XM_019912349.1	NW_017852302.1	2217.0	0.93	0.000	ADP-ribosylation factor-like protein 6-interacting protein 4
XM_019912353.1	NW_017852302.1	504.3	0.77	0.000	uncharacterized LOC109542898%2C transcript variant X1
XM_019912354.1	NW_017852302.1	2551.3	0.86	0.000	U7 snRNA-associated Sm-like protein LSm11
XM_019912358.1	NW_017852302.1	409.1	0.84	0.000	protein artichoke-like
XM_019912359.1	NW_017852302.1	94.1	0.98	0.007	uncharacterized LOC109542907
XR_002172465.1	NW_017852302.1	119.1	-0.89	0.000	

XM_019912366.1	NW_017852302.1	3573.5	0.89	0.002	uncharacterized LOC109542908
XM_019912369.1	NW_017852304.1	5641.3	-0.58	0.000	apoptosis-resistant E3 ubiquitin protein ligase 1%2C transcript variant X1
XM_019912385.1	NW_017852305.1	3.6	-1.33	0.004	uncharacterized LOC109542925
XM_019912391.1	NW_017852305.1	89.1	-1.44	0.000	T-box transcription factor TBX3-like
XM_019912397.1	NW_017849649.1	257.7	0.57	0.009	uncharacterized LOC109542933
XM_019912400.1	NW_017852305.1	1364.2	1.04	0.000	high mobility group protein HMGI-C
XM_019912404.1	NW_017852305.1	1565.3	0.26	0.002	ubiquitin carboxyl-terminal hydrolase FAM188A homolog%2C transcript variant X1
XM_019912407.1	NW_017852305.1	1861.0	0.58	0.002	UBA-like domain-containing protein 2
XM_019912411.1	NW_017852305.1	17738.3	-0.35	0.008	clathrin heavy chain
XM_019912417.1	NW_017852305.1	2640.9	0.43	0.006	histone acetyltransferase type B catalytic subunit
XM_019912419.1	NW_017852305.1	5831.9	-1.06	0.000	probable cation-transporting ATPase 13A3
XM_019912431.1	NW_017852305.1	422.9	0.83	0.001	rac GTPase-activating protein 1%2C transcript variant X1
XM_019912433.1	NW_017852305.1	311.4	1.44	0.000	glucose dehydrogenase [FAD%2C quinone]-like
XM_019912442.1	NW_017852305.1	375.3	0.71	0.000	sex-lethal homolog%2C transcript variant X1
XM_019912447.1	NW_017852305.1	3386.8	-0.41	0.004	protein retinal degeneration B
XM_019912448.1	NW_017852305.1	4411.3	-0.54	0.000	integral membrane protein GPR155
XM_019912449.1	NW_017852305.1	2362.2	-0.31	0.005	ATP-dependent RNA helicase dbp2-like
XM_019912461.1	NW_017852305.1	8269.5	-0.52	0.002	microtubule-associated protein 1B-like
XM_019912473.1	NW_017852305.1	4573.8	0.42	0.009	NADH dehydrogenase [ubiquinone] iron-sulfur protein 8%2C mitochondrial
XM_019912509.1	NW_017852305.1	11078.1	1.46	0.001	scavenger receptor class B member 1-like%2C transcript variant X1
XM_019912511.1	NW_017852305.1	1562.8	1.47	0.000	scavenger receptor class B member 1-like%2C transcript variant X1
XM_019912520.1	NW_017852305.1	95.1	-0.51	0.007	T-box transcription factor TBX10
XM_019912530.1	NW_017852305.1	2123.7	-0.51	0.001	activating signal cointegrator 1 complex subunit 1-like
XM_019912567.1	NW_017852305.1	222025.2	-1.07	0.000	uncharacterized LOC109543047
XM_019912568.1	NW_017852305.1	2696.6	0.88	0.000	APOBEC1 complementation factor-like%2C transcript variant X1
XM_019912593.1	NW_017852308.1	664.1	0.51	0.001	uncharacterized LOC109543071
XM_019912609.1	NW_017852309.1	692.1	0.80	0.000	rho GTPase-activating protein 19
XM_019912614.1	NW_017852309.1	3666.9	-0.27	0.001	uncharacterized LOC109543087%2C transcript variant X1
XM_019912622.1	NW_017849664.1	419.1	0.42	0.001	protein arginine N-methyltransferase 3-like
XM_019912620.1	NW_017852309.1	1937.9	0.44	0.000	uncharacterized LOC109543091%2C transcript variant X1
XM_019912629.1	NW_017852310.1	1875.0	0.46	0.000	E3 ubiquitin-protein ligase TRIM33
XM_019912679.1	NW_017845697.1	10468.3	-0.45	0.008	sortilin-related receptor-like
XM_019912643.1	NW_017852311.1	491.2	0.71	0.001	collagen alpha-1(XI) chain-like
XM_019912645.1	NW_017852311.1	4727.2	-0.44	0.000	structural maintenance of chromosomes protein 3

XM_019912650.1	NW_017852311.1	2379.1	-0.42	0.001	E3 ubiquitin-protein ligase RFW2-like
XM_019912661.1	NW_017852311.1	2939.0	-0.47	0.000	peroxisomal membrane protein 11C
XM_019912666.1	NW_017852312.1	54.8	-1.35	0.001	A disintegrin and metalloproteinase with thrombospondin motifs 12-like
XM_019912672.1	NW_017852312.1	292.6	0.65	0.000	ankyrin repeat%2C SAM and basic leucine zipper domain- containing protein 1
XM_019912676.1	NW_017852312.1	1319.1	1.07	0.001	uncharacterized LOC109543129
XM_019912687.1	NW_017852312.1	7683.0	-0.63	0.001	uncharacterized LOC109543138%2C transcript variant X1
XM_019912706.1	NW_017852312.1	1636.8	0.47	0.000	ubiquitin-like protein 5
XM_019912713.1	NW_017852312.1	5388.3	1.21	0.000	uncharacterized LOC109543152
XM_019912718.1	NW_017852312.1	797.2	0.82	0.000	RE1-silencing transcription factor B-like
XM_019912719.1	NW_017852312.1	1575.0	-1.22	0.000	cell division control protein 42 homolog
XM_019912726.1	NW_017852312.1	710.8	0.82	0.000	Y+L amino acid transporter 2%2C transcript variant X1
XM_019912733.1	NW_017852312.1	445.0	0.64	0.001	poly [ADP-ribose] polymerase 14-like
XM_019912744.1	NW_017852312.1	1489.8	0.55	0.003	2-acylglycerol O-acyltransferase 1-like%2C transcript variant X1
XM_019912771.1	NW_017852312.1	3563.0	1.51	0.000	putative serine protease F56F10.1
XM_019912772.1	NW_017852312.1	2275.8	0.68	0.000	thioredoxin domain-containing protein 5 homolog
XM_019912776.1	NW_017849691.1	5003.6	-0.98	0.000	ATP-binding cassette sub-family G member 4-like
XM_019912773.1	NW_017852312.1	5027.3	1.03	0.000	mucin-2-like
XM_019912784.1	NW_017852312.1	2024.2	1.07	0.000	uncharacterized LOC109543198
XM_019912785.1	NW_017852312.1	2577.9	1.23	0.000	uncharacterized LOC109543199
XM_019912789.1	NW_017852312.1	1959.5	1.00	0.000	uncharacterized LOC109543204
XM_019912791.1	NW_017852312.1	1718.6	0.91	0.005	uncharacterized LOC109543206
XM_019912792.1	NW_017852312.1	6256.8	1.09	0.001	uncharacterized LOC109543207
XM_019912793.1	NW_017852312.1	2174.4	1.11	0.000	uncharacterized LOC109543208
XM_019912795.1	NW_017852312.1	1251.8	1.13	0.001	uncharacterized LOC109543211
XM_019912796.1	NW_017852312.1	3876.4	1.23	0.000	uncharacterized LOC109543212
XM_019912799.1	NW_017852312.1	2054.7	1.04	0.000	uncharacterized LOC109543214
XM_019912806.1	NW_017852313.1	1720.9	-0.22	0.010	dual specificity mitogen-activated protein kinase kinase 7-like%2C transcript variant X1
XM_019912824.1	NW_017852313.1	7236.7	-0.33	0.010	protein phosphatase 1 regulatory subunit 15B%2C transcript variant X1
XM_019912842.1	NW_017852313.1	4355.2	0.60	0.000	putative tricarboxylate transport protein%2C mitochondrial%2C transcript variant X1
XM_019912864.1	NW_017852313.1	8200.5	0.40	0.003	NADH dehydrogenase [ubiquinone] flavoprotein 1%2C mitochondrial
XM_019912872.1	NW_017852315.1	2897.0	0.51	0.001	calcium-transporting ATPase type 2C member 1
XM_019912873.1	NW_017852315.1	1763.6	0.35	0.002	periodic tryptophan protein 1 homolog
XM_019912874.1	NW_017852315.1	1831.3	0.42	0.000	alpha- and gamma-adaptin-binding protein p34-like

XM_019912892.1	NW_017852320.1	1778.7	-0.30	0.005	UV radiation resistance-associated gene protein%2C transcript variant X1
XM_019912897.1	NW_017852320.1	2259.6	0.28	0.004	pyruvate dehydrogenase [acetyl-transferring]-phosphatase 1%2C mitochondrial
XM_019912910.1	NW_017852320.1	596.7	0.45	0.001	mediator of RNA polymerase II transcription subunit 29
XM_019912911.1	NW_017852320.1	1613.1	0.65	0.000	uncharacterized LOC109543289%2C transcript variant X1
XM_019912927.1	NW_017849725.1	110.9	-0.85	0.003	protein ovo-like%2C transcript variant X1
XM_019912926.1	NW_017852320.1	984.0	-0.70	0.000	ataxin-1%2C transcript variant X1
XM_019912934.1	NW_017852320.1	1734.5	-0.65	0.003	BTB/POZ domain-containing protein 6-like%2C transcript variant X1
XM_019912944.1	NW_017852320.1	5370.3	-0.88	0.001	facilitated trehalose transporter Tret1-like
XM_019912962.1	NW_017852320.1	3076.0	-0.99	0.000	uncharacterized LOC109543313
XM_019912968.1	NW_017852320.1	5557.2	-0.79	0.000	transmembrane and coiled-coil domains protein 2%2C transcript variant X1
XM_019912995.1	NW_017852320.1	5608.4	0.51	0.000	mitochondrial import receptor subunit TOM20 homolog B-like
XM_019912996.1	NW_017852320.1	609.2	-1.16	0.008	organic cation transporter protein-like
XM_019913002.1	NW_017852320.1	442.1	-0.76	0.004	discoidin domain-containing receptor tyrosine kinase B-like
XR_002172485.1	NW_017849730.1	339.4	-1.16	0.000	uncharacterized LOC109543333
XM_019913023.1	NW_017849741.1	29.9	-1.29	0.002	histidine-rich glycoprotein-like
XM_019913020.1	NW_017852324.1	10365.2	1.20	0.000	uncharacterized LOC109543346
XM_019913022.1	NW_017852324.1	3487.4	-0.36	0.007	disintegrin and metalloproteinase domain-containing protein 10
XM_019913039.1	NW_017852326.1	750.0	0.70	0.000	serine/threonine-protein kinase Aurora-2-like
XM_019913050.1	NW_017852326.1	2435.2	0.50	0.000	mitochondrial inner membrane protein OXA1L%2C transcript variant X1
XM_019913058.1	NW_017852326.1	810.4	-0.94	0.000	uncharacterized LOC109543373%2C transcript variant X1
XM_019913062.1	NW_017852326.1	36.6	-1.03	0.003	cytosol aminopeptidase-like
XM_019913063.1	NW_017852327.1	37342.5	-1.36	0.000	uncharacterized LOC109543375
XM_019913066.1	NW_017852327.1	4324.0	-1.80	0.000	putative uncharacterized protein DDB_G0290989
XM_019913067.1	NW_017852327.1	21758.0	-1.18	0.000	leucine-rich repeat-containing protein 40
XM_019913069.1	NW_017852328.1	110.3	-1.22	0.002	cathepsin L-like
XM_019913072.1	NW_017852328.1	907.4	-0.72	0.000	beta-1%2C4-galactosyltransferase 1-like
XM_019913074.1	NW_017852328.1	82.1	-1.08	0.010	cathepsin L1-like
XM_019913092.1	NW_017849749.1	131.8	0.73	0.003	uncharacterized protein C19orf52-like
XM_019913090.1	NW_017852328.1	1995.0	-0.69	0.007	glutamate receptor ionotropic%2C kainate 2-like%2C transcript variant X1
XM_019913094.1	NW_017852328.1	2330.8	-1.41	0.000	protein toll-like%2C transcript variant X1
XM_019913096.1	NW_017852328.1	21.9	-1.48	0.000	tyrosine-protein kinase receptor torso
XM_019913097.1	NW_017852328.1	4195.4	0.69	0.000	double-stranded RNA-specific editase Adar%2C transcript variant X1

XM_019913102.1	NW_017852328.1	912.9	-1.11	0.000	insulin-like growth factor-binding protein complex acid labile subunit%2C transcript variant X1
XM_019913106.1	NW_017852328.1	1991.3	0.25	0.009	probable nucleoporin Nup54
XM_019913113.1	NW_017852328.1	52.0	-1.78	0.000	serine proteinase stubble
XM_019913116.1	NW_017852328.1	6045.5	-0.35	0.000	F-box only protein 28-like%2C transcript variant X1
XM_019913123.1	NW_017852328.1	11490.2	-0.91	0.000	glycerol-3-phosphate acyltransferase 4
XM_019913125.1	NW_017852328.1	1691.8	-0.73	0.000	beta-1%2C4-glucuronyltransferase 1-like
XM_019913134.1	NW_017852328.1	1269.6	-0.77	0.000	lactosylceramide 4-alpha-galactosyltransferase-like
XM_019913139.1	NW_017852328.1	640.8	0.42	0.002	metaxin-1
XM_019913145.1	NW_017852328.1	428.5	-0.40	0.005	uncharacterized LOC109543432
XM_019913153.1	NW_017852328.1	547.3	0.39	0.000	non-structural maintenance of chromosomes element 1 homolog
XM_019913157.1	NW_017852328.1	682.1	0.36	0.000	trafficking protein particle complex subunit 5
XM_019913170.1	NW_017852328.1	2482.9	0.37	0.002	mitochondrial pyruvate carrier 2-like heterogeneous nuclear ribonucleoprotein A1%2C A2/B1 homolog%2C transcript variant X1
XM_019913186.1	NW_017852328.1	3865.9	-0.39	0.002	tolloid-like protein 1
XM_019913188.1	NW_017852328.1	4397.2	-0.54	0.000	endothelin-converting enzyme 1-like
XM_019913196.1	NW_017852329.1	1897.0	0.87	0.003	peptidoglycan-recognition protein 2-like
XM_019913215.1	NW_017852329.1	784.2	0.63	0.006	fatty acid-binding protein%2C liver
XM_019913216.1	NW_017852329.1	9520.0	0.87	0.000	glucose dehydrogenase [FAD%2C quinone]-like
XM_019913228.1	NW_017852332.1	94.9	1.06	0.002	uncharacterized LOC109543498%2C transcript variant X1
XM_019913234.1	NW_017852335.1	624.6	-1.36	0.000	uncharacterized LOC109543501
XM_019913238.1	NW_017852336.1	676.5	1.00	0.001	O-acyltransferase like protein-like
XM_019913249.1	NW_017852336.1	257.8	1.09	0.003	cytochrome P450 6B1-like
XM_019913251.1	NW_017852336.1	1556.7	0.37	0.006	mitochondrial amidoxime reducing component 2-like%2C transcript variant X1
XM_019913255.1	NW_017849790.1	1518.3	0.99	0.000	epidermal growth factor receptor substrate 15-like 1%2C transcript variant X1
XM_019913260.1	NW_017852336.1	1973.0	0.30	0.002	sister chromatid cohesion protein DCC1
XM_019913266.1	NW_017852336.1	582.3	0.35	0.002	mitochondrial amidoxime reducing component 2-like%2C transcript variant X1
XM_019913271.1	NW_017849791.1	1517.9	0.99	0.000	cysteine-rich protein 2-binding protein%2C transcript variant X1
XM_019913269.1	NW_017852336.1	502.5	0.50	0.000	rho guanine nucleotide exchange factor 18%2C transcript variant X1
XM_019913278.1	NW_017852336.1	2553.8	-0.41	0.000	adhesion G-protein coupled receptor G4-like
XM_019913301.1	NW_017852336.1	446.1	-0.95	0.001	carnosine N-methyltransferase
XM_019913310.1	NW_017852336.1	417.5	0.47	0.000	tRNA (adenine(37)-N6)-methyltransferase-like%2C transcript variant X1
XM_019913311.1	NW_017852336.1	929.9	0.24	0.001	calcium and integrin-binding protein 1-like
XM_019913317.1	NW_017852336.1	1346.2	0.75	0.010	

XM_019913320.1	NW_017852336.1	1359.4	0.47	0.001	ubiquinone biosynthesis monooxygenase COQ6%2C mitochondrial%2C transcript variant X1
XR_002172507.1	NW_017852336.1	147623.4	-0.96	0.000	uncharacterized LOC109543549
XR_002172508.1	NW_017852336.1	185884.4	-0.89	0.000	uncharacterized LOC109543550
XR_002172509.1	NW_017852336.1	3390.4	-1.21	0.000	uncharacterized LOC109543551
XM_019913330.1	NW_017852336.1	1783.3	0.32	0.000	cob(II)yrinic acid a%2Cc-diamide adenosyltransferase%2C mitochondrial-like
XM_019913341.1	NW_017852336.1	8269.8	-0.59	0.003	uncharacterized LOC109543563%2C transcript variant X1
XM_019913348.1	NW_017852336.1	5035.5	0.32	0.002	protein LTV1 homolog
XM_019913349.1	NW_017852336.1	4020.9	-1.23	0.000	E3 ubiquitin-protein ligase MYLIP vacuolar protein sorting-associated protein 18 homolog%2C transcript variant X1
XM_019913359.1	NW_017849803.1	2670.6	-0.42	0.000	protein nessun dorma-like
XM_019913366.1	NW_017852336.1	685.1	0.90	0.000	protein nessun dorma-like
XM_019913368.1	NW_017852336.1	319.9	0.65	0.003	uncharacterized LOC109543585
XM_019913377.1	NW_017852336.1	1155.1	0.93	0.001	uncharacterized LOC109543588
XM_019913381.1	NW_017852336.1	2396.2	0.80	0.005	farnesyl pyrophosphate synthase%2C transcript variant X1
XM_019913385.1	NW_017852336.1	16032.2	0.88	0.000	UPF0415 protein C7orf25 homolog
XM_019913404.1	NW_017849817.1	816.0	0.38	0.002	protein CASC3
XM_019913402.1	NW_017852336.1	2372.7	-0.48	0.004	pre-mRNA-splicing factor SPF27
XM_019913419.1	NW_017852337.1	485.9	0.52	0.000	small nuclear ribonucleoprotein F tRNA (adenine(58)-N(1))-methyltransferase catalytic subunit TRMT61A-like
XM_019913421.1	NW_017852337.1	1266.0	0.48	0.001	uncharacterized LOC109543619
XM_019913429.1	NW_017849817.1	329.3	0.61	0.000	beta-1%2C3-galactosyltransferase brn
XM_019913430.1	NW_017852337.1	1160.5	0.80	0.004	uncharacterized LOC109543622
XM_019913432.1	NW_017852337.1	512.8	0.46	0.002	putative glutamate synthase [NADPH]%2C transcript variant X1
XM_019913433.1	NW_017852337.1	317.2	0.64	0.000	transforming growth factor-beta-induced protein ig-h3
XM_019913435.1	NW_017852337.1	9976.4	-0.51	0.001	uncharacterized LOC109543630
XM_019913437.1	NW_017852337.1	13828.3	-0.78	0.001	dual specificity tyrosine-phosphorylation-regulated kinase 4%2C transcript variant X1
XM_019913443.1	NW_017852337.1	3720.0	-0.61	0.002	decaprenyl-diphosphate synthase subunit 2-like%2C transcript variant X1
XM_019913451.1	NW_017852337.1	960.7	-1.41	0.000	ATP-binding cassette sub-family B member 7%2C mitochondrial
XM_019913469.1	NW_017852337.1	431.6	0.77	0.001	LYR motif-containing protein 2
XM_019913472.1	NW_017852337.1	5074.6	-0.57	0.000	uncharacterized LOC109543677
XM_019913492.1	NW_017852338.1	316.6	0.62	0.002	cilia- and flagella-associated protein 44
XR_002172513.1	NW_017852338.1	498.2	-1.13	0.001	AF4/FMR2 family member 4
XM_019913510.1	NW_017852339.1	184.2	-0.95	0.000	NEDD8 ultimate buster 1-like
XM_019913514.1	NW_017852339.1	2603.9	-0.57	0.000	
XM_019913521.1	NW_017852339.1	2341.0	-0.48	0.000	

XM_019913522.1	NW_017852339.1	1910.4	-0.69	0.001	beta-1%2C4-mannosyltransferase egh-like
XM_019913523.1	NW_017852339.1	3717.2	-0.71	0.001	beta-1%2C4-mannosyltransferase egh-like
XM_019913524.1	NW_017852339.1	3263.2	0.42	0.006	proteasome inhibitor PI31 subunit-like%2C transcript variant X1
XM_019913526.1	NW_017852339.1	374.1	0.54	0.000	mitochondrial inner membrane protease subunit 1-like
XR_002172514.1	NW_017852339.1	29.3	-0.93	0.003	uncharacterized LOC109543705 SH3 domain-containing RING finger protein 3%2C transcript variant X1
XM_019913529.1	NW_017852339.1	2473.1	-0.25	0.003	
XM_019913538.1	NW_017852339.1	919.8	-0.60	0.001	RNA-binding protein 33-like%2C transcript variant X1
XM_019913546.1	NW_017852339.1	979.9	-1.24	0.000	G-protein coupled receptor moody-like
XM_019913583.1	NW_017849874.1	201.9	-0.43	0.004	rho GTPase-activating protein 42-like
XM_019913589.1	NW_017852340.1	4193.7	0.68	0.004	phosphoglycerate kinase
XM_019913608.1	NW_017852340.1	7944.2	1.37	0.002	D-arabinitol dehydrogenase 1-like mediator of RNA polymerase II transcription subunit 31%2C transcript variant X1
XM_019913619.1	NW_017852340.1	1035.5	-0.44	0.003	
XM_019913634.1	NW_017852340.1	1859.8	0.60	0.000	histone-lysine N-methyltransferase pr-set7
XM_019913639.1	NW_017852340.1	568.5	0.44	0.006	uncharacterized LOC109543774
XM_019913651.1	NW_017849902.1	24989.2	0.30	0.007	60S ribosomal protein L5-like electron transfer flavoprotein-ubiquinone oxidoreductase%2C mitochondrial
XM_019913655.1	NW_017852341.1	29688.9	-0.79	0.006	
XM_019913663.1	NW_017852342.1	918.8	0.44	0.005	uncharacterized LOC109543795%2C transcript variant X1
XR_002172528.1	NW_017852342.1	384.1	0.82	0.000	uncharacterized LOC109543804
XM_019913675.1	NW_017852342.1	1641.6	-0.49	0.009	phosphofurin acidic cluster sorting protein 1
XM_019913676.1	NW_017852342.1	796.5	0.53	0.000	BRCA1-associated RING domain protein 1-like
XM_019913680.1	NW_017852342.1	643.2	0.63	0.000	exosome complex component RRP46
XM_019913696.1	NW_017852342.1	2745.3	0.43	0.002	protein lin-52 homolog polycomb group protein FERTILIZATION-INDEPENDENT SEED 2-like%2C transcript variant X1
XM_019913745.1	NW_017852342.1	3008.2	0.49	0.000	
XM_019913757.1	NW_017852342.1	1068.4	0.46	0.002	kelch-like protein 30%2C transcript variant X1
XM_019913763.1	NW_017852342.1	243.8	2.07	0.000	proton-coupled folate transporter-like
XM_019913768.1	NW_017852342.1	599.9	0.38	0.002	uncharacterized LOC109543853%2C transcript variant X1
XM_019913776.1	NW_017852342.1	158.6	1.15	0.000	Werner Syndrome-like exonuclease
XM_019913783.1	NW_017852342.1	515.4	0.83	0.001	POC1 centriolar protein homolog A-like
XM_019913784.1	NW_017852343.1	5766.3	-0.47	0.001	nuclear receptor coactivator 2%2C transcript variant X1
XM_019913812.1	NW_017849935.1	2029.4	-0.61	0.004	uncharacterized LOC109543883
XM_019913823.1	NW_017849936.1	2030.5	-0.61	0.004	uncharacterized LOC109543893
XM_019913826.1	NW_017852346.1	524.3	0.38	0.006	pre-mRNA-splicing factor 18-like
XM_019913837.1	NW_017852348.1	572.0	-0.68	0.000	tubby-related protein 4
XM_019913853.1	NW_017852348.1	2619.9	0.99	0.000	polyadenylate-binding protein 4-like%2C transcript variant X1

XM_019913860.1	NW_017852348.1	922.0	0.46	0.000	uncharacterized LOC109543925
XM_019913862.1	NW_017852348.1	1353.5	0.46	0.000	protein Star%2C transcript variant X1
XM_019913867.1	NW_017852348.1	1463.7	0.29	0.001	probable U3 small nucleolar RNA-associated protein 11
XM_019913878.1	NW_017852348.1	3060.5	-0.36	0.000	protein TAPT1 homolog%2C transcript variant X1
XM_019913887.1	NW_017852348.1	269.3	-1.01	0.001	uncharacterized LOC109543944
XM_019913888.1	NW_017852348.1	77.1	1.42	0.000	probable histone-lysine N-methyltransferase set-23
XM_019913890.1	NW_017852348.1	4095.7	-0.33	0.000	insulin-degrading enzyme stress-activated map kinase-interacting protein 1%2C transcript variant X1
XM_019913894.1	NW_017852348.1	1610.6	-0.66	0.000	
XM_019913909.1	NW_017852348.1	97.2	-0.77	0.001	phosphatase and actin regulator 4-B%2C transcript variant X1
XM_019913911.1	NW_017852348.1	6010.8	0.69	0.000	phosphoserine phosphatase
XM_019913912.1	NW_017852348.1	2507.7	-0.87	0.000	histone deacetylase complex subunit SAP18
XM_019913933.1	NW_017852348.1	1186.4	0.44	0.000	NEDD8-activating enzyme E1 catalytic subunit
XM_019913945.1	NW_017852348.1	133.3	-1.22	0.003	uncharacterized LOC109543982
XM_019913946.1	NW_017852349.1	8408.1	1.53	0.000	probable methylmalonate-semialdehyde dehydrogenase [acylating]%2C mitochondrial%2C transcript variant X1
XM_019913958.1	NW_017852350.1	3586.3	-0.35	0.008	transcription-associated protein 1%2C transcript variant X1
XM_019914004.1	NW_017852350.1	413.3	0.41	0.006	zinc finger protein OZF-like
XM_019914026.1	NW_017852350.1	10743.3	0.86	0.000	uncharacterized LOC109544033%2C transcript variant X1 putative inorganic phosphate cotransporter%2C transcript variant X1
XM_019914030.1	NW_017852350.1	5021.8	-0.59	0.000	
XM_019914046.1	NW_017852350.1	621.5	0.66	0.000	nitrogen permease regulator 3-like protein
XM_019914091.1	NW_017845758.1	37863.5	-1.50	0.000	ATP-binding cassette sub-family G member 4-like
XM_019914057.1	NW_017852350.1	1226.6	0.93	0.000	cyclin-dependent kinase 1
XM_019914080.1	NW_017852350.1	514.6	0.71	0.008	DNA replication factor Cdt1-like tRNA (adenine(58)-N(1))-methyltransferase non-catalytic subunit TRM6
XM_019914088.1	NW_017852350.1	363.2	0.63	0.000	
XM_019914093.1	NW_017852350.1	751.0	0.60	0.000	WW domain-containing oxidoreductase
XM_019914118.1	NW_017852350.1	768.1	1.67	0.000	rutC family protein UK114
XM_019914124.1	NW_017852350.1	1861.9	0.39	0.001	probable prefoldin subunit 4
XM_019914138.1	NW_017852350.1	846.8	0.48	0.000	nuclear pore complex protein Nup88
XM_019914153.1	NW_017852351.1	2076.4	-0.36	0.002	uncharacterized LOC109544113%2C transcript variant X1
XM_019914159.1	NW_017852352.1	2180.9	0.73	0.006	uncharacterized LOC109544118
XM_019914160.1	NW_017852352.1	720.2	-0.59	0.001	protein lap4-like
XM_019914164.1	NW_017852353.1	2189.5	-0.40	0.000	male-specific lethal 1 homolog ubiquinone biosynthesis O-methyltransferase%2C mitochondrial%2C transcript variant X1
XM_019914168.1	NW_017852353.1	572.2	0.69	0.000	
XM_019914172.1	NW_017852353.1	3554.1	-0.35	0.000	prefoldin subunit 2

XM_019914175.1	NW_017852353.1	29.1	-0.82	0.007	sal-like protein 4
XM_019914180.1	NW_017850005.1	156.8	1.08	0.005	uncharacterized LOC109544136
XM_019914181.1	NW_017852355.1	2108.2	0.92	0.003	5-oxoprolinase
XM_019914185.1	NW_017852355.1	3542.7	-0.48	0.008	transmembrane protein 245%2C transcript variant X1
XM_019914201.1	NW_017852355.1	337.5	0.53	0.001	DNA polymerase epsilon subunit 2
XM_019914202.1	NW_017852355.1	182.7	-1.00	0.003	tubulin beta chain-like dual specificity protein phosphatase CDC14B-like%2C transcript variant X1
XM_019914203.1	NW_017852355.1	281.2	-1.03	0.002	
XM_019914207.1	NW_017852355.1	19610.0	1.36	0.000	probable cytochrome P450 6a13 microtubule-associated protein RP/EB family member 1%2C transcript variant X1
XM_019914221.1	NW_017852355.1	6992.6	0.50	0.000	
XM_019914230.1	NW_017852355.1	299.1	1.32	0.000	uncharacterized LOC109544171%2C transcript variant X1
XM_019914234.1	NW_017852355.1	9803.1	-0.29	0.006	eukaryotic translation initiation factor 3 subunit J
XM_019914243.1	NW_017850018.1	532.1	0.46	0.005	CMP-sialic acid transporter 1-like
XM_019914242.1	NW_017852355.1	13535.0	1.01	0.001	esterase B1-like
XM_019914249.1	NW_017852355.1	819.5	0.90	0.001	m-AAA protease-interacting protein 1%2C mitochondrial
XM_019914262.1	NW_017852355.1	667.7	0.64	0.000	DNA replication licensing factor Mcm5
XM_019914275.1	NW_017850019.1	562.9	0.47	0.003	CMP-sialic acid transporter 1-like
XM_019914279.1	NW_017852358.1	1970.1	-0.99	0.000	uncharacterized LOC109544210
XM_019914280.1	NW_017852358.1	348.6	0.90	0.009	uncharacterized LOC109544211
XM_019914288.1	NW_017852358.1	917.2	-0.84	0.003	glucose dehydrogenase [FAD%2C quinone]-like
XM_019914295.1	NW_017852358.1	997.9	0.34	0.005	uncharacterized LOC109544226
XM_019914296.1	NW_017852358.1	2588.1	0.79	0.000	flotillin-2%2C transcript variant X1 serine/threonine-protein phosphatase 4 catalytic subunit%2C transcript variant X1
XM_019914303.1	NW_017852358.1	3353.7	0.14	0.008	
XR_002172552.1	NW_017852358.1	38.6	1.23	0.001	uncharacterized LOC109544233%2C transcript variant X1
XM_019914314.1	NW_017852358.1	304.1	1.15	0.000	NAD-dependent protein deacylase Sirt4 serine/threonine-protein phosphatase Pgam5%2C mitochondrial-like%2C transcript variant X1
XM_019914315.1	NW_017852358.1	1746.9	0.42	0.001	
XM_019914321.1	NW_017850023.1	4040.5	-0.31	0.001	putative U5 small nuclear ribonucleoprotein 200 kDa helicase
XM_019914336.1	NW_017852358.1	4332.1	-0.49	0.004	ceramide synthase 6
XM_019914337.1	NW_017852358.1	727.4	0.41	0.006	mediator of RNA polymerase II transcription subunit 30
XM_019914340.1	NW_017852358.1	2827.1	0.52	0.007	ecto-NOX disulfide-thiol exchanger 2
XM_019914342.1	NW_017852358.1	473.2	-0.37	0.000	uncharacterized LOC109544253 mitochondrial import inner membrane translocase subunit TIM16-like
XM_019914351.1	NW_017852358.1	777.0	0.45	0.005	
XM_019914353.1	NW_017852358.1	445.5	0.54	0.000	diphthamide biosynthesis protein 1%2C transcript variant X1
XM_019914356.1	NW_017852358.1	2415.0	0.34	0.000	regulation of nuclear pre-mRNA domain-containing protein 1B

XM_019914360.1	NW_017852358.1	389.6	0.60	0.000	ankyrin repeat domain-containing protein 49-like%2C transcript variant X1
XM_019914363.1	NW_017852358.1	1213.7	0.46	0.004	uncharacterized LOC109544270%2C transcript variant X1
XM_019914375.1	NW_017852358.1	555.3	1.17	0.006	glucose dehydrogenase [FAD%2C quinone]-like
XM_019914383.1	NW_017852358.1	165.8	0.89	0.001	mannose-binding protein C
XM_019914389.1	NW_017852359.1	463.5	0.69	0.000	uncharacterized protein C19orf52-like
XM_019914406.1	NW_017852359.1	4146.8	0.28	0.004	chromatin assembly factor 1 subunit A-like%2C transcript variant X1
XR_002172561.1	NW_017852359.1	1920.6	0.59	0.000	uncharacterized LOC109544319
XM_019914434.1	NW_017852360.1	2785.4	-0.22	0.008	guanine nucleotide-binding protein G(s) subunit alpha%2C transcript variant X1
XM_019914441.1	NW_017852360.1	18329.8	-1.76	0.000	dystroglycan%2C transcript variant X1
XM_019914459.1	NW_017852362.1	1434.5	-0.60	0.000	homeodomain-interacting protein kinase 2-like%2C transcript variant X1
XM_019914463.1	NW_017850048.1	1960.1	0.41	0.003	glucosamine-6-phosphate isomerase-like%2C transcript variant X1
XR_002172564.1	NW_017852362.1	362.0	-0.57	0.000	uncharacterized LOC109544346
XM_019914468.1	NW_017852363.1	614.2	0.71	0.003	myelin transcription factor 1
XM_019914486.1	NW_017852363.1	655.8	1.15	0.000	protein abnormal spindle-like%2C transcript variant X1
XM_019914495.1	NW_017850060.1	1345.5	0.97	0.000	anaphase-promoting complex subunit 4-like
XM_019914500.1	NW_017852363.1	9305.6	1.33	0.001	glucose 1%2C6-bisphosphate synthase%2C transcript variant X1
XM_019914505.1	NW_017852363.1	451.0	0.45	0.008	ribonuclease P/MRP protein subunit POP5%2C transcript variant X1
XM_019914507.1	NW_017852363.1	9523.3	-0.35	0.000	armadillo segment polarity protein%2C transcript variant X1
XM_019914524.1	NW_017852363.1	476.6	0.73	0.000	peptidyl-prolyl cis-trans isomerase H
XM_019914527.1	NW_017852363.1	1579.3	-0.79	0.000	zinc finger protein 33A-like
XM_019914552.1	NW_017852366.1	2775.1	-0.58	0.001	matrix metalloproteinase-2-like
XM_019914558.1	NW_017852366.1	7108.3	-0.37	0.005	protein split ends%2C transcript variant X1
XR_002172582.1	NW_017852366.1	13.1	1.65	0.000	uncharacterized LOC109544438
XM_019914620.1	NW_017852366.1	2373.0	0.91	0.000	cytochrome b5-related protein
XR_002172584.1	NW_017852366.1	1742.8	0.86	0.002	uncharacterized LOC109544447
XM_019914649.1	NW_017850082.1	1597.1	0.40	0.000	prefoldin subunit 3-like
XM_019914654.1	NW_017852366.1	1595.5	0.31	0.005	protein-associating with the carboxyl-terminal domain of ezrin
XM_019914659.1	NW_017852366.1	7071.9	-0.57	0.000	autism susceptibility gene 2 protein-like%2C transcript variant X1
XM_019914667.1	NW_017852366.1	304.0	0.91	0.001	uncharacterized LOC109544472
XM_019914674.1	NW_017852366.1	8392.4	-0.72	0.000	protein alan shepard%2C transcript variant X1
XM_019914688.1	NW_017852366.1	4572.9	0.42	0.009	WD repeat domain phosphoinositide-interacting protein 2-like%2C transcript variant X1
XM_019914694.1	NW_017852366.1	14785.8	-0.72	0.000	Niemann-Pick C1 protein%2C transcript variant X1
XM_019914701.1	NW_017852366.1	39.2	1.35	0.001	titin-like

XM_019914706.1	NW_017850091.1	5534.3	0.28	0.000	secretion-regulating guanine nucleotide exchange factor-like
XM_019914731.1	NW_017852366.1	783.5	0.54	0.001	gastrula zinc finger protein XICGF49.1-like
XM_019914735.1	NW_017852366.1	3909.5	-0.64	0.009	integrin alpha-PS1-like%2C transcript variant X1 TATA-binding protein-associated factor 172%2C transcript variant X1
XM_019914739.1	NW_017852366.1	2772.6	-0.75	0.000	
XM_019914757.1	NW_017852366.1	3403.0	0.75	0.001	atypical protein kinase C-like
XM_019914763.1	NW_017852366.1	2485.2	0.58	0.000	ribosomal L1 domain-containing protein 1-like
XM_019914774.1	NW_017852366.1	2687.3	0.33	0.002	thioredoxin domain-containing protein 9
XM_019914784.1	NW_017850103.1	1071.1	-0.34	0.005	UPF0536 protein C12orf66 homolog
XR_002172594.1	NW_017852366.1	90.0	-1.22	0.006	uncharacterized LOC109544536
XM_019914804.1	NW_017852366.1	1491.0	-1.10	0.000	serine protease persephone-like
XM_019914808.1	NW_017852366.1	2171.4	0.53	0.003	rho GTPase-activating protein 20-like%2C transcript variant X1
XM_019914814.1	NW_017852366.1	1015.2	0.68	0.000	protein wntless
XM_019914816.1	NW_017852366.1	78.2	1.17	0.000	golgin subfamily A member 6-like protein 22
XM_019914827.1	NW_017852366.1	6751.1	-0.70	0.000	leucine-rich repeat extensin-like protein 3
XM_019914851.1	NW_017852366.1	3668.6	-0.21	0.001	splicing factor U2AF 50 kDa subunit
XM_019914856.1	NW_017852366.1	959.4	0.39	0.000	U3 small nucleolar RNA-associated protein 15 homolog
XM_019914857.1	NW_017852366.1	1135.0	0.53	0.001	1-acyl-sn-glycerol-3-phosphate acyltransferase alpha zinc finger HIT domain-containing protein 3%2C transcript variant X1
XM_019914879.1	NW_017852366.1	2173.4	0.39	0.007	
XM_019914910.1	NW_017850143.1	197.2	-1.51	0.000	uncharacterized LOC109544609 eukaryotic translation initiation factor 3 subunit D%2C transcript variant X1
XM_019914913.1	NW_017852366.1	6525.0	0.56	0.000	
XM_019914915.1	NW_017852366.1	3648.0	0.63	0.004	nuclear autoantigenic sperm protein%2C transcript variant X1 evolutionarily conserved signaling intermediate in Toll pathway%2C mitochondrial-like
XM_019914919.1	NW_017852366.1	1598.9	0.37	0.003	
XM_019914923.1	NW_017852366.1	439.1	0.64	0.000	cytosolic endo-beta-N-acetylglucosaminidase
XM_019914934.1	NW_017852366.1	1498.5	0.23	0.003	protein transport protein SFT2
XM_019914945.1	NW_017850165.1	2629.1	-0.94	0.000	ATP-binding cassette sub-family G member 4-like
XM_019914944.1	NW_017852366.1	10188.8	-0.53	0.000	glutaredoxin-C4-like%2C transcript variant X1
XM_019914948.1	NW_017852366.1	37.3	0.83	0.006	uncharacterized LOC109544638
XM_019914949.1	NW_017852366.1	325.4	0.87	0.000	voltage-dependent T-type calcium channel subunit alpha-1G-like
XM_019914951.1	NW_017852366.1	25.0	-1.29	0.008	pancreatic triacylglycerol lipase
XM_019914953.1	NW_017852366.1	42.4	-0.85	0.004	uncharacterized LOC109544644
XM_019914955.1	NW_017852366.1	1960.9	0.54	0.000	transcription factor A%2C mitochondrial-like
XM_019914959.1	NW_017852366.1	6401.6	-0.65	0.000	glucose-induced degradation protein 4 homolog
XM_019914980.1	NW_017852366.1	1083.7	0.45	0.000	GTPase Era%2C mitochondrial
XM_019914985.1	NW_017852366.1	1294.9	0.46	0.002	probable trans-2-enoyl-CoA reductase%2C mitochondrial

XM_019914997.1	NW_017852366.1	381.2	0.95	0.005	amyloid protein-binding protein 2
XM_019915004.1	NW_017852366.1	337.8	1.80	0.000	sulfotransferase 1C4%2C transcript variant X1
XM_019915008.1	NW_017852366.1	966.6	0.49	0.000	U6 snRNA-associated Sm-like protein LSm3
XM_019915010.1	NW_017852366.1	207.0	0.73	0.001	DNA polymerase delta small subunit
XM_019915022.1	NW_017852366.1	19.3	-1.15	0.006	coiled-coil domain-containing protein 96-like
XM_019915035.1	NW_017852368.1	779.8	0.38	0.000	coiled-coil domain-containing protein 134-like
XM_019915047.1	NW_017852368.1	460.7	0.71	0.000	origin recognition complex subunit 3
XM_019915048.1	NW_017852368.1	1093.2	0.28	0.008	beta-catenin-like protein 1
XM_019915053.1	NW_017852368.1	11271.8	2.28	0.000	group XV phospholipase A2-like
XM_019915062.1	NW_017852369.1	1313.7	-0.46	0.000	tyrosine-protein kinase Abl-like
XM_019915063.1	NW_017852369.1	2795.4	-0.62	0.000	protein Shroom
XM_019915070.1	NW_017852369.1	10467.3	0.45	0.000	clustered mitochondria protein homolog%2C transcript variant X1
XM_019915072.1	NW_017852369.1	6711.5	0.65	0.000	ATP-dependent RNA helicase DHX36-like%2C transcript variant X1
XM_019915078.1	NW_017852369.1	1383.7	0.36	0.000	tRNA dimethylallyltransferase%2C mitochondrial
XR_002172607.1	NW_017852369.1	348.8	0.56	0.005	uncharacterized LOC109544769%2C transcript variant X1
XM_019915105.1	NW_017852369.1	971.8	-1.28	0.000	caspace-1-like
XM_019915116.1	NW_017852369.1	1043.3	0.48	0.001	uncharacterized protein C16orf52 homolog A
XM_019915117.1	NW_017852369.1	2648.7	0.53	0.004	NHP2-like protein 1 homolog
XR_002172610.1	NW_017845819.1	674.2	0.42	0.002	THAP domain-containing protein 4-like%2C transcript variant X1
XM_019915146.1	NW_017852369.1	3810.7	-0.37	0.009	calpain-A-like%2C transcript variant X1
XR_002172609.1	NW_017850202.1	71.6	-1.35	0.000	uncharacterized LOC109544800
XM_019915159.1	NW_017852369.1	515.6	0.58	0.008	uncharacterized LOC109544807
XM_019915162.1	NW_017852369.1	5489.9	-0.25	0.001	poly(A) polymerase type 3
XM_019915172.1	NW_017852369.1	5816.6	-0.65	0.003	uncharacterized LOC109544820%2C transcript variant X1
XM_019915178.1	NW_017852369.1	1296.2	0.75	0.000	nardilysin-like%2C transcript variant X1
XM_019915181.1	NW_017852369.1	543.5	0.57	0.000	CWF19-like protein 2 homolog
XM_019915183.1	NW_017852369.1	1223.1	0.76	0.002	uncharacterized LOC109544827%2C transcript variant X1
XM_019915193.1	NW_017852369.1	4475.4	-0.66	0.001	uncharacterized LOC109544832%2C transcript variant X1
XM_019915197.1	NW_017852369.1	1474.6	0.52	0.005	serine/threonine-protein kinase VRK1-like
XM_019915204.1	NW_017850216.1	1632.4	-0.36	0.000	regulator complex protein LAMTOR1
XM_019915203.1	NW_017852369.1	9169.5	-0.49	0.005	uncharacterized LOC109544838%2C transcript variant X1
XM_019915210.1	NW_017852369.1	2469.4	0.47	0.000	uncharacterized LOC109544841
XM_019915211.1	NW_017852369.1	214.8	0.81	0.000	zinc transporter ZIP3-like%2C transcript variant X1
XM_019915221.1	NW_017852369.1	3853.5	-0.71	0.000	protein enabled%2C transcript variant X1
XM_019915242.1	NW_017852369.1	486.4	0.62	0.001	uncharacterized LOC109544861%2C transcript variant X1
XM_019915244.1	NW_017852369.1	3672.4	-0.57	0.006	band 7 protein AGAP004871-like%2C transcript variant X1

XM_019915250.1	NW_017852369.1	3717.4	0.59	0.000	monoacylglycerol lipase ABHD12-like%2C transcript variant X1
XM_019915278.1	NW_017850235.1	587.3	1.02	0.000	uncharacterized LOC109544872
XM_019915275.1	NW_017852369.1	312.8	0.79	0.007	paired box protein Pax-8%2C transcript variant X1
XM_019915286.1	NW_017852369.1	3182.3	1.85	0.000	sphingomyelin phosphodiesterase-like%2C transcript variant X1
XM_019915326.1	NW_017845823.1	859.9	0.42	0.000	cleavage stimulation factor subunit 2-like
NW_017850235.1_1947-2566	NW_017850235.1	299.5	0.97	0.000	#N/A
XM_019915292.1	NW_017852369.1	4747.4	-1.00	0.002	L-lactate dehydrogenase-like%2C transcript variant X1
XM_019915295.1	NW_017852369.1	15717.1	-0.66	0.000	translocon-associated protein subunit alpha
XM_019915316.1	NW_017852369.1	236.3	-0.49	0.002	dendritic arbor reduction protein 1-like%2C transcript variant X1
XM_019915318.1	NW_017852369.1	586.1	0.63	0.004	otoferlin-like
XR_002172619.1	NW_017852369.1	1990.8	-0.71	0.000	uncharacterized LOC109544905%2C transcript variant X1
XM_019915334.1	NW_017852369.1	17.7	-0.96	0.008	uncharacterized LOC109544910%2C transcript variant X1
XM_019915338.1	NW_017850244.1	1715.0	-1.40	0.002	esterase FE4-like
XM_019915339.1	NW_017852369.1	558.2	1.01	0.000	maternal embryonic leucine zipper kinase-like
XM_019915346.1	NW_017852369.1	45.8	-1.25	0.002	L-lactate dehydrogenase B chain-like
XM_019915353.1	NW_017852370.1	1519.1	0.60	0.003	uncharacterized LOC109544931%2C transcript variant X1
XR_002172622.1	NW_017850246.1	370.5	-0.85	0.000	uncharacterized LOC109544932
XM_019915359.1	NW_017852370.1	1299.3	1.11	0.000	serine/threonine-protein kinase SIK2-like%2C transcript variant X1
XM_019915367.1	NW_017852371.1	1716.3	1.01	0.000	nucleoprotein TPR-like
XM_019915368.1	NW_017852371.1	12063.6	-0.38	0.004	transmembrane protease serine 9-like
XM_019915381.1	NW_017852371.1	4185.9	0.82	0.000	protein regulator of cytokinesis 1-like%2C transcript variant X1
XM_019915387.1	NW_017852371.1	1048.4	0.33	0.001	transcription initiation factor TFIIID subunit 8-like
XM_019915396.1	NW_017852371.1	3186.9	0.57	0.000	serine-arginine protein 55-like
XM_019915397.1	NW_017852371.1	1594.4	0.47	0.000	intron-binding protein aquarius%2C transcript variant X1
XM_019915446.1	NW_017845826.1	654.7	0.82	0.000	uncharacterized LOC109544968
XM_019915405.1	NW_017852371.1	1329.4	0.40	0.000	protein SDE2 homolog
XM_019915406.1	NW_017852371.1	7735.1	-0.47	0.002	autophagy-related protein 2 homolog B
XM_019915408.1	NW_017852371.1	2377.9	0.45	0.000	tryptophan--tRNA ligase%2C cytoplasmic
XM_019915409.1	NW_017852371.1	1098.3	0.38	0.002	m7GpppN-mRNA hydrolase
XM_019915411.1	NW_017852371.1	773.4	0.56	0.001	zinc finger protein 16-like
XM_019915413.1	NW_017852371.1	8533.8	-0.52	0.001	microsomal glutathione S-transferase 1-like
XM_019915414.1	NW_017852371.1	2724.2	-0.32	0.000	protein daughterless%2C transcript variant X1
XM_019915442.1	NW_017852371.1	2078.0	0.35	0.006	uncharacterized LOC109544988%2C transcript variant X1
XM_019915451.1	NW_017852371.1	3229.9	1.03	0.000	G2/mitotic-specific cyclin-B
XM_019915471.1	NW_017852371.1	1485.7	0.43	0.000	integrator complex subunit 9
XM_019915481.1	NW_017852371.1	5655.5	-0.36	0.000	transmembrane emp24 domain-containing protein bai

XM_019915491.1	NW_017852371.1	611.6	0.85	0.000	NADPH oxidase 5%2C transcript variant X1
XM_019915495.1	NW_017852371.1	1082.1	0.42	0.000	ADP-ribosylation factor-like protein 2
XM_019915502.1	NW_017852371.1	1716.2	0.66	0.000	UPF0160 protein
XM_019915507.1	NW_017852371.1	282.9	-1.69	0.000	paired box pox-meso protein
XM_019915517.1	NW_017852372.1	2429.9	-0.66	0.000	septin-interacting protein 1
XM_019915518.1	NW_017852372.1	2179.8	0.43	0.000	histone-lysine N-methyltransferase setd3-like mitochondrial import inner membrane translocase subunit Tim9-like
XM_019915523.1	NW_017852372.1	408.4	0.68	0.000	
XM_019915536.1	NW_017852373.1	230.1	1.31	0.002	cytochrome P450 6k1-like%2C transcript variant X1 chromodomain-helicase-DNA-binding protein Mi-2 homolog%2C transcript variant X1
XM_019915540.1	NW_017852374.1	8046.6	-0.53	0.000	
XM_019915555.1	NW_017852374.1	1715.2	0.74	0.000	exodeoxyribonuclease-like
XR_002172637.1	NW_017850264.1	71.8	0.62	0.004	uncharacterized LOC109545080 mitochondrial amidoxime reducing component 2-like%2C transcript variant X1
XM_019915578.1	NW_017852375.1	2076.4	0.98	0.000	protein-L-isoaspartate(D-aspartate) O-methyltransferase%2C transcript variant X1
XM_019915582.1	NW_017852375.1	917.5	0.65	0.000	
XM_019915591.1	NW_017852375.1	1073.6	0.68	0.001	glycerate kinase
XM_019915595.1	NW_017852376.1	7168.5	-0.57	0.000	23 kDa integral membrane protein-like%2C transcript variant X1
XM_019915604.1	NW_017850268.1	1797.2	0.42	0.000	centromere/kinetochore protein zw10 homolog
XM_019915610.1	NW_017852377.1	932.8	0.34	0.007	uncharacterized LOC109545114
XM_019915611.1	NW_017852377.1	1686.3	-0.87	0.007	probable cytochrome P450 28d1
XM_019915626.1	NW_017852377.1	1247.4	0.40	0.000	probable phenylalanine--tRNA ligase%2C mitochondrial
XM_019915630.1	NW_017852377.1	774.9	0.56	0.000	WD repeat-containing protein 89%2C transcript variant X1 endoplasmic reticulum metalloproteinase 1%2C transcript variant X1
XM_019915639.1	NW_017852377.1	8645.2	-0.42	0.002	
XM_019915642.1	NW_017852377.1	20.4	-0.93	0.001	cuticle protein 8-like
XM_019915661.1	NW_017852377.1	1709.8	0.52	0.000	probable ATP-dependent RNA helicase Dbp73D
XM_019915663.1	NW_017852377.1	994.0	0.80	0.000	uncharacterized LOC109545149%2C transcript variant X1
XM_019915667.1	NW_017852377.1	4958.9	-0.61	0.001	basic salivary proline-rich protein 1-like%2C transcript variant X1
XM_019915685.1	NW_017852377.1	545.9	0.45	0.000	D-beta-hydroxybutyrate dehydrogenase%2C mitochondrial-like
XM_019915686.1	NW_017852377.1	93.4	-1.13	0.004	transcription elongation factor spt5-like probable phospholipid hydroperoxide glutathione peroxidase%2C transcript variant X1
XM_019915687.1	NW_017852377.1	1806.5	0.94	0.000	
XM_019915693.1	NW_017852377.1	1480.0	0.46	0.006	39S ribosomal protein L11%2C mitochondrial-like
XM_019915706.1	NW_017852377.1	6159.5	-1.45	0.000	spatacsin%2C transcript variant X1
XM_019915709.1	NW_017852377.1	395.9	0.33	0.002	actin-related protein 8-like
XM_019915710.1	NW_017852377.1	587.1	0.50	0.000	leucine-rich repeat protein 1
XM_019915711.1	NW_017852377.1	1957.2	0.42	0.002	WD repeat-containing protein 74

XM_019915712.1	NW_017852377.1	2260.0	0.46	0.000	DDB1- and CUL4-associated factor 5%2C transcript variant X1
XM_019915727.1	NW_017852377.1	2079.7	-0.84	0.000	GTP-binding protein Rit2-like
XM_019915736.1	NW_017850281.1	1906.2	0.82	0.000	ATP-dependent RNA helicase DBP2-like
XM_019915735.1	NW_017852377.1	5514.1	0.95	0.000	serine/threonine-protein kinase Nek8-like
XM_019915737.1	NW_017852377.1	250.6	0.66	0.008	protein dead ringer%2C transcript variant X1
XM_019915743.1	NW_017852377.1	18.8	-1.01	0.009	paternally-expressed gene 3 protein-like
XM_019915746.1	NW_017852378.1	1830.4	-0.45	0.000	probable cation-transporting ATPase 13A3
XM_019915748.1	NW_017852378.1	789.4	-0.47	0.001	probable cation-transporting ATPase 13A4
XM_019915749.1	NW_017852378.1	1102.7	-0.48	0.000	probable cation-transporting ATPase 13A3
XM_019915750.1	NW_017852378.1	333.5	-0.48	0.000	uncharacterized LOC109545207
XM_019915752.1	NW_017852378.1	1336.8	-0.72	0.000	histone deacetylase 11%2C transcript variant X1
XM_019915758.1	NW_017852380.1	600.8	0.49	0.008	unconventional myosin-VIIa-like
XM_019915759.1	NW_017852380.1	109.9	-0.68	0.006	coiled-coil domain-containing protein 65-like
XM_019915763.1	NW_017852380.1	294.2	0.64	0.000	dimethyladenosine transferase 2%2C mitochondrial
XM_019915765.1	NW_017852380.1	17.3	-1.49	0.000	enhancer of split malpha protein-like UDP-N-acetylglucosamine--peptide N- acetylglucosaminyltransferase 110 kDa subunit
XM_019915766.1	NW_017852380.1	19302.9	-0.69	0.000	E3 ubiquitin-protein ligase SMURF1%2C transcript variant X1
XM_019915767.1	NW_017852380.1	3176.9	-0.38	0.000	E3 ubiquitin-protein ligase SMURF1%2C transcript variant X1
XM_019915776.1	NW_017850281.1	6559.1	0.85	0.000	ATP-dependent RNA helicase p62-like
XM_019915777.1	NW_017852380.1	628.4	-1.37	0.001	runt-related transcription factor 2-like
XM_019915778.1	NW_017852380.1	1908.6	0.26	0.007	U5 small nuclear ribonucleoprotein 40 kDa protein
XM_019915795.1	NW_017852380.1	6955.2	0.76	0.006	L-xylulose reductase-like
XM_019915796.1	NW_017852380.1	580.7	-0.95	0.000	uncharacterized LOC109545241%2C transcript variant X1
XM_019915825.1	NW_017852380.1	1626.5	0.49	0.006	protein BUD31 homolog phosphoribosyl pyrophosphate synthase-associated protein 2%2C transcript variant X1
XM_019915826.1	NW_017852380.1	5101.8	0.26	0.000	phosphoribosyl pyrophosphate synthase-associated protein 2%2C transcript variant X1
XM_019915840.1	NW_017852380.1	12781.9	-1.03	0.000	myosin-IA%2C transcript variant X1
XM_019915842.1	NW_017852380.1	2558.2	-0.20	0.009	testis-expressed sequence 2 protein
XM_019915845.1	NW_017852380.1	1386.9	0.47	0.001	bifunctional coenzyme A synthase-like
XM_019915852.1	NW_017852380.1	708.3	-0.36	0.004	protein aveugle
XM_019915856.1	NW_017852380.1	1146.4	-0.62	0.002	cytochrome b5 reductase 4%2C transcript variant X1
XM_019915861.1	NW_017852380.1	5402.6	-0.28	0.002	fatty-acid amide hydrolase 2
XM_019915887.1	NW_017852380.1	3355.8	-0.36	0.000	uncharacterized LOC109545289%2C transcript variant X1
XM_019915891.1	NW_017852380.1	5314.7	0.84	0.000	androgen-induced gene 1 protein-like
XM_019915900.1	NW_017852380.1	1491.2	0.42	0.002	cAMP-regulated phosphoprotein 19
XM_019915903.1	NW_017852380.1	46.8	-0.96	0.002	odorant receptor 46a-like%2C transcript variant X1
XM_019915911.1	NW_017852380.1	5228.6	-0.60	0.000	kinesin-like protein unc-104%2C transcript variant X1

XM_019915925.1	NW_017852380.1	7439.2	-0.23	0.002	putative RNA-binding protein Luc7-like 2%2C transcript variant X1
XM_019915939.1	NW_017852380.1	1430.3	1.44	0.000	uncharacterized LOC109545321%2C transcript variant X1
XM_019915944.1	NW_017852380.1	2099.5	1.57	0.000	uncharacterized LOC109545322%2C transcript variant X1
XM_019915946.1	NW_017852380.1	11975.1	1.58	0.000	adenylosuccinate lyase
XM_019915947.1	NW_017852380.1	15.5	1.02	0.007	uncharacterized LOC109545324%2C transcript variant X1
XM_019915956.1	NW_017850342.1	601.6	0.34	0.001	uncharacterized LOC109545327
XM_019915962.1	NW_017852380.1	2648.2	1.02	0.000	inositol-3-phosphate synthase%2C transcript variant X1
XM_019915965.1	NW_017852380.1	5544.8	-1.15	0.000	major royal jelly protein 3-like
XM_019915981.1	NW_017852380.1	14694.6	-0.82	0.001	speckle-type POZ protein-like%2C transcript variant X1
XM_019915989.1	NW_017852380.1	15765.3	-1.20	0.000	sialin%2C transcript variant X1
XM_019915994.1	NW_017852380.1	19080.5	2.54	0.000	probable low-specificity L-threonine aldolase 2%2C transcript variant X1
XM_019915997.1	NW_017852380.1	6857.7	-0.77	0.000	protein tweety%2C transcript variant X1
XM_019916002.1	NW_017852380.1	927.9	0.85	0.000	uncharacterized LOC109545349%2C transcript variant X1
XM_019916004.1	NW_017852380.1	2006.6	-1.10	0.000	uncharacterized LOC109545350%2C transcript variant X1
XM_019916012.1	NW_017852380.1	9506.4	-0.64	0.000	ubiquitin carboxyl-terminal hydrolase 31
XM_019916026.1	NW_017852380.1	419.7	0.65	0.000	M-phase phosphoprotein 6
XM_019916030.1	NW_017852380.1	23789.0	-1.09	0.000	protein charybde-like%2C transcript variant X1
XM_019916034.1	NW_017852380.1	3446.8	-0.86	0.002	uncharacterized LOC109545370
XM_019916037.1	NW_017852380.1	6595.6	-0.72	0.000	protein charybde-like
XM_019916040.1	NW_017852380.1	272.3	-1.20	0.000	homeobox protein unc-4-like%2C transcript variant X1
XM_019916047.1	NW_017852380.1	1046.0	-0.87	0.000	B9 domain-containing protein 1-like
XM_019916048.1	NW_017852380.1	542.0	-0.68	0.004	protein charybde-like
XM_019916049.1	NW_017852380.1	511.6	0.83	0.007	enhancer of split mbeta protein-like
XM_019916050.1	NW_017852380.1	854.5	0.69	0.004	uncharacterized LOC109545386%2C transcript variant X1
XR_002172664.1	NW_017852380.1	130.0	-0.50	0.006	uncharacterized LOC109545387
XM_019916053.1	NW_017852380.1	641.7	1.11	0.000	zinc finger and BTB domain-containing protein 8A-like%2C transcript variant X1
XM_019916057.1	NW_017852380.1	24.7	-1.34	0.002	protein gooseberry-neuro-like
XM_019916059.1	NW_017852381.1	1302.6	-0.43	0.000	calmodulin-binding transcription activator 2-like
XM_019916067.1	NW_017852381.1	15.1	1.67	0.000	probable E3 ubiquitin-protein ligase makorin-1
XR_002172666.1	NW_017852381.1	106.7	-1.16	0.002	uncharacterized LOC109545411
XM_019916077.1	NW_017852381.1	3330.9	-0.33	0.008	rho guanine nucleotide exchange factor 5%2C transcript variant X1
XM_019916081.1	NW_017852381.1	2816.2	-0.30	0.000	DNA-directed RNA polymerase II subunit RPB2%2C transcript variant X1
XM_019916083.1	NW_017852381.1	1288.7	0.30	0.006	calcium homeostasis endoplasmic reticulum protein%2C transcript variant X1
XM_019916090.1	NW_017852381.1	5900.8	1.04	0.000	solute carrier family 25 member 35-like%2C transcript variant X1

XM_019916092.1	NW_017852381.1	710.5	0.80	0.000	tRNA methyltransferase 10 homolog A%2C transcript variant X1
XM_019916099.1	NW_017852381.1	6035.3	-0.38	0.007	dual specificity testis-specific protein kinase 2%2C transcript variant X1
XM_019916106.1	NW_017852381.1	1119.3	-0.88	0.000	BMP and activin membrane-bound inhibitor homolog
XM_019916107.1	NW_017852381.1	1743.4	0.37	0.001	B-cell CLL/lymphoma 7 protein family member A
XM_019916116.1	NW_017852381.1	279.0	0.74	0.005	aminopeptidase M1-A-like%2C transcript variant X1
XM_019916128.1	NW_017850378.1	38926.9	-1.52	0.000	ATP-binding cassette sub-family G member 4-like
XM_019916142.1	NW_017850384.1	447.1	-1.03	0.000	acyl-CoA:lysophosphatidylglycerol acyltransferase 1-like
XM_019916148.1	NW_017852381.1	589.4	1.00	0.000	myosin-10-like
XM_019916153.1	NW_017852381.1	20938.7	-0.51	0.001	protein transport protein Sec61 subunit alpha
XM_019916163.1	NW_017852381.1	247.5	0.47	0.001	zinc finger protein 664-like
XM_019916173.1	NW_017852381.1	6252.4	0.74	0.000	upstream activation factor subunit spp27
XM_019916189.1	NW_017852381.1	1296.1	0.54	0.000	G protein-coupled receptor kinase 2%2C transcript variant X1
XM_019916197.1	NW_017852381.1	530.9	0.72	0.000	protocadherin-like wing polarity protein stan
XM_019916221.1	NW_017852381.1	1684.9	0.61	0.000	histone RNA hairpin-binding protein
XM_019916222.1	NW_017852381.1	3917.8	-0.65	0.004	glycerol-3-phosphate acyltransferase 1%2C mitochondrial%2C transcript variant X1
XM_019916228.1	NW_017852381.1	839.6	0.50	0.000	tRNA-splicing ligase RtcB homolog
XM_019916230.1	NW_017852381.1	1645.6	0.37	0.006	TBC1 domain family member 7
XM_019916231.1	NW_017852381.1	1306.9	0.65	0.000	uncharacterized LOC109545491
XM_019916233.1	NW_017852381.1	1205.6	0.73	0.000	uncharacterized LOC109545494
XM_019916234.1	NW_017852381.1	9675.6	0.27	0.005	MICOS complex subunit Mic60%2C transcript variant X1
XR_002172671.1	NW_017852381.1	84.3	-2.20	0.000	uncharacterized LOC109545496
XM_019916250.1	NW_017852381.1	889.3	0.48	0.002	probable receptor-like protein kinase At5g18500
XM_019916253.1	NW_017852381.1	170.2	0.66	0.003	pancreatic triacylglycerol lipase-like%2C transcript variant X1
XM_019916255.1	NW_017852381.1	1000.6	0.45	0.001	quinone oxidoreductase-like protein 2 homolog
XM_019916256.1	NW_017852381.1	591.4	0.37	0.008	THO complex subunit 6 homolog
XM_019916258.1	NW_017852381.1	2774.8	-0.40	0.001	uncharacterized LOC109545511
NW_017850402.1_948-1527	NW_017850402.1	120.4	1.80	0.000	#N/A
XM_019916272.1	NW_017852381.1	2643.4	0.65	0.000	peroxiredoxin-2-like
XM_019916278.1	NW_017852381.1	70.5	-1.02	0.000	cilia- and flagella-associated protein 58-like
XM_019916279.1	NW_017852381.1	1201.4	-0.52	0.000	lateral signaling target protein 2 homolog
XM_019916280.1	NW_017852381.1	518.5	0.55	0.000	copper homeostasis protein cutC homolog
XM_019916284.1	NW_017852381.1	12301.4	1.23	0.004	glycine dehydrogenase (decarboxylating)%2C mitochondrial
XM_019916297.1	NW_017852381.1	2642.9	0.24	0.005	COP9 signalosome complex subunit 7b%2C transcript variant X1
XM_019916313.1	NW_017850408.1	288.0	0.58	0.000	mitochondrial inner membrane protease subunit 1-like
XM_019916315.1	NW_017852381.1	428.2	0.53	0.000	cell cycle checkpoint control protein RAD9A-like

XM_019916320.1	NW_017852381.1	13.7	-1.02	0.008	uncharacterized LOC109545555
NW_017850408.1_c8738-1508	NW_017850408.1	3567.7	-0.75	0.001	#N/A
XM_019916328.1	NW_017852381.1	2180.7	0.72	0.001	patched domain-containing protein 3%2C transcript variant X1
XM_019916331.1	NW_017852381.1	1601.0	0.76	0.001	uncharacterized LOC109545562%2C transcript variant X1
XM_019916334.1	NW_017852381.1	1091.8	0.30	0.009	TGF-beta-activated kinase 1 and MAP3K7-binding protein 1-like
XM_019916335.1	NW_017852381.1	168.9	0.87	0.000	DNA repair protein RAD51 homolog 4-like
XM_019916347.1	NW_017852381.1	5991.1	-0.38	0.004	NECAP-like protein CG9132
XM_019916364.1	NW_017852381.1	3724.5	1.04	0.001	elongation of very long chain fatty acids protein 7-like
XM_019916367.1	NW_017852381.1	1154.0	-0.83	0.006	TWiK family of potassium channels protein 18-like
XM_019916368.1	NW_017852381.1	79.5	0.94	0.002	glutamate receptor ionotropic%2C kainate 2-like
XM_019916374.1	NW_017852381.1	66.5	-0.74	0.002	homeotic protein empty spiracles-like
XM_019916375.1	NW_017852381.1	126.0	0.82	0.000	DNA helicase MCM9-like%2C transcript variant X1
XM_019916394.1	NW_017852381.1	1683.9	0.93	0.000	anillin-like
XM_019916405.1	NW_017852382.1	7247.7	-0.24	0.003	pre-mRNA-processing factor 39
XM_019916409.1	NW_017852382.1	1833.8	-1.22	0.000	A disintegrin and metalloproteinase with thrombospondin motifs
XM_019916414.1	NW_017852382.1	7420.2	0.24	0.003	16%2C transcript variant X1
XM_019916425.1	NW_017852382.1	10418.0	-0.48	0.001	ATP-dependent zinc metalloprotease YME1L1
XM_019916435.1	NW_017852382.1	580.7	0.65	0.000	transmembrane protein 214-A
XM_019916437.1	NW_017852382.1	7870.2	-0.42	0.006	glycosaminoglycan xylosylkinase homolog%2C transcript variant X1
XM_019916450.1	NW_017852382.1	3295.7	-0.39	0.002	peptidyl-prolyl cis-trans isomerase FKBP8%2C transcript variant X1
XM_019916454.1	NW_017852382.1	691.2	0.49	0.002	BSD domain-containing protein 1-A-like%2C transcript variant X1
XM_019916464.1	NW_017852382.1	2347.7	-0.41	0.003	probable cardiolipin synthase (CMP-forming)
XM_019916470.1	NW_017852382.1	1886.6	0.55	0.002	DNA-directed RNA polymerase III subunit RPC7
XM_019916505.1	NW_017852382.1	263.8	-1.35	0.000	probable ubiquitin-conjugating enzyme E2 C
XM_019916506.1	NW_017852382.1	3178.9	-0.28	0.000	coiled-coil and C2 domain-containing protein 2A
XM_019916511.1	NW_017850438.1	3124.6	-0.82	0.007	BTB/POZ domain-containing protein 9%2C transcript variant X1
XM_019916508.1	NW_017852382.1	25967.4	-0.81	0.002	1-acyl-sn-glycerol-3-phosphate acyltransferase alpha-like
XM_019916525.1	NW_017850439.1	1721.4	-0.83	0.007	23 kDa integral membrane protein-like
XM_019916528.1	NW_017852382.1	2921.7	-0.60	0.000	1-acyl-sn-glycerol-3-phosphate acyltransferase alpha-like
XM_019916532.1	NW_017852382.1	5132.7	0.75	0.003	CREB-regulated transcription coactivator 1-like%2C transcript variant X1
XM_019916533.1	NW_017852382.1	167.6	1.66	0.000	aldose reductase-like
XM_019916542.1	NW_017852383.1	7658.0	-0.36	0.002	dynein regulatory complex subunit 7
XM_019916549.1	NW_017852383.1	1029.4	-1.00	0.003	RB1-inducible coiled-coil protein 1%2C transcript variant X1
XM_019916571.1	NW_017852384.1	2153.2	-0.74	0.001	integrin beta-PS-like
					serine protease easter-like

XM_019916572.1	NW_017852385.1	1033.2	-0.79	0.000	piezo-type mechanosensitive ion channel component-like
XM_019916578.1	NW_017852408.1	559.5	0.75	0.001	plexin domain-containing protein 2-like
XM_019916601.1	NW_017852555.1	59.7	0.81	0.002	tubulin epsilon chain-like
XM_019916604.1	NW_017852582.1	2658.7	0.99	0.000	uncharacterized LOC109545762
XM_019916607.1	NW_017852599.1	250.7	-0.71	0.003	disco-interacting protein 2
XR_002172695.1	NW_017852715.1	879.6	-0.70	0.000	uncharacterized LOC109545787
XM_019916633.1	NW_017852745.1	78.4	0.83	0.002	collagen alpha-2(XI) chain-like
XM_019916658.1	NW_017852893.1	192.2	0.81	0.001	protein SDE2 homolog
XM_019916667.1	NW_017850500.1	1251.5	0.27	0.005	polyphosphoinositide phosphatase-like
XM_019916668.1	NW_017850500.1	3268.8	0.44	0.001	eukaryotic translation initiation factor 3 subunit K-like
XM_019916672.1	NW_017850502.1	3806.1	-0.49	0.000	serine/threonine-protein kinase 10-like
XM_019916673.1	NW_017850503.1	4816.8	-0.50	0.000	serine/threonine-protein kinase 10-like
XM_019916674.1	NW_017850504.1	526.1	-0.37	0.007	uncharacterized LOC109545832
XM_019916678.1	NW_017850520.1	5533.8	0.28	0.000	secretion-regulating guanine nucleotide exchange factor-like
XM_019916692.1	NW_017845860.1	301.2	-0.48	0.003	uncharacterized LOC109545848
XM_019916691.1	NW_017850547.1	86.5	-0.78	0.003	cytochrome P450 4d2-like%2C transcript variant X1
XM_019916694.1	NW_017850548.1	63.4	-0.78	0.005	cytochrome P450 4d2-like
XM_019916696.1	NW_017850552.1	72.4	0.64	0.001	disheveled-associated activator of morphogenesis 2-like
XM_019916701.1	NW_017845861.1	310.4	-0.50	0.001	uncharacterized LOC109545859
XM_019916699.1	NW_017850558.1	945.6	-0.47	0.009	serine/threonine-protein kinase 3-like
XM_019916704.1	NW_017850561.1	376.5	-0.34	0.009	signal-induced proliferation-associated 1-like protein 2
XM_019916714.1	NW_017845862.1	3550.6	0.32	0.001	T-complex protein 1 subunit eta-like
XM_019916717.1	NW_017850575.1	1222.4	-0.69	0.000	monocarboxylate transporter 12-like
XM_019916721.1	NW_017850592.1	30.3	-1.30	0.004	homeotic protein proboscipedia-like
XM_019916736.1	NW_017850625.1	77.9	1.03	0.009	proline-rich nuclear receptor coactivator 2-like
XR_002172707.1	NW_017850625.1	89.3	1.18	0.009	uncharacterized LOC109545894
XM_019916746.1	NW_017850652.1	7526.0	0.85	0.003	aldose reductase-like
XM_019916751.1	NW_017850658.1	405.2	0.51	0.000	DNA polymerase delta catalytic subunit-like
XM_019916756.1	NW_017850661.1	35.8	-1.33	0.003	homeotic protein proboscipedia-like
XM_019916757.1	NW_017850662.1	36.0	-1.34	0.003	homeotic protein proboscipedia-like
XM_019916763.1	NW_017850671.1	8401.1	-0.29	0.002	spectrin beta chain-like
XM_019916770.1	NW_017850687.1	861.4	0.42	0.000	cleavage stimulation factor subunit 2-like
XM_019916776.1	NW_017845868.1	680.2	-0.40	0.005	uncharacterized LOC109545931
XM_019916773.1	NW_017850703.1	2782.5	-0.48	0.002	dynamamin-like
XM_019916778.1	NW_017850708.1	870.9	-0.57	0.004	ATP-binding cassette sub-family G member 4-like
XR_002172714.1	NW_017850709.1	661.3	1.18	0.000	uncharacterized LOC109545936

XM_019916790.1	NW_017850717.1	263.3	0.57	0.008	uncharacterized LOC109545945
XM_019916798.1	NW_017850731.1	646.7	1.06	0.005	sideroflexin-1-like
XM_019916799.1	NW_017850733.1	33.7	0.80	0.000	dnaj homolog subfamily C member 24-like
XM_019916805.1	NW_017850746.1	1140.0	0.30	0.007	RNA polymerase II-associated factor 1 homolog
XM_019916806.1	NW_017850747.1	2146.0	0.29	0.003	RNA polymerase II-associated factor 1 homolog
XR_002172717.1	NW_017850753.1	661.2	1.18	0.000	uncharacterized LOC109545966
XM_019916809.1	NW_017850761.1	1335.5	0.27	0.004	polyphosphoinositide phosphatase-like
XM_019916810.1	NW_017850761.1	2369.7	0.49	0.000	eukaryotic translation initiation factor 3 subunit K-like
XM_019916816.1	NW_017850775.1	3018.2	0.35	0.005	caprin homolog%2C transcript variant X1
XM_019916818.1	NW_017850775.1	1519.6	-0.60	0.002	protein shuttle craft-like
XR_002172719.1	NW_017850780.1	302.8	0.35	0.010	uncharacterized LOC109545979
XM_019916820.1	NW_017850780.1	1049.4	0.55	0.004	apoptosis-stimulating of p53 protein 2-like
XM_019916821.1	NW_017850781.1	877.5	0.56	0.005	apoptosis-stimulating of p53 protein 2-like
XR_002172720.1	NW_017850781.1	303.4	0.34	0.010	uncharacterized LOC109545983
XM_019916828.1	NW_017850802.1	1476.7	-0.85	0.000	GTP-binding protein Rit1-like
XM_019916831.1	NW_017850811.1	35.3	1.07	0.001	uncharacterized LOC109545992
XM_019916835.1	NW_017850821.1	19.1	-1.03	0.004	uncharacterized LOC109545998
XM_019916839.1	NW_017850822.1	19.1	-1.03	0.004	uncharacterized LOC109546002
XM_019916840.1	NW_017850823.1	19.1	-1.03	0.004	homeobox protein OTX-like
XM_019916860.1	NW_017850846.1	532.1	0.52	0.000	uncharacterized LOC109546024
XR_002172724.1	NW_017850888.1	1282.8	-0.74	0.000	uncharacterized LOC109546042%2C transcript variant X1
XM_019916882.1	NW_017845920.1	49.8	1.02	0.003	carbohydrate sulfotransferase 1-like
XM_019916881.1	NW_017850890.1	131.4	-1.00	0.000	organic cation transporter-like protein
XR_002172726.1	NW_017850892.1	643.4	-0.89	0.000	uncharacterized LOC109546046
XM_019916886.1	NW_017850913.1	12058.2	1.05	0.000	uncharacterized LOC109546052
XM_019916896.1	NW_017850933.1	518.3	1.11	0.000	uncharacterized LOC109546061
XM_019916905.1	NW_017850947.1	1861.4	0.92	0.000	poly(A) RNA polymerase gld-2 homolog A-like
XM_019916916.1	NW_017850948.1	3454.1	-1.62	0.000	uncharacterized LOC109546080
XM_019916917.1	NW_017850949.1	2469.9	-1.60	0.000	uncharacterized LOC109546081
XR_002172729.1	NW_017850963.1	12.6	-1.46	0.002	uncharacterized LOC109546083%2C transcript variant X1
XM_019916923.1	NW_017850979.1	56094.1	1.22	0.002	pectinesterase B-like
XM_019916927.1	NW_017850986.1	2045.4	0.35	0.006	ribosome production factor 2 homolog
XM_019916931.1	NW_017851001.1	64.7	1.11	0.007	serine protease snake-like
XM_019916933.1	NW_017851006.1	637.3	-1.01	0.000	uncharacterized LOC109546099%2C transcript variant X1
XM_019916936.1	NW_017851008.1	456.0	0.38	0.001	oligoribonuclease%2C mitochondrial-like
XR_002172733.1	NW_017851035.1	481.8	-0.70	0.001	uncharacterized LOC109546115%2C transcript variant X1

XM_019916950.1	NW_017851049.1	1345.7	0.97	0.000	anaphase-promoting complex subunit 4-like
XR_002172736.1	NW_017851065.1	463.2	-0.73	0.007	uncharacterized LOC109546124
XR_002172737.1	NW_017851065.1	205.7	-0.76	0.004	uncharacterized LOC109546126
XM_019916962.1	NW_017851077.1	1040.9	0.65	0.000	protein farnesyltransferase subunit beta%2C transcript variant X1
XM_019916973.1	NW_017851084.1	24.1	1.28	0.006	uncharacterized LOC109546141
XM_019916990.1	NW_017851084.1	41896.3	1.69	0.000	amidophosphoribosyltransferase-like
XM_019916995.1	NW_017851084.1	651.9	0.55	0.000	exosome complex component RRP4
XM_019916998.1	NW_017851084.1	18065.4	-0.35	0.003	spectrin alpha chain%2C transcript variant X1
XM_019917010.1	NW_017851084.1	397.0	0.55	0.007	protein ARV1
XM_019917028.1	NW_017851084.1	13110.2	2.08	0.000	branched-chain-amino-acid aminotransferase%2C cytosolic
XM_019917055.1	NW_017845975.1	62.9	-1.57	0.000	probable cytochrome P450 9f2
XM_019917057.1	NW_017851084.1	873.5	2.01	0.000	cytochrome P450 4c3-like%2C transcript variant X1
XM_019917081.1	NW_017851087.1	2962.3	-0.31	0.000	centrosome-associated zinc finger protein CP190
XM_019917088.1	NW_017851087.1	1315.1	0.36	0.003	splicing factor 3A subunit 3
XM_019917091.1	NW_017851087.1	3638.5	-0.24	0.000	protein YIPF5
XM_019917100.1	NW_017851087.1	12732.3	-2.13	0.000	uncharacterized LOC109546220
XM_019917106.1	NW_017851087.1	1634.5	0.33	0.003	nitric oxide-associated protein 1
XM_019917120.1	NW_017851087.1	7988.6	-0.40	0.004	actin-binding LIM protein 1
XM_019917129.1	NW_017851087.1	1717.6	-0.55	0.004	disintegrin and metalloproteinase domain-containing protein 10-like
XM_019917134.1	NW_017851087.1	51024.0	1.50	0.000	probable phosphoserine aminotransferase
XM_019917145.1	NW_017851087.1	610.5	0.36	0.001	uncharacterized LOC109546250
XM_019917146.1	NW_017851087.1	8782.7	0.67	0.008	succinyl-CoA:3-ketoacid coenzyme A transferase 1%2C mitochondrial
XM_019917150.1	NW_017851087.1	14880.2	1.30	0.000	putative inorganic phosphate cotransporter
XM_019917154.1	NW_017851087.1	137.7	0.80	0.001	hexosaminidase D-like
XM_019917157.1	NW_017851087.1	405.0	-1.08	0.002	chondroitin proteoglycan-2-like
XM_019917159.1	NW_017851087.1	245.1	-1.06	0.000	glutamate receptor-interacting protein 1%2C transcript variant X1
XM_019917173.1	NW_017851087.1	563.1	0.53	0.008	methionine synthase reductase-like
XM_019917202.1	NW_017851087.1	1375.7	0.55	0.003	U3 small nucleolar RNA-interacting protein 2
XR_002172754.1	NW_017846000.1	590.3	-0.70	0.000	uncharacterized LOC109546291%2C transcript variant X1
XR_002172757.1	NW_017851105.1	8406.7	0.85	0.003	aldose reductase-like
XM_019917221.1	NW_017851106.1	4208.5	-0.56	0.000	uncharacterized LOC109546301
XM_019917224.1	NW_017851114.1	721.7	1.88	0.000	uncharacterized LOC109546305
XM_019917227.1	NW_017851115.1	5910.9	0.48	0.000	transcription factor Dp-1%2C transcript variant X1
XM_019917232.1	NW_017851115.1	1384.5	0.92	0.000	GATA-binding factor A-like%2C transcript variant X1
XM_019917237.1	NW_017851121.1	190.3	1.37	0.003	uncharacterized LOC109546318

XM_019917240.1	NW_017851122.1	808.5	0.79	0.000	WD repeat-containing protein 46
XM_019917246.1	NW_017851125.1	578.6	0.35	0.001	crossover junction endonuclease MUS81
XM_019917247.1	NW_017851125.1	703.4	0.44	0.001	60S ribosome subunit biogenesis protein NIP7 homolog
XM_019917248.1	NW_017851125.1	651.9	0.48	0.000	SET and MYND domain-containing protein 5
XM_019917251.1	NW_017851125.1	2045.0	0.33	0.001	formin-binding protein 4-like
XM_019917252.1	NW_017851125.1	1109.9	-0.25	0.005	uncharacterized LOC109546337
XM_019917254.1	NW_017851125.1	3932.8	1.06	0.000	uncharacterized LOC109546339
XM_019917256.1	NW_017851125.1	3711.5	1.12	0.000	uncharacterized LOC109546340
XM_019917258.1	NW_017851131.1	5054.5	-0.23	0.001	cytosolic carboxypeptidase-like protein 5
XM_019917259.1	NW_017851131.1	751.3	-0.24	0.002	GA-binding protein subunit beta-2%2C transcript variant X1
XM_019917261.1	NW_017851131.1	983.6	0.45	0.000	8-oxo-dGDP phosphatase NUDT18%2C transcript variant X1
XM_019917284.1	NW_017851136.1	1.8	1.25	0.010	proton-coupled amino acid transporter 1-like
XM_019917285.1	NW_017851136.1	8598.5	-0.54	0.002	uncharacterized LOC109546363%2C transcript variant X1 cleavage and polyadenylation specificity factor subunit 1%2C transcript variant X1
XM_019917297.1	NW_017851136.1	1065.2	0.61	0.000	EH domain-binding protein 1%2C transcript variant X1
XM_019917301.1	NW_017851136.1	6267.6	-0.51	0.000	EH domain-binding protein 1%2C transcript variant X1
XM_019917321.1	NW_017851136.1	1370.2	0.43	0.002	OCIA domain-containing protein 1
XM_019917322.1	NW_017851136.1	969.7	-0.84	0.003	capon-like protein%2C transcript variant X1 vasoactive intestinal polypeptide receptor 2-like%2C transcript variant X1
XM_019917326.1	NW_017851136.1	12190.0	-1.51	0.000	pancreatic lipase-related protein 3-like
XM_019917332.1	NW_017851136.1	120.1	1.49	0.001	pancreatic lipase-related protein 3-like
XM_019917333.1	NW_017851136.1	1295.1	1.03	0.006	laminin subunit gamma-1
XM_019917336.1	NW_017851136.1	958.7	1.17	0.000	sialin%2C transcript variant X1
XR_002172772.1	NW_017851137.1	92.5	0.55	0.005	uncharacterized LOC109546390
XM_019917344.1	NW_017851138.1	5365.4	1.01	0.000	uncharacterized LOC109546393
XM_019917345.1	NW_017851138.1	825.6	-0.38	0.006	uncharacterized LOC109546394%2C transcript variant X1
XM_019917351.1	NW_017851139.1	1004.7	0.41	0.004	1%2C2-dihydroxy-3-keto-5-methylthiopentene dioxygenase-like
XM_019917355.1	NW_017851142.1	1861.3	0.92	0.000	poly(A) RNA polymerase gld-2 homolog A
XM_019917381.1	NW_017851142.1	761.5	0.61	0.000	uncharacterized LOC109546422
XM_019917396.1	NW_017851149.1	7868.3	-0.44	0.009	sortilin-related receptor-like
XM_019917402.1	NW_017851152.1	28358.0	-1.02	0.000	choline/ethanolamine kinase
XM_019917415.1	NW_017851153.1	18.6	-1.41	0.000	iodotyrosine deiodinase 1-like
XM_019917424.1	NW_017851153.1	738.2	0.42	0.000	cyclin-dependent kinase 7
XM_019917426.1	NW_017851153.1	11126.0	1.34	0.000	uncharacterized LOC109546460
XM_019917447.1	NW_017851153.1	2285.9	0.27	0.005	prefoldin subunit 1
XM_019917449.1	NW_017851153.1	800.8	0.69	0.000	uncharacterized LOC109546472%2C transcript variant X1
XM_019917469.1	NW_017851157.1	6413.4	-0.38	0.001	translation initiation factor IF-2-like

XM_019917472.1	NW_017851157.1	40747.8	-0.55	0.001	uncharacterized LOC109546494
XR_002172784.1	NW_017851157.1	622.4	0.65	0.002	uncharacterized LOC109546498%2C transcript variant X1
XM_019917482.1	NW_017851159.1	5593.1	-0.78	0.000	uncharacterized LOC109546505
XM_019917484.1	NW_017851159.1	67.9	0.92	0.003	zinc finger and BTB domain-containing protein 8A.2
XM_019917490.1	NW_017851159.1	585.3	0.40	0.004	rhomboid-related protein 2
XM_019917499.1	NW_017851160.1	186.5	1.00	0.000	kinesin-like protein KLP2
XM_019917500.1	NW_017851160.1	96.3	0.82	0.001	uncharacterized LOC109546521
XM_019917515.1	NW_017851160.1	12859.9	-0.58	0.000	BAG domain-containing protein Samui%2C transcript variant X1 zinc finger and BTB domain-containing protein 24-like%2C transcript variant X1
XM_019917517.1	NW_017851160.1	756.8	0.81	0.000	
XM_019917524.1	NW_017851160.1	3953.8	0.54	0.000	importin subunit alpha-1-like
XM_019917533.1	NW_017851160.1	588.7	-0.71	0.000	multiple inositol polyphosphate phosphatase 1
XM_019917534.1	NW_017851160.1	170.5	-0.57	0.006	uncharacterized LOC109546544 PEST proteolytic signal-containing nuclear protein-like%2C transcript variant X1
XM_019917535.1	NW_017851160.1	1336.1	-0.27	0.007	
XM_019917541.1	NW_017851160.1	899.1	0.44	0.007	5-methylcytosine rRNA methyltransferase NSUN4
XM_019917542.1	NW_017851160.1	1488.9	0.94	0.000	uncharacterized LOC109546550
XM_019917544.1	NW_017851160.1	20.2	1.20	0.009	uncharacterized LOC109546552
XM_019917547.1	NW_017851162.1	2110.1	0.29	0.002	protein ABHD4-like U3 small nucleolar RNA-associated protein 4 homolog%2C transcript variant X1
XM_019917555.1	NW_017851162.1	1346.5	0.64	0.000	
XM_019917577.1	NW_017851165.1	1501.3	0.42	0.000	peptidyl-prolyl cis-trans isomerase-like 2
XM_019917579.1	NW_017851165.1	5455.6	0.50	0.000	ubiquitin-conjugating enzyme E2-24 kDa%2C transcript variant X1
XM_019917584.1	NW_017851165.1	1398.2	1.74	0.000	regucalcin-like%2C transcript variant X1
XM_019917604.1	NW_017851169.1	811.5	0.85	0.000	multidrug resistance-associated protein 4-like
XM_019917605.1	NW_017851169.1	529.3	0.73	0.000	multidrug resistance-associated protein 4-like
XM_019917607.1	NW_017851169.1	150.7	0.74	0.007	multidrug resistance-associated protein 4-like
XM_019917608.1	NW_017851169.1	191.5	0.92	0.000	probable multidrug resistance-associated protein lethal(2)03659 inositol polyphosphate 5-phosphatase OCRL-1%2C transcript variant X1
XM_019917619.1	NW_017851170.1	2099.1	0.29	0.000	
XM_019917641.1	NW_017851170.1	453.6	-0.52	0.007	GTP-binding protein Di-Ras2
XM_019917661.1	NW_017846163.1	812.2	-1.60	0.000	gonadotropin-releasing hormone receptor-like
XM_019917696.1	NW_017851171.1	119.5	1.01	0.006	facilitated trehalose transporter Tret1-like
XM_019917697.1	NW_017851171.1	120.3	1.13	0.000	protein spaetzle-like
XM_019917699.1	NW_017851171.1	2264.0	0.25	0.004	MOB kinase activator-like 4 actin cytoskeleton-regulatory complex protein PAN1-like%2C transcript variant X1
XM_019917705.1	NW_017851173.1	2225.7	-0.51	0.009	
XM_019917728.1	NW_017851174.1	13.9	1.00	0.002	cuticle protein 7-like

XM_019917737.1	NW_017851174.1	1056.7	-0.62	0.003	sodium/potassium/calcium exchanger 3%2C transcript variant X1
XM_019917741.1	NW_017851174.1	1894.4	0.53	0.000	cytochrome P450 302a1%2C mitochondrial-like
XM_019917742.1	NW_017851174.1	29021.2	1.07	0.000	fumarate hydratase%2C mitochondrial-like
XM_019917745.1	NW_017851174.1	8483.9	0.83	0.003	arginase-1 RB-associated KRAB zinc finger protein-like%2C transcript variant X1
XM_019917746.1	NW_017851174.1	2006.2	-0.64	0.000	
XM_019917752.1	NW_017851174.1	141.8	0.77	0.005	protein CROWDED NUCLEI 1-like
XM_019917764.1	NW_017846193.1	965.5	0.36	0.001	N-alpha-acetyltransferase 15%2C NatA auxiliary subunit-like
XM_019917777.1	NW_017846193.1	929.8	0.34	0.002	DNA-directed RNA polymerase III subunit RPC3-like
XM_019917784.1	NW_017851174.1	2313.2	0.29	0.001	ubiquitin-protein ligase E3C
XM_019917791.1	NW_017851174.1	5317.4	-0.34	0.003	1-acyl-sn-glycerol-3-phosphate acyltransferase gamma-like
XM_019917820.1	NW_017851174.1	477.9	1.56	0.000	pseudouridine-5'-phosphatase-like%2C transcript variant X1
XM_019917840.1	NW_017851174.1	4118.9	-0.69	0.001	UMP-CMP kinase 2%2C mitochondrial-like voltage-dependent L-type calcium channel subunit beta-2%2C transcript variant X1
XM_019917841.1	NW_017851174.1	2459.0	-1.05	0.000	
XM_019917861.1	NW_017846219.1	3712.4	0.32	0.003	T-complex protein 1 subunit eta-like
XM_019917858.1	NW_017851174.1	1783.4	0.56	0.000	FACT complex subunit Ssrp1 zinc finger CCHC-type and RNA-binding motif-containing protein 1-like
XM_019917890.1	NW_017851181.1	315.5	0.62	0.000	
XM_019917892.1	NW_017851181.1	373745.5	-1.30	0.000	apolipoporphins%2C transcript variant X1
XM_019917912.1	NW_017851181.1	16254.4	0.70	0.000	malate dehydrogenase%2C mitochondrial
XR_002172815.1	NW_017844965.1	571.5	-0.69	0.006	uncharacterized LOC109546798
XM_019917917.1	NW_017851181.1	5853.4	-0.31	0.010	protein zyg-11 homolog
XM_019917921.1	NW_017851181.1	2668.1	0.35	0.006	histone chaperone asf1
XM_019917926.1	NW_017851181.1	8181.3	-1.15	0.000	solute carrier family 26 member 10-like%2C transcript variant X1
XM_019917934.1	NW_017851181.1	1909.8	-0.69	0.000	carbohydrate sulfotransferase 11%2C transcript variant X1
XM_019917936.1	NW_017851181.1	9395.6	2.39	0.000	inositol oxygenase
XM_019917956.1	NW_017851181.1	394.7	0.78	0.000	low-density lipoprotein receptor-related protein 1-like jmc domain-containing histone demethylation protein 1%2C transcript variant X1
XM_019917959.1	NW_017851181.1	3617.7	-0.50	0.001	
XM_019917971.1	NW_017851181.1	184.8	0.99	0.009	uncharacterized LOC109546834
XM_019917991.1	NW_017846261.1	33.7	0.80	0.000	dnaj homolog subfamily C member 24-like
XM_019917990.1	NW_017851181.1	19125.3	-1.32	0.001	apolipoprotein D-like
XM_019917996.1	NW_017851181.1	1148.2	0.69	0.000	tubulin gamma-1 chain-like
XM_019918001.1	NW_017851181.1	252.1	1.23	0.002	cytochrome P450 4C1-like%2C transcript variant X1 putative fatty acyl-CoA reductase CG5065%2C transcript variant X1
XM_019918004.1	NW_017851181.1	187.7	1.99	0.000	
XM_019918018.1	NW_017851185.1	343.6	0.63	0.000	uncharacterized LOC109546865

XM_019918019.1	NW_017851185.1	738.7	0.65	0.008	aurora kinase B
XM_019918020.1	NW_017851185.1	2635.7	0.46	0.000	proline-rich protein PRCC%2C transcript variant X1
XM_019918045.1	NW_017851187.1	4595.3	0.60	0.000	chromosome-associated kinesin KIF4%2C transcript variant X1 receptor expression-enhancing protein 5-like%2C transcript variant X1
XM_019918051.1	NW_017851187.1	19228.3	-0.57	0.000	
XM_019918053.1	NW_017851187.1	840.1	0.63	0.000	probable 28S ribosomal protein S16%2C mitochondrial
XM_019918059.1	NW_017851187.1	123.4	1.30	0.000	tetratricopeptide repeat protein 30A neutral and basic amino acid transport protein rBAT%2C transcript variant X1
XM_019918060.1	NW_017851187.1	1900.1	0.37	0.000	
XM_019918068.1	NW_017851187.1	1532.9	0.78	0.001	cyclin-dependent kinases regulatory subunit-like
XM_019918071.1	NW_017851187.1	2689.9	-0.45	0.000	activin receptor type-1%2C transcript variant X1
XM_019918082.1	NW_017851187.1	536.6	-0.37	0.007	zinc finger Y-chromosomal protein 2-like%2C transcript variant X1
XM_019918083.1	NW_017851187.1	7552.5	-0.45	0.000	protein bicaudal D
XM_019918085.1	NW_017851187.1	732.7	0.69	0.005	uncharacterized LOC109546913%2C transcript variant X1
XM_019918090.1	NW_017851187.1	1661.8	-1.56	0.000	uncharacterized LOC109546919
XR_002172826.1	NW_017851187.1	78.5	-1.24	0.009	uncharacterized LOC109546921
XM_019918104.1	NW_017851190.1	157.5	-0.88	0.007	piggyBac transposable element-derived protein 3-like ADP-ribosylation factor GTPase-activating protein 2%2C transcript variant X1
XM_019918105.1	NW_017851192.1	3502.7	-0.31	0.009	
XM_019918113.1	NW_017851192.1	8444.0	-0.96	0.000	ATP-binding cassette sub-family G member 4-like
XM_019918124.1	NW_017851196.1	5003.7	-0.58	0.000	beta-TrCP%2C transcript variant X1
XR_002172831.1	NW_017851201.1	7.3	1.33	0.005	uncharacterized LOC109546961 ubiquitin carboxyl-terminal hydrolase calypso%2C transcript variant X1
XM_019918150.1	NW_017851201.1	682.8	0.41	0.001	
XM_019918174.1	NW_017851204.1	761.8	0.58	0.000	cytochrome c oxidase assembly factor 5
XM_019918175.1	NW_017851204.1	27553.5	0.45	0.002	calmodulin
XM_019918196.1	NW_017846291.1	9744.7	-0.58	0.002	baculoviral IAP repeat-containing protein 2-like
XM_019918194.1	NW_017851209.1	636.6	-0.98	0.001	histamine H2 receptor-like
XM_019918212.1	NW_017851209.1	2477.1	-1.34	0.000	peptidoglycan-recognition protein LE-like%2C transcript variant X1
XM_019918218.1	NW_017851209.1	2879.4	-0.28	0.009	TATA element modulatory factor%2C transcript variant X1
XM_019918236.1	NW_017851216.1	692.0	-1.17	0.005	cytochrome b5-like
XM_019918243.1	NW_017851217.1	1094.6	1.04	0.000	uncharacterized LOC109547027
XM_019918244.1	NW_017851217.1	1011.6	0.91	0.000	protein ovarian tumor locus-like
XM_019918255.1	NW_017851223.1	4553.7	-0.34	0.006	AMMECR1-like protein%2C transcript variant X1
XM_019918258.1	NW_017851223.1	547.3	0.39	0.000	non-structural maintenance of chromosomes element 1 homolog
XM_019918260.1	NW_017851223.1	2482.5	0.37	0.002	mitochondrial pyruvate carrier 2-like
XM_019918261.1	NW_017851223.1	733.6	0.77	0.003	toll-like receptor Tollo
XM_019918262.1	NW_017851223.1	600.7	0.49	0.000	lysine-specific histone demethylase 1A%2C transcript variant X1

Appendix 3.2 Table containing all KEGG pathways with 2 or more enzymes associated with differentially expressed flight genes identified using a differential expression analysis.

Pathway	Pathway ID	number of representative enzymes	Enzyme sequence accession numbers
Biosynthesis of antibiotics	map01130	37	XM_019899042.1, XM_019915292.1, XM_019915346.1, XM_019898758.1, XM_019901306.1, XM_019913589.1, XM_019901341.1
Purine metabolism	map00230	14	XM_019917912.1, XM_019915591.1, XM_019905419.1
Pyruvate metabolism	map00620	8	XM_019899143.1, XM_019905168.1, XM_019902592.1, XM_019899997.1, XM_019909244.1, XM_019909039.1, XM_019916272.1, XM_019906204.1, XM_019915687.1, XM_019899247.1, XM_019899143.1
Glycine, serine and threonine metabolism	map00260	8	XM_019899878.1
Glutathione metabolism	map00480	7	XM_019917912.1, XM_019899042.1, XM_019915292.1, XM_019915346.1, XM_019898758.1, XM_019901306.1, XM_019903625.1, XM_019910050.1, XM_019917742.1, XM_019910050.1
Amino sugar and nucleotide sugar metabolism	map00520	6	XM_019906902.1
Cysteine and methionine metabolism	map00270 map00561	6	XM_019905419.1
Glycerolipid metabolism		6	XM_019912417.1, XM_019899639.1, XM_019901314.1, XM_019904139.1

Methane metabolism	map00680	6	XM_019915946.1, XM_019904632.1, XM_019917028.1, XM_019917912.1, XM_019899042.1, XM_019915292.1, XM_019915346.1, XM_019898758.1, XM_019899073.1, XM_019910396.1, XM_019901306.1, XM_019913911.1, XM_019899073.1, XM_019915591.1, XM_019900363.1, XM_019903625.1, XM_019913435.1, XM_019916990.1, XM_019907193.1, XM_019909244.1, XM_019917134.1, XM_019913385.1, XM_019910318.1, XM_019907029.1, XM_019915826.1, XM_019905419.1, XM_019911961.1, XM_019913589.1, XM_019899668.1, XM_019917742.1, XM_019902406.1, XM_019916962.1, XM_019913385.1, XM_019899247.1, XM_019915962.1, XM_019911961.1, XM_019904647.1, XM_019917742.1, XM_019901341.1
Terpenoid backbone biosynthesis	map00900	6	XM_019905992.1
Glycolysis / Gluconeogenesis	map00010	5	XM_019917146.1
Drug metabolism - other enzymes	map00983	5	XM_019904099.1, XM_019901421.1
Alanine, aspartate and glutamate metabolism	map00250	5	XM_019917028.1
Porphyrin and chlorophyll metabolism	map00860	5	XM_019916315.1, XM_019916364.1
Carbon fixation pathways in prokaryotes	map00720	5	XM_019906856.1, XM_019897898.1, XM_019911852.1, XM_019911849.1
Valine, leucine and isoleucine degradation	map00280	4	XM_019917028.1, XM_019910290.1, XM_019913946.1, XM_019917146.1

Galactose metabolism	map00052	4	XM_019912417.1, XM_019899639.1, XM_019901314.1, XM_019904139.1
Sphingolipid metabolism	map00600	4	XM_019906856.1, XM_019911961.1, XM_019905459.1, XM_019911961.1 XM_019914463.1, XM_019897898.1, XM_019911852.1, XM_019911849.1, XM_019911961.1, XM_019905459.1, XM_019911961.1, XM_019904647.1
Aminoacyl-tRNA biosynthesis	map00970	4	XM_019916315.1, XM_019916364.1, XM_019910424.1
Folate biosynthesis	map00790	4	XM_019897951.1, XM_019904007.1, XM_019913894.1
Pyrimidine metabolism	map00240	4	XM_019905168.1, XM_019902592.1, XM_019899997.1, XM_019906207.1, XM_019905720.1, XM_019899788.1, XM_019899789.1
Nicotinate and nicotinamide metabolism	map00760	4	XM_019906883.1
One carbon pool by folate	map00670	4	XM_019914336.1, XM_019901577.1, XM_019906362.1, XM_019906856.1
Pentose and glucuronate interconversions	map00040	4	XM_019910318.1
Carbon fixation in photosynthetic organisms	map00710	4	XM_019901419.1, XM_019910125.1, XM_019899542.1, XM_019915408.1, XM_019915181.1, XM_019915626.1
Pentose phosphate pathway	map00030	4	XM_019912864.1, XM_019907741.1
Citrate cycle (TCA cycle)	map00020	4	XM_019903766.1, XM_019908753.1, XM_019911686.1, XM_019904030.1
Propanoate metabolism	map00640	4	XM_019917028.1, XM_019917912.1, XM_019915292.1, XM_019915346.1, XM_019898758.1, XM_019900363.1, XM_019917134.1, XM_019917351.1
Glyoxylate and dicarboxylate metabolism	map00630	3	

N-Glycan biosynthesis	map00510	3	XM_019906883.1, XM_019900285.1, XM_019912014.1, XM_019900285.1
Metabolism of xenobiotics by cytochrome P450	map00980	3	XM_019917936.1, XM_019903766.1, XM_019908753.1, XM_019915962.1 XM_019902845.1, XM_019902369.1, XM_019912321.1, XM_019899330.1, XM_019916334.1, XM_019909702.1, XM_019899407.1, XM_019914203.1, XM_019904175.1, XM_019908130.1, XM_019908753.1, XM_019907109.1, XM_019912897.1, XM_019911906.1, XM_019902668.1, XM_019914303.1
Phosphatidylinositol signaling system	map04070	3	XM_019910290.1
Inositol phosphate metabolism	map00562	3	XM_019916284.1, XM_019904956.1, XM_019913911.1, XM_019915591.1, XM_019900363.1, XM_019917134.1, XM_019910318.1, XM_019905419.1
Fructose and mannose metabolism	map00051	3	XM_019907860.1, XM_019911961.1 XM_019905168.1, XM_019902592.1, XM_019899997.1, XM_019902438.1, XM_019912417.1, XM_019899639.1, XM_019901314.1, XM_019904139.1, XM_019911517.1, XM_019914951.1, XM_019899299.1, XM_019915181.1, XM_019917332.1, XM_019916253.1, XM_019898846.1, XM_019904616.1, XM_019916923.1, XM_019902086.1, XM_019902087.1, XM_019908951.1, XM_019899377.1, XM_019903785.1, XM_019905720.1, XM_019899788.1, XM_019899789.1
Arginine and proline metabolism	map00330	3	
Pantothenate and CoA biosynthesis	map00770	3	

Drug metabolism - cytochrome P450	map00982	3	XM_019915946.1, XM_019910396.1, XM_019913435.1, XM_019916990.1, XM_019902453.1 XM_019902845.1, XM_019902369.1, XM_019912321.1, XM_019899330.1, XM_019916334.1, XM_019909702.1, XM_019899407.1, XM_019914203.1, XM_019904175.1, XM_019908130.1, XM_019908753.1, XM_019907109.1, XM_019912897.1, XM_019911906.1, XM_019902668.1, XM_019914303.1 XM_019898051.1, XM_019902845.1, XM_019902369.1, XM_019912321.1, XM_019899330.1, XM_019916334.1, XM_019909702.1, XM_019899407.1, XM_019914203.1, XM_019904175.1, XM_019908130.1, XM_019908753.1, XM_019907109.1, XM_019912897.1, XM_019911906.1, XM_019902668.1, XM_019914303.1
Riboflavin metabolism	map00740	3	XM_019903625.1 XM_019897898.1, XM_019911852.1, XM_019911849.1 XM_019904956.1, XM_019907373.1, XM_019907274.1, XM_019907285.1, XM_019910013.1, XM_019899241.1, XM_019905720.1, XM_019899788.1, XM_019899789.1, XM_019907538.1 XM_019902438.1, XM_019907860.1, XM_019901561.1, XM_019908289.1, XM_019908288.1 XM_019907504.1, XM_019903054.1, XM_019901341.1
Thiamine metabolism	map00730	3	
Glycosaminoglycan degradation	map00531	3	
Ascorbate and aldarate metabolism	map00053	3	
Other glycan degradation	map00511	3	
Glycosphingolipid biosynthesis - ganglio series	map00604	2	
Biosynthesis of unsaturated fatty acids	map01040	2	

Starch and sucrose metabolism	map00500	2	XM_019904632.1, XM_019910318.1, XM_019917742.1
T cell receptor signaling pathway	map04660	2	XM_019903625.1
Arginine biosynthesis	map00220	2	XM_019910318.1
Arachidonic acid metabolism	map00590	2	XM_019906204.1, XM_019898811.1, XM_019915687.1
Nitrogen metabolism	map00910	2	XM_019900633.1
Ubiquinone and other terpenoid-quinone biosynthesis	map00130	2	XM_019897898.1, XM_019911852.1, XM_019911849.1
Glycerophospholipid metabolism	map00564	2	XM_019906883.1
Cutin, suberine and wax biosynthesis	map00073	2	XM_019899407.1

Appendix 4.1 Populations, regions, site locations, and beetle numbers. Sample sizes are given for the full data set after filtering (n), the number of specimens in the south (C_s), intermediate (C_i) and north (C_n) genetic clusters at each sample location, and the number in the 125-specimen subsampled dataset (n_s). Individual cluster assignments were determined based on principal component 1 (PC1) values for the full data set ($n=294$) as follows: $PC1 < -5.5$ = south cluster; $PC1 > -0.6$ = north; and $PC1$ of -5.5 to -0.6 = intermediate.

Population	Region	Site	Latitude	Longitude	Collection year	n	O_s	O_i	O_n	n_s
Edson	North	1	53.702	-116.847	2014	3	0	0	3	2
Edson	North	2	53.770	-116.961	2014	2	0	0	2	1
Edson	North	3	53.777	-116.686	2014	4	0	0	4	1
Edson	North	4	53.833	-116.992	2014	3	0	0	3	1
Edson	North	5	53.398	-115.850	2016	17	0	1	16	5
Edson	North	6	53.831	-116.569	2016	20	0	0	20	5
Battle Lake	Intermediate	1	52.941	-114.284	2018	11	0	11	0	10
Canmore	South	1	51.067	-115.287	2014	10	10	0	0	10
Grande Prairie	North	1	54.570	-119.420	2015	8	0	0	8	0
Grande Prairie	North	2	54.190	-118.680	2015	6	0	0	6	5
Grande Prairie	North	3	54.656	-119.007	2016	20	0	0	20	5
Grande Prairie	North	4	54.606	-118.224	2016	19	0	0	19	5
Hinton	Intermediate	1	53.380	-117.543	2017	22	0	22	0	8
Hinton	Intermediate	2	53.344	-117.583	2016	30	0	19	11	8
Jasper	Intermediate	1	53.463	-118.237	2015	2	0	2	0	2
Jasper	Intermediate	2	53.160	-117.530	2015	3	0	3	0	3
Jasper	Intermediate	3	53.208	-117.348	2015	3	0	3	0	1
Jasper	Intermediate	4	53.400	-117.247	2015	1	0	1	0	3
Jasper	Intermediate	5	53.503	-117.734	2015	3	0	2	1	3
Lac La Biche	North	1	55.622	-112.881	2018	6	0	0	6	2
Lac La Biche	North	2	55.389	-112.976	2018	3	0	0	3	3
Lac La Biche	North	3	55.382	-112.990	2018	4	0	0	4	2

Lac La Biche	North	4	55.397	-112.972	2018	4	0	0	4	0
Lac La Biche	North	5	55.395	-112.972	2018	3	0	0	3	1
Lac La Biche	North	6	55.390	-112.989	2018	1	0	0	1	1
Lac La Biche	North	7	55.431	-112.072	2018	1	0	0	1	1
Lac La Biche	North	8	55.413	-112.005	2018	5	0	0	5	5
Slave Lake	North	1	54.863	-115.163	2017	13	0	0	13	0
Slave Lake	North	2	55.139	-115.343	2018	5	0	0	5	4
Slave Lake	North	3	54.933	-115.452	2018	4	0	1	3	4
Slave Lake	North	4	54.744	-115.798	2018	7	0	0	7	0
Slave Lake	North	5	55.613	-114.326	2016	19	0	2	17	8
Whitecourt	North	1	54.393	-116.286	2018	5	0	2	3	2
Whitecourt	North	2	54.354	-115.782	2018	5	0	0	5	4
Whitecourt	North	3	54.493	-115.538	2018	5	0	3	2	2
Whitecourt	North	4	54.376	-115.691	2016	17	0	0	17	8

Appendix 4.2 Discriminant analysis of principal components (DAPC) of 201 individuals from five northern populations, excluding intermediate-cluster individuals as in Figure 4.1B.

